Winter 12-18-2019

Hydro-Climatic Dynamics of Lake Watershed Systems in a Changing Climate

Mussie Tekie Beyene
University of Maine, mussie.beyene@maine.edu

HYDRO-CLIMATIC DYNAMICS OF LAKE WATERSHED SYSTEMS IN A CHANGING CLIMATE

By

Mussie Tekie Beyene

B.S., University of Asmara, 2004

M.S., University of Maine, 2016

A DISSERTATION

Submitted in Partial Fulfillment of the

Requirements for the Degree of

Doctor of Philosophy

(in Civil and Environmental Engineering)

The Graduate School

The University of Maine

December 2019

Advisory Committee:

Shaleen Jain, Ph.D., Professor of Civil and Environmental Engineering, Advisor

Aria Amirbahman, Ph.D., Professor of Civil and Environmental Engineering

Jean MacRae, Ph.D., Associate Professor of Civil and Environmental Engineering

Ramesh C. Gupta, Ph.D., Professor of Mathematics and Statistics

Firooza Pavri, Ph.D., Professor of Geography

HYDRO-CLIMATIC DYNAMICS OF LAKE WATERSHED SYSTEMS IN A CHANGING CLIMATE

By Mussie Tekie Beyene

Dissertation Advisor: Dr. Shaleen Jain

An Abstract of the Dissertation Presented
in Partial Fulfillment of the Requirements for the
Degree of Doctor of Philosophy
(in Civil and Environmental Engineering)
December 2019

In the northern hemisphere, winter climate conditions are showing dramatic year-to-year swings. To date, implications of a changing winter climate pattern on individual or regional lakes are poorly understood, particularly in cold regions where seasonal ice appears on lake surfaces. This dissertation investigates the significance of yearly winter climate condition on the health and function of freezing lakes by modeling and characterizing the response of lake ice phenology (and related socio-ecological systems) to winter weather-climate variability. In Chapter 2, several case studies on winter limnology are reviewed to develop a tentative socio-ecological framework that demonstrates the local and regional implications of the changing nature of lake ice, and the extent to which the resulting impacts span human and environmental systems. The performances of ice-out date models that incorporate winter degree-days as covariates in Chapter 3 imply that winter temperatures (as degree-days) govern the variability of lake ice-out dates across the three climatic regions in Maine. In Chapter 4, the influence of antecedent winter degree-days on spring ice-out dates is described by determining the winter degree-day thresholds that engender early/late spring ice-out dates. In Chapter 5, quantile regression models were developed to characterize the heterogeneous effect of diverse El Niño-Southern Oscillation (ENSO) events on North American wintertime air temperatures at specific

quantiles as well as the entire distribution. Chapter 6 extends the work in Chapter 5 and describes the potential asymmetry in the nature of ENSO related ice-out date anomalies for North American lakes both locally and regionally. In conclusion, the findings here imply that characterizing the relationship between winter climate patterns and lake ice season in cold regions offers forecast of lake structure and function at a seasonal or longer time scale across multiple spatial scales.

DEDICATION

To my parents, who instilled in me the virtue of education.

ACKNOWLEDGEMENTS

The fear of God is the beginning of Wisdom... (Proverbs 9:10).

I am indebted to many people for making my Ph.D. experience unforgettable. First and foremost, I would like to thank my advisor Professor Shaleen Jain for his excellent guidance, caring, patience and making my Ph.D. experience productive and stimulating. The joy and enthusiasm he has for his research was contagious and motivational for me, even during the tough time in my Ph.D. pursuit. I am also thankful for the excellent example he has provided me as a successful professor and researcher.

I would also like to thank my committee members Professor Gupta, Professor MacRae, Professor Amirbahman and Professor Pavri for their interesting and critical feedback. I feel proud and honored that you accepted to be on my committee.

My deepest appreciation to the rest of the Civil and Environmental faculty at the University of Maine and especially Professor William Davids, for their brilliant counsel and support.

I gratefully acknowledge the funding sources that made my Ph.D. work possible. I was funded by Senator Mitchell's Center for Sustainability Solutions for my first three years and was honored to be a graduate fellow. My Ph.D. work was also supported by the National Science Foundation Awards 0904155 and 1055934, and National Oceanic and Atmospheric Administration (NOAA) award NA 14OAR 4320158.

Completing this work would have been all the more difficult were it not for the support of my colleagues and close friends. Nirajan Dhakal, Anne Lausier, Ali Aljoda, Nuha Abdullah, Prashanta, Haifei Chen, Rakibul Khan, and Alex Gray, I am lucky to have had colleagues like you. Thank you for your friendship, motivations and creating the best work environment for me to succeed. I am also indebted to Amamihe Onwuachumba, Tesfahiwet Zerayesus, Fidel Odunze, Wang Yang Arnaud, Bipush Osti, Cinny, Matt Valles, Bereket

Yohannes, and Milkias Tesfamariam for their amazing friendship, energy and humor throughout my time in graduate school. You have a friend for life.

Finally, I would like to dedicate this dissertation to my parents Tekie and Azeb and my siblings Michael and Mehret, whose love, understanding and support are with me in whatever I pursue. They are my ultimate role models.

TABLE OF CONTENTS

LIST OF TABLES

LIST OF FIGURES

CHAPTER 1
GENERAL INTRODUCTION

1.1 Effect of Climate Variability on Northern Lakes Ecosystem

Lakes play a critical role in the cold northern regions where the air temperature fall below 0°C in winter (December-February). As hosts to a diverse array of cold-water species, lakes serve as hubs for many hydrogeochemical cycles, moderate climate, and provide ecosystem services to local human and terrestrial life. Accordingly, alteration in the physical, biological and chemical attributes of lakes have a number of ecological and socio-economic ramifications. Over the last century, there have been unprecedented changes in northern cold regional climate patterns [156]. Limnological studies show that these deviations combined with land use changes are engendering shorter ice cover durations and warmer temperatures, increased likelihood of algal blooms and elevated water quality concerns, depletion of cold-water fishes and spread of invasive species, and loss of ecosystem health and services for various lakes [62, 134]. Given that regional and global climate models are projecting progressively large changes in the cold regions climate by mid 21^{st} century [156], the ability of local lakes to sustain present day range of aquatic species or provide life giving services to terrestrial life is at risk.

In order to understand the impact of climate variability and change on cold regions lake ecosystem, the relative role of seasonal climate and limnology in regulating lake health and functioning need to be characterized. To this end, there have been a number of published studies that examine the import of open-water season (e.g. spring and summer) lake processes in determining the physical, chemical and biological attributes of cold region lakes. In contrast, the effect of winter and related limnological activities on lake ecosystems is poorly understood often stemming from the misconception that low light level and cold-water temperatures in winter brings lake processes to a standstill [141]. However,

recent studies show that limnological activities in winter are not only equivalent to that of other seasons but also govern the lake structure, stability and productivity in following seasons [2, 70, 169]. The fact that Global Atmospheric Circulation Models (GCM) are predicting the changes in climate patterns to be more pronounced in the winter season further heightens the urgency to study the significance of winter on cold region lake ecosystem.

1.2 Lake Ice Phenology and Its Links to Seasonal Climate Variables

About half of the world's 117 million lakes are found poleward of 40^oN and during winter, these lakes are often covered in ice ([165]). The appearance of a stable ice on lake surfaces has an important ecological and social significance. It creates a cold, dark, calm, and oxygen limited under-ice lake environment such that lake heterotrophs and mixotrophs flourish over the autotrophs, and cold-water species gain competitive advantage over warm water ones [e.g., 132, 141]. On the other hand, frozen lakes are used by local people as inexpensive roadways to remote communities, industrial development sites, and hunting and trapping grounds [109, 135]. They also serve as venues for popular winter recreational activities such as skating and ice fishing.

Lake ice formation, growth and decay is an outcome of the heat exchange between lake and atmosphere at lake surface, integrated over time [174]. It begins to form from weeks to months after daily air temperatures fall below 0°C (32°F) and the date when ice completely covers lake surface is commonly referred to as the ice in (or freeze up) date. Geographically, the ice-in date for lakes in the Northern Hemisphere lakes primarily varies with latitude and to a lesser extent by lake depth, elevation and distance from the oceans, with shallow lakes in high latitude and altitude freezing as early as October 1^{st} [109, 176, 178]. The rate of ice growth in a lake is determined by the winter meteorological conditions particularly the freezing degree days (FDD). Consequently, in the high latitudes it can grow to several meters thick [109]. For most lakes, the appearance of an ice cover on

lakes is a seasonal phenomenon (i.e. does not remain for the entire year), although multi-year and permanent ice-covers have been found in mountainous, high latitude lakes. In spring, lake ice begins to melt some time after daily air temperatures rise above freezing point and the date when ice completely clears from the surface of a lakes is called the lake ice-out (or break up) dates ([111]). Geographically, the ice-out date for northern lakes primarily fluctuates with latitude and to a lesser extent elevation, with shallow high latitude and altitude lakes having their ice-out dates as late as July [109, 176, 178].

However, over the last century, lake ice phenology in the northern hemisphere is recording a rapid rise in the frequency of unusually short ice seasons (including ice free winters). Weyhenmeyer et al. [171] found an increase in the year-to-year variability of lake ice-in and ice-out date for northern cold regions during the 1961-1990 period, with the greatest rise observed in regions that experience freezing temperatures for only short period of time. Benson et al. [20] reported that for studied northern lakes, the frequency of 50-year, 25-year, and 10-year extreme late freeze and melt date events increased in recent periods. Furthermore, Sharma et al. [147] estimates that a mere 2°C increase in the mean annual air temperature results in a shift in the ice regime of 35,300 lakes from a stable ice cover to an intermittent ice cover.

To elucidate the observed changes in the lake ice season and predict future changes due to climate change and variability, there have been empirical and model studies that assess the efficacy of seasonal weather-climate variables in modulating the ice characteristics and phenology of northern lakes. Given that the ice in and out dates for most lakes occurs during fall/early winter and spring respectively, the focus of most research publications has been in characterizing and quantifying the efficacy of fall and spring climate variables in determining the timing and length of the lake ice cover period. For instance, Hodgkins et al. [77] estimated that the monotonic trends in New England lakes towards earlier ice-out dates correspond to the warming of the mean spring (March-April) air temperature by 1.4-1.5°C during 1850-2000 period. In contrast, the relative role of winter

weather-climate variability in determining the lake ice season is poorly understood and characterized even though winter provides the bulk of freeze energy needed to form and thicken ice on lake surface. The [156] reports that for cold regions the warming of climate will be more pronounced in winter as compared with other seasons under future climate scenario. Furthermore, recent climate studies have also found that under future climate, the frequency and intensity of extreme El Niño-Southern Oscillation (ENSO) events, which is leading source of inter-annual winter climate variability for subtropical regions, is projected to increase [39, 40]. Taken together, these findings indicate that in the upcoming decades, winter may not provide present day freeze energy such that for some cold region lakes, complete lake ice cover may not either form or the ice cover may not last until spring.

1.3 Thesis Outline

In a series of studies, this dissertation demonstrates the significance of yearly winter conditions on the health and function of cold region lakes by characterizing the response of lake ice phenology (and related socio-ecological system) to winter weather-climate variability at local and regional scales. All studies were based the long-term ice phenology records for various North American lakes and high-quality climate datasets either from nearby stations or gridded climate dataset. The next chapter (Chapter 2) provides a synthesis of lake ice case studies to assess the multiple pathways (and feedbacks) by which perturbations triggered by shorter ice cover season can cascade throughout the lake-watershed system and alter lake structure, stability and function the following seasons. Chapter 3 presents an empirical modeling framework to examine the significance of seasonal meteorological variables, especially the winter freezing and melting degree days (AFDD and AMDD) in determining the lake ice season. In Chapter 4, the efficacy of winter weather-climate variability in producing early/late spring ice out dates is investigated, including the identification of winter degree-day thresholds. Chapter 5 models and quantifies the asymmetry in ENSO related North American winter air temperature

anomalies at specific quantiles as well as the entire distribution. In chapter 6, heterogeneity in the nature of ENSO related ice-out date anomalies for North American lakes is characterized both locally and regionally.

CHAPTER 2
HYDROCLIMATIC CHANGE AND THRESHOLDS IN LAKE-ICE AS LENSES TO DELINEATE SOCIAL-ECOLOGICAL SYSTEMS VULNERABILITY

2.1 Introduction

Of the world,s 117 million lakes, nearly half freeze over periodically [165]. For the people living near these lakes, the appearance of lake ice has social, cultural, and economic significance. For hundreds of years, the shinto priests who lived at the shrine near the edge of Lake Suwa (Japan), have held their religious purification ritual following the complete freezing of the lake [146]. Skiing and skating on frozen lakes is a long-standing tradition in Canada and Nordic countries [98, 135]. In remote northern Canadian regions, lake ice sheets have been used as aircraft landing sites, thus allowing for uninterrupted access to and from local communities during the winter season [13]. On the other hand, lake ice acts as a lid over the lake water body restricting the transmission of light, oxygen, wind movement from the overlying atmosphere (Figure 2.1). Consequently, lake organisms and biogeochemical processes that can operate under relatively cold, dark, calm, and oxygen limited lake environment often dominate during the ice cover season [21, 70, 141]. Anomalous winter and spring season, in particular ones with warmer seasonal temperatures and high winter precipitation, impede ice growth and cause shorter or no ice cover season in cold region lakes. Recent studies point to both interannual climate variability, for example, due to El Niño-related weather [22, 23, 24, 138], and long-term warming trends [115] as causative factors.

In regions where lakes freeze, the shortening of the ice cover period not only affects human activities, but it also contributes to lake water quality decline with manifold implications. For instance, in the summer of 2012, the surface of Lake Auburn—a southern

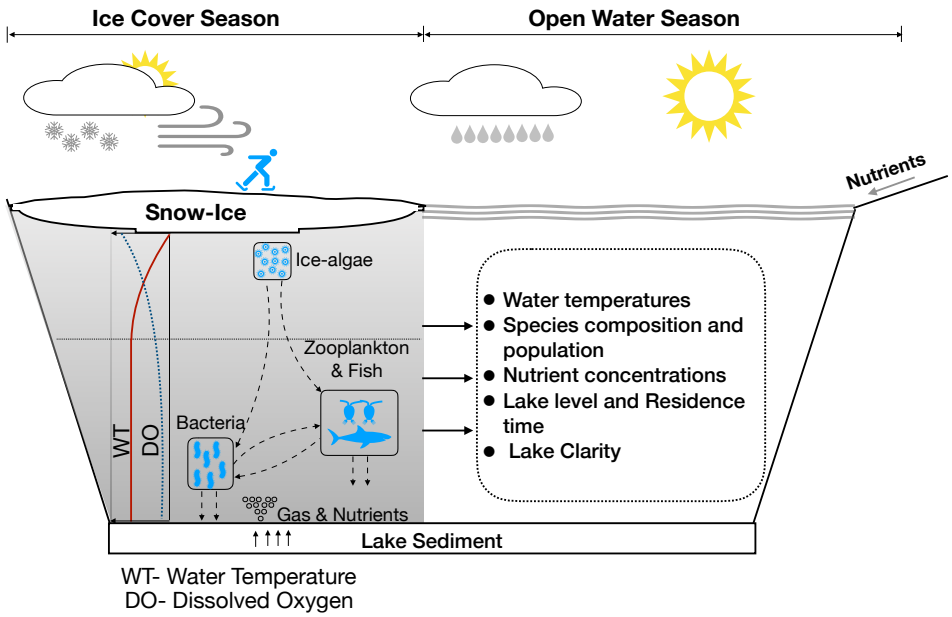

Figure 2.1. Conceptual diagram of expected winter activities in northern lakes.

Maine (USA) lake with no history of water quality issues—turned green stemming from severe algal blooms. In subsequent weeks, severe anoxic conditions developed at the lake bottom and killed the lake's entire cold-water trout population. Williams [177] suggests that the 2012 event at Lake Auburn were triggered by the early end to the ice cover season and high summer water temperatures caused by the unusually mild winter and high sediment flux into the lake due to heavy springtime rains. Weather- and climate-induced contrasts in lake physical conditions and trophic status during spring and summer seasons are also evident in European lakes, wherein milder winters with shorter ice periods or ice-free conditions appear to lead to larger algal biomass, thus contributing to water quality declines [e.g., 126, 170].

Despite the ubiquity of ice on the world's lakes, the nature and predictability of winter weather-climate conditions that cause unusually short or no ice cover season in lakes has received limited attention in the literature [22, 24, 25]. This stems from the prevailing reasoning that the warming and/or lengthening of the spring period is the primary driver

of the trend towards the early end of the lake ice cover season, particularly for lakes where the ice cover season ends in late spring or early summer months [e.g., 51, 77, 155, 175]. The rapid warming of winter climate conditions over the past few decades has led to a sharp rise in the frequency of extremely short ice seasons, including no complete ice cover (NCIC) and ice-free winters in the northern hemisphere lakes [20, 147]. Beyene and Jain [22, 24] found a strong non-linear relationship between winter temperatures and spring ice-out dates, and that existence of winter degree-day thresholds, which if exceeded cause dramatic changes in the spring ice out dates of North American lakes. Finally, winter weather-climate variability in the extra-tropics has been found to correspond with large-scale atmospheric-oceanic circulation patterns (e.g., El Niño-Southern Oscillation —ENSO), which can be forecasted up to six months ahead [45, 81, 137]. This implies that characterizing the linkages between winter weather-climate conditions and ice phenology in northern lakes may offer a pathway towards effective lake-related management and planning by enabling season-ahead (or longer) predictions of lake ice conditions in the northern hemisphere from local-to-regional scales.

In limnology, there is a paucity of information about the overall effects of shorter or no ice cover season on the nature, stability, and function of seasonally ice covered lakes [132, 141]. A recent global under-ice lake ecology study by Hampton et al. [70] elaborated that the under-ice lake environment maintains substantial biological activity (e.g., autotrophic productivity) and nutrient (e.g., Dissolved Nitrogen) level, which for some lakes such as Lake Baikal (Russia) and Lake Erie even exceeds than that of summer. Moreover, there are case-studies that have examined the impact of shifts in lake ice phenology on the physical, chemical, and biological constituents of freezing lake(s) during the open water season. For instance, Adrian et al. [2] found a significant positive correlation between ice duration and maximum spring algal biomass at Lake Müggelsee (Germany). Finally, there is multiple evidence of the cultural and economic consequences of a short or no lake ice cover season at local and regional scales [147]. Synthesizing these

findings allows for understanding and mapping of the overall response of freezing lakes and related socio-ecological systems to changes in the annual ice cover period (and its climate drivers) at a watershed or larger spatial scale, during the year.

Given the increasing concern over the consequence of projected winter climate warming (trend and variability) in cold regions, there is a need to motivate the study of winter limnology in seasonally ice-covered lakes. To this end, this study intends to articulate the presence of winter thermal thresholds in lake ice which if exceeded can have cross-seasonal implications on lake ecology and ecosystem services, and the extent to which the impacts can span human and environmental systems. The next section elucidates how inter-annual winter climate variability influences the ice cover duration using findings from recent lake ice studies. and illustrations using ice phenology and climate records. Following this, a review of a full range of lake ecosystem response to shorter/ no ice cover period in freezing lakes is presented. This includes a tentative social-ecological framework that maps the multiple pathways and feedback by which perturbations stemming from short ice cover period may cascade across the lake-watershed system. The final section describes the commingling effect of a changing watershed processes and lake ice phenology in diminishing lake water quality.

2.2 Delineation of Lake-Watershed Processes Within the Context of Lake Ice

We reviewed over 40 peer-reviewed case studies that examined the response of one or more lake-watershed parameter(s) to the early end of the ice cover period (Table A.1). Based on the findings of these case studies, we describe in the following paragraphs the potential impact of shorter/no ice cover season on the physical, chemical, biological and social attributes of lakes in northern cold regions. The schematic in Figure 2.2 also summarizes the response and feedback of key lake ecological and social components and processes to shorter/no ice cover period at a watershed scale, including the confidence placed in each response.

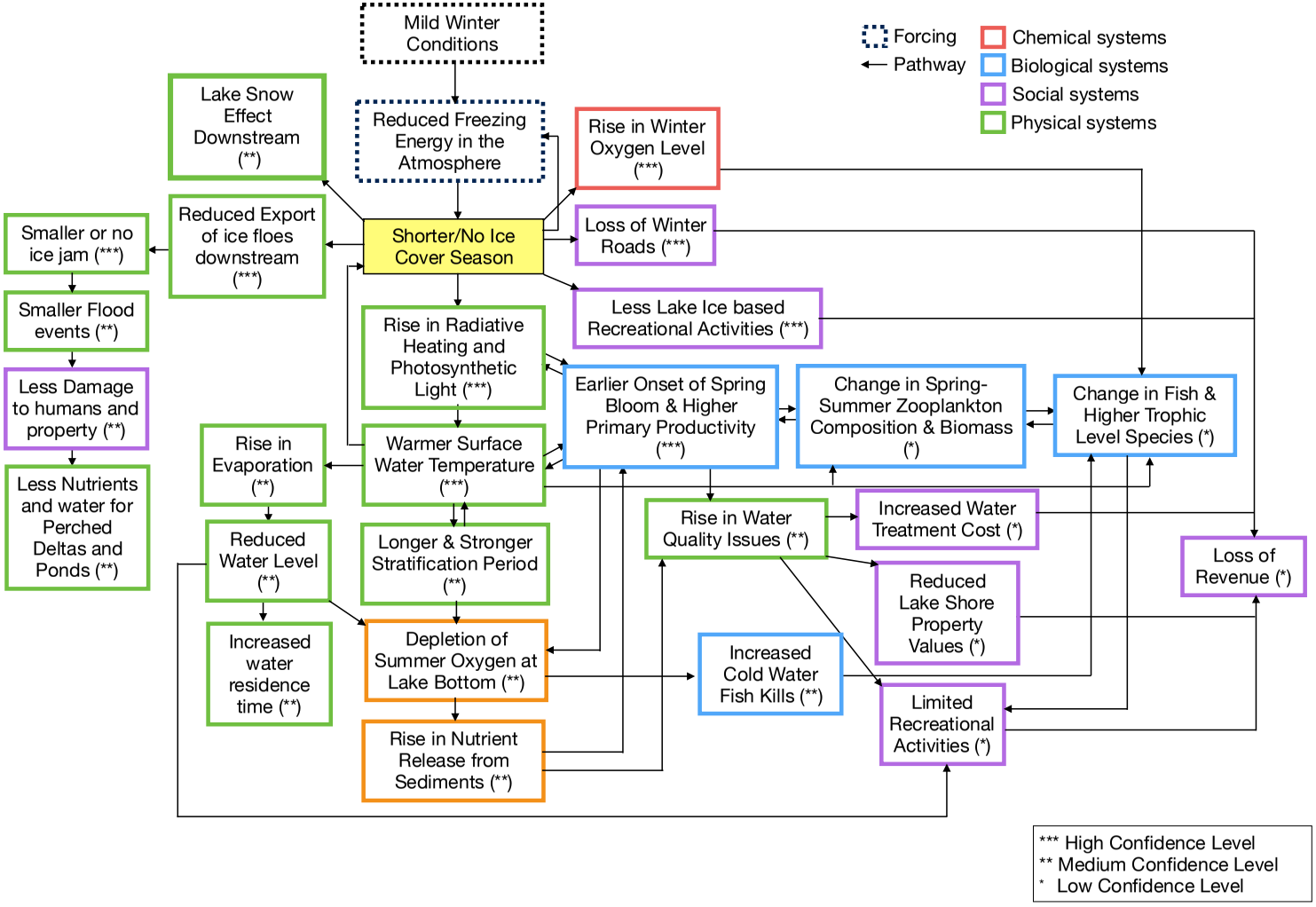

Figure 2.2. Conceptual schema of the response of lake watershed processes to shorter or no ice cover season.

Seasonal Thermal Structure and Mixing Regime: when the surface of lakes is covered in ice, only a small fraction of the atmospheric heat input reaches the lake water column. This is because ice reflects back 30-90% of the incoming solar insolation into the atmosphere [109]. The early end of the lake ice season by weeks to months therefore favors a substantial rise in the atmospheric heat inputs into the lake water volume. For lakes in the northern cold regions, this can lead to warmer spring and summer lake water temperatures [e.g., 14, 64, 127, 186], earlier onset of spring turnover and summer stratification period [e.g., 88, 133, 186], and upsurge in spring/summer sensible and latent heat flux [139]. In some lakes, the absence of lake ice during winter triggers dramatic changes in the lake's mixing regime such as a shift from cold monomictic to dimictic or from dimictic to warm monomictic [e.g., 6, 135]. However, the persistency and degree to which shorter or no ice duration affects the thermal structure of northern cold region lakes depends on lake specific factors such as water clarity, morphometry, and water residence time, which determine the distribution of extra added heat in lake volume [64].

Nutrient Cycling: During long ice cover periods, dissolved oxygen can get exhausted at lake bottom (hypolimnion) due to the consumption of oxygen for benthic respiration and decomposition of organic matter near sediment [96, 131]. This is especially the case for lakes where the volume of hypolimnion water is small, and the amount of organic matter near the lake bottom are high. The exhaustion of oxygen at the hypolimnion creates an anoxic (reducing) environment at lake water-sediment interface, which promotes the release of nutrients such as reactive manganese, iron and phosphorous [27, 90, 154]. For some northern lakes, shorter or no ice cover season may, therefore, decrease the likelihood of an anoxic conditions from developing at lake sediments during the winter season, which in turn reduces the availability of nutrients in the water column. On the other hand, the early end to the lake ice season in lakes often leads to the early onset of the spring-summer lake stratification period, where there is limited mixing between epilimnion (upper) and hypolimnion waters [135]. In shallow lakes or lakes where there is a strong thermocline at a

lower depth, the lengthening of the stratification season enhances the development of an anoxic conditions at the sediment-water interface, which in turn favors the release of reactive nutrients from sediments to the overlying water column [55].

Aquatic species and trophic interaction: During complete ice cover period in lakes, the surface snow-ice cover acts as a lid, creating dark, less turbid and cold under-ice lake environment [141]. These conditions generally favor heterotrophic processes and lower plankton biomass as the low light setting restricts autotrophic plankton productivity, and the non-turbulent conditions promote sinking of non-motile algae [70]. Thus, the early onset of ice-free period can lead to a substantial increase in spring and summer algal biomass [2, 133, 169], change in the seasonal composition and succession of plankton species [27, 63, 68, 140] for various cold region lakes. Significant mismatches in the response of predator and prey plankton species caused by shorter ice cover season can also engender the re-organization of the lake food web [179]. However, the extent to which shorter or no ice duration alters the plankton abundance, community and trophic relationships in lakes depend on factors such as snow-ice conditions, nutrient availability and spring/summer climate [3]. The cold, dark and oxygen-limited lake environment during ice cover season also provides an optimum environment for native cold-water fish species [75]. Therefore, the early end to the lake ice season commingling with warmer lake water temperatures diminish the survival advantage of these native fish species and promote the spread of invasive warm water fish species [56, 69, 135]. It also reduces the likelihood of winter fish kills, as there is less potential for anoxic conditions to develop at the lake bottom during short or no ice cover period [55]. On the other hand, early ice-out dates may correspond to the lengthening of summer stratification period in lakes, and in shallow lakes or lakes with strong thermocline at lower depth, this promotes the occurrence of anoxic conditions and fish kills in the hypolimnion waters during summer/fall season [177].

Economic and Cultural Values: Over half of a billion people live in northern cold regions where lakes periodically freeze [147]. For these people, lake ice has social, cultural,

economic, and recreational importance as evidenced by the long-term ice phenology records kept for hundreds of years, and the abundance of ice festivals each year. Consequently, shorter or no lake ice cover season can have a range of implications. It can contribute to increased economic hardship and scarcity of provisions, as lake ice offers an inexpensive roadway to remote communities and industrial development sites, access to traditional hunting, fishing and trapping grounds, and a venue for popular winter recreational activities [97, 108, 135]. For example, in Manitoba (Canada), mild winter conditions in 2010 prompted the closure of 2200 km of winter roads (composed of lake and river ice), impeding the transport of food, gas and construction materials to more than 30,000 first nations people (Carlson, 2010). This created scarcity of provisions in many First Nations communities such that a state of emergency was declared. On the other hand, the ice fishing derby at Gull Lake (Minnesota, USA) alone gathers tens of thousands of anglers, generating over $1 million in revenue to local businesses, and $150,000 for charities annually. In addition, we noted earlier that shorter or no ice season might lead to increased algal biomass and loss of cold-water fishes in cold region lakes. These conditions may put off recreational activities during the open water season, increase water treatment costs, and reduce lake-shore property prices [135].

Local climate: The presence of complete ice cover limits the thermal exchange between the relatively warm lake waters under ice and overlying cold air [109]. In medium-to-large sized lakes, the premature end of the lake ice season during winter or early spring thus promotes the development of severe downwind fog and precipitation (e.g., lake snow effect) that have a significant economic impact [36, 47]. For instance, due to the lesser than average ice-cover extent over Lake Ontario during the winter of 2007, the town of Redfield, in New York State received about 141 inches of lake effect snowfall over seven days. This event impacted the transportation infrastructure, caused widespread power outrage and damaged buildings.

Ice Jams: Temperate and boreal lakes can be major producers of floating ice that flow down rivers. When these ice blocks get stuck in a narrow river channel, they may create an ice jam, which in spring produce flood events that supply nutrients and sediments to perched ponds and deltas [135]. Shorter or no ice duration may reduce the likelihood of ice jams from developing in rivers, which in turn may result in the loss of these unique habitats.

2.3 Climatic Drivers and Winter Thermal Thresholds in Lake Ice

The long-term ice phenology records for many northern cold region lakes exhibit significant secular trends towards later ice-in and earlier ice-out dates [e.g., 20, 77, 115]. However, the trends in the ice phenology of most lakes are also marked by significant year-to-year variability which enhance or reverse the trend in the lake ice dates [66, 145, 171]. For instance, for the 1870-2010 period, ice-out dates for Lake Auburn display a significant ($p < 0.05$) long-term trend towards earlier ice-out dates, where the mean ice-out date shifts from April 27^{th} for the 1870-1900 period to April 17^{th} for the 1980-2008 period (see Figure 2.3). Yet, there were three years during the 1870-1900 period, when the ice-out date was earlier than April 17^{th}, while there were five years when the ice-out date was later than April 27^{th} during the 1980-2010 period. Weyhenmeyer et al. [171], after examining the ice phenology of 1213 lakes, concluded that in recent period, there was an increase in the inter-annual variability of ice-in and ice-out dates of northern hemisphere lakes. In cold regions, the chain of events that modulate the inter-annual variability of lake ice phenology at local and regional scales often involve large-scale oceanic-atmospheric circulation (teleconnections) patterns, regional weather regimes, and local meteorological conditions that accelerate or impede lake ice growth or melt [e.g., 25, 32, 66, 112, 142, 169].

At local scales, lake ice formation, growth, and decay is an outcome of the thermal energy transfer between lake and overlying atmosphere, integrated over time and space (for large lakes) [11, 35, 109]. Air temperature generally represents the surplus/deficit heat

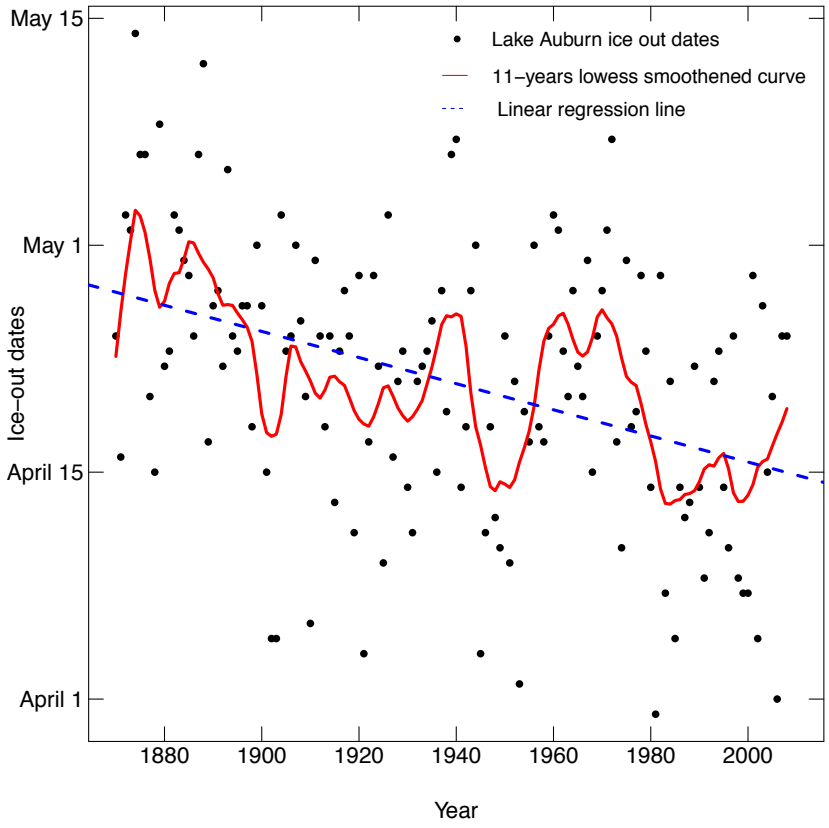

Figure 2.3. Trends and variability in the spring ice-out dates at Lake Auburn from 1850-2010.

energy in the atmosphere, and is therefore a good predictor of lake ice growth/decay [e.g., 111, 129]. For lakes with seasonal ice cover, the mechanisms by which winter and spring air temperatures govern the ice cover duration are not the same [25, 174]. This can be illustrated by contrasting the 2005/06 and 2006/07 lake ice evolution at Lake Auburn using a 1-D freshwater lake thermodynamic model FLake [122].

The ice-in date is the date when the surface of lake completely freezes. For Lake Auburn, the ice-in dates for the 2005/06 and 2006/07 ice cover season were December 18^{th} and 10^{th} respectively (Figures 2.4a & b). After the ice-in date, the ice cover begins to

thicken rapidly. For the two ice cover seasons, significant thickening of lake ice occurred during winter (December to February) (Figures 2.4a & b). Moreover, the rate of daily ice growth corresponds to the daily freezing degree days —the extent (in degrees) to which daily air temperatures fell below freezing (Figures 2.4e &f). At the end of February, the winter ice cover thickness in 2007 is twice as much to that of 2006 (Figure 2.4a & b). At the beginning of March, the ice cover stops growing and even starts to thin (melt) when the daily air temperatures rise above the freezing point (Figures 2.4a & b). In both seasons, the rate at which the ice melts daily mirrors the daily melting degree days—the extent (in degrees) to which daily air temperatures rises above freezing (Figures 2.4e & f). Since the ice growth to be melted during the 2006/07 lake ice season was higher than that for 2005/06 season, the ice out date—the date when ice completely cleared from the lake surface in 2006/07 was about 18 days later than in 2005/06 ice cover season (Figures 2.4a & b).

For northern cold region lakes, the efficacy of local winter temperature conditions in regulating the year-to-year variability of lake ice season can be determined and highlighted by characterizing the antecedent winter AFDDs and/or AMDDs that produce early and late spring ice-out dates. Figure 2.5 depicts the antecedent winter AFDDs and AMDDs for the spring ice-out dates at Lake Auburn from 1950-2010. The winter AFDDs and AMDDs that correspond to unusually early and late ice out dates can be estimated by generating the joint probability density estimates (of winter AFDDs and AMDDs) for the earliest and latest 15 ice-out dates at Lake Auburn during the 1950-2010 period (see Beyene and Jain [22] for more information on the methodology). The majority ($> 66\%$) of the earliest ice-out dates had both winter AMDDs greater than 37 Degree Day Fahrenheit (DDF) and winter AFDDs less than 600 DDF (Figure 2.5). Less than 20% of the latest 15 ice out dates occurred under any one of these winter conditions. Such disparity in the winter degree-days associated with the earliest and latest spring ice-out dates implies that for Lake Auburn, there are antecedent winter degree-days thresholds which if exceeded or not

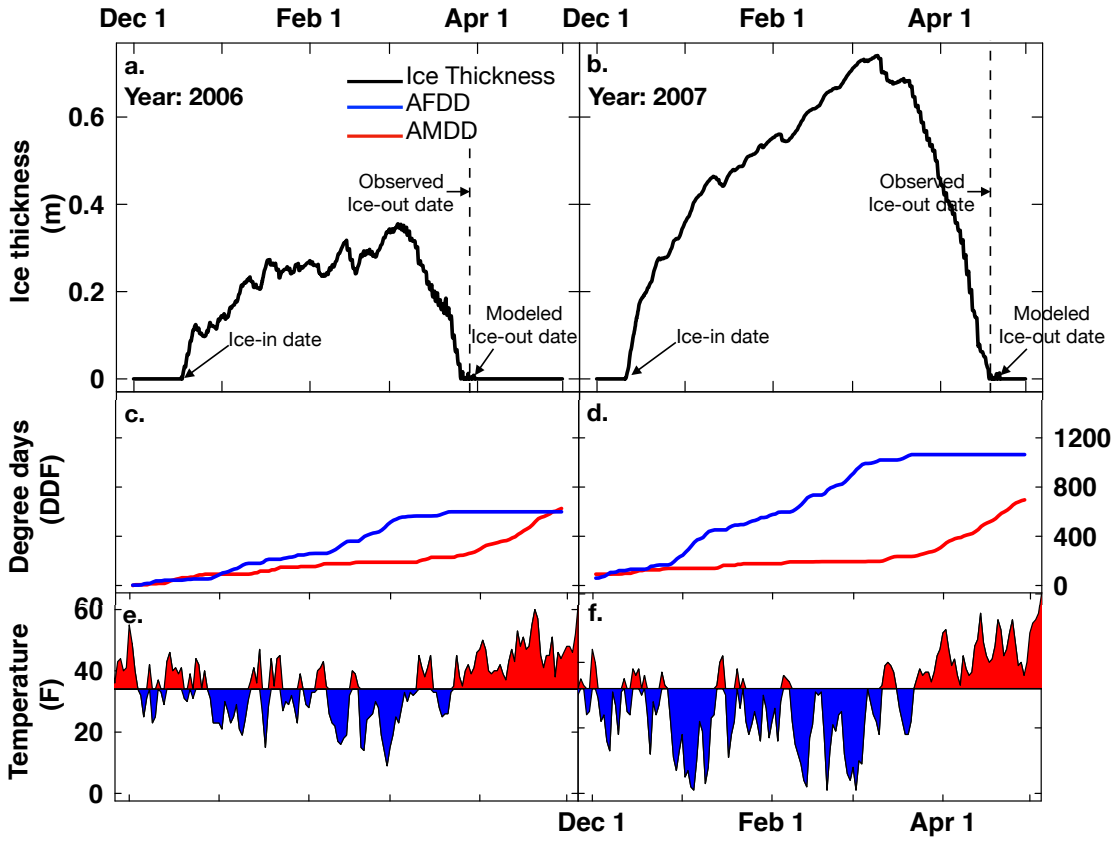

Figure 2.4. Contrasting the ice phenology and prevailing temperature conditions at Lake Auburn for 2006/07 and 2007/08. Contrasting the ice phenology and prevailing temperature conditions at Lake Auburn for 2006/07 and 2007/08. (a) and (b) Simulated lake ice evolution for 2006 and 2007 respectively. (c) and (d) Winter and spring accumulated freezing and melting degree days for 2006/07 and 2007/08. (e) and (f) daily winter and spring temperature for 2006/07 and 2007/08.

exceeded predispose the lake to have an early/late ice-out dates in spring. The studies by Beyene and Jain [22, 24] point to the presence of winter degree days that govern the variability of spring ice-out dates across North American lakes.

Large-scale winter teleconnection patterns regulate the timing of the lake ice in/out date by promoting warm and cold and/or wet and dry spells that delay or accelerate lake ice formation/melt [32]. Linkages between large-scale teleconnection patterns and lake ice cover season in northern regions can be quantified by estimating the relative change in the likelihood of local winter temperature conditions (that correspond to specific ice in/out dates) during different climate phases. This can be illustrated using Lake Auburn. Climate

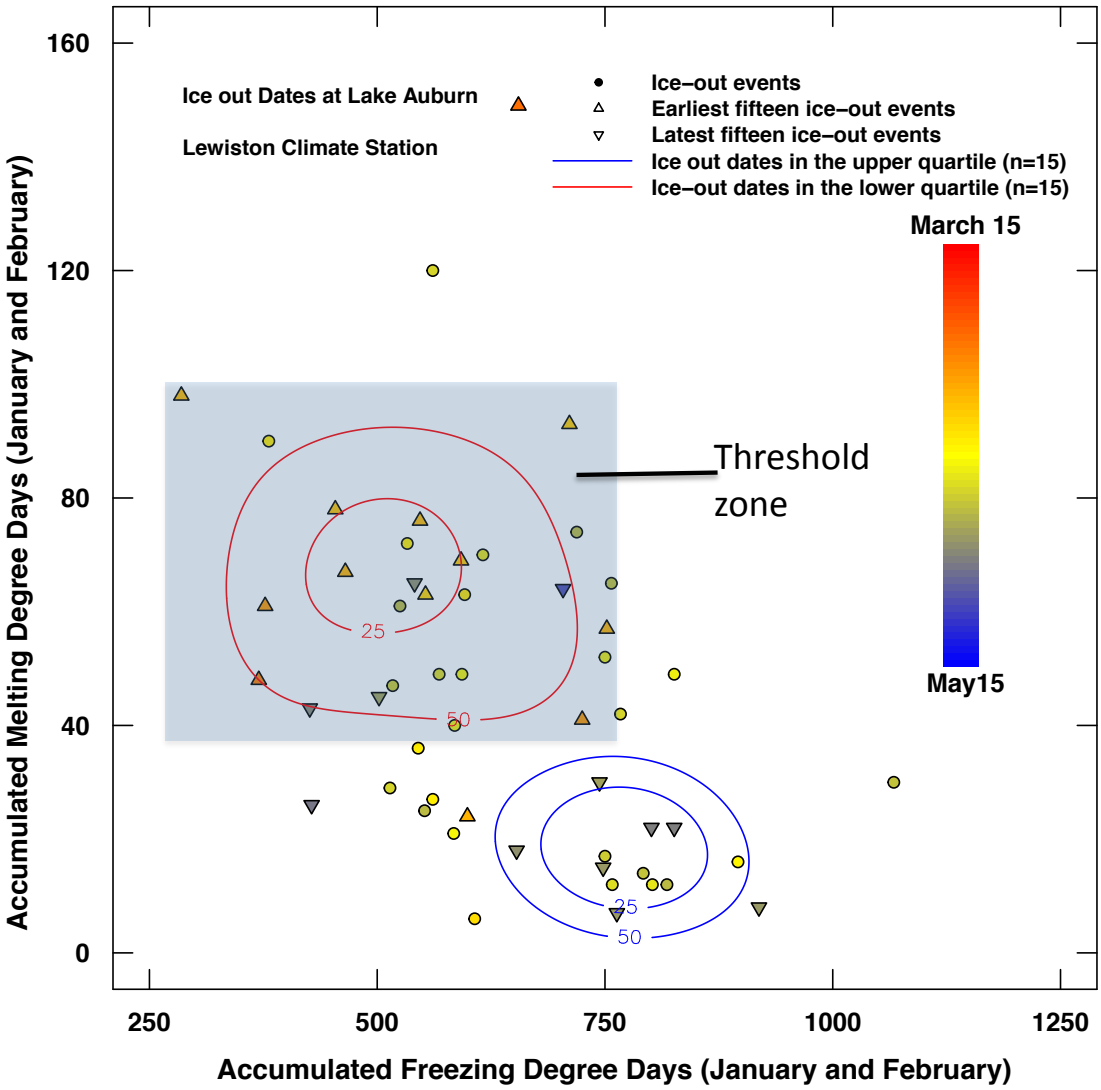

Figure 2.5. The joint probability density of winter AFDD and AMDD for the earliest and latest 15 ice out dates at Lake Auburn from 1950-2010. The joint probability density of winter AFDD and AMDD for the earliest and latest 15 ice out dates at Lake Auburn from 1950-2010. The density contours were generated using non-parametric kernel density estimators (Silvermann, 1986).

studies have found that winter meteorological conditions over the eastern North America are modulated by major teleconnection patterns such as the Tropical/Northern Hemisphere (TNH) and the El Niño-Southern Oscillation (ENSO) pattern [e.g., 16, 23, 34]. Moreover, it was noted earlier that winters with AFDD less than 600 degree-day Fahrenheit correspond to early spring ice-out dates at Lake Auburn. During strongly negative Tropical/Northern

Hemisphere (TNH) phases (TNH < -0.47), there is about 76% chance that the winter AFDD at Lake Auburn will be less than 600 DDF, which is approximately 80% more likely than other TNH phases. Similarly, during positive (warm) ENSO years, there is an 80% increase in the likelihood of winters with AFDDs less than 600 DDF at Lake Auburn, while there is a 20% decrease in their probability during cold (negative) ENSO phases.

2.4 Commingling Effect of Watershed Processes and Lake Ice Phenology on Lake Water Quality

There have been marked declines in the water quality of cold region lakes over the last century where in some cases, lakes have undergone shifts and transitions from a clear water state to a turbid state [e.g., 50, 121, 185]. Changes in the ice phenology of cold region lakes towards shorter or no ice cover season can contribute to the decline in lake water quality from seasonal to annual time scales, through multiple pathways (Figure 2.6). For example, the absence of winter snow-ice cover on the lake surface typically raises the availability of photosynthetic light and suspended nutrients in the water column due to the decline lake surface albedo, and increase in wind-induced water movement [141]. These conditions can lead to an increase in winter and spring algal biomass in lakes [3, 169]. On the other hand, shorter or no ice cover season often corresponds to a rise in the amount of short wave radiation absorbed in the lake water volume during winter and spring, which in turn promotes warmer spring-summer water temperatures [14, 64], and earlier commencement of the summer stratification period [88, 133]. Such stable and warm lake water conditions provides favorable conditions for harmful algal communities such as Cyanobacteria to flourish on the lake surface during the summer [37, 128]. The early onset of the summer stratification period also enhances the development of anoxic conditions at the sediment-water interface for lakes with strong thermoclines at a lower depth, which in turn favors the release of reactive nutrients and pollutants from sediments to overlying water column during wind induced mixing [55]. However, the extent to which shorter or no ice

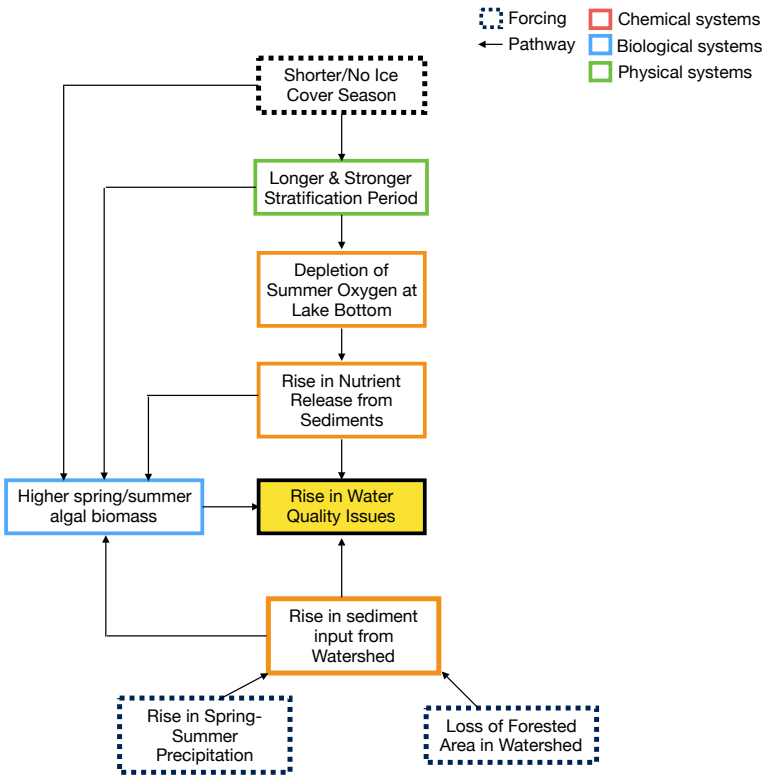

Figure 2.6. Conceptual diagram of the commingling effect of shorter ice cover duration and higher sediment flow on the water quality of northern lakes.

cover season influences lake geo-chemical and biological cycles and in turn the state of the water quality, hinges upon the ice cover characteristics and phenology, lake morphometry, and the availability and chemistry of nutrients in the lake water column and sediments [3, 64].

On the other hand, there has been an overall rise in the amount of sediments and nutrients delivered into cold region lakes since the turn of the 21^{th} century [e.g., 74, 157]. This can diminish lake water quality by raising the abundance of nutrients and pollutants in the lake water column, and promoting algal growth. The climatic parameter that is often found to explain rises in sediment and nutrient loading entering cold region lakes is the spring-summer rains. Changes in the magnitude and frequency of heavy spring-summer

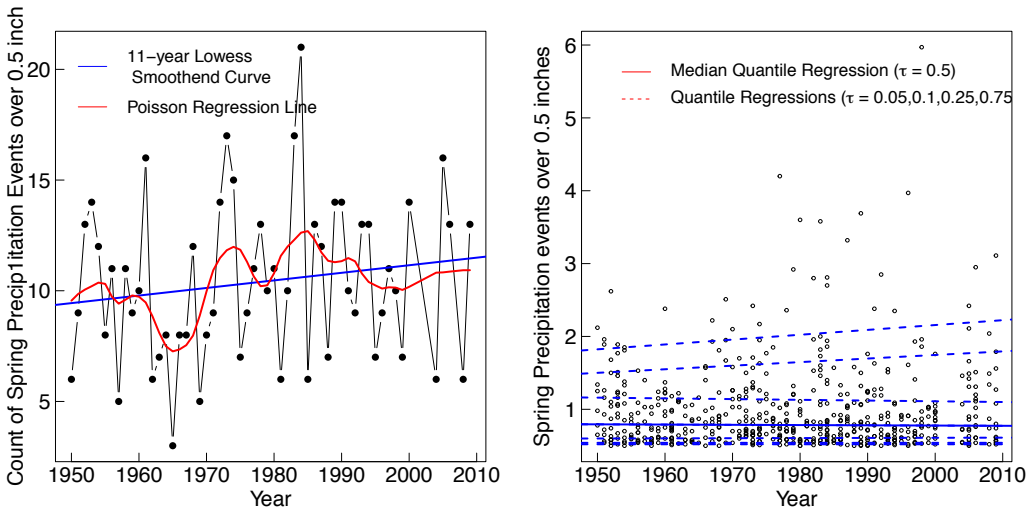

Figure 2.7. Trends and decadal variability in the annual frequency and magnitude of heavy spring rainfall events at Lake Auburn from 1950-2010. Trends and decadal variability in the annual frequency and magnitude of heavy spring rainfall events at Lake Auburn from 1950-2010. (a) 11- and 60-year smoothened patterns in the annual frequency of daily spring rainfall events exceeding 0.5 inches. (b) Regressing daily spring rainfall events (exceeding 0.5 inches) against time across five select quantiles.

storm events over headwater catchments can trigger changes in the sediment and nutrient entering lakes, as heavy rains in spring and summer are often accompanied by high pulse of water discharge and sediment load into lakes [42, 94, 151]. According to IPCC (2013), it is likely that the intensity and frequency of heavy spring-summer precipitation events have increased over the second half of the 21^{th} century for most northern North American and European regions including regions where the annual precipitation is decreasing. For Lake Auburn, for example, the trends in the magnitude of heavy spring-summer precipitation events, across seven select quantiles, reveal that the intensities of heavy spring summer storms (quantile, $\tau > 0.75$) have significantly risen over the last half century (Figure 2.7).

2.5 Concluding Remarks

In the northern hemisphere, the year-to-year variability of the lake ice season is rising dramatically. This is disconcerting as we lack a complete understanding of the risk of short/no ice induced effects on lakes and related systems. Here, our synthesis elucidates that characterizing the linkages between winter weather-climate variability and lake ice phenology affords seasonal (or longer) outlooks of the lake ice cover season at local and regional scales. It also outlines the potential ramification of short/no lake ice season (and its winter climate drivers) on a range of ecological, social, hydrological, and climatic variables. Collectively, this review offers for the first time a general framework by which the nature and predictability of short/no ice cover seasons and its impacts on linked socio-ecological systems can be examined and understood both at local and regional scales. Nevertheless, we are not at a stage where we can estimate the risk of short/no ice induced effects on lakes and related systems. To this end, we recommend future works in the following research areas:

- *Under-Ice Limnology*: comprehensive knowledge of the physical, chemical, and biological processes/activities that underpin the under-ice limnology will enable the identification and characterization of connections and feedbacks between under-ice and ice-free seasons. It would also explain the mechanisms by which shifts in the lake ice cover phenology (and related limnology) affect lake structure, stability, and function. However, any progress in the under-ice limnology study will entail an improvement in the current sampling procedures, methodologies, and instruments for seasonally ice-covered lakes as detailed by Block et al. [29]. Moreover, there are lake processes/activities that are endemic to the ice cover period. So the under-ice lake activities should also not be gaged using limnological metrics that are used for detecting the metabolism during the ice-free seasons [70].

- *Climate Forecast*: in the past four decades, seasonal-to-annual climate forecast has improved considerably, stemming from better climate models and additional data [e.g., 152]. Moreover, the greatest source of seasonal winter climate skill in the extra-tropics is the El Nino-Southern Oscillation (ENSO) pattern, whose development and teleconnections are well studied [81]. However, climate diagnostic studies have primarily focused on assessing ENSO induced shifts in the mean climate, which offers little information on the changes in the likelihood of winter climate conditions that engender short/no ice cover season. Future climate works on ENSO-winter climate teleconnections are needed where approaches and frameworks that assess ENSO related climate shifts across the entire distribution, as well as specific quantiles, are applied.

CHAPTER 3
MODELING LAKE ICE-OUT DATES: A LINEAR-CIRCULAR REGRESSION FRAMEWORK

3.1 Introduction

In temperate regions, there has been an increase in the inter-annual variability of the lake ice phenology over the past few decades [e.g., 102, 171]. This has led to the rise in the frequency of unusually short ice cover periods. For instance, Beyene and Jain [22] found that the inter-annual winter climate variability, linked to the northern hemisphere atmospheric teleconnection patterns, promote early ice-out dates in Maine lakes. Winter limnology studies show that the shortening of the ice cover season in lakes has detrimental effect on lake ecology and services [70, 135]. The year-to-year variability in the timing of spring lake ice-out dates is primarily a response to prevailing winter and spring meteorological conditions, as they control the surplus/deficit in the energy balance at lake surface determining lake ice growth/melt [e.g., 108, 111]. Aside from spring temperatures however, the efficacy of seasonal meteorological variables particularly during winter, in modulating the timing of the spring ice-out dates of lakes is not well known. Given that winter climate variability over the northern Temperate and Arctic regions, is influenced by large-scale oceanic-atmospheric circulation patterns, determining the role of winter on the variability of ice out dates would offer seasonal or longer outlook on the ice-cover season of lakes, both at local and regional scale.

The mechanisms by which winter and spring climate variability affect the timing of spring lake ice-out date are different. Winter meteorological conditions govern ice-cover processes related to the characteristics (e.g. type, thickness) of the winter ice that melts in spring. For instance, winter air temperatures (particularly the accumulated freezing and melting degree days - AFDD and AMDD) determine the cold content available at lake

surface to cool and thicken the ice cover [e.g., 109]. Winter snowfall on the other hand, can alter the composition of the ice-cover by promoting snow-ice formation, as well as reduce the thickness of lake ice, due to its insulating effect [e.g., 1, 164]. In contrast, spring climate variables control ice processes that govern the rate of melt. Spring air temperature, for example, influences the thermal energy available in the atmosphere to overcome the freeze content and melt the winter ice cover, while spring snowfall can reduce the melt rate by increasing the surface albedo and cold content of the ice cover [e.g., 174]. Modeling offers the opportunity to disentangle the dependence of year-to-year variability of lake ice-out dates to winter and spring weather and climate processes.

In empirical lake ice studies, ice phenology models, conditioned on seasonal climate variable(s), are often built using traditional regression method. The underlying assumption in this method is that the response variable (e.g., ice in/out dates) is a linear continuous variable, which has a true start point and magnitude. However, given that day-of-year variable is inherently unbounded (no start and end point) and cyclical, representing time variables as a linear variable results in the (i) loss of the periodic nature of time-of-year (ii) order and rank of ice in/out date variables to change with respect to the choice of origin [e.g., 107]. For instance, if using the Julian calendar, December 31$^{\text{st}}$ and January 1$^{\text{st}}$ are always 364/365 magnitudes apart and (say) January 1$^{\text{st}}$ and September 1$^{\text{st}}$ have a magnitude of 1 and 242 respectively. On the other hand, if using the water year, December 31$^{\text{st}}$ and January 1$^{\text{st}}$ are 1 magnitude apart and January 1st and September 1$^{\text{st}}$ have a magnitude of 124 and 1 respectively. According to Mallows [117], choosing data appropriate for model is a critical first step in statistical model building, as erroneous representation of the phenomenon under consideration in model produces model uncertainty that is much more than simple statistical inefficiency. This highlights the need for an alternate approach for characterizing day-of-year variables in regression models for ice phenology such that (a) the order of ice in/out dates are insensitive to the choice of

reference point and (b) the distributional assumptions employed for analyses take into account cyclical nature of time-of-year.

One such approach is the use of circular (angular) regression method, where the day-of-year variable is represented as a point on the circumference of a unit circle [86, 119]. In a circle, the beginning coincides with the end, and as such representing day-of-year variables as circular variables captures the periodicity and order of calendar days, independent of the choice in reference point. Furthermore, the circular regression approach employs unimodal circular distributions most notable of which is the standard von Mises distribution [119]. In addition, in circular regression models where the covariates are linear variable(s) (e.g., temperature, snowfall), link functions such as $2tan^{-1}(.)$ are used to map the covariate variable from the real line onto a unit circle. Consequently, the circular regression method is employed here in developing ice-out models of increasing complexity, to clarify the efficacy of winter and spring temperatures and snowfall in modulating the variability of spring ice dates in Maine lakes.

For this study, the historical ice-out and climate data for 12 Maine lakes are used. The next section discusses source of the ice out and meteorological data and delineation of winter and spring season for this study. The methodology section provides a concise summary on the theory of circular regression, and the framework applied here for building and assessing circular regression models for ice-out dates. The result section discusses diagnostic results from model outputs and residuals for selected lakes. It also provides an assessment if winter and spring degree-days and snowfall are adequate in explaining the variability in the spring ice-out dates in Maine lakes.

3.2 Data

3.2.1 Lake Ice-out Date Data

Lake ice-out date refers to the date in spring, when winter ice completely disappears from the lake surface [77]. The annual spring ice-out dates from 1950-2010 for the 12

studied Maine lakes were obtained from a publication by USGS [76]. Data from this database is selected because of the consistency over site of observation, and ice-out date definition for each lake. Furthermore, the main criteria for selecting these lakes is that they had more than 50 years of ice-out date data. Morphometric data for the twelve lakes are given in Table B.1.

3.2.2 Temperature and Snowfall Data

The 1950-2010 daily temperature and snowfall data for each lake are obtained from the nearest United States Historical Climatology Network (USHCN) stations. Data from USHCN stations are preferred, because of the long period of serially complete data, genuine quality assurance and control checks imposed on data. The procedures undertaken by USHCN for data quality control are described in Williams et al. [173]. Appropriate modeling of lake ice-out dates and meteorological variables necessitates that stations have more than 30 years of complete data. In this study,a year is considered complete if it contained 90% of the winter and spring temperature and snowfall data. Climate data from seven USHCN stations are used in this study.

Mohseni et al. [123] has shown that climate data from meteorological stations, as far as 200 kilometers (km) from site, can be applicable in predicting stream water temperatures. Here, the distance between lake and nearby meteorological station is on average about 20 km, while the maximum distance is about 80 km (see Figure 3.1).

3.2.3 Seasonal Degree-day Indices

The net energy balance at lake surface determines the formation, growth and melt of surface ice cover, and air temperature is directly or indirectly related to the net long wave radiation, sensible heat and latent heat flux. Consequently, seasonal winter temperature indices such as accumulated freezing and melting degree days (AFDD and AMDD) have often been used to approximate the available freeze/thaw energy to form/melt lake ice [e.g., 8, 95, 109]. When calculating seasonal AFDD/AMDD, lake and glacial ice studies,

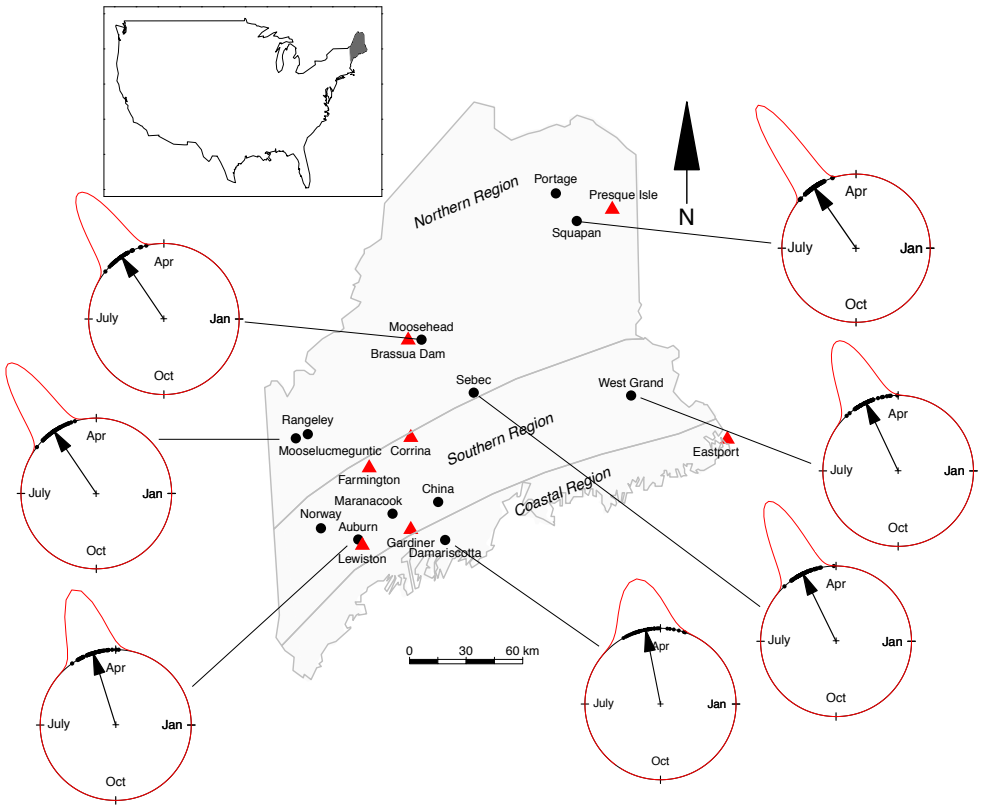

Figure 3.1. Location of selected Maine lakes, and the circular plots of their spring ice-out dates. Location of selected Maine lakes, and the circular plots of their spring ice-out dates. For each circular plot, the arrow denote the mean ice out date, while the red curves denote the fitted von-Mises distribution.

different temperature thresholds are employed for freezing/melting of water/ice, to compensate for different atmospheric conditions or sampling problems. However in this study, the AFDD (AMDD) during the ice cover period is computed, as the daily degree-days below (above) freezing of water (0°C or 32°F) summed over the total number of days when daily average temperature was below (above) freezing.

3.2.4 Delineating Winter and Spring Period in Maine

In lake ice studies, the winter season provides the bulk of freezing energy to grow lake ice, and consequently the winter accumulated freezing degree days (AFDD) have often be used to gage the freezing energy available to form and grow ice. Thus to delineate the winter months during the lake ice cover period in Maine, the smoothened mean profile of AFDD from 1950-2010 over the period between December 1^{st} and April 30^{th} is generated using non-parametric kernel estimators for each station (see Figure 3.2). Across the six stations, the mean (median) date when 90% of the winter and spring AFDD is attained lies prior to March 10^{th}. Thus in this study, winter season represents the period between December and February months, and spring season refers to the period between March and April.

3.3 Methodology

3.3.1 Circular Data: Lake ice-out dates

Circular/directional data is the data that can be represented as locations (points) on the circumference of a unit circle [e.g., 107]. They are encountered in various scientific fields, and are usually expressed as angles from an arbitrarily selected zero reference and sense of rotation. Examples of this type of data include readings of wind direction or animal orientation, relative to a reference direction. In addition to data that are initially measured as angles, circular data also applies to measurements such as time of day/year that show periodicity. In general, circular data have no natural ranking, since the origin and sense of rotation is arbitrary [e.g., 60]. Furthermore, measurements are cyclical just as in a circle, the beginning coincides with the end (i.e., points 0 and 2π coincide). Thus the use of conventional statistical methods in analyzing circular data often results in misleading or absurd results. For further discussions on the nature of circular data, reader is referred to books by Mardia and Jupp [119], Jammalamadaka and Sengupta [86], and Fisher and Lee [61].

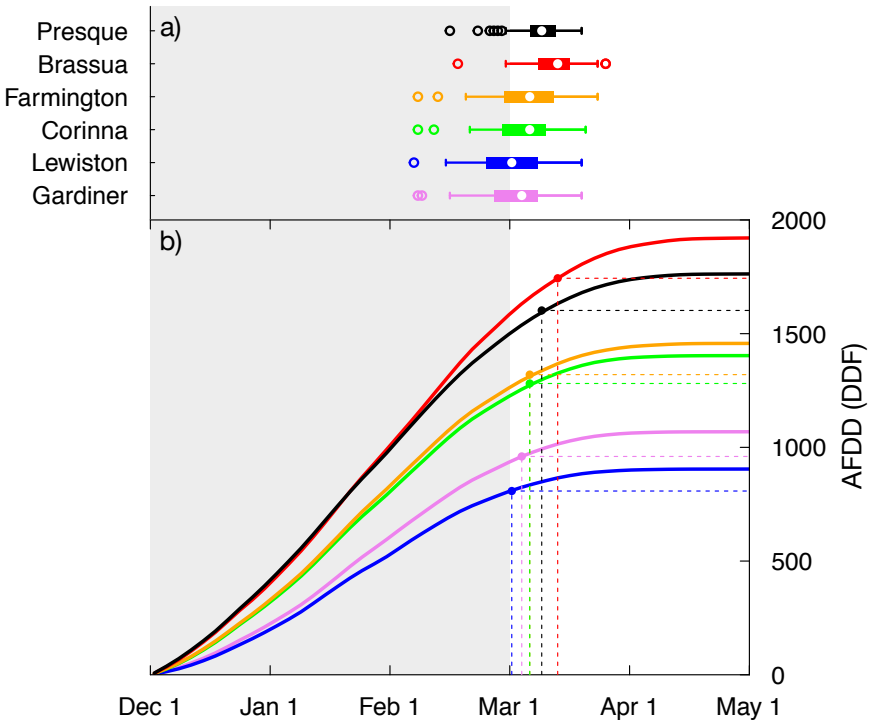

Figure 3.2. 1950-2010 profile of AFDD growth as a function of days between December 1st and April 30th for six USHCN stations in Maine. 1950-2010 profile of AFDD growth as a function of days between December 1st and April 30th for six USHCN stations in Maine. (a) Annual dates from 1950-2010 when 90% of the winter and spring AFDD is attained for six USHCN stations. (b) 1950-2010 mean smoothened profile of AFDD as a function of the days between December 1st and April 30th for six USHCN stations.

3.3.2 Summary statistics for the ice-out dates of studied lakes

As illustrated in earlier sections, circular statistical approaches are more appropriate method for describing calendar data such as lake ice-out dates. Thus, the historical ice-out date of studied lakes are transformed to angular data by computing

$$\theta_i = D_i \frac{2\pi}{D_{year}} \tag{3.1}$$

where D_{year} represents the number of days in a year. The variable D_i is the spring lake ice out date in Julian day, and θ_i is its angular value in radians. Since θ_i also corresponds to the polar coordinates $(\cos\theta_i, \sin\theta_i)$ of a location on a unit circle $(r = 1)$, the historical spring ice-out dates of lakes can graphically be depicted as points on a unit circle.

The 1950-2010 climatology of the spring ice-out dates across studied lakes are characterized by estimating the mean and spread. For a sample of n ice-out dates, the sample mean ($\hat{\bar{\theta}}$) and variance ($\hat{\rho}$) are determined by computing

$$\hat{\bar{\theta}} = \arctan(\frac{S}{C}) \tag{3.2}$$

$$\hat{\rho} = 1 - \sqrt{(S^2 + C^2)} \tag{3.3}$$

where

$$S = \frac{\sum_{i=1}^{n} \sin\theta_i}{n}$$

and

$$C = \frac{\sum_{i=1}^{n} \cos\theta_i}{n}$$

C and S represent the x and y coordinates of the mean lake ice-out date on the unit circle. The measure of dispersion (ρ) for angular data on a unit circle, ranges from $\rho = 0$ (corresponds to all ice-out dates occurring on the same date of the year) to $\rho = 1$ (indicates maximum variability). Alternatively, the circular standard deviation (σ) can be calculated using the equation

$$\hat{\sigma} = \sqrt{-2\ln(1-\rho)} \tag{3.4}$$

Figure 3.1 and Table 3.1 present the summary statistics for the historical ice out dates of studied lakes. For the 1950-2010 period, they show that the mean spring ice-out dates of Maine lakes range from mid-April in coastal and southern interior lakes to early May in northern interior lakes. Moreover, contrasting the circular standard deviation of the ice-out dates for studied lakes indicate that coastal lakes have greater variability in their timing of their spring ice out dates as compared to their inland counterparts.

3.3.3 Linear-Circular (L-C) correlation

Linear-circular correlation ($R_{x\theta}$, Mardia [118]) approach is utilized to measure the linear association between winter/spring climate variables and spring lake ice out dates. Suppose X and θ denote the variables seasonal temperature/snowfall and spring ice out

Lakes	Circular Statistics					
	Mean		Standard Deviation	von Mises Distribution		
	μ_o	Date (Julian Day)		θ (SE)	κ (SE)	Watson's U^2 statistic (p-value)
Damariscotta	1.74	April 11 (101)	11.37	1.74 (0.03)	24.59 (4.41)	0.07 ($p > 0.1$)
China	1.80	April 14 (104)	10.16	1.80 (0.03)	35.32 (6.35)	0.07 ($p > 0.1$)
Maranacook	1.84	April 17 (107)	9.55	1.84 (0.02)	39.64 (7.13)	0.06 ($p > 0.1$)
Auburn	1.86	April 18 (108)	8.73	1.86 (0.02)	44.3 (8.18)	0.04 ($p > 0.1$)
West Grand	2.00	April 26 (116)	8.61	2.00 (0.02)	41.89 (7.54)	0.07 ($p > 0.1$)
Norway	1.92	April 21 (111)	7.57	1.92 (0.02)	65.37 (12.42)	0.08 ($p > 0.1$)
Sebec	2.03	April 28 (118)	7.28	2.03 (0.02)	65.49 (11.89)	0.08 ($p > 0.1$)
Mooselucmeguntic	2.15	May 5 (125)	7.17	2.15 (0.02)	66.34 (12.17)	0.05 ($p > 0.1$)
Rangeley	2.17	May 6 (126)	7.16	2.17 (0.02)	66.17 (11.94)	0.05 ($p > 0.1$)
Moosehead	2.16	May 5 (125)	7.62	2.16 (0.02)	60.36 (10.88)	0.05 ($p > 0.1$)
Squapan	2.11	May 3 (123)	6.05	2.11 (0.01)	88.12 (16.91)	0.04 ($p > 0.1$)
Portage	2.17	May 6 (126)	5.78	2.17 (0.01)	100 (18.68)	0.04 ($p > 0.1$)

SE- Standard Error

Table 3.1. Summary Statistics of ice out dates from 1950-2010 for selected Maine lakes using circular statistical approach Summary Statistics of ice out dates from 1950-2010 for selected Maine lakes using circular statistical approach

date (in radians) respectively, Linear-circular correlation coefficient is defined as the multiple correlations between X and angular components $(\cos\theta, \sin\theta)$, assuming that the circular variable can be described by a random vector $v = (\cos\theta, \sin\theta)^{\mathrm{T}}$ in a plane [118]. For n pairs of X and θ, this can mathematically be written as

$$R_{x\theta} = \sqrt{\frac{r_{xc}^2 + r_{xs}^2 - 2r_{xc}r_{xs}r_{cs}}{1 - r_{cs}^2}} \tag{3.5}$$

where the correlations are: $r_{xc} = cor(X, \cos\theta)$, $r_{xs} = cor(X, \sin\theta)$, and $r_{cs} = cor(\cos\theta, \sin\theta)$. If the winter/spring climate variable and spring lake ice-out dates do not exhibit covariability, then $R_{x\theta}$ will approach zero. In contrast, if climate variable and spring lake ice-out dates are strongly associated with each other, then $R_{x\theta}$ will be close to ± 1. Under the null hypothesis of no correlation between X and θ, the test statistics follows the distribution

$$\frac{(n-3)R_{x\theta}^2}{1 - R_{x\theta}^2} \sim F_{2,n-3} \tag{3.6}$$

given that X is normally distributed [119, page 246]. In this study, correlation coefficients are taken as significant,if the hypothesis that there is no correlation between the two variables is unlikely with a probability of 0.95. For comprehensive expositions on linear-circular correlation coefficient and other forms of linear-circular correlation techniques, the reader is referred to books by [86, 119].

3.3.4 Circular-Circular (C-C) correlation

The circular-circular correlation ($r_{\theta\phi}$) approach is used to assess the rotational association between two time series of lake ice-out dates. For n pairs of θ and ϕ, this can be mathematically expressed as [86, *page* 176]

$$r_{\theta\phi} = \frac{\sum_{i=1}^{n} \sin(\theta_i - \overline{\theta}) \sin(\phi_i - \overline{\phi})}{\sqrt{\sum_{i=1}^{n} \sin^2(\theta_i - \overline{\theta}) \sin^2(\phi_i - \overline{\phi})}} \tag{3.7}$$

where $\overline{\theta}$ and $\overline{\phi}$ are the sample mean directions. If $r_{\theta\phi}$ is close to zero, it suggests that the two time series of lake ice out dates are rotationally independent. On the other hand, when $r_{\theta\phi}$ approaches ± 1, it indicates that there is a strong rotational association between the two time series of lake ice-out dates. Under the null hypothesis of no correlation between ϕ and θ, the test statistics

$$t = \sqrt{f} r_{\theta\phi} \tag{3.8}$$

follows a standard normal distribution. The term f is given by

$$f = N \frac{\sum_{i=1}^{n} \sin^2(\theta_i - \overline{\theta}) \sum_{i=1}^{n} \sin(\phi_i - \overline{\phi})}{\sum_{i=1}^{n} \sin^2(\theta_i - \overline{\theta}) \sin^2(\phi_i - \overline{\phi})} \tag{3.9}$$

Here, circular correlation coefficients are taken as significant, if the hypothesis that there is no correlation between the two time series of ice out dates was unlikely with a probability of 0.95. For further discussions on circular-circular correlation coefficient or other forms of linear-circular correlation techniques, the reader is referred to comprehensive expositions in the published literature [86, 119].

3.3.5 Linear-Circular Regression

Figure 3.3 shows the procedural framework applied here for inferring the efficacy of winter and spring climate parameter(s) on the variability of lake ice-out dates. The framework employs preliminary circular diagnostic methods described in earlier sections, as well as assess outputs from candidate ice-out models of varying complexity, developed using the circular regression approach described below. In the latter approach, model building was done in stages beginning with the null model, which presumes that spring ice-out date variability is dependent exclusively on the spring AFDD and AMDD. Subsequently, spring snowfall, winter AFDD and AMDD, and winter snowfall are sequentially added in the following models and fitted. Model parameter significance and outputs across candidate

models are then compared to assess the relevance of winter and/or spring climate variables in controlling the variability of spring ice-out dates across Maine lakes.

3.3.5.1 von Mises Distribution

The von Mises distribution, first proposed by von Mises in 1918, is the most common and best studied of unimodal circular distributions. The reasons for its popularity is (a) its results are easier to interpret, as its inference techniques are well developed (b) it is flexible with regards to the effect of parameters (c) it has an in-built measure for scale (dispersion) [86]. Thus, it plays a central role in circular statistics, akin to the Normal distribution for linear data analysis. The von Mises probability density function (PDF) for random variable ϕ is given by

$$f(\phi;\mu,\kappa) = \frac{1}{2\pi I_0(\kappa)} e^{\kappa\cos(\phi-\mu)}, \qquad 0 \leq \phi, 0 \leq \mu < 2\pi, \kappa > 0 \tag{3.10}$$

where $I_0(.)$ is the modified Bessel function of zeroth order, μ is the mean direction and κ is the concentration parameter. When $\kappa > 0$, the density is unimodal and symmetrical about the μ and as κ increases, the distribution increasingly becomes tightly clustered. For $\kappa > 2$, the distribution can be well approximated by a Normal distribution with mean μ and variance $1/\kappa$ [61].

The appropriateness of von Mises distribution in representing the probability distribution of ice-out dates for studied lakes are verified using Watson's U^2 test [113]. This test compares the mean squared deviation between the empirical cumulative distribution function (CDF) and true CDF, at all data points, to the deviation against the critical value at alpha level. Results show that the assumption the probability structure for lake ice-out dates has a von Mises distribution can not be rejected at 90% significance level for all lakes (see Table 3.1).

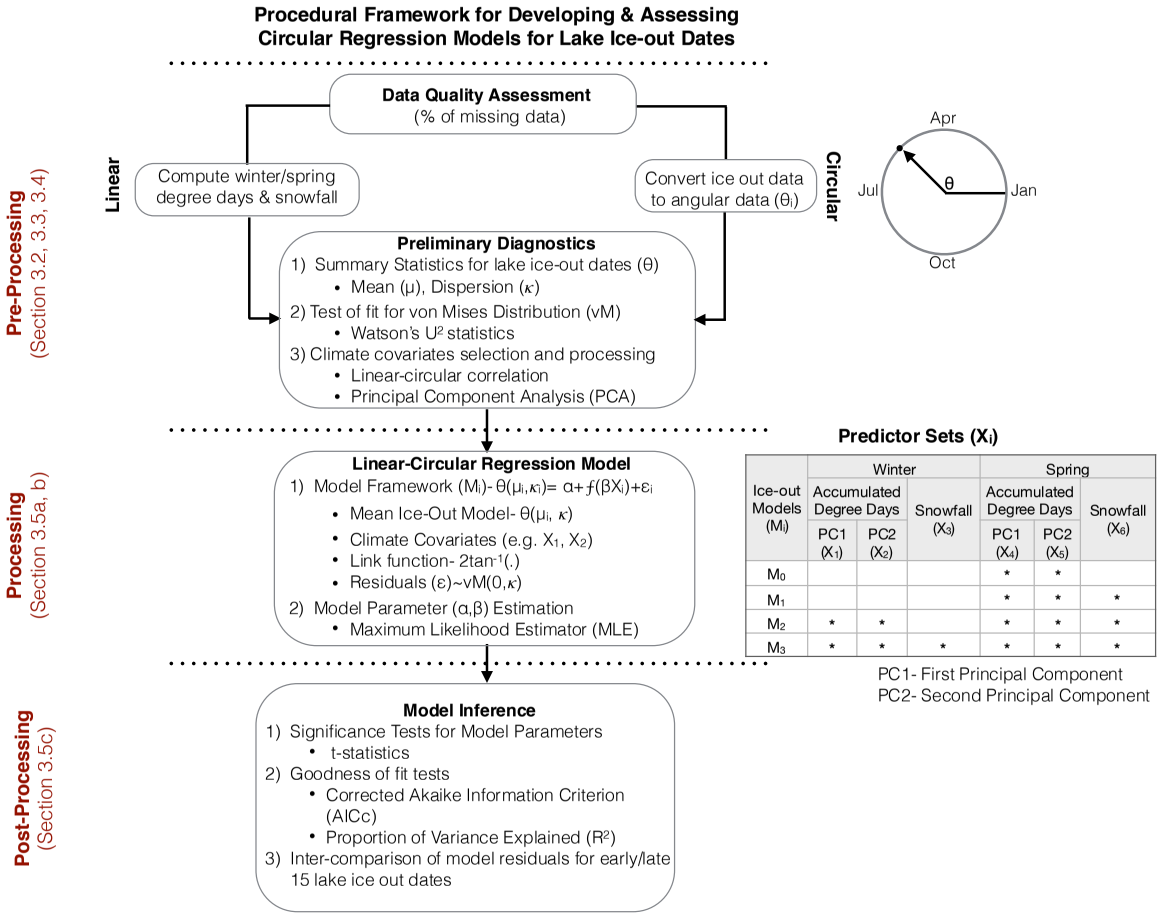

Figure 3.3. Procedural framework for developing and assessing circular regression models for ice-out dates Procedural framework for developing and assessing circular regression models for ice-out dates: three preliminary diagnostic techniques, circular regression model framework and parameter estimation method and three approaches for assessing model outputs and performance.

3.3.5.2 Model Framework and Fitting

In the linear-circular regression models with von Mises distribution, winter and/or spring climate variables are described as linear covariates, and the lake ice out dates is represented as a circular response variable. In general, the response of lake ice-out date of to seasonal climate variables can be modeled by regressing either (a) the mean direction (μ), (b) the dispersion (κ), (c) or both the mean direction (μ) and dispersion of ice out dates to winter/spring climate variables. In the present study, we focus on the first model, and therefore model the mean direction μ of ice-out dates to climate covariates x_i as

$$\mu_i = \mu_0 + g(x_i\beta) + \epsilon_i \tag{3.11}$$

where β corresponds to the vector of regression parameters to be estimated, μ_0 is the circular mean of the dependent variable, $g(.)$ is the link function and ϵ_i is the residual term from the von Mises $vM(0, \kappa)$ distribution. The purpose of the link function $g(.)$ is to convert linear variables to circular ones. Possible choice of link functions are discussed in Fisher and Lee [61] and Jammalamadaka and Sengupta [86], however, in this study we used

$$g(u) = 2\tan^{-1}(.) \tag{3.12}$$

The maximum likelihood estimates (MLE), for the parameters (μ_0, β, and κ) of a homoscedastic von Mises regression model, are the values that maximize the log-likelihood function

$$L(\beta|X) = -N\log I_0(\kappa) + \kappa\sum_{i=1}^{N}\cos(\theta_i - \mu_0 - 2\tan^{-1}(\beta X_i)) \tag{3.13}$$

Often, the determination of the maximum likelihood estimates requires the use of iterative procedures. The circular package [4] in the R statistical computing environment, provided the optimizing algorithm to estimate μ, β, and κ. Furthermore, large sample asymptotic variance is used to estimate standard errors for the parameters, and to test hypotheses [61].

3.3.5.3 Model Diagnostics and Inference

Model inference on the relative importance of winter/spring climate variables on spring ice out dates is based on (a) parameter significance tests, and (b) comparing model fitness. Significance tests for model parameter estimates indicate whether there is a detectable relationship between the response variable and predictive variable(s) under focus, for a given level of certainty. In the present study, the significance of model parameter estimates for winter/spring degree-days and snowfall are determined using t-statistics. Model parameters are considered significant, if the significance level (p) is less than 0.10. On the other hand, if models are successively fitted in order of increasing complexity, comparing the relative fit for successive pairs of models provides an alternative means of assessing the null hypothesis that the omitted (added) term(s) has no significant contribution on the spring ice-out date variability. In this study, Model 0 (M_0), Model 1 (M_1), and Model 2 (M_2) are special cases of M_1, M_2, and M_3 respectively, and thus, comparison of say M_0 and M_1 using goodness of fit tests is a test of the hypothesis that spring snowfall has no influence on the timing of spring lake ice-out dates. The relative fit across models is determined using coefficient of determination (R^2) and bias-corrected Akaike Information Criterion ($AICc$). The coefficient of determination (R^2), which measures the variability explained by the model, was computed for each model by squaring the circular-circular correlation between observed and model simulated ice out dates [114]. In addition, to balance between model complexity and model fitting of data, the corrected Akaike Information criterion ($AICc$) was employed. AICc is a likelihood-based criterion that quantifies the relative amount of information lost, if a given ice out model is used to approximate the underlying process that generates the observed lake ice out dates. Assuming that the ice-out model residuals have a von Mises distribution with concentration parameter $\hat{\kappa}$, the $AICc$ of a given model is given as

$$AICc = 2n \log I_0(\hat{\kappa}) - 2n\hat{\kappa} + \frac{n(n+1)}{n-l-2} \tag{3.14}$$

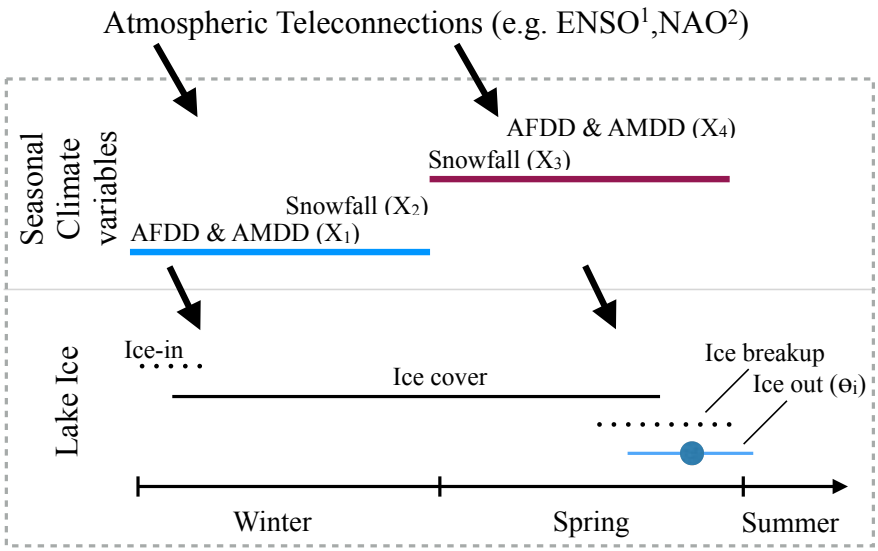

Figure 3.4. Schema depicting the seasonal evolution of lake ice and linked climatic variables. Schema depicting the seasonal evolution of lake ice and linked climatic variables. The climate covariates (X) and ice out date (θ) are shown along the winter-spring seasonal timeline.

where $I_0(.)$ is the modified Bessel function of zeroth order, n is the sample size and l is the number of estimated parameters (degrees of freedom) in the model.

3.4 Results

3.4.1 Seasonal Meteorological Covariates

Six seasonal meteorological variables were considered in the development of our circular regression models for ice out dates (see Figure 3.4). This section provides a rational, both physical and statistical for the inclusion of these variables.

3.4.1.1 Seasonal winter degree-days and lake ice-out

The thickness of winter ice cover over lakes determines the amount of heat energy needed to melt and clear the ice from lake surface. The preceding winter AFDD and AMDD quantities can have strong influence on the timing of lake ice-out dates in spring. In this study, the winter AFDD (AMDD) is computed as the daily degree-days below

(above) freezing (0°C or 32°F) summed over the total number of days during December and February when daily average temperature was below (above) freezing.

Linear-circular (L-C) correlation tests between winter AFDD and AMDD and spring ice-out dates for studied Maine lakes shows that the preceding winter AFDD has a significant positive correlation (ρ = 0.25-0.53, $p < 0.05$) with the spring ice out dates for lakes across all three-climate regions in Maine (see Table B.2-B.7). This indicates that the higher winter AFDDs—i.e., the larger the freeze content to grow ice—the longer for the winter ice to clear in spring, and vice versa. Spatial comparison of the correlation coefficient across studied lakes show that the correlation between spring ice out dates and winter AFDDs is higher in coastal and southern interior regions (ρ = 0.31-0.53) as compared with northern interior regions (ρ = 0.24-0.45). The underlying physical reasoning for the reduced influence of winter AFDD on the variability of spring ice out dates of northern interior regions are (a) formation and growth of ice in northern interior Maine lakes begins in fall, which reduces the role of winter AFDD variability on lake ice thickness (b) lake ice-out dates in the northern interior regions often occur later in spring (May-June), which allows spring climate variables to moderate the effect of winter AFDD on the spring ice out dates.

On the other hand, seasonal winter AMDD shows a significant negative correlation ($|\rho|$ = 0.25-0.55, $p < 0.05$) with spring lake ice out dates primarily in coastal and southern interior regions (see Table B.2-B.7). This implies that the higher winter AMDDs—i.e., the lower the cold content in the ice cover—the earlier than usual spring ice-out dates and vice versa. Spatially, the relative correlation between winter AMDD and spring lake ice out dates decreases towards interior Maine regions. The major factor for the reduced influence of winter AMDD on spring ice-out dates of inland Maine lakes is that over the region, daily temperatures during December and February months seldom, if ever, exceed freezing point (0°C or 32°F).

3.4.1.2 Principal Component Analysis for winter degree-days

There is a significant ($p < 0.1$) negative correlation between winter AFDD and AMDD for most Maine regions (see Table B.2-B.7). Consequently, using both winter degree-day indices as predictor variables in lake ice-out date regression models generates parameter estimates for winter AFDD and AMDD that are less reliable and physically meaningful, due to collinearity effect. Fekedulegn et al. [57] showed that transforming the original variables into a new set of orthogonal uncorrelated variables using principal component analysis (PCA) eliminates this effect. Thus PCA (using the covariance matrix) was performed on the time series of winter AFDD and AMDD at each meteorological station. Across the six meteorological stations, the first principal component (PC1) of winter degree-days represents 97-99.5% of the total variability and therefore may be considered as the dominant pattern of winter degree-day variability (see Table A8). Furthermore given that the magnitude and variance of winter AFDD is much larger than that of winter AMDD for all stations, the loading of winter AFDD in each PC1 pattern is positive and over 0.99, whereas the loading of winter AMDD is negative and less than 0.03 (see Table B.8). The result implies that PC1 patterns primarily reflect the winter AFDD conditions over lakes, and as such positive (negative) PC1 indices represent above (below) average winter AFDDs. Spatially, there is a strong positive correlation ($\rho > 0.91$) between PC1 patterns across stations, which shows strong regional coherence in the temporal pattern of winter AFDD variability in Maine. On the other hand, the second principal component (PC2) reproduces only 0.5-3.0% of the total variability in winter degree-days across the six meteorological stations (see Table B.8). Furthermore for each PC2 pattern, the loading of winter AFDD is negative and less than 0.03, while the loading of winter AMDD is positive and over 0.99 (see Table B.8). This suggests that PC2 scores predominantly represent the winter AMDD conditions over lakes and positive (negative) PC2 phases imply above (below) normal winter AMDD. There is a strong positive correlation ($\rho > 0.83$) between

the PC2 patterns across stations, which implies strong spatial synchroneity in the pattern of winter AMDD variability in Maine.

3.4.1.3 Winter snowfall

Winter snowfall can affect the thickness and type of winter ice cover and in turn the timing of spring ice out dates by (a) reducing rate of ice growth in winter by adding insulation, (b) increasing the winter cold (freeze) content of lake ice, and (c) promoting the development of snow ice, thereby affecting the composition of the winter ice cover over lakes [1]. In this study, time series of winter snowfall for the study period was determined by summing the daily total snowfall recorded at each station from the beginning of December to the end of February for each year.

L-C correlation results show that winter snowfall has a significant positive correlation ($\rho = 0.28$-0.43, $p < 0.05$) with spring lake ice-out dates chiefly in coastal and southern interior regions (see Table B.2-B.7). This means that the higher winter snowfall, the longer the duration of winter ice. Furthermore, the coefficient and significance of this linear association decreases towards the interior regions. Again this is mainly because lake ice out date in deep interior regions occurs relatively later in spring (May-June), which allows spring climate conditions to have more influence on the timing of ice breakup date. It should be noted that winter snowfall has little or no correlation with the two principal components of winter degree-days (see Table B.2-B.7). This indicates that the relationship between winter snowfall and spring ice-out dates is independent of the prevailing winter temperature conditions.

3.4.1.4 Seasonal spring degree-days and lake ice-out

Spring is the period when the bulk of the ice melting process occurs. Williams [174] showed that spring temperature largely determine the melt rate of winter ice cover. Hodgkins [76] based on their correlation results suggested that the prevailing average spring (March-April) temperatures explain 50-70% of the variability in the timing of spring ice-out

dates in New England lakes. In this study, the spring AFDD (AMDD) is computed as the daily degree-days below (above) freezing (0°C or 32°F) summed over the total number of days during March and April when daily average temperature was below (above) freezing.

L-C correlation results show that seasonal spring AFDD has significant negative correlation ($|\rho|$ = 0.35-0.65, $p < 0.05$) with lake ice out dates across all climate regions in Maine (see Supplementary Table B.2-B.7). This implies that the higher the spring AFDDs—i.e., the higher the cold content in lake ice—the later the spring ice out dates and vice versa. Moreover, the role of spring AFDD on spring lake ice-out dates of Maine lakes across the three climate divisions appears to be uniform, as the correlation coefficients do not show any systematic spatial patterns.

On the other hand, seasonal spring AMDD has significant positive correlation (ρ = 0.73-0.84, $p < 0.05$) with lake ice out date in all climate regions (see Supplementary Table B.2-B.7). This suggests that the higher the spring AMDD—i.e., the higher the melt energy at lake surface—the earlier the timing of ice out dates. Spatially, the strength of correlation between spring AMDD and lake ice-out dates increases towards the interior regions. This is mainly because lake ice out date in deep interior regions occurs relatively later in spring (May-June), which allows spring temperatures to have more influence on the timing of ice breakup date.

3.4.1.5 Principal Component Analysis for spring degree-days

There is a significant ($p < 0.1$) negative correlation between spring AFDD and spring AMDD in all stations (see Table B.2-B.7). To reduce collinearity effect, the spring AFDD and AMDD variables at each lake are orthogonalized into two principal components and these principal components are included as predictor variables in the ice out date regression models.

Across the six stations, the first principal component (PC1) of spring degree-days represents 77%-87% of the total variability in spring AFDD and AMDD, and therefore may

be considered as the leading pattern of local spring degree-day variability (see Table B.9). Furthermore, in each of the PC1 patterns, the loadings for spring AFDD (AMDD) is of negative (positive) sign, which implies that when PC1 is in the positive phase, spring AFDD (AMDD) is lower (higher) than normal (see Table B.9). However, the loading of spring AFDD and AMDD in PC1 pattern varies across different climate regions in Maine with spring AMDD having relatively higher loading than spring AFDD in stations found in southern interior and coastal regions and vice versa for stations found in northern interior regions. This is because even in spring months, daily temperatures get below 32°F for a significant period of time in northern interior Maine regions. Spatially, there is a strong positive correlation ($\rho > 0.87$) between spring PC1 patterns across stations, which suggests that there is spatial coherence between spring PC1 patterns across Maine regions.

The second principal component (PC2) for spring degree-days reproduces 17-23% of the total variability across the six stations (see Table B.9). Furthermore, in each of the PC2 patterns, the loading for spring AFDD and AMDD are both positive implying positive (negative) PC2 phases are related to higher (lower) than normal spring AFDD and AMDDs over lakes (see Table B.9b). AFDD and AMDD values gage the range of the seasonal temperature distribution. As such seasonal conditions where both the AFDD and AMDD are either high or low occur are indicative of a change in the variability of seasonal temperatures. Consequently, PC2 indices show a strong positive correlation ($\rho > 0.68$) with the intra-seasonal standard deviation of spring temperatures at all stations where positive (low) spring PC2 phases are related to high (low) intra-seasonal spring temperature variability in all stations (see Figure B.1). Similar to spring PC1 of spring degree days, the loading of spring AFDD and AMDD in PC1 pattern varies across different climate regions in Maine although here spring AMDD having relatively lower loading than spring AFDD in stations found in southern interior and coastal regions and vice versa for stations found in northern interior regions. There is a strong spatial correlation ($\rho > 0.68$)

between the PC2 patterns of spring degree-days across the six stations, which implies of a regional synchroneity in the PC2 variability patterns across Maine regions.

Another important result of note is that the two principal components for spring degree-days show little or no correlation with that of the winter degree-days in all regions (see Table B.2-B.7). This indicates that there is no problematic climatic persistence between winter and spring degree day variability.

3.4.1.6 Spring snowfall

Spring snow accumulation can reduce the melt rate of ice cover by (a) increasing the albedo (thereby lowering radiation absorption) of the ice cover (b) increasing the cold content of the ice cover. In this study, the annual spring snowfall from 1950–2010 was determined by summing the daily total snowfall from the beginning of March to the end of April for each year.

L-C correlation results reveal that spring snowfall has significant positive correlation ($0.28 \leq \rho \leq 0.55$, $p < 0.05$) with the timing of spring ice-out dates of studied lakes across all climate regions in Maine (see Table B.2-B.7). This suggests that the more spring snowfall, the longer the duration of ice over lakes. Furthermore, the correlation coefficients across different regions indicate that the correlation coefficient for spring snowfall is lower in northwestern Maine regions ($0.28 \leq \rho \leq 0.31$) as compared with other regions ($0.41 \leq \rho \leq 0.55$).

3.5 Results

3.5.1 Model Output and Inference

The four circular models for each lake describe the variability of spring ice out dates, as a function of the prevailing winter and/or spring degree-days, and snowfall. Key model results are summarized in Table B.10-B.13 for studied lakes. The $2\tan^{-1}(.)$ used as link function between covariates and ice-out dates (see equation 3.10 and 3.11), has both

transformative and multiplicative effect on changes in the covariates. For instance, a coefficient of -0.001 associated with spring PC1 implies that an increase by 1 unit in spring PC1 is associated with a multiplicative decrease of $2\tan^{-1}$(-0.001) radians or 6.6 days in spring ice-out dates.

Model 0 (M_0), a model that explains spring ice-out date variability as a function of the two principal components for spring degree-days, captures over 50% of the total variability in ice-out dates of studied lakes (see Supplementary Table 5a and Figure 3.5). The prevailing spring temperatures have a strong control over the timing of spring ice-out dates in Maine lakes. However, the efficacy of spring degree-days in modulating the timing of spring ice-out dates is not the uniform across Maine lakes, as the performance of M_0 in studied lakes shows variations at regional, and to a lesser extent local scales (see Table B.10). For instance, the explained variance (R^2) by M_0 for studied coastal and southern interior Maine lakes is less than 60%, while for most northern interior lakes, M_0 represents at least 65% of the total variance. Also in Northern interior Maine regions, M_0 captures over 70% of the total variance in high altitude lakes such as Lake Rangeley and Lake Mooselucmeguntic, while this is much lower in relative low altitude lakes such as Lake Portage and Lake Squapan. At local scale, the M_0 for relatively large, deep lakes such as Lake Damariscotta and Moosehead shows higher unexplained variance as compared with that of relatively small, shallow lakes in the same climate division.

In M_0, the coefficient for PC1 of spring degree-days is negative, and statistically significant ($p < 0.1$) across all lakes, while the parameter for PC2 is positive and statistically significant for studied lakes, with the exception of Lake Damariscotta and Lake Norway (see Table B.10). Thus, positive PC1 phases (lower than average spring AFDD and higher spring AMDD) are related to earlier than normal spring ice-out dates in lakes, whereas positive PC2 indices (higher than normal spring AFDD and AMDD) are linked to later than normal spring ice-out dates. Furthermore, PC2 indices represent the intra-seasonal variance in spring degree-days, and these results suggest that the timing of

spring ice-out dates in Maine lakes is not only sensitive to the magnitude of spring degree-days, but also on the intra-seasonal variability of spring temperatures. Comparing the parameter estimates for PC1 and PC2 patterns across the M_0 of studied lakes reveals that in general the coefficient for PC1 (PC2) is of higher (lower) magnitude in southern interior and coastal Maine lakes relative to northern interior lakes (see Table B.10).

Model 1 (M_1), which includes spring snowfall in addition to the two principal components of spring degree days to explain spring ice-out date variability, captures 56-75% of the total variability in the ice-out date of studied lakes (See Table B.11 and Figure 3.5). Assessing the R^2 and AICc of M_1 relative to that of M_0 across studied lakes, indicates that the dependence of spring ice-out dates in Maine lakes to spring snowfall shows regional variations based on climatic divisions, and to a lesser extent altitude. For instance, Figure 3.5 shows that the change in R^2 and $AICc$ from M_0 to M_1 is higher in northern interior Maine lakes such as Lake Portage and Lake Sebec, as compared to that of southern and coastal lakes such as Lake Damariscotta and West Grand. Also for northern interior regions, the change in model fitness from M_0 to M_1 is higher in lower altitude lakes such as Lake Moosehead and Lake Portage, relative to that of high altitude lakes such as Lake Rangeley and Lake Mooselucmeguntic.

In M_1, the coefficient for spring snowfall is positive and statistically significant for all studied lakes, except for Lake Mooselucmeguntic (see Table B.11). This implies that the higher the spring snowfall, the later the spring ice out dates. Comparison of parameter estimates for spring snowfall across the M_1 models studied lakes shows that the parameter coefficients for spring snowfall are of lower magnitude in northwestern lakes (Rangeley and Mooselucmeguntic) as compared with lakes in other Maine regions. This result is in consensus with the correlation analysis that the northwestern high altitude lakes have lesser sensitivity to spring snowfall than lakes in other regions.

Model 2 (M_2), with two principal components of winter degree-days in addition to the predictor variables in M_1, explains 67-77% of the variability in ice-out dates in studied

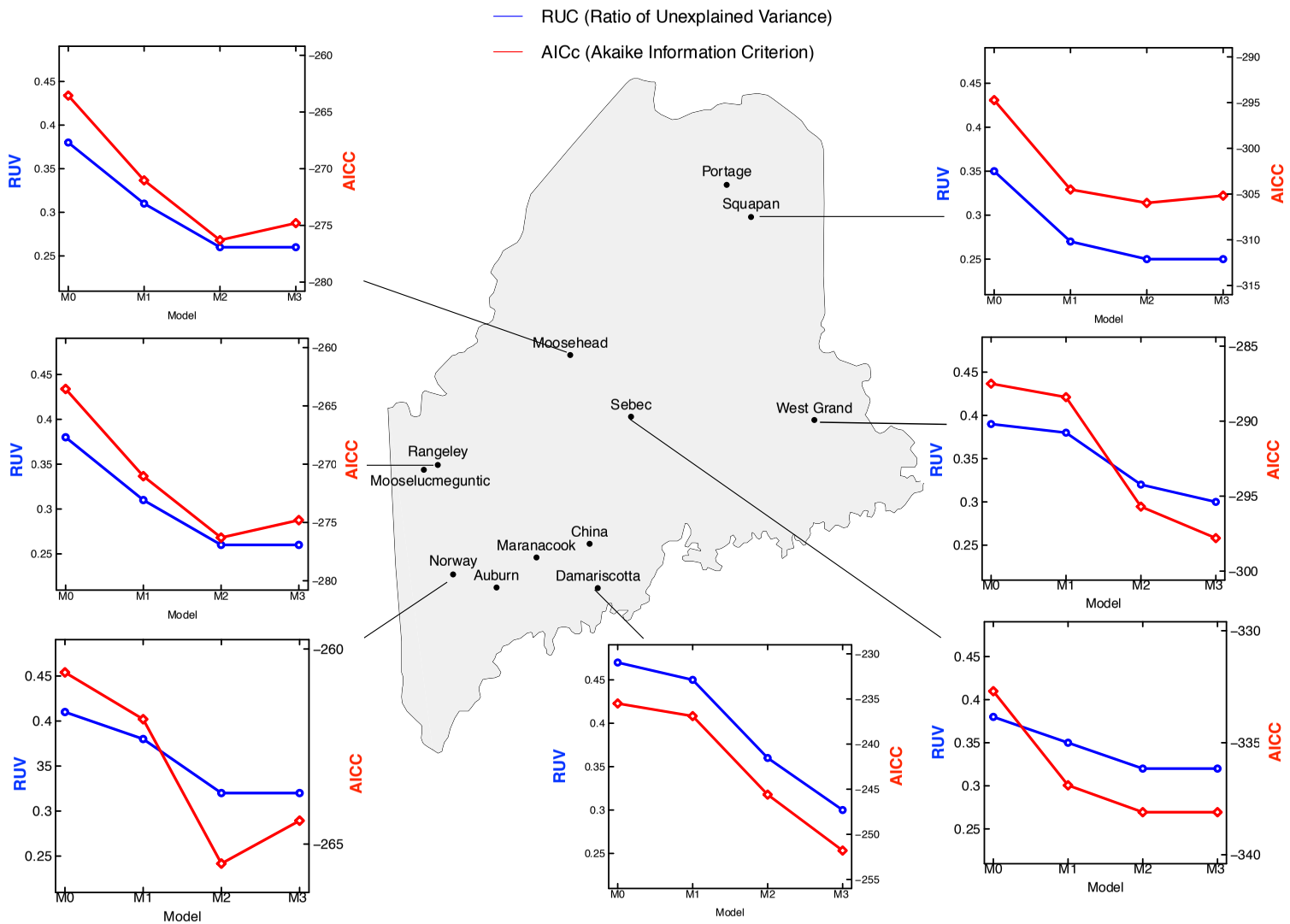

Figure 3.5. Relative performance of candidate ice-out models for select Maine lakes. Relative performance of candidate ice-out models for select Maine lakes. M_0, M_1, M_2 and M_3 denote the four candidate ice-out models developed for each lake.

lakes (see Table B.12 and Figure 3.5). Comparison of model fitness metrics between M_2 and M_1 indicates that the efficacy of winter degree-days in modulating the timing of spring ice-out dates in Maine lakes, is higher in large, deep coastal and southern Maine lakes as compared with small, shallow and northern interior lakes. For instance, the relative change in R^2 and AICc from M_1 to M_2 is higher for southern and coastal lakes such as Lake Damariscotta and Lake West Grand, as compared to that of northern interior lakes such as Lake Portage and Lake Rangeley. Also in northern interior regions, the improvement in model fitness from M_1 to M_2 is higher in large, deep lakes such as Moosehead, as compared with small, shallow lakes such as Squapan or Portage.

In M_2, the coefficient for PC1 of winter degree-days is positive and statistically significant ($p < 0.1$) across all studied lakes, while the parameter for PC2 is negative and statistically significant only for coastal lakes (see Table B.12). In general, this implies that positive PC1 phases (higher than normal winter AFDDs) are associated with later than average spring lake ice-out dates, while positive PC2 phases (higher than normal winter AMDDs) are related to earlier than average spring lake ice out dates. Comparison of parameter estimates for PC1 and PC2 of winter degree-days across the M_2 models of studied lakes reveals that the coefficient for PC2 is of higher magnitude in coastal lakes, relative to lakes in other Maine regions. This indicates that coastal and southern interior lakes have higher sensitivity to PC2 indices (i.e., winter AMDD), as compared with those in northern interior lakes. This conclusion is consistent with the finding in the correlation analysis from earlier section.

Model 3 (M_3), which includes winter snowfall in addition to M_2 predictor variables to model spring ice-out dates, captures 68-77% of the total variability of ice-out dates in studied lakes (see Table B.13 and Figure 3.5). Assessing the change in model fitness metrics between M_2 and M_3 for studied lakes indicates that the modulating influence of winter snowfall on spring ice-out dates is higher for coastal Maine lakes. For instance, figure 3.5 shows that the relative change in R^2 and $AICc$ from M_3 to M_2 is higher for

southern and coastal lakes such as Lake Damariscotta and Lake Auburn as compared to that of northern interior lakes such as Lake Portage and Lake Rangeley.

In M_3, the parameter for winter snowfall is positive and statistically significant for coastal Maine lakes such as Maranacook, Damariscotta and China and Auburn (see Table B.13). This implies that the higher the winter snowfall over lakes, the later the spring ice-out dates. Comparison of parameter estimates for winter snowfall in M_3 models across studied lakes shows that the coefficient for winter snowfall in coastal lakes in higher in coastal lakes as compared to lakes in other Maine regions. This implies that the sensitivity of spring ice out dates to winter snowfall is higher in coastal lakes as compared with interior Maine regions.

3.5.1.1 Model Residual Diagnostics

By determining the incremental information added by incorporating winter and/or spring climate variables, the previous section assessed the overall efficacy of winter and spring climate variables, in modulating the timing of spring ice-out dates in Maine lakes. However, this provides limited insight into the role of these variables in producing unusually early/late spring ice-out dates in Maine lakes. Thus in this section, the import of winter and/or spring variables in producing large departures in the timing of spring ice out events in Maine lakes, was assessed by contrasting the residuals for the earliest and latest 10 ice-out dates, across candidate models (i.e., M_0-M_3). The premise in such assessments is that majority improvement in the model estimation of the earliest/latest ice out events, after the inclusion of a seasonal climate variable/s, implies the importance of the seasonal climate variable on the occurrence of these events. Figure 3.6 and figure B.2 depict inter-model residuals for various ice out dates, and the gray area in these plots represents regions where the estimate made by complex model has lesser error than that of the reduced model(s). In general, the pattern of M_0 residuals for the earliest and latest 10 ice-out dates reveals that the ice-out date models, conditioned on the two principal

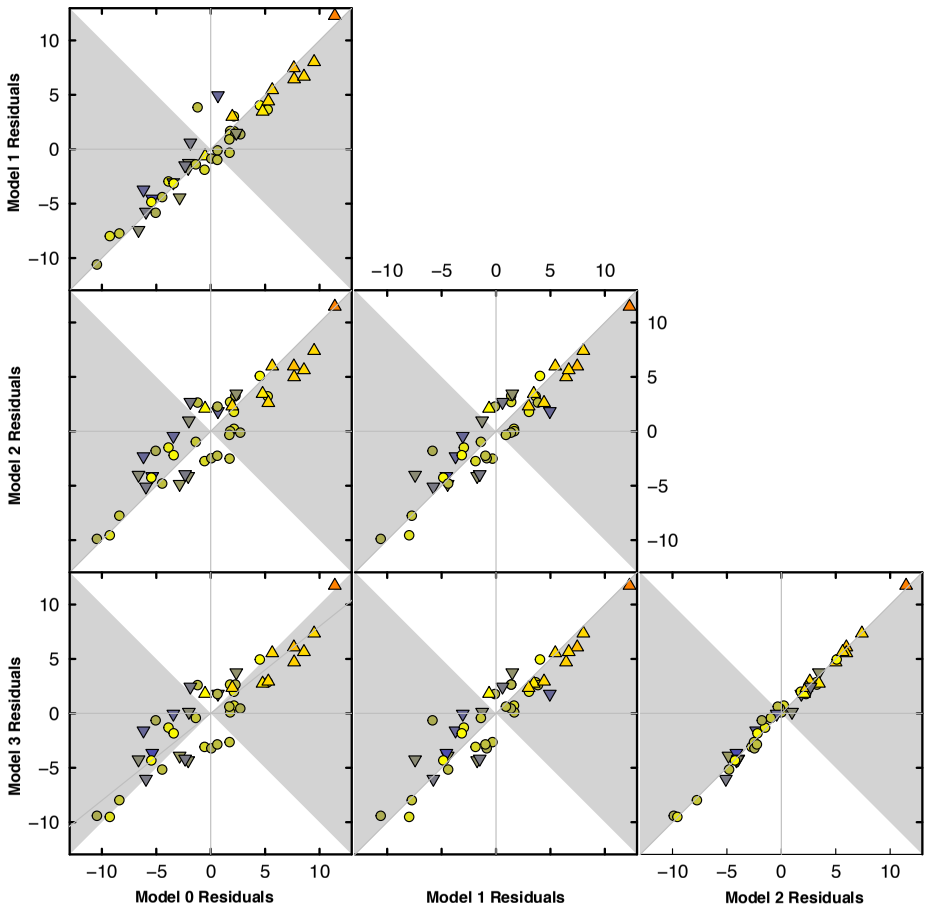

Figure 3.6. Inter-model residual comparison for ice-out dates at Lake Auburn. Inter-model residual comparison for ice-out dates at Lake Auburn. Model residuals are calculated as the difference between observed and model predicted ice-out dates.

components of spring degree-days, performs poorly when estimating ice-out dates before mid-April for coastal and southern interior lakes and after May 10^{th} for northern interior lakes. Counting the number of earliest/latest 10 lake ice-out events (upper and lower triangles) falling in the gray area of M_1-M_0 residual plot for studied lakes, reveals that for lake Sebec, Portage, Mooselucmeguntic, Squapan, Norway and Auburn, more than half of the residuals for both the earliest and latest 10 spring ice out dates are in the gray area of M_1-M_0 sub-space. For instance, it can be observed in Figure S5k that the M_1-M_0 residuals for 7 (8) of the 10 earliest (latest) ice-out dates at Lake Portage are in the gray area within M_1-M_0 space. This indicates that the efficacy of spring snowfall in engendering early/late ice-out dates in Maine lakes, is the highest in northern interior regions. Similarly, tallying the number of earliest/latest 10 ice-out events within the gray area of M_2-M_1 residual plots, for studied lakes, shows that for Lake Sebec, Moosehead, West Grand, Norway, Damariscotta, China and Auburn, more than 60% of both the earliest and latest ice out events are within the gray area of M_2-M_1 subspace. For instance, Figure 3.6 shows that the M_2-M_1 residuals for 9 of the 10 earliest (latest) ice-out dates at Lake Norway are in the gray area within M_2-M_1 space. This indicates that the efficacy of daily winter temperatures, in producing early/late ice out dates in Maine lakes, is the highest in coastal and southern interior lakes, and large northern interior lakes. Finally, counting the number of earliest/latest 10 ice-out events within the gray area of M_3-M_2 residual plots, for studied lakes, shows that for Lake Maranacook, China, Damariscotta and Sebec, 70% or more of the earliest 10 ice out events are within the gray area of M_3-M_2 sub-space. For example, the M_3-M_2 residuals for 8 of the 10 earliest ice out dates at Lake Damariscotta are in the gray area, within M_3-M_2 space (see figure B.2). This implies that the antecedent winter snowfall quantity, over coastal regions, has a significant modulating effect on the occurrence/non-occurrence of the earliest ice-out dates of lakes.

High coherence in model residuals for pairs of lakes, indicates how well the ice-out model performs in estimating the spring ice-out dates for these lakes. For instance, if the

M_0 residuals for two lakes are highly correlated, in years where M_0 overestimates (underestimates) the ice-out date for one of these lakes, M_0 also tends to overestimate (underestimate) the ice-out date for the other lake as well. Therefore, the pairwise (circular) correlation between model residuals of selected lakes was determined, across the four ice-out models developed. Results show that across the four ice-out models, the strength of correlation between model residuals for two lakes varies depending on the similarity/difference in their respective climate division, and to a lesser extent proximity from each other (see Figure 3.7). For instance, correlation between model residuals for Lake China and Lake Maranacook across M_0 to M_3 ranges from 0.82-0.87, while these correlations between Lake China and Lake Presque ranges from 0.20-0.27. This is because ice-cover seasons for lakes in the same climate regions have similar sensitivity to winter and spring meteorological variables, given that the prevailing climate conditions over lakes, in the same climate divisions are analogous. On the other hand, the correlation between model residuals for two lakes in general decreases with increasing complexity of ice-out date models (see Figure 3.7).

In addition to these four seasonal climate variables studied in this paper, the year-to-year variability of spring lake ice-out dates can be modulated by other climatic/non-climatic variables such as wind, cloudiness or lake depth. As such, it is not surprising to observe years where all four models for studied lakes under-perform by relatively large margins ($>$ 5 days). For example, the four ice-out date models developed for all twelve lakes overestimate the timing of spring ice out dates for the year 2002. To understand the underlying climatic factors, the prevailing meteorological conditions during the winter and spring of 2002 were scrutinized. It was noted that during the winter and spring of 2002, there was unusually high amount of precipitation in the form of rain. Given that rainfall promotes the melting of lake ice by reducing albedo and freeze content of surface lake ice the four candidate ice out models are vulnerable to overestimation, when rainfall has a significant influence in modulating the timing of ice out date of lakes.

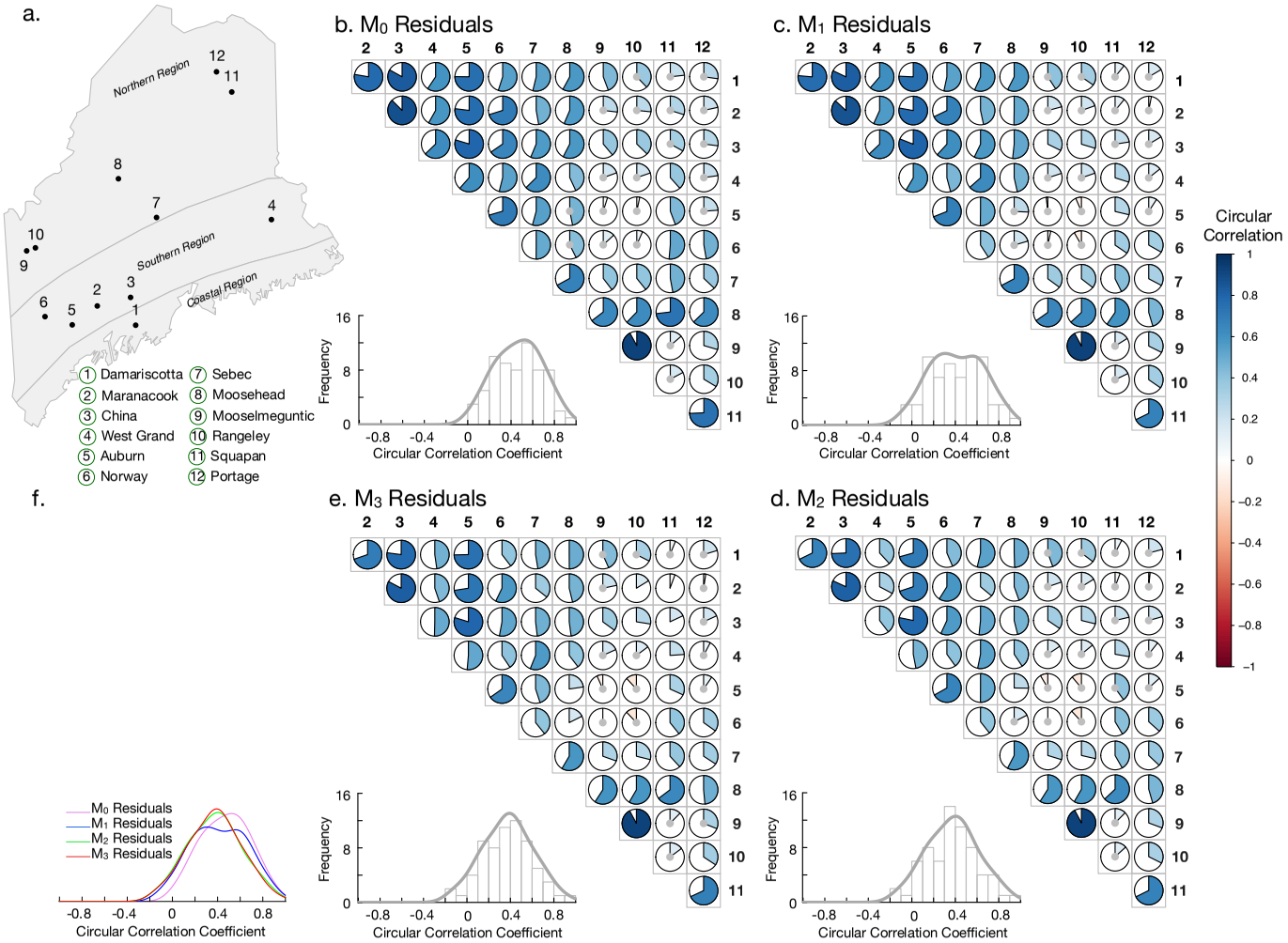

Figure 3.7. Circular correlations in model residuals for selected Maine lakes across M_0 to M_3.

3.5.1.2 Comparison of Circular Regression Models to Standard Linear Regression Models

As noted in the introduction, linear models/methods are not appropriate for analyzing ice-out date(a circular random variable) due to model specification. However Table 3.1 shows that the kappa for ice out dates of studied lakes is greater than 26, and according to Fisher and Lee [61], von Mises distribution with $\kappa > 2$ can be well approximated using normal distribution. Thus using the traditional linear regression (TLR) method, ice-out models of varying complexity were developed for studied lakes (see Table B.14-B.17), and for two of these lakes, the resulting model coefficients and model errors were compared to that of circular models (see Table 3.2 and 3.3). Results reveal that TLR models with only spring degree-days explain over 50% of the total variance in ice out date for Lake Damariscotta and Lake Squapan. They also show that the inclusion of winter meteorological variables in TLR models for ice out dates reduces model estimate error for both lakes. The consistency in TLR and circular regression model is generally expected for cases with small variance. However in lakes where the timing of ice out dates shows large variance ($\kappa > 2$), the difference in model results and performance between TLR models and circular regression models is expected to be prominent. As such, the linear-circular framework developed in this study offers a parsimonious statistical approach to model the effect of linear meteorological variables on lake ice phenology, particularly in a changing climate wherein warmer temperatures are poised to induce increased variability in ice-out dates.

3.6 Discussion and Conclusions

This study presented a circular regression framework for modeling ice-out dates, conditioned on a suite of winter and spring climate variables (i.e. degree days and snowfall), to determine the import of winter and spring climate conditions on the timing of ice-out dates in Maine lakes. Winter/spring AFDD and AMDD variables were

Model Type	Model	Regression Coefficients						Model Fitness		
		Winter			Spring			R^2	MAE (days)	RMSE (days)
		PC1 (10^{-4})	PC2 (10^{-4})	Snowfall (10^{-4})	PC1 (10^{-4})	PC2 (10^{-4})	Snowfall (10^{-3})			
Circular Regression	M_0				-6.9 ***	2.2		0.53	5.4	6.9
Linear Regression	M_0				-13.3 ***	4.2		0.53	5.4	6.9
Circular Regression	M_1				-6.2 ***	2.5	1.5 ***	0.55	5.2	6.7
Linear Regression	M_1				-12.3 ***	4.9	2.9	0.54	5.2	6.7
Circular Regression	M_2	1.0 ***	-9.7 ***		-5.1 ***	1.4	1.6 **	0.64	4.4	5.8
Linear Regression	M_2	2.1 **	-19.3 ***		-10.2 ***	2.8	3.3 *	0.64	4.4	5.8
Circular Regression	M_3	1.1 ***	-7.5 ***	1.5 ***	-4.6 ***	7.9	1.7 ***	0.70	4.4	5.6
Linear Regression	M_3	2.3 **	-14.8 **	3.0 **	-9.2 ***	1.7	3.3 **	0.69	4.4	5.6

MAE- Mean Absolute Error
RMSE- Root Mean Squared Error
* significant at $p < 0.10$ significance level, ** significant at $p < 0.05$ significance level, *** significant at $p < 0.01$ significance level.

Table 3.2. Comparing key statistics of circular and linear regression models for Lake Damariscotta ($\kappa = 25$). Comparing key statistics of circular and linear regression models for Lake Damariscotta ($\kappa = 25$).

Model Type	Model	Regression Coefficients						Model Fitness		
		Winter			Spring			R^2	MAE (days)	RMSE (days)
		PC1 (10^{-4})	PC2 (10^{-4})	Snowfall (10^{-4})	PC1 (10^{-4})	PC2 (10^{-4})	Snowfall (10^{-3})			
Circular Regression	M_0				-3.7 ***	3.4 ***		0.65	2.9	3.6
Linear Regression	M_0				-7.4 ***	6.9 ***		0.65	2.9	3.6
Circular Regression	M_1				-3.3 ***	3.9 ***	1.5 ***	0.73	2.3	3.2
Linear Regression	M_1				-6.5 ***	7.7 ***	3.0 ***	0.73	2.3	3.2
Circular Regression	M_2	0.5 **	-0.1		-3.2 ***	3.9 ***	1.3 ***	0.74	2.2	3.0
Linear Regression	M_2	0.9 *	-1.8		-6.4 ***	7.8 ***	2.5 **	0.74	2.2	3.0
Circular Regression	M_3	0.4 **	-1.0	0.3 *	-3.2 ***	4.0 ***	1.3 ***	0.75	2.2	3.0
Linear Regression	M_3	0.9 *	-1.8	0.5	-6.3 ***	8.0 ***	2.6 ***	0.75	2.2	3.0

MAE- Mean Absolute Error
RMSE- Root Mean Squared Error
* significant at $p < 0.10$ significance level, ** significant at $p < 0.05$ significance level, *** significant at $p < 0.01$ significance level.

Table 3.3. Comparing key statistics of circular and linear regression models for Lake Squapan ($\kappa = 88$). Comparing key statistics of circular and linear regression models for Lake Squapan ($\kappa = 88$).

orthogonalized into two principal components to reduce collinearity effect in ice-out date models, and these principal components were included as predictor variables in the circular regression models for ice-out dates. Parameter significance tests and inter-model fitness tests (R^2 and AICc) across candidate ice-out date models revealed that for Maine lakes:

(a) The joint effect of seasonal spring degree-days (AFDD and AMDD) and the intra-seasonal variance in spring temperatures explains more than half of the total variability in spring lake ice-out dates in Maine. Spatially, the modulating influence of spring temperature conditions on lake ice-out dates increases towards northern interior Maine regions.

(b) The relative role of spring snowfall in engendering early/late ice out dates in Maine lakes is the strongest in northern interior region.

(c) The efficacy of the antecedent winter degree-days (AFDD and AMDD) in modulating variability of lake ice-out dates is significant, across all climate regions in Maine. However, the strongest effects are observed in large, coastal lakes.

(d) The relative influence of winter snowfall on lake ice-out date variability is significant, ($p < 0.1$) only in coastal Maine regions.

A diagnostic analysis of years in which all four ice-out models developed most underperformed by more than 5 days, indicated unexplained variance likely stemming from other hydro-climatic processes and lake dynamics. In closing, we put forward the following remarks, and discuss emerging research directions.

1. This study focused on the efficacy of different climatic and non-climatic variables in modulating the inter-annual variability of spring ice out dates of temperate lakes. Results indicate that in addition to spring degree-days, the state of the winter degree-days and winter and spring snowfall contributes significantly to the overall year-to-year variability of ice-out dates including the occurrence of early/late spring ice out dates of Maine lakes. Future works on this topic is still needed including determining the role of other climatic/non-climatic variables on the inter-annual lake

ice-out date variability, the use of different link functions in circular ice-out date models and performance of non-parametric circular regression approach for modeling ice-out dates.

2. Large-scale teleconnections patterns produce North American climate anomalies at a regional-scale. For Maine, it has been shown that the Tropical/ Northern Hemisphere (TNH) and North Atlantic Oscillation (NAO) patterns influence inter-annual winter temperature variability [22]. Given that the Climate Prediction Centers in North America and Europe routinely provides skillful forecast of these climate patterns, winter meteorological conditions derived from such information can be incorporated in circular ice-out date models conditioned on winter climate variables, to provide season-ahead outlooks on the spring time lake ice season in Maine.

3. Data involving time-of-year variables are prevalent in hydrology and hydrometeorology and to date, conventional approaches that characterize date-of-year variables as linear continuous data are often employed to analyze such data. A number of studies have shown that such approaches produce erroneous results [86]. This study presents a systematic framework and highlights (a) the applicability of circular statistical approaches in modeling circular/periodic data such as lake ice phenology (b) the availability of circular counterparts for traditional linear data analysis techniques for environmental systems analysis and modeling.

CHAPTER 4
WINTERTIME WEATHER-CLIMATE VARIABILITY AND ITS LINKS TO EARLY SPRING ICE-OUT IN MAINE LAKES

4.1 Introduction

In the spring of 2010, a number of lakes in Maine, a state situated in the northern New England region of the United States with over 5500 lakes, recorded their earliest ice-out dates (a term used interchangeably with ice breakup/ice-off/ice thawing date in this study) in over a century (Bayly 2010). This resulted in the hasty enactment of a new open-water fishing season Bill and cancellation of major ice-fishing derbies throughout the state. Furthermore, the early end to annual ice-season raised fears that the water quality in Maine lakes will plummet stemming from algal blooms and shortening of the annual clear water phase, as studies have shown that the lengthening of the ice-free period in temperate and Arctic lakes directly and indirectly promotes algal growth [e.g., 2, 134]. With increases in urbanization and associated nutrient loading in lakes being projected for various regions in Maine, the effect of late winter/early spring lake ice off events on the ecological and social systems linked to Maine lakes promises to be more severe. These issues thus necessitate detailed climatological analysis to understand the potential drivers of early spring ice-out events in Maine lakes.

The nature of attendant variability and change in the timing of lake ice out merits an assessment of the individual and joint effects of climatic variability and change. In Maine, only modest monotonic trends towards early ice-out are observed, however, as noted by Hodgkins et al. [77], recent decades show appreciable change gleaned from decadal scale smoothing analysis towards early ice-out. It was also noted that this changes in ice-out dates correspond to 1.4°C to 1.5°C change (over a 150 years record) in the mean spring (March-April) temperatures over the New England region. On inter-annual time scales, the

present study shows that there is a significant year-to-year swing in the timing of ice out dates in Maine lakes. Furthermore, the chain of events that modulate lake phenology involve interlinked large-scale atmospheric circulations, weather patterns, and warm and cold spells that accelerate or impede the lake ice-in buildup and melt. For example, the winter of 1983, a strong El Niño year in the tropical Pacific, was characterized by a persistent above normal surface pressure anomalies over eastern Northern American regions. This resulted in the mean winter air temperature over lake Sebec to rise by 2.5°C, which in turn resulted the lake to experience spring ice out 9 days earlier than the median ice out date for the period 1950-2010. This exemplifies that the role of inter-annual large-scale atmospheric circulation patterns (teleconnections) on the variability of lake ice out date in Maine is strong and thus must be properly characterized in the context of the observed changes in lake ice phenology for the region. Furthermore, due to their gradual evolution, persistence and oscillatory behavior, large-scale teleconnection patterns have the potential to (a) offer seasonal and longer time scale predictability of ice breakup dates, premised on appropriately derived variables (b) alter the temporal pattern of variability of lake ice out dates through long term changes in the frequency and amplitude of coupled oceanic atmospheric processes, such as El Niño-Southern Oscillation (ENSO), which has undergone significant changes in recent decades.

Few regional ice phenology studies have examined the linkages between ice breakup/freeze up dates, local climate and large-scale atmospheric/oceanic oscillations in North American and European lakes [e.g., 5, 32, 142]. For instance, a recent study by Sánchez-López et al. [142] found that North Atlantic Oscillation (NAO) pattern affects the timing of ice breakup in Spanish alpine lakes through its influence on one or more climate variables during winter and early spring. In most of these studies, correlation or other linear analysis method is employed to determine the strength of association between atmospheric/oceanic oscillations, local climate variables and ice phenology. However, given that (a) the influence of teleconnection patterns on local climatic variables is asymmetric

[e.g., 79, 138] (b) the relationship between local climatic variables (e.g. temperature, snowfall, precipitation) and lake ice processes is non-linear [e.g., 8, 108, 109], a fuller exposition of the interrelationships between weather-climate and lake variables as they induce variability and change in lake ice phenology is still less understood. While large scale teleconnection patterns have been shown to have linear relationship with ice-out dates, perhaps a more systematic characterization warrants identification of thresholds in climate variables (e.g. accumulated degree-days) whose exceedance or non-exceedance may lead to large shifts in the ice-out dates or what is often termed as NCIC (no complete ice cover) on lakes.

The timing of lake ice breakup date is strongly modulated by temporally (and in some cases spatially) integrated thermal fluxes at the surface of ice-cover, which in turn is determined by prevailing meteorological conditions and limnological factors during the ice cover season. As such the role of seasonal thermal forcing on the lake ice-system is non-linear and involves thermal thresholds. A number of studies have established that local air temperature is related to a various thermal fluxes over lake ice and therefore can reasonably explain the variation in ice off dates [e.g., 77, 111, 155] For the New England lakes, Hodgkins et al. [77] also showed the existence of a significant ($p<0.05$) correlation between the historical spring ice out dates and spring (March-April) temperatures. However given that (a) the timing of ice-out events in New England lakes is shifting towards early spring dates, and (b) the natural and/or anthropogenic forced climate warming is projected to continue for the Northeast region (IPCC 2007) which sets the winter period to provide the bulk of the thermal energy to form and thicken the ice cover over lakes, it is imperative that the relationship between spring time ice-out dates and antecedent winter temperatures including thresholds be characterized so as to anticipate the timing of early spring ice breakup dates.

The primary focus of this paper is thus to characterize the role of antecedent winter teleconnections, with origins in the tropical oceans, in driving early spring ice breakup

events in Maine lakes, where ice-out dates have been studied from the standpoint of long-term trends, yet empirical diagnosis of linkages between lake ice-out dates, antecedent winter temperatures and teleconnection patterns has not been pursued. Thus the three objectives of this study are:

1. Analysis of the leading pattern of anomaly in the ice-out dates of Maine lakes.

2. Characterization of the link between spring ice out dates and antecedent winter temperatures (and derived degree-day variables) including the identification of thresholds within seasonal winter temperatures whose exceedance/non-exceedance engenders anomalous ice breakup events.

3. Quantification of the influence of select large-scale atmospheric circulation patterns, that operate at inter-annual time scale, on the winter degree-days quantities and lake ice breakup dates in Maine.

4.2 Study Site and Background

4.2.1 Study Site

Maine has an astonishing range in climate with the climate gradient found in only three degrees of latitude in Maine occurs over 20 degrees of latitude in Europe [85]. Based on monthly average temperatures and precipitation data from 1895-2007, NOAA National Climate Data Center broadly classifies Maine into three climatological regions: Northern, Southern interior and Coastal. The mountainous, Northern division of Maine experiences some of the lowest temperatures and highest snowfalls in the eastern United States during winter and early spring while the waters of the Gulf of Maine moderate the continental winter climate typical of its interior regions keeping it mild along the coastal regions [85, 106]. Annual mean temperature in the Northern region is 4.4°C while in the Southern regions and Coastal regions are 6.7 °C and 7.8°C respectively.

4.2.2 Lake Ice-cover Dynamics

Lake ice cover formation, growth and melt rates are outcomes of an energy balance at the surface of lake [8, 108], which can be written as

$$\phi_N = \phi_{SW}(1-\alpha)(1-\beta) + (\phi_{Li} - \phi_{Lo}) - \phi_E - \phi S + \phi p \tag{4.1}$$

Where ϕ_N = Net energy at surface, ϕ_{SW} =Incident short wave radiation, α =Surface albedo, β =Fraction that penetrates surface, ϕ_{Li}=Incoming long wave radiation, ϕ_{Lo} =Outgoing long wave radiation, ϕ_E =Latent heat flux, ϕ_S = Sensible heat flux and ϕp =heat from precipitation. However, explicitly calculating using equation 4.1 requires detailed information on various environmental and lake parameters such as surface albedo, long and short wave radiation, snow/ice density, wind speed which are often not available at weather stations near lakes. Analytical studies on ice often employ degree-day methods for a first order approximation of the bulk growth and melt rate of ice over a period based on the physical basis that air temperature strongly relates to sensible heat flux, net long wave radiation and to a certain extent latent heat flux over lake/ice cover surface [8, 108]. The most basic of the degree-day formulation used is given as:

$$AFDD = \sum_{i=1}^{i=n} (T_o - T_i)\Delta t, T_o > T_i \tag{4.2}$$

$$AMDD = \sum_{i=1}^{i=n} (T_i - T_o)\Delta t, T_i, > T_o \tag{4.3}$$

Where $AFDD$ = Accumulated freezing degree-days, $AMDD$= Accumulated melting degree-days, T_i = Air temperature and T_o=Base temperature. The time interval Δt is usually chosen as one day. Although the base temperature T_o can vary depending on physical, meteorological and atmospheric conditions over lakes, it is often taken as 0°C (32°F). The basic assumption in equation (4.2) and (4.3) is that AFDD represents a negative net radiation at surface meaning the lake is losing heat energy to the atmosphere while AMDD signifies a positive net radiation at surface indicating the lake is gaining heat

energy from atmosphere. For further details on the different analytic models that couple lake ice growth and melt with accumulated degree-days and/or their underlying thermodynamic principles, reader is referred to a book by Leppäranta [109] and articles by Ashton [11] and Leppäranta [108].

4.2.3 Teleconnection Patterns

Teleconnection patterns usually refer to quasi-periodic and persistent perturbance in the atmospheric pressure and circulation pattern that span over large geographical areas due to any remote forcing such as particular sea surface temperature or atmospheric pressure patterns [43, 124]. Monthly or seasonal teleconnection indices describe the large-scale changes in atmospheric wave and/or jet stream patterns that influence temperature, precipitation and storm-tracks at continental scales. Using rotated principal component analysis method, a number of atmospheric and oceanic oscillation patterns have been identified [16, 49].

There may be several atmospheric/oceanic teleconnections originating in the Atlantic and Pacific that influence Maine winter climate. However given that (a) the main focus of this study is on extra-tropical winter teleconnection patterns that operate at inter-annual time scale (b) the seasonality, evolution and persistence in many of these oceanic/atmospheric teleconnections are still less understood, we selected only two major mid-latitudinal winter teleconnection patterns for further analyses, which are discussed below. For interested reader, additional analyses on the atmospheric/oceanic patterns that may influence winter temperature variability in Maine are presented in Appendix C.2.

The Tropical/Northern Hemisphere (TNH) is a prominent wintertime (November-February) mode of oceanic-atmospheric circulation pattern with primary center of action over the Pacific northwestern coast of the United States and a separate center of action of opposite sign over the Hudson Bay. A weaker yet broad center of action, having same sign to that of the Pacific center extends across Mexico and Cuba [16]. According to

NOAA climate prediction center, fluctuation in TNH indices represent large-scale departures both in the amplitude and location of the climatological mean Hudson Bay trough and also position and eastward extension of the Pacific jet stream. For the New England region of the United States, monthly or seasonal TNH indices reflect the atmospheric circulation pattern upwind of the region. For instance during pronounced negative phases of TNH, the trough normally located over Hudson Bay moves further north and is unusually weak resulting in the northward shift of the polar jet stream. This flow pattern prevents the normal buildup of cold air over central and eastern Canada, and transport of frigid polar air into New England. This in combination with enhanced flow of marine air from the Atlantic result in the occurrence of relatively warm winters to the New England (see Figure C.2).

TNH variability is sensitive to strong ENSO forcing although it is largely driven by the inherent atmospheric dynamics within the extra-tropics. Circulation patterns during pronounced negative phase of TNH have been closely correlated with that of strong El Niño episodes [17, 163]. El Niño is predictable on a seasonal-to-inter-annual and longer time scales [81, 137].

The North Atlantic Oscillation (NAO) is the synchronous fluctuation of the pressure gradient between the Icelandic low and the Azores high on time scales from daily to multi-decadal ([83]). Its monthly or seasonal indices reflect change in the intensity and location of the North Atlantic jet stream, which affects heat and moisture transport to the surrounding continent and waters ([83]).

NAO is strongly related to the leading structure of variability of wintertime sea level pressure (SLP) over the Northern hemisphere, the Arctic Oscillation (AO) [160]. The maps between the two modes of variability are almost indiscernible (except for the Pacific region) and correlation between their monthly indices exceeds 0.7 [48]. Wallace [166] argues that the NAO and AO are a single phenomenon viewed through two paradigms. Marshall et al. [120] characterizes NAO as the North Atlantic regional manifestation of AO. In this study,

we restrict our focus to NAO variability and its impacts on temperature in Maine. While TNH patterns describe the change in the atmospheric circulation upwind of the New England region, NAO reflect the circulation on the downstream side. During pronounced positive NAO phases, the polar jet front is further north yet zonally oriented bringing in modified Pacific air into New England, causing a cool to warm winter without major coastal storm development [34]. In contrast during strong negative NAO phases, high-pressure system tends to form over Greenland, producing a blocking pattern over the North Atlantic, anomalous cooling of sea surface temperatures (SSTs) and deepening of the East coast trough [34, 72]. This produces meridional flow pattern across the eastern United States and New England causing the influx of colder air and greater number of coastal storms into the region: a prime mix for heavy and frequent snow-storms. The actual number of storms and snowfall totals however will depend on exactly where the limb of the jet streams is relative to New England [34]. The primary mechanism for NAO variability is thought to be the internal dynamics within the north Atlantic atmosphere [120]. Such inherent atmospheric variability displays little temporal coherence on longer time scale, and therefore month-to-month or year-to-year sign and amplitude of NAO has been highly unpredictable. However, recent studies have demonstrated the link between winter AO pattern and preceding summer Arctic sea ice and fall land snow cover which provides potential long-range (weeks in advance) predictability of winter AO/NAO [45, 71]. Furthermore, a few studies have shown that there is an association between sea surface temperatures in the tropical Pacific/North Atlantic and winter NAO and this promises to enhance the predictability of NAO in the Atlantic basin in the future [80, 104].

4.3 Data Provenance and Method

4.3.1 Historical observations of lake ice out dates in Maine

Lake ice-out date refers to the time when ice-cover completely clears from a lake [77]. For the study period (1950-2010), serially complete ice out data for the selected eight

Maine lakes were obtained from a USGS publication [76] and from website publication by the Department of Conservation for the state of Maine Google. Geo-morphological detail of the selected eight lakes is provided in Table 4.1.

4.3.2 Local winter temperature and derived metrics

The daily mean temperature data from January to April for different regions in Maine were obtained from local United States Historical Climatology Network (USHCN) stations. Data from USHCN stations was preferred as it imposes genuine quality assurances and quality control checks [93, 136]

It is necessary that the station data used have nearly complete daily temperature data for the study period in order to study the link between seasonal winter degree-days and lake ice-out dates/teleconnection patterns. Thus in this paper, a year is considered missing if it does not contain temperature data for at least 75% of the winter days (January-February). Furthermore, a station is used only when a station has daily temperature data for at least 55 years out of possible 61. Therefore out of the available twelve USHCN stations in Maine, only six are used. At each of these stations, the accumulated freezing (melting) degree days during winter were calculated as the daily degree days below (above) 0°C summed over the total number of days during winter the daily average temperature was below (above) freezing.

4.3.3 Gridded winter climate and sea surface temperature anomalies

Long term (1950-2010) gridded monthly 500mb geopotential heights, sea and land surface temperatures and wind speed data for January and February were retrieved from National centers for environmental prediction (NCEP) reanalysis dataset [91]. These monthly metrics were later averaged and their climatologial (1950-2010) mean removed to create gridded winter climate and sea surface temperature anomalies dataset.

Lake	Latitude(°N)	Longitude (°E)	Surface area ($10^6 m^2$)	Mean Depth (m)	Elevation (m)
Damariscotta	44.14	−69.49	18.96	9.14	17
China	44.43	−69.55	15.94	8.53	60
Maranacook	44.34	−69.95	7.46	9.14	64
Auburn	44.15	−70.25	9.15	10.97	90
West Grand	45.24	−67.84	58.54	11.28	91
Norway	44.23	−70.58	3.73	5.48	128
Sebec	4.26	−69.23	25.74	12.80	98
Mooselucmeguntic	44.91	−70.89	66.2	18.28	447
Rangeley	44.95	−70.70	25.5	18.29	463
Moosehead	45.66	−69.69	305.42	16.76	313
Squapan	46.57	−68.32	20.72	6.40	183
Portage	46.78	−68.50	8.54	3.05	220

Table 4.1. Geomorphic data for selected Maine lakes.

4.3.4 Historical winter TNH and NAO indices

The January and February monthly indices for TNH and NAO patterns during the study period (1950-2010) were obtained from NOAA National Weather Service Climate Prediction Center (NWS CPC). These monthly indices were later averaged to compute the mean winter indices of the selected circulation patterns.

4.3.5 Kernel density estimations

Kernel density estimations is a well known non-parametric method for estimating (in any number of dimensions) the probability density function of a random variable based on a random sample [144, 149]. It entails the construction of a window of certain width h and fitting of a symmetric probability density function $k(.)$ (e.g. Gaussian, triangular, Epanechnikov) to the observation in each window [150]. The estimated density for any value is simply the sum of estimates from the density function of each window. For n number of available data point with d-dimensions of vector x, the multi-dimensional probability density function $\rho(x, h, n)$, is estimated by centering preferred kernel function k and scale h at each data point X_i

The attractive feature of this technique is that the probability density function used is local and hence not globally affected by outliers. Also since it makes weak prior assumption of the underlying probability density function, it is data driven, robust and portable across data sets although not efficient in extrapolating beyond extreme values. For more details on the topic of univariate and multivariate kernel density estimation, refer to Silverman [149] and Scott [144].

In the current study, Gaussian kernel is used to develop probability density estimates for (a) characterizing the threshold degree-days above/below which are associated with the earliest and latest 15 ice out dates for the eight studied lakes (b) assessing the change in the empirical probability density of winter density of degree-days during different phases of TNH and NAO. Furthermore, Silverman reference bandwidth method, which is the most

popular and practical technique of estimating the global bandwidth h for Gaussian kernels [148], was used for estimating the optimal bandwidth h_{opt}

$$h_{opt} = \frac{0.9\sigma}{n^5} \tag{4.4}$$

where $\sigma = min(s, R/1.34)$ where $s^2 = \frac{1}{n-1}\sum_{i=1}^{i=n}(x_i - \bar{x})^2$ and R is the inter-quartile range of the data.

4.3.6 Bootstrap Method

The bootstrap method is a non-parametric technique introduced by [53] that is used extensively in carrying out test of hypothesis or estimation of the sampling distribution of some statistics by either constructing confidence interval or attaching standard error to an estimate. This method is particularly useful when analyzing data for which the distribution is unknown or when random sampling from a population is not possible due to small sample size. The sampling distribution is determined empirically by randomly re-sampling with replacement from the original sample, with the same original sample size. The desired statistic and its distribution can be determined from each bootstrapped sample and the distribution of each statistics. For more details on the bootstrap method, the reader is referred to [53].

In this study, 10000 bootstrap replication of size n are generated from the historical data of studied lakes to generate an empirical probability distribution when sub-sample size is less than 30. The (1-α) x 100% confidence intervals for bootstrap estimates are obtained using the percentile method. That is, the two end points of the n_b=10000 bootstrap distribution are taken at the ($\alpha/2$) 100^{th} and (1- $\alpha/2$) 100^{th} percentiles.

4.3.7 Principal Component Analysis

As a method for reducing the dimensionality of a dataset containing of a large number of inter-related variables, principal components analysis (PCA) has found wide spread use

in the fields of hydrology and atmospheric sciences [172]. The reduction in dimensionality is attained by projecting the original variables onto the eigenvectors of the spatial cross-correlation (covariance) matrix of the variables. This results in a new set of orthogonal variables (patterns) called principal components (PCs) that are (a) linear combination of the original variables (b) uncorrelated with each other (c) able to retain maximum possible fraction of the variance in the original data using fewer patterns. The PCA solution also yields eigenvalues, which describe the variance explained by each PC and eigenvectors (loadings), which basically express the association between the PC and the original variables. For more details on the topics of principal component analysis, reader is referred to a book by Jolliffe [89] and Wilks [172]. In this study, principal component analysis was applied on the (a) ice out date of eight lakes (b) the winter degree-days (AFDD and AMDD) of six USHCN stations to determine the leading variability patterns that represents the historical variation in ice out date and winter degree-days in Maine. Three results are obtained from PCA solution: the principal components, which are time series of ice out dates/winter degree-days; the amount of variance explained by the PCs and the spatial pattern or loadings associated with the PCs.

4.4 Results

4.4.1 Statistics of Early/Late Ice-out Events in Maine

Figure 4.1b depicts the earliest ten ice-out years for each of the eight Maine lakes from 1950-2010. While these lakes are found in different climate divisions (see Figure 4.1a), approximately 70% of the earliest ice-out years were common to three or more of these lakes. This temporal synchrony in the earliest ice-out years indicates that there is strong coherence among Maine lakes in their pattern of early ice-out dates. Furthermore, approximately 75% of the earliest ice-out years occurred after the 1970s suggesting that recently there is an increased tendency in these lakes to experience early ice-breakup dates. To succinctly express the role of inter-annual winter climate variability in the context of

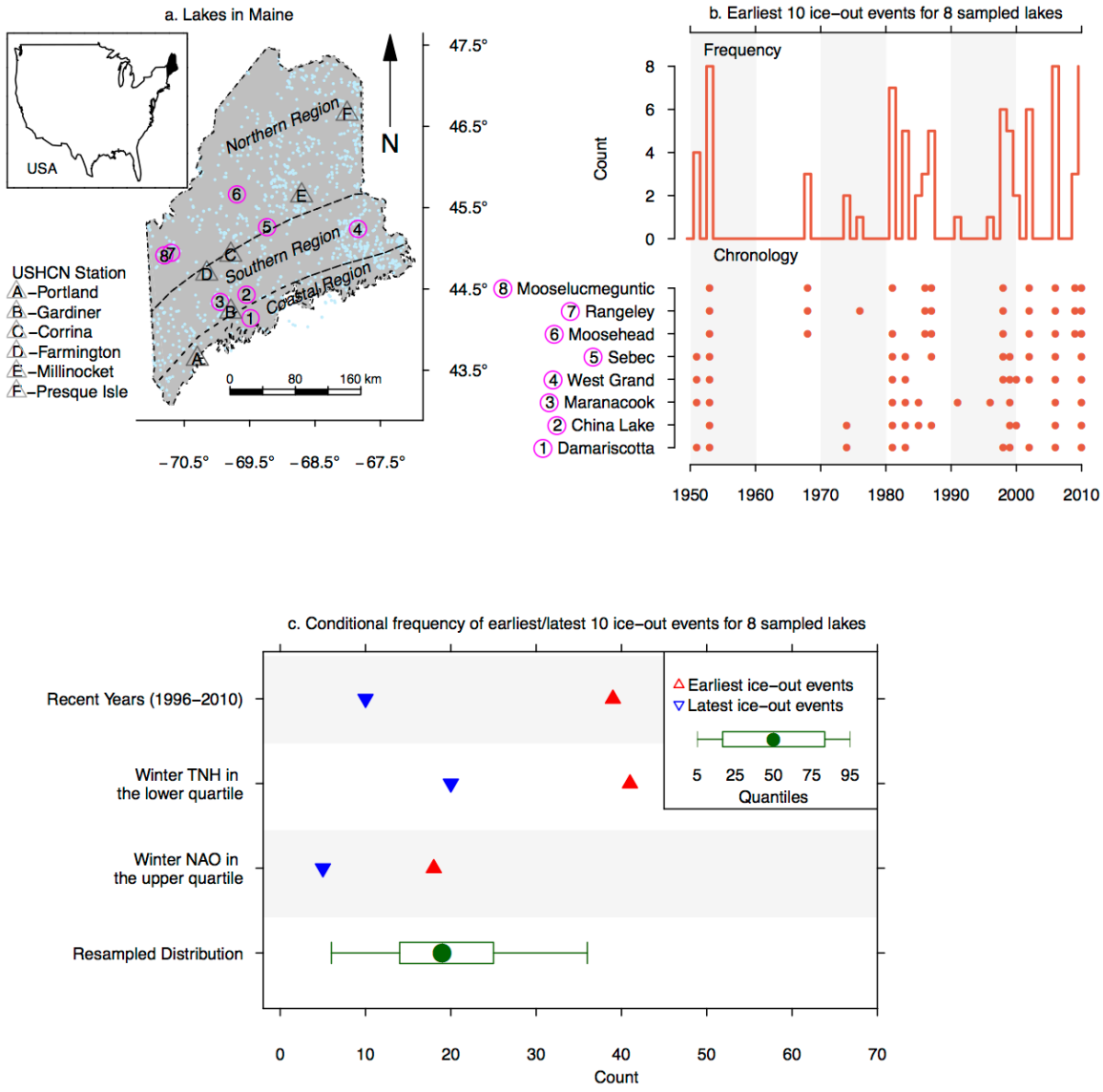

Figure 4.1. Temporal pattern for the earliest/latest 10 ice out years for selected Maine lakes from 1950-2010 and their conditional distribution to inter-annual winter climate patterns.

extreme ice-out date patterns in these lakes, the unconditional probability distributions of the earliest and latest ten ice breakup events for each of the eight lakes during randomly chosen 15 years was compared with that of the frequency for (a) the last 15 years of the most recent period (1996-2010) (b) the 15 years when the average winter TNH index was in its lower quartile (TNH < -0.47) (c) the 15 years when the average winter NAO index was in its upper quartile (NAO$>$ 0.2). Out of possible 80, 39 of the earliest ten ice breakup

events for the eight Maine lakes occurred during the last fifteen years of the study period (1950-2010) representing at 97^{th} quantile of the unconditional distribution (see Figure 4.1c). Furthermore, only 10 out of the possible 80 latest ice-out events occurred during these years, which is at the 10^{th} quantile. This is a reflection of the observed pattern in the timing of the mean ice-out date towards earlier dates for New England lakes, which has been described in detail by Hodgkins et al. [77]. However, 41 out of the possible 80 earliest ice-out events also occurred during the fifteen years when the average winter TNH index was at its lower quartile for the study period (see Figure 4.1c). What makes this result interesting is that only three out of the fifteen years, when winter TNH in its pronounced negative phase, were post 1996. This in turn suggests that there is relatively modest influence of the recent pattern or trend in the earliest ice breakup events on the results for TNH events. Yet the mechanisms by which seasonal winter weather/climate variability preconditions lake ice cover towards early ice breakup dates in Maine is poorly characterized and understood. Figure 4.1c also shows that 20 out of the possible 80 ten latest ice-out events also occurred during the fifteen years when TNH was at its lowest quartile, representing at 55^{th} quantile. On the other hand, 5 out of the possible 80 latest ice-out events (5^{th} quantile) and 19 out of the 80 earliest ice-out events (50^{th} quantile) occurred during winters when the average NAO was at his highest quantile (see Figure 4.1c). These observational analyses indicates that (a) inter-annual variability is a significant determinant of extreme ice out dates (b) winter teleconnection patterns such as TNH and NAO influence the timing and frequency of extreme ice breakup dates in Maine lakes. For the sake of completeness, the major spatial and temporal pattern of variability of ice out dates in Maine lakes was investigated by applying PCA on the ice-out date of eight Maine lakes with serially complete data for the period 1950-2010. The first principal component (PC1) alone reproduces more than 80% of the total variance and therefore may be considered as the leading pattern of lake ice-out date variability in these lakes (see Figure 4.2a). The homogeneity of signs in lake loading (correlation coefficients between the

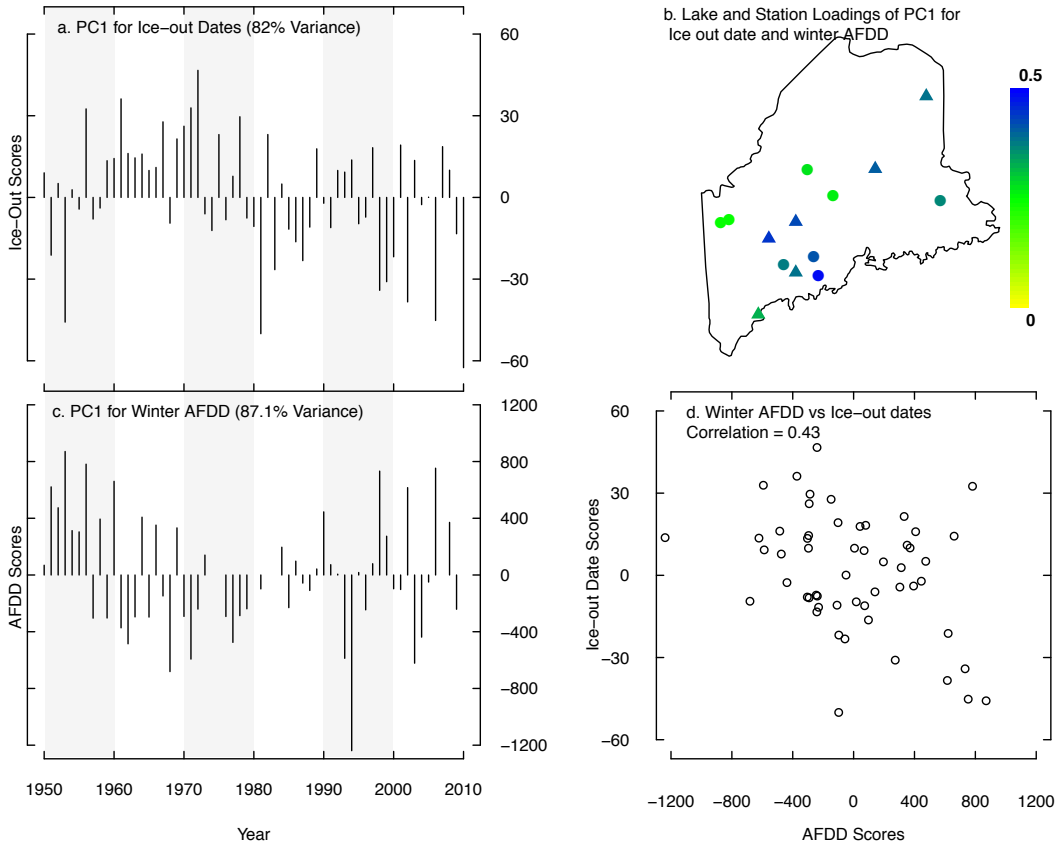

Figure 4.2. PC for winter AFDD. The PC1 of lake ice out date corresponds to the major temporal pattern of ice out date for eight lakes while the PC1 of winter AFDD represents the major temporal pattern for winter AFDD in the five USHCN stations.

lake ice out dates and the PC) of PC1 reflects synchronous variation in all eight lakes although lakes near the coast display slightly higher loadings as compared with lakes found in the inlands (see Figure 4.2b).

The temporal pattern of PC1 shows a sequence of relatively strong positive scores (corresponding to later than average ice-breakup dates in lakes) in the 1960s and 70s that were later overtaken by a series of relatively strong negative scores (signifying earlier than average ice breakup dates) since the early 1980s. Although no secular trend for PC1 time series was found, the sequence of PC1 scores is a reflection of the recent pattern of lake ice out date in Maine towards earlier dates (see Figure 4.2a). Furthermore, the PC1 time series also shows high year-to-year fluctuation in ice out dates. This suggests that

inter-annual variation in ice-out date has an important role on the timing of ice-off dates in these lakes. It should be noted that the these observations applies to other Maine lakes as well as the PC1 times series for the eight lakes had a significant correlation ($|r|$=0.98, $p<$ 0.05) with the PC1 time series of sixteen Maine lakes (see Appendix C.1).

4.4.2 Linking ice-out dates to winter degree-day thresholds in Maine

The major temporal pattern of winter AFDD in Maine was examined by applying principal component analysis on the winter AFDD time series of six stations. The first principal component (PC1) represents 87% of the variability in AFDD in the six USHCN stations and thus may be considered as the leading pattern of winter AFDD variability in Maine (see figure 4.2c). The homogeneity of signs in station loading in PC1 reflects synchronous variation in winter AFDD in all stations (see figure 4.2b). Time series of PC1 (see Figure 4.2c) shows high year-to-year variation in winter AFDD but no secular trend (see Figure 4.2c). Comparison of the PC1 of ice-out date and winter AFDD time series shows a significant ($|r|$=0.4, $p < 0.05$) correlation between the PC1 of winter AFDD and ice-out date (see Figure 4.2d). This indicates that the timing of spring ice out date in Maine lakes is influenced by the variability of the preceding winter temperature.

Appropriate characterization of the link between spring ice-out dates and antecedent winter temperature further clarifies the role of local winter temperature variability on the timing of spring ice breakup. Initially, the general relationship between spring ice out and winter degree-days in Maine was investigated using Pearson's correlation tests. Results show there is a significant ($p < 0.05$) positive correlation between local winter AFDD and ice-breakup dates of selected Maine lakes that is lower winter AFDD quantities are associated with early ice out dates and vice versa. Seasonal AFDD quantities explain 15-20% ($p < 0.05$) of the total variability in ice-out dates (see Table B.2-B.7). No systematic regional difference exists in the correlation coefficients between winter AFDD and lake ice out dates although there is considerable difference in the quantity of winter

AFDD between stations and the variability and timing of lake ice breakup dates in the three climate regions of Maine. On the other hand, seasonal winter AMDD shows significant ($p < 0.05$) negative correlation with the spring lake ice-off dates indicating that higher AMDD magnitudes are linked to earlier ice out dates and vice versa. Winter AMDD quantities account for 10-28% ($p < 0.05$) of the total variability in the lake ice thawing dates (see Table B.2-B.7). Furthermore, there is an inland-coastal gradient in the correlation coefficient between AMDD and lake ice out date of lakes suggesting that for those lakes near the coast such as Damariscotta or China lake, the occurrence and magnitude of the non-freezing winter days (AMDD) has stronger effect on the ice-off dates than that of lakes found deep in the interior (Rangeley, Mooselmeguntic).

Visual inspection of the relationship between winter temperatures (degree-days) and ice-out dates of selected lakes reveals that ice-out dates in Maine have higher sensitivity to warmer winter temperatures (lower AFDD and higher AMDD) than colder ones. This is due to the fact that ice-cover produced during warmer winters requires relatively lower thermal forcing to melt in spring as compared with those produced during colder winters and thus is less affected by meteorological conditions in spring. This explains for the modest correlation results between winter temperatures and ice out dates as correlation tests can only gauge the average linear relationships. Furthermore, it reveals that simple linear models provide somewhat partial characterization of the threshold winter degree-days above/below, which engenders anomalous spring ice breakup dates in spring in lakes. However, non-parametric kernel density estimation method would be better suited to derive the existing relationship between ice breakup dates and antecedent winter degree-days as it makes no priori assumptions about such association or distributions. Thus to develop the relationship between variability in spring ice breakup dates especially the anomalous ones to antecedent winter temperatures, the joint density contours of the seasonal winter AFDDs and AMDDs for the earliest and latest 15 ice-out dates for selected lakes were generated using non-parametric kernel density estimators.

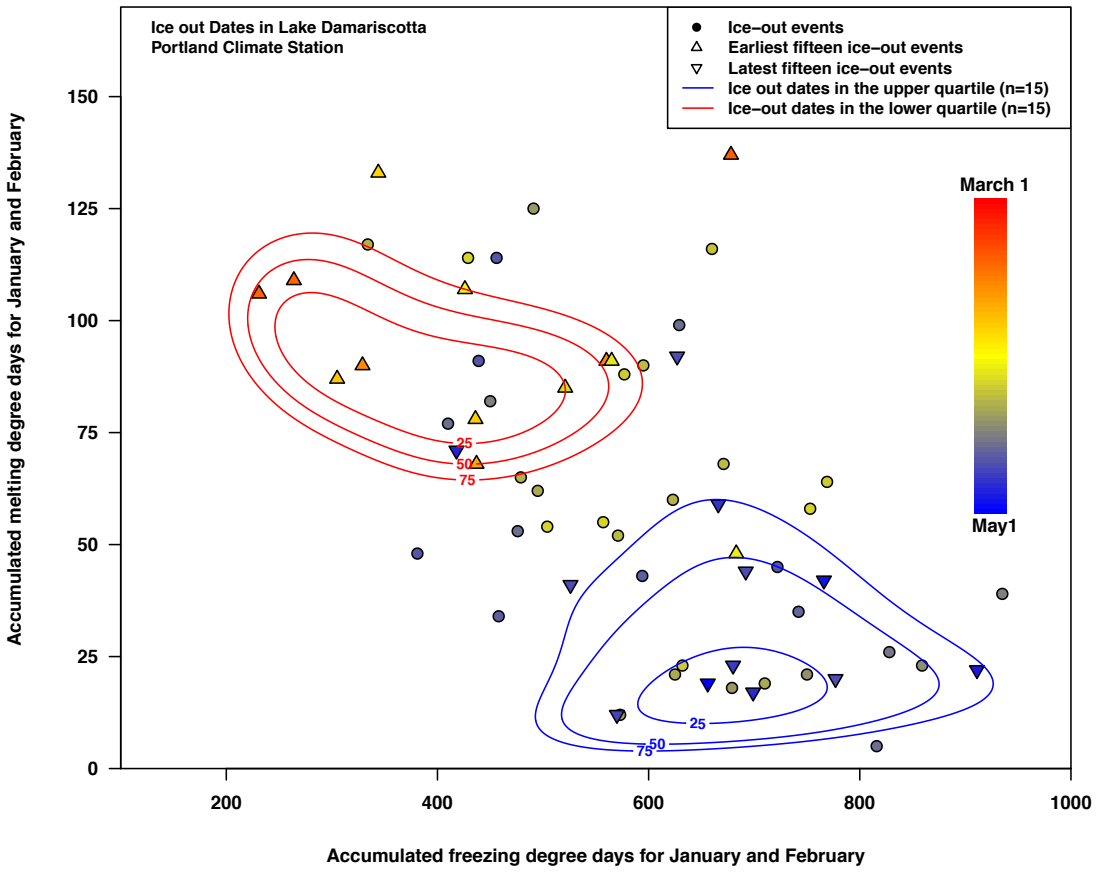

Figure 4.3. Joint probability density of winter AFDD and AMDD for the earliest and latest 15 ice-out dates at Lake Damariscotta.

The red and blue contours in Figure 4.3 show the joint probability density estimates of preceding winter AFDD and AMDD quantities for the earliest and latest ice-off events in spring respectively. It can be observed that more than 75% of the earliest 15 ice-out events at Lake Damariscotta occurred when the winter AMDD quantity was over 35 degree days centigrade (DDC) while nearly 75% of the latest 15 ice-out events had winter AFDD values below 325 DDC. This separation in AMDD and to a lesser extent AFDD quantities imply the presence of winter degree-day thresholds above/below which precondition the ice cover formed during winter to bring about early spring ice out dates in lake Damariscotta. Other lakes also show the presence of winter AFDD and AMDD thresholds that precede early/late spring ice out events (see Figure C.4). Based on these results, it can be

concluded that variability in spring ice-out events in Maine lakes is dependent on the exceedance/non-exceedance of the threshold degree-days during the antecedent winter.

4.4.3 Linking Winter Temperature Variability to Large-Scale Teleconnection Patterns

The most relevant large-scale teleconnection patterns that influence seasonal winter degree-days quantities in Maine were identified by correlating the time series of PC1 for both seasonal winter AFDDs and AMDDs to the geo-potential height at 500mb (see Figure 4.4). The time series of PC1 for AFDD have statistically significant ($\rho > 0.4$, $p < 0.05$) correlations with the geopotential height anomaly time series over eastern North America and the Pacific Northwestern region of U.S. and Canada, which is reminiscent of the Tropical/Northern hemisphere teleconnection pattern (see Figure 4.4a and c). In contrast, the time series of PC1 for AMDD show significant correlation ($\rho >$0.4, $p < 0.05$) with the geo-potential height anomaly time series over Iceland and Atlantic Ocean, consistent with North Atlantic Oscillation (NAO) pattern (see Figure 4.4b and d). While the major thrust of this study will thus be to understand the role of winter TNH and NAO patterns on spring ice breakup dates, results from ancillary analyses relating PC1 of winter degree days in Maine with global sea surface temperatures and upper air geopotential heights, and putative links to known oceanic/atmospheric modes of climate (such as Atlantic tripole, Atlantic multi-decadal oscillation) is presented in Appendix C.2.

Pearson's correlation tests between local temperatures (as recorded by stations) in Maine and average winter TNH indices show that TNH has a significant ($p < 0.05$) negative correlation with local winter temperatures (see Table C.2). That is, negative phases generally are associated with warmer winters (lower AFDD and/or higher AMDD) and vice versa. TNH patterns explain about 10%-17% ($p < 0.05$) of the total variability in AFDD quantities recorded at all stations and 9-10% ($p < 0.05$) of the total variability in AMDD at Farmington and Corinna stations. The correlation coefficient between TNH and

local winter degree-days also has an inland-coastal gradient with inland stations displaying higher correlation coefficients than that of the coastal. Winter NAO patterns show significant positive correlations (at $p < 0.05$) with local winter temperatures in some of the southern and coastal stations (Portland, Gardiner, Farmington and Millinocket) (see Table C.2). The variance explained by NAO indices ranges from 10%-19% of total AMDD variation recorded at these stations. No significant correlation between NAO phases and winter AFDD quantities was registered at any of the stations. The absence of a significant association between NAO and winter AFDD or mean winter temperature implies that NAO phases mainly influence the warm tail distribution of seasonal winter temperatures while having little or no effect on the mode or cold tail distributions of winter temperatures. Furthermore, partial correlation analysis indicates that the linear relationship between TNH (NAO) and temperature metrics is relatively insensitive to NAO (TNH) indices (see Table C.2).

A closer inspection of the composite geo-potential heights patterns to opposing extreme phases of TNH/NAO shows asymmetry, and differences in the local amplitudes of the anomaly patterns for Maine (see Figure 4.4a-d). The relative effect of this potentially nonlinear atmospheric response to strong TNH and NAO patterns on winter temperature variability in Maine was investigated by comparing their empirical density function of winter degree-days. The empirical density function during lower quartile TNH phases (TNH < -0.47) shifts toward lower winter AFDDs as compared with the other phases (TNH > -0.47) in all six stations (see Figure 4.5 and Figure C.6). Thus, the observed that TNH patterns affect the mode and lower tail of the seasonal winter temperatures distribution in Maine. This effect is exemplified in figure 4.5a-c where during lower quartile TNH phases (red line), there is a marked shift in the empirical density estimate of Portland winter temperatures towards warmer degree-days (especially in AFDD). On the other hand, it was noted that NAO patterns influence the warm tail of seasonal winter temperatures in southern and coastal regions as the empirical density function during

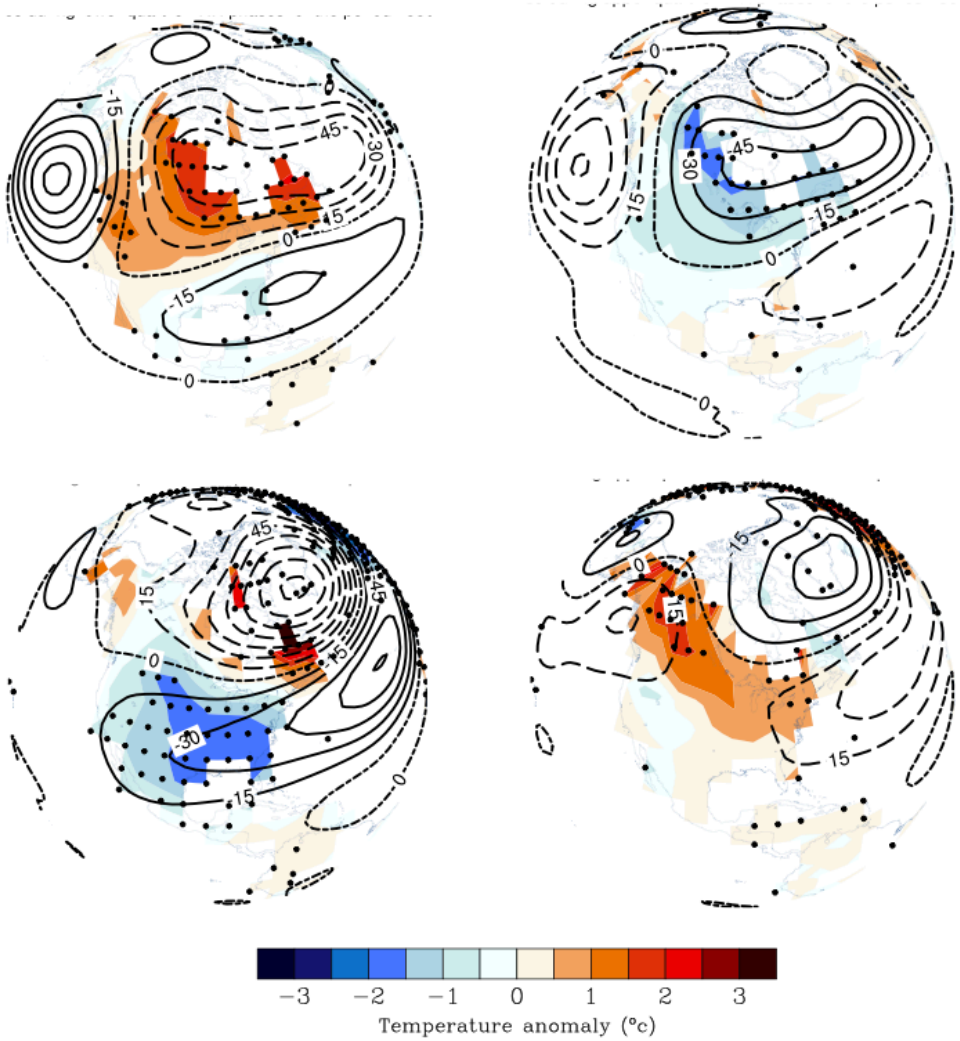

Figure 4.4. Seasonal 500mb geopotential height composites and surface temperature anomalies during lower quartile TNH phases (TNH<-0.47) (a-b) and upper quartile NAO phases (NAO>0.2) (c-d) during winter for the period 1950-2010.

upper quartile NAO phases shifts towards higher AMDDs as compared with other phases in most southern stations (see Figure 4.5d-f and Figure C.6). This effect is illustrated in Figure 4.5d-f where during upper quartile NAO phases (red line), there is a strong shift in the empirical density estimate of Portland's winter temperatures towards warmer degree-days (especially in AMDD).

The observed effects of winter TNH/NAO variability on the statistics of winter degree days may provide prospects for spring ice out prediction in Maine premised on the

probability that the threshold winter AFDD and AMDD quantities, that are associated with early and late spring ice breakup events of lakes, is exceeded. In this regard Figure 4.3 shows that 75% of the earliest 15 ice-out events in lake Damariscotta had winter AFDD below 325 DDF. During lower quartile TNH phases (upper quartile NAO phases), there is approximately 76% (63%) chance that the accumulated freezing degree-days at lake Damariscotta will be less than 325 DDC, which is approximately 80% (27%) more likely as compared with the other winter TNH (NAO) phases. This exemplifies that forecasts of TNH and NAO indices can be used in the season-ahead or longer prediction of early/late spring ice out events in Maine lakes premised on the exceedance probability of the threshold winter degree-days.

4.4.4 Teleconnection patterns and Lake Ice-off Dates

The overall strength to which winter TNH and NAO patterns precondition spring lake ice-out dates in Maine lakes were determined empirically by comparing the median ice out date of the eight lakes during lower quartile TNH phases ($TNH < -0.47$) and upper quartile NAO phases to the unconditional median ice out date for 15 randomly chosen years in the study period (see Figure 4.6). During upper quartile winter NAO ($NAO > 0.2$) years, the median ice-out date for most lakes showed shifts towards earlier dates. However these shifts were only significant ($p<0.05$) in the coastal lakes (China and Maranacook). On the other hand during lower quartile TNH ($TNH < -0.47$) years, all lakes including those found in the deep interior regions such as Rangeley and Mooselmeguntic, whose climatological median ice out date for the period in this study is in late-April to early-May period, displayed significant ($p < 0.05$) shifts towards earlier dates than the unconditional median ice breakup date. Similar results were obtained when the threshold for these teleconnection patterns were altered for different percentiles (see Figure C.3). These diagnostic analyses provide an empirical basis regarding the efficacy of

pronounced negative TNH phase and pronounced positive NAO phase in bringing about shifts in the timing of ice breakup dates of Maine lakes towards earlier dates.

4.5 Discussion and Conclusion

In this paper, we studied inter-annual variability in spring ice out dates in Maine lakes and its association with preceding winter weather-climate variability. The influence of antecedent winter degree-days on spring ice-out dates of selected eight Maine lakes was characterized by determining the threshold winter accumulated freezing and melting degree-day (AFDD and AMDD), the exceedance (non-exceedance) of which engenders early (late) spring ice-out dates. Winter teleconnections such as TNH and NAO were determined to impact the timing of spring ice out dates in Maine through their influence on the winter degree-days. In closing, we offer the following observations, and discuss emerging research directions.

1. The results in this study show that significant season-ahead information regarding springtime lake ice-out resides within the wintertime temperature patterns for Maine lakes, even though the bulk of the ice-out date variability seems to be driven by spring temperature conditions. For the eight lakes used in this study, our correlation analysis indicates that spring (March-April) temperatures accounts for more than half ($p < 0.05$) of the total variability in the lake ice breakup dates for the study period (see Appendix B). However, linkages identified in this study between ice-out and wintertime weather and climate patterns are important for two other reasons: (a) recent early lake ice-out events in a number of southern and coastal Maine lakes signal a shift towards early spring (mid to late March) dates which reduces the role of spring climate conditions on early spring ice breakup dates and (b) the natural and/or anthropogenic forced climate warming is projected to continue for the Northeast region (IPCC 2007) which sets the winter period to provide the bulk of the freezing energy to form and thicken the ice cover over lakes; it is imperative that the

role of winter weather/climate variability on the ice-breakup dates of lakes in the Northeast regions be understood so as to anticipate major changes in the lake ice breakup regimes.

2. The majority of publications on lake ice phenology employ seasonal mean temperature as the choice of metrics for analyzing the link between local air temperatures and lake ice freeze up/breakup. The often-cited reason for such selection is that the use of degree-days over seasonal mean temperature does not improve regression/correlation results [111, 178]. However the determination of winter degree day thresholds that determine the timing of spring ice out in this study indicates that variability in seasonal and/or episodic temperatures are as important as seasonal mean temperatures in influencing lake ice phenology. Our correlation analyses also show that spring lake ice out in coastal/southern Maine lakes (such as Damariscotta and China lakes) was more sensitive to seasonal winter AMDD (warm tail of seasonal temperature) than seasonal mean temperature (see Appendix B). In addition to these results, the use of seasonal mean temperature is also less intuitive about the seasonal ice cover growth and melt processes that affect lake ice formation and duration. Thus we believe that future ice phenology studies should take into account the role of intra-seasonal temperature variability on the inter-linkages between seasonal temperature and ice cover duration.

3. The extensive use of linear regression/correlation in ice phenology studies has limited the way in which the links between lake ice phenology, local climate variables and teleconnections have been characterized and understood. In this study our use of non-parametric methods (e.g. kernel density estimates, bootstrap) has allowed (a) improved characterization of the empirical seasonal temperature and ice out dates relationship which is inherently non-linear (b) better insight into how teleconnection patterns influence seasonal temperature variability (c) better description of the link

between teleconnection patterns and ice phenology in Maine lakes. For instance, it was shown in this study that NAO patterns largely influence the warm tail of seasonal winter temperature for coastal and southern climate regions while TNH patterns regulate the mean and cold tail of seasonal winter temperatures for all regions. Furthermore, the effect of teleconnection patterns on the timing of ice out dates were better characterized by determining how these patterns influence the exceedance / non-exceedance probability of the lake winter degree-day thresholds. It should also be noted that comparison of the threshold winter degree days between nearby lakes can provide better insights into the modulating effects of lake variables (e.g. morphometry or altitude) on the link between teleconnection patterns, local climate variable and lake ice phenology.

4. It is evident from our results that pronounced negative phases of TNH influence the frequency and occurrence of early spring ice breakup in Maine lakes. While variability in TNH pattern is largely determined by the internal dynamics within the mid-latitude atmosphere, studies have shown that pronounced negative TNH phase accompany strong El Niño episodes in the Tropical Pacific [17, 163]. El Niño is relatively well documented and well understood ocean-atmospheric phenomena and recent evidences have shown that precursor signals to El Niño events can be observed in the tropical Pacific up to 18 months in advance and their magnitude estimable 9 month ahead [81, 137]. Furthermore, there are predictions in the inter-decadal time scale that there will be an increase in frequency of El Niño events in a warming climate [39, 161]. It is hoped that the development of El Niño episodes over multiple seasons and its skillful forecasts (and its close association with TNH variability) can provide outlooks on seasonal to decadal patterns of early spring ice-out dates in Maine lakes.

5. So what do shifts in the ice out dates mean to the future of Maine lakes? Studies have shown that moderate to dramatic shifts in lake ice phenology induced by climate have cascading effects on the physical, chemical and biological processes in temperate lakes [65, 69]. For instance, during the post-1980 era, shifts towards earlier ice out dates due to winter NAO and ENSO patterns has been linked to changes in the timing, composition and magnitude of spring blooms in European and North American lakes [e.g., 2, 65, 130] although factors endogenous to the lake (e.g. nutrient availability, traits of plankton species and tropic state) may modulate the extent and intensity of change for other lakes [e.g., 3, 82]. Furthermore, depending on the external (e.g. light, temperature and supply of nutrients) and internal (e.g. residence time, underwater light regime and mixing characteristics) factors, changes in the timing and duration of ice cover have also been observed to directly and/or indirectly influence timing and duration of spring turnover [6], water temperatures and heat budget [e.g., 6, 135], lake chemical variables [e.g., 87, 168], seasonal composition and biomass of zooplankton species [e.g., 2, 68], food-web interactions [e.g., 69, 158], cold and warm aquatic species composition and habitat [135], and socio-economic values [135] of temperate and arctic lakes. Our study establishes the relative role played for winter weather-climate variability on spring ice-out dates in Maine lakes and confirms the prospect of season-ahead forecasts based on climatic indices. Carefully designed lake modeling studies, that integrate weather-climate information, as well as lake-specific parameters have the potential to explicate the likelihood for transitions in lake ecosystems and functions stemming from a multitude of commingling factors (early ice out, nutrient loading, lake sediment entrainment, and increased radiative heating the lake, and mixing). In Maine, numerous lake-related activities stand to benefit from seasonal ahead forecasts, as well as identification of thresholds linked to dramatic changes in limnology induced by climate and urbanization (among other factors).

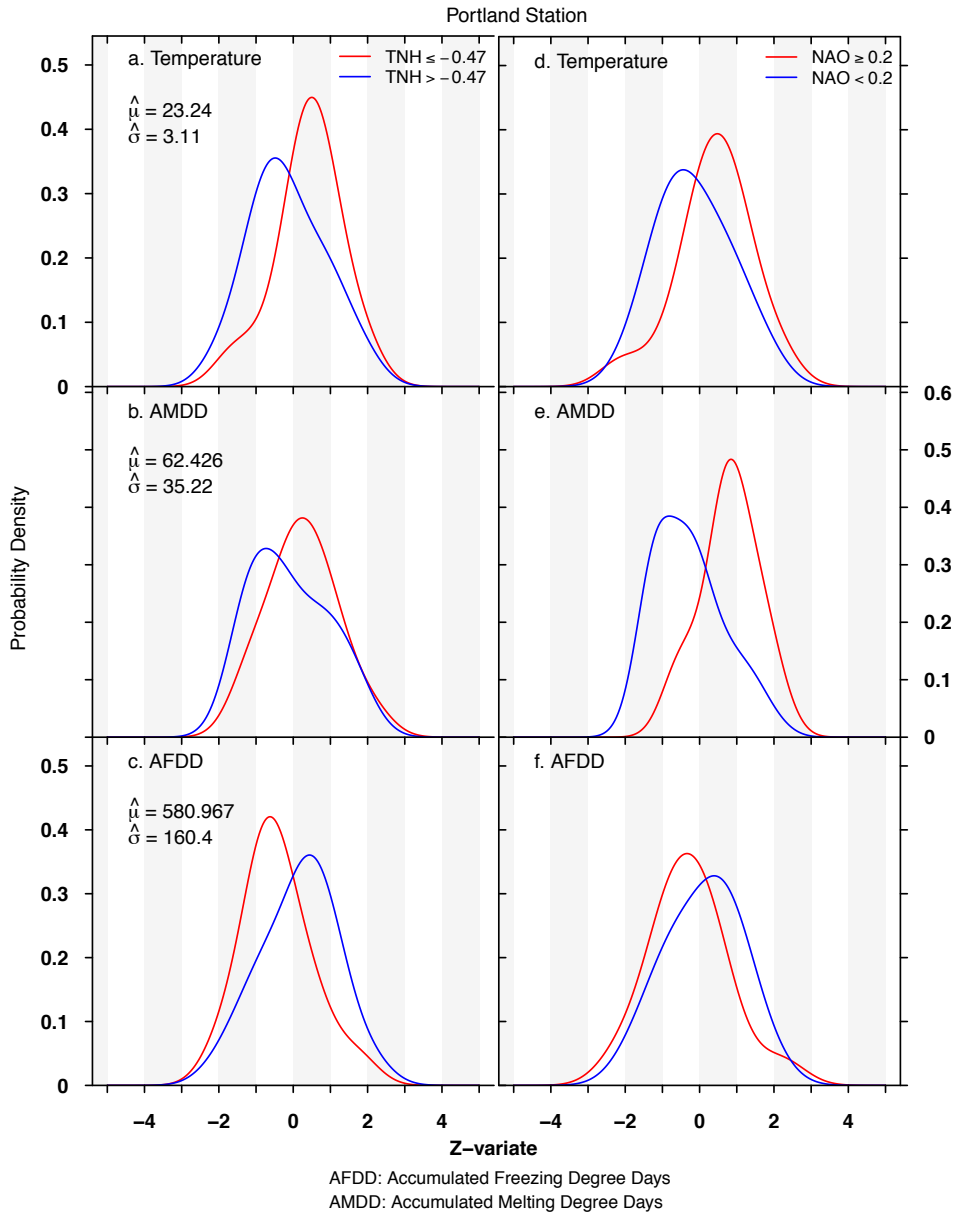

Figure 4.5. Conditional probability density curves for winter temperature (and derived variables) in Portland during contrasting phases of (a-c) TNH (d-f) and NAO.

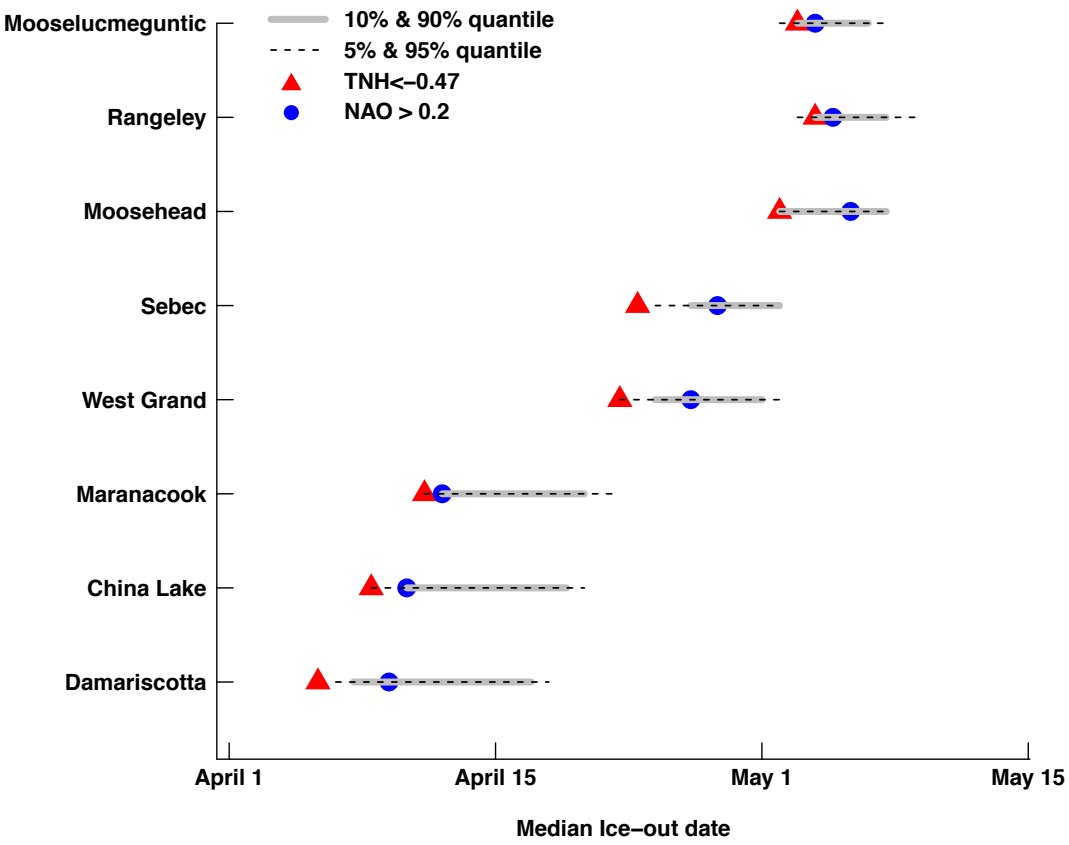

Figure 4.6. The median ice out dates of eight selected lakes from 1950-2010 during lower quartile TNH phases (TNH<-0.47) and upper quartile NAO phases (NAO>0.2).

CHAPTER 5
NORTH AMERICAN WINTERTIME TEMPERATURE ANOMALIES: THE ROLE OF EL NIÑO DIVERSITY AND DIFFERENTIAL TELECONNECTIONS

5.1 Introduction

ENSO events differ in their evolution, strength and spatial pattern of tropical Pacific sea surface temperature (SST) anomalies [e.g., 40, 41]. These contrasts contribute to the observed inter-ENSO variation and their global climate teleconnections, as asymmetry in amplitude and location of tropical Pacific heat sources excite differential Rossby wave trains that induce distinct climate anomalies worldwide [e.g., 18, 79, 183, 184]. To better understand the nature of teleconnections, a broader characterization of ENSO diversity, based on empirical and physical considerations, is needed [e.g., 7, 92, 103, 105, 162]. To this end, two issues cloud the understanding of ENSO-related climatic risk: a. ENSO diversity: differences in the SST anomaly patterns linked to El Niño/La Niña events, and b. differential sensitivity to ENSO: across the range of ENSO amplitudes, the local-to-regional climate impacts vary.

From the standpoint of local and regional patterns of climatic risk under varied ENSO conditions, understanding the heterogeneous nature of shifts in the empirical probability distributions (EPDF) as a whole (as is traditionally done), as well as, for select quantiles is an open problem. Changes in the mean EPDFs conditioned on ENSO patterns have been examined. For instance, Yu et al. [183] broadly describe central Pacific (CP) ENSO impact on US mean winter surface air temperature (SAT) as a northwest-southeast pattern, while this is northeast-southwest for eastern Pacific (EP) ENSO. On the one hand analysis of SAT composites conditioned on ENSO states allow assessment of conditional mean, however, concordant changes across the range of temperatures, including the extremes are

also implied. As noted in recent studies [40, 41],in general, ENSO events do not conform to a particular canonical tropical Pacific SST pattern. In many cases, a better representation would be based on superposition of distinct tropical Pacific SST anomalies patterns derived, for example, using Principal Component Analysis (PCA) approach. Furthermore, the response of the mean winter SAT to ENSO patterns largely reflect the relative shift in the central part of the conditional distribution, while SAT thresholds in numerous environmental and societal systems (such as lake ice) are sensitive to alterations in the distributional tails induced by teleconnections [22]. Also, the assumption of an ENSO-induced symmetric shift in the distributional tails is simplistic for many North American locations, because of the complex interplay between local and regional land-atmospheric processes operative at different time scales. Thus, it is critical that a comprehensive analysis of the modulating influence of diverse ENSO patterns on local North American winter-time SAT be made across different parts of the SAT distribution as well as the entire distribution.

The present study assesses differential sensitivity of local North American wintertime SAT, across the entire variability range, to ENSO diversity with focus on understanding how asymmetries in the location of tropical Pacific winter SST anomalies affect risk of key winter SAT thresholds in North American regions. Two key questions in this regard are: (a) what is the relative contribution of the leading empirical patterns of winter SST variability in Niño regions, towards the modulation of conditional winter SAT distribution over North America, (b) for a given SAT threshold, what are the relative sensitivities to ENSO covariates?, and in general, what is the location-specific and regional nature of conditional EPDFs corresponding to archetypical ENSO flavors? We investigate these questions based on a conditional quantile function approach [100], which allows modeling of quantile-specific functional relationships be-tween ENSO indices and local North American wintertime SATs that provide comprehensive description of the location and magnitude of maximum SST anomalies in the tropical Pacific.

5.2 Data and Methods

North American SAT: Monthly time series of gridded (0.5°x0.5° resolution), land-only, SAT data were obtained from NOAA GHCN Climate Anomaly Monitoring System (GHCN CAMS) dataset [54]. Winter season (December-February) SAT anomaly fields from 1951 to 2016 were computed for North America, as departures from the 1951-2016 climatology. Equatorial Pacific Sea Surface Temperature: Observational, gridded (2°x2° resolution) SST data from 1951-2016 was obtained from extended, reconstructed sea surface temperature (ERSST) V4 dataset prepared by NOAA National Centers for Environmental Prediction Reanalysis [153]. Moreover, monthly SST indices for the four tropical Pacific Niño regions, which are based on ERSST dataset, were also obtained from NOAA Climate Prediction Center. These four indices are defined based on spatially averaged SST anomalies over select spatial domains: Niño 1+2 (0°-10°S, 90°W-80°W) Niño 3 (5°S-5°N, 150°W-90°W), Niño 4 (5°S-5°N, 160°E-150°W), and Niño 3.4 (5°S-5°N, 170°-120°W) (see Figure D.1). Taken together, the four indices span the tropical Pacific region, and are routinely used for monitoring of the ENSO state (NOAA CPC, 2016). Quantile Functions: SAT is the principal variable considered in this study, and in particular, we focus on its empirical probability distribution throughout North America. We do so using conditional quantile function, so as to understand the full nature of its sensitivity to the ENSO state. Quantiles (τ) are locations in a distribution that correspond to the rank order of values in that distribution. For in-stance, in a given distribution, 75% of the population have values greater than the $\tau = 0.25^{th}$ quantile point, while 25% of the population have values less than that. Quantile regression, first proposed by Koenker and Bassett Jr [100], involves one-sample quantile concept towards estimation of the quantiles of a conditional distribution, such that the conditional quantiles of the response variable, Y, are defined as functions of known covariates, X [101]. Given that the respective quantile functions are determined independently, this approach (a) allows detection of heterogeneity in the response of different quantiles, (b) is robust against outliers in the response variable

distribution, and (c) has no distributional assumption. As such, it provides a relatively complete description of conditional distribution of the response variable, Y (in our case, SAT), especially when changes in tail behavior (upper and lower quantiles) are of interest. In the present study, this approach is particularly appropriate, as it allows for analyses of asymmetric teleconnections, a feature noted in a number of previous studies, yet not quantified at regional scales. As a first step, we estimate the conditional quantile functions of SAT at each grid point to the covariate set comprised of indices corresponding to the two leading patterns of Niño SST (see Section 5.3.2 for a detailed discussion). Linear quantile models have the form, $Y(\tau)$=$\beta(\tau)X + \epsilon(\tau)$, where $\beta(\tau)$ is the parameter estimate for each quantile and $\epsilon(\tau)$ denotes the error term for each quantile with an unknown distribution. Unlike in conventional linear regression where parameters are estimated by solving for minimization of sum of squared errors, $\beta(\tau)$ in quantile functions are obtained by solving for the minimization of the sum of weighted absolute residuals

$$argmin|\sum_{i=1}^{i=n}\rho(\tau)(Y_i - \beta(\tau)X_i)| \tag{5.1}$$

where n is sample size ($n = 66$) for a North American field and $\rho^{(tau)}$ is the check function where

$$\rho^{(\tau)}(\epsilon_i) = \left\{ \begin{array}{c} (\tau - 1)\epsilon_i;\ \epsilon_i < 0 \\ (\tau)\epsilon_i;\ \epsilon_i > 0 \end{array} \right\} \tag{5.2}$$

$\epsilon_i$is the difference between observed and estimated Y_i at selected τ^{th} quantile. This limits the influence of outliers and other extreme data on parameter estimation at each quantile. Computations for parameter estimates were done using quantile regression implementation, Koenker [99] within the R computing environment.

A potential problem with modeling multiple linear quantile functions is that, estimated independently, the conditional quantile lines may cross, producing an invalid distribution. To alleviate the crossing problem in quantile regression, a procedure introduced by Bondell et al. [31], which imposes a non-crossing constraint to the solution of Equation 5.1, is used in this work. Moreover studies show that conditional heteroscedasticity may be common

(but certainly not exclusively) in small to moderate samples, which may lead to misleading inference regarding the significance of parameter estimates. Thus for testing the significance of parameter estimates (β) in quantile functions for winter SATs, we employed the wild bootstrap method [58], a procedure that has been shown to be resistant by the nature of the conditional distribution of residuals. Finally, given the spatial interdependence of winter SATs among neighboring North American grid points, the re-sampling procedure in the wild bootstrap method was modified such that the approach tests the field significance Livezey and Chen [110] and not the local significance of parameter estimates. In this paper, parameter estimates in quantile functions are considered field significant, when the null hypothesis that the parameter estimate is equal to zero can be rejected at 0.95^{th} confidence level.

5.3 Results

5.3.1 Inter ENSO SAT Variability in North America

At local scale, the differential response of North American winter SAT quantiles to ENSO events can be demonstrated by contrasting composite maps of the contemporaneous NA and TP SSTA, conditioned on the winter SAT quantiles (τ) at two North American locations, Lake Superior (47.7°N, 87.5°W) and Fort Nelson (57.8°N, 122.7°W), separated into five groups: $\tau < 0.1$, $0.1 < \tau < 0.25$, $0.25 < \tau < 0.75$, $0.75 < \tau < 0.9$, and $\tau > 0.9$. Two noteworthy features of the results presented in figure 5.1 are: (a) there is a strong association between local winter SATs and the large-scale climate patterns over North America, particularly during unusual winters. For instance, during the years when wintertime SATs at Lake Superior/Fort Nelson exhibited pronounced deviations ($\tau < 0.25$ or $\tau > 0.75$), large swathes of North America also had colder/milder than normal wintertime SATs (see Figure 5.1a-j), and (b) over North America, local wintertime air SATs across different quantiles show differential sensitivity to the location and amplitude of tropical Pacific SST anomaly associated with ENSO events. For instance, during the

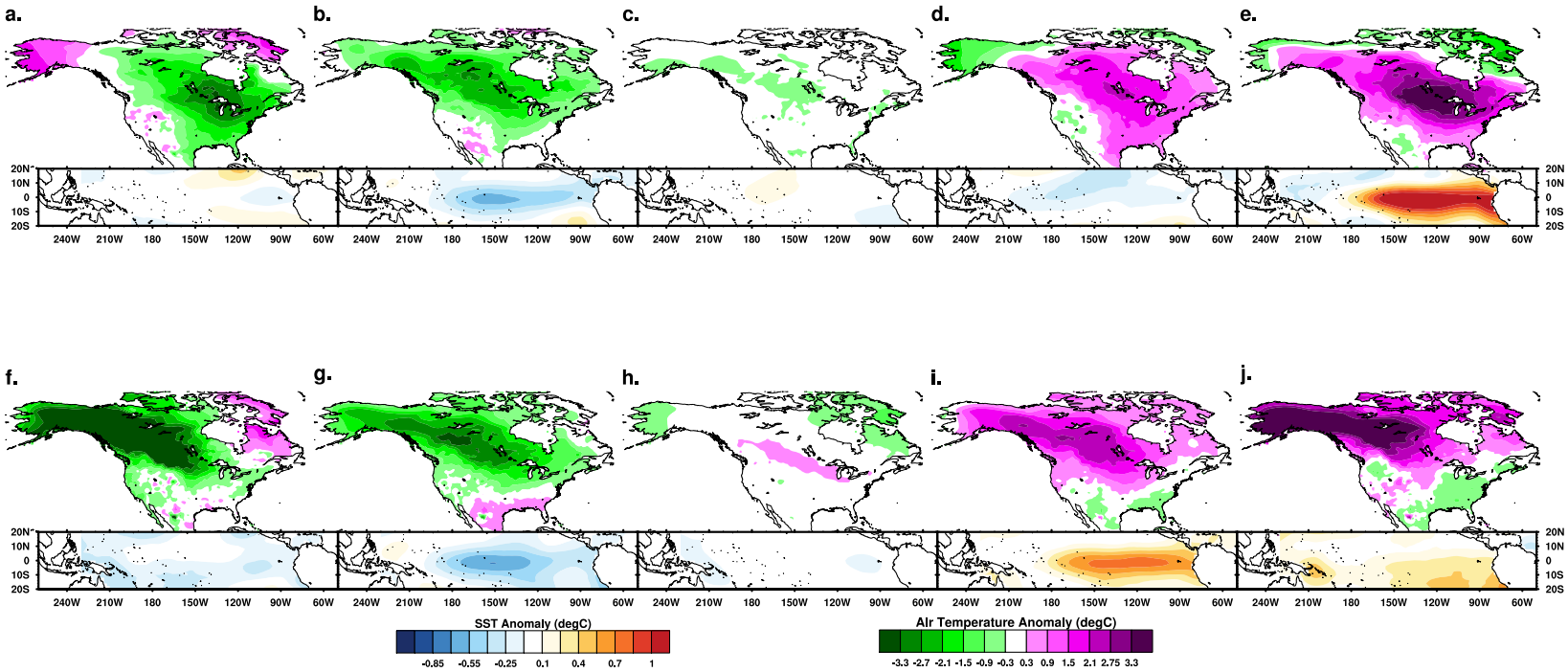

Figure 5.1. Composite maps of contemporaneous North American surface air and tropical Pacific sea surface temperature anomalies Composite maps of contemporaneous North American surface air and tropical Pacific sea surface temperature anomalies, conditioned on local winter (December-February) air temperatures quantiles at Lake Superior (**a-e**), and Fort Nelson (**f-j**). The winter temperature quantile ranges are **a,f** $\tau < 0.1$ (n=6), **b,g** $0.1 < \tau < 0.25$ (n=10), **c,h** $0.25 < \tau < 0.75$ (n=34), **d,i** $0.75 < \tau < 0.9$ (n=10), and **e,i** $\tau > 0.9$ (n=6)

warmest 10% ($\tau > 0.90$) winters at Lake Superior, the contemporary eastern tropical Pacific SSTs were unusually warm. However, it is the SSTs in the central TP and not the eastern TP that show unusual cooling during cold but not extremely cold winters ($0.1 < \tau < 0.25$) at Lake Superior, suggesting asymmetry in the sensitivity of wintertime SATs at Lake Superior to (a) the warming of SSTs in the central and eastern tropical Pacific, (b) the warm and cold phases of ENSO. Similarly, during the cold ($0.1 < \tau < 0.25$) and warm ($0.75 < \tau < 0.9$) winters at Fort Nelson, the central tropical Pacific winter SSTs were colder and warmer than normal respectively. However, there was little or no unusual SST cooling/warming in the central tropical Pacific during the coldest/warmest 10% winters at Fort Nelson, indicating the variable nature of correspondence between ENSO and different SAT quantile groups (see Figure 5.1f-j). Overall, these results suggest that ENSO induced changes on local winter SAT variability of North American regions differs depending on: (a) the amplitude and location of SST anomaly (associated with ENSO) (b) sensitivity of different parts (quantiles) of the winter SAT distribution to ENSO patterns, revealing heterogeneity in the strength of teleconnection that are largely missed by conditional moment based approaches (such as linear regression). Thus, results presented above provide stratified composites (based on five quantile groupings) and highlight the nature of local North American wintertime climate and ENSO variability as asymmetric, non-linear and sensitive to the location of the TP anomaly [7, 79, 183, 184]. As such, a robust characterization of the ENSO-related climatic risk requires the use of an appropriate set of ENSO indices that comprehensively capture the diversity in TP SST pattern, as well as a set of quantile-specific functional relationships with remote climatic variables (gridded NA-SAT).

5.3.2 ENSO Diversity

As noted earlier, a robust approach to ENSO-related climatic risk characterization would entail carefully chosen set of ENSO indices that reflect the detailed nature of tropical

	PC1	PC2	PC3	PC4
Standard Deviation	1.86	0.64	0.28	0.10
Proportion of Variance	0.87	0.10	0.02	0.003
Cumulative Proportion	0.87	0.97	0.99	1.00

PC	Niño1.2	Niño3	Niño3.4	Niño4
PC1	0.46	0.52	0.52	0.48
PC2	-0.73	-0.14	0.22	0.62
PC3	-0.46	0.50	0.44	-0.58
PC4	-0.17	0.67	-0.69	0.19

Table 5.1. Empirical orthogonal modes of wintertime SST variability in Niño regions Empirical orthogonal modes of wintertime SST variability in Niño regions: (a) proportion of variance explained (b) loadings of Niño regions

Pacific SST anomalies. Trenberth and Stepaniak [162] suggested that at least two indices be used to describe the strength and spatial distribution of SST anomalies associated with ENSO events. To this end, we derived the leading empirical patterns of wintertime SST variability in Niño regions by performing PCA on the normalized winter season Niño SST anomalies from 1951-2016 (see Table 5.1). Niño SST anomalies have historically been used to identify the development, type and strength of El Niño/La Niña events.

The first principal component (PC1) represents 87.3% of the total Niño wintertime SST variability and may be considered as the leading pattern of inter-annual winter SST variability across Niño regions (eastern and central equatorial Pacific) (see Table 5.1a). Moreover, the Niño loadings for PC1 are of the same sign indicating synchronous SST variation across all Niño regions (see Table 5.1b). Correlations between PC1 time series and tropical Pacific winter SST anomalies reveal that positive PC1 patterns have a spatial structure akin to the mature El Niño condition: peak SST warming concentrated in eastern equatorial Pacific enclosed by a boomerang shaped cold anomalies in higher latitudes (see Figure D.2). In the PC1 time series, the magnitude of positive and negative anomalies show asymmetry in their magnitude, indicating that warm wintertime SST events along the tropical Pacific are of a higher magnitude as compared to cold events. The second principal component (PC2) represents 10.5% of the total winter SST variability across the Niño regions. The loadings in PC2 are characterized by an east-west dipole pattern in the equatorial Pacific with SSTs in Niño-1+2 (eastern Pacific) region varying out of phase with

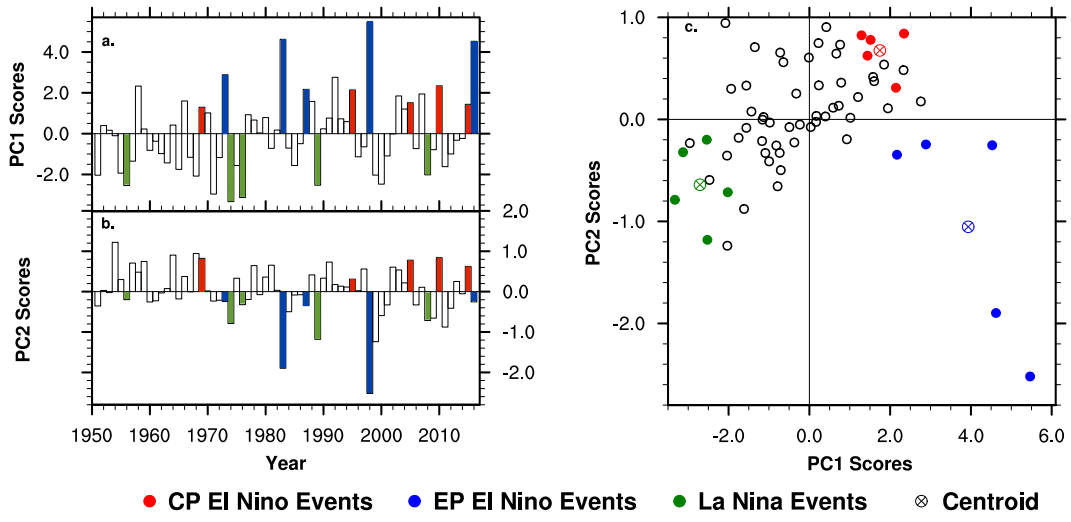

Figure 5.2. The two leading modes (PC1 and PC2) of winter SST variability for Niño regions for the 1951-2016 period The two leading modes (PC1 and PC2) of winter SST variability for Niño regions for the 1951-2016 period: **a** PC1 **b** PC2. **c** Location of select five Eastern Pacific El Niño (1973, 1983, 1998, 2007 and 2016), Central Pacific El Niño (1969, 1995, 2005,2010, and 2015) and La Niña (1956, 1974, 1976, 1989 and 2008) years.

Niño-4 (Central-western Pacific) regions. Correlation between PC2 indices and tropical Pacific winter SST anomalies reveals that positive PC2 patterns have a spatial structure resembling El Niño Modoki [7]: warm SST anomalies confined in the central TP flanked by cold SST anomalies (see Figure D.2b). Some studies have suggested that PC2 corresponds to part of typical El Niño evolution where the warming in the central TP precedes the warming of the eastern TP by few months [159]. However, that is not the case here given that the PCA analysis is based on the DJF months where ENSO events are at their mature stage. In the PC2 time series, negative anomalies have higher magnitudes than extreme positive ones (see Figure 5.2), and this result indicates that the negative anomalies are stronger in the central Pacific than in eastern Pacific while extreme warming is more intense in eastern Pacific than in central Pacific regions during winter. PC2 patterns mainly describe the east-west asymmetry in the location of maximum warming/cooling of wintertime SSTs in the tropical Pacific during diverse El Niño/La Niña events.

Figure 5.2c shows the distribution of the different El Niño/La Niña flavors, selected by majority agreement across various identification methods available in published literatures (see Table D.1), within PC1 and PC2 phase space. EP-El Niño events are found in the fourth quadrant where the PC1 and PC2 indices are positive and negative respectively. This indicates that the maximum SST warming during these events is concentrated around eastern equatorial Pacific and the western south American coast (Niño 1+2 and Niño 3) as some of the warming in central equatorial Pacific (Niño 3.4 and Niño 4) SSTs due to positive PC1 pattern is attenuated or even reversed by the cooling effect in the region due to negative PC2 phases. On the other hand, CP-El Niño events are found in the first quadrant where PC1 and PC2 indices are both positive. This in turn implies that the peak anomalous SST warming in the tropical Pacific during these episodes are located within central equatorial Pacific region; some of the anomalous SST warming in Niño 1+2 and Niño 3 due to positive PC1 phase is offsetted/reversed by the opposite phase of PC2 in the region. The strong La Niña episodes are found in the third quadrant where PC1 and PC2 patterns are both negative, which suggests that the greatest SST cooling in the Niño regions is concentrated along the central equatorial Pacific. These results reveal that the joint indices of the two leading pattern of tropical Pacific SST variability allow characterization of the strength and location of maximum SST anomaly corresponding to diverse El Niño/La Niña events. The separability of ENSO event types aids for meaningful interpretation of teleconnections; analysis to that end is pursued next.

5.3.3 Response of North American Wintertime SAT Distribution to Leading Empirical Patterns of SST Variability in Niño regions

The role of ENSO patterns in shaping local North American winter SAT variability can be expressed as superposition of the leading patterns of wintertime SST variability in Niño regions [e.g., 18]. As noted in the previous section, NA winter SATs at different quantiles may show differential sensitivities to ENSO events depending on their amplitude and

location of TP SST anomalies. In other words, the analysis of NA-SAT teleconnection can be viewed as modulation of the distribution of wintertime SATs, conditioned upon tropical Pacific SSTs, represented by the two leading principal components of winter SSTA in TP. At a grid point or location, an additional consideration for robust estimates of the climatic risk would be the allowance for SAT quantile-specific sensitivities to the two ENSO indices. To this end, quantile functions for wintertime SATs that incorporate the joint PC1-PC2 indices as covariates were generated at three key quantile thresholds ($\tau = 0.25, 0.50$, and 0.75) over North America. Furthermore, the field significance of derived coefficients for PC1 and PC2 were computed using wild bootstrap method, which accounts for heteroscedastic residuals. Figure 5.3a-f show that the slope coefficients for PC1 and PC2 patterns across the three SAT quantiles. The relationship between North American winter SATs and PC1, across the three SAT quantiles (see Figure 5.3a, c and e), has a broad north-south dipole pattern, wherein the slope coefficient for PC1 is significantly ($p \leq 0.05$) positive for most northern areas (except for Baffin Island and northern Quebec) and significantly negative for southeastern and south-central regions. However, the strength and significance of PC1 to winter SATs at $\tau = 0.75$ is less to that of $\tau = 0.25$ and 0.50 for a majority of the North American region. Taken together, these results indicate that the relative warming (cooling) of SSTs across the entire Niño regions increases the relative likelihood of warm (cold) wintertime SATs for northern US and Canadian regions, and vice versa for southern North American regions, primarily by modulating the cold tails of the SAT range rather than the warm tails.

On the other hand, PC2 phases have a direct relationship with winter SATs in the western US states and northeastern edges of Canada (Baffin Island and northern Quebec), while it has an inverse relationship with winter SATs in central and eastern half of North America, across the three SAT quantiles (see Figure 5.3b, d and f). Yet, the strength and significance of the relationship between PC2 and wintertime SAT is not uniform across the three SAT quantiles as the magnitude and significance of slope for PC2 against winter

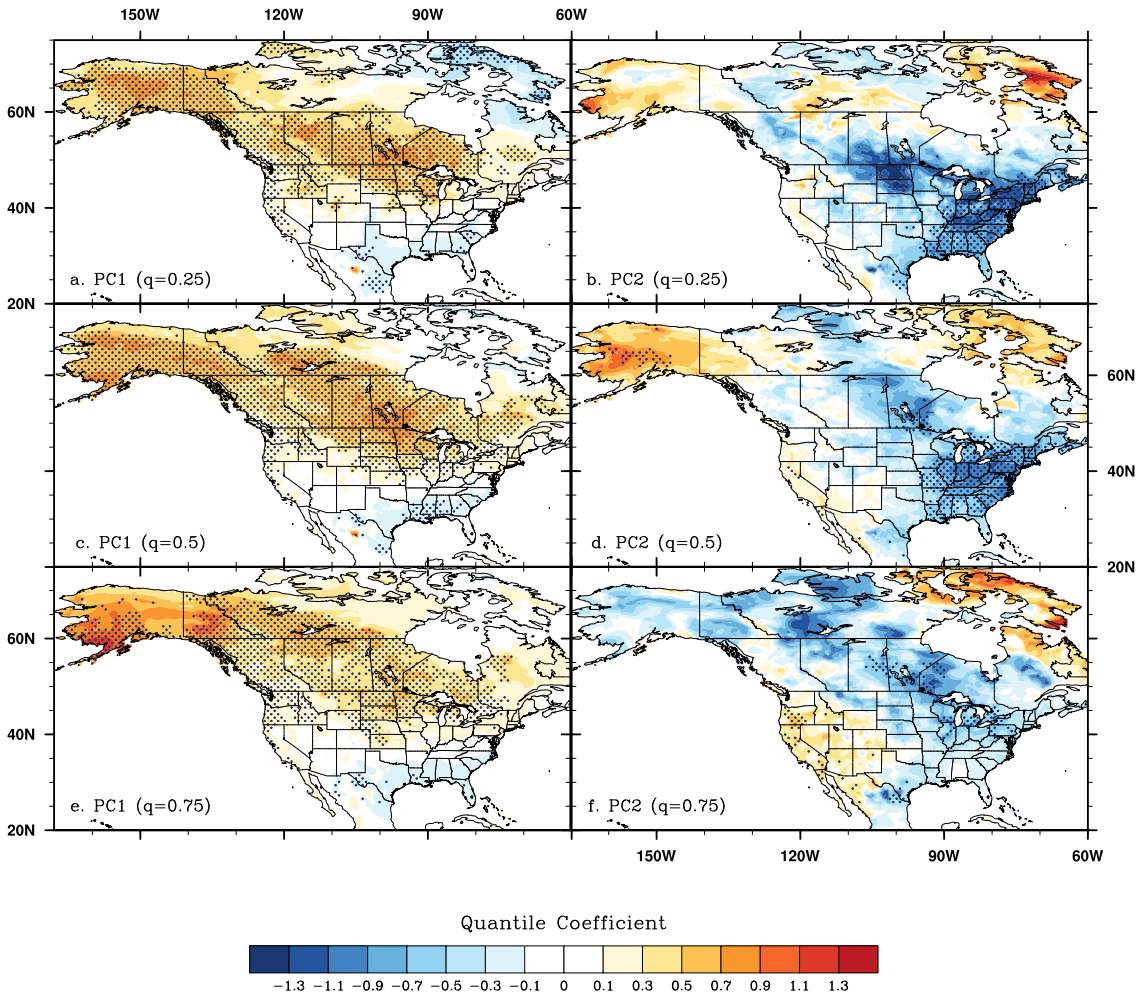

Figure 5.3. Regression analysis for North American winter temperatures at various quantiles Regression analysis for North American winter temperatures at various quantiles: **a,b** $\tau = 0.25$ **c,d** $\tau = 0.50$ and **e,f** $\tau = 0.75$ quantiles against PC1 and PC2 patterns. Stippled regions signifies quantile regression coefficients at 5% field significance level.

SATs weakens with increasing quantiles especially for eastern and southeastern US states. These results suggest that the relative warming (cooling) of SSTs in the CP as compared with EP regions raises the relative exceedance probability of warm (cold) winters in central and eastern North America mainly by influencing the lower (cold SAT) tails of the SAT probability distribution rather than the upper (warm SAT) tails. Asymmetry in the response of North American wintertime SATs across different SAT quantiles to PC1 and PC2 patterns reveals that the two leading patterns of winter SST anomaly in the tropical Pacific modulate not only the conditional mean but also the scale and higher moments

(e.g., kurtosis, skewness) of the conditional winter SAT variability range. These findings are in stark contrast from the conventional linear regression results wherein: (a) the sensitivity of wintertime SATs to PC1 and PC2 indices, across the entire SAT quantiles is uniform, (b) ENSO indices affect the conditional mean and not the spread or other aspects of the conditional SAT distribution. Furthermore, similar analyses using de-trended NA SAT time series were performed (see Appendix D.3) and results show that for most North American regions, the de-trending process does not result in significant changes in the parameter estimates for PC1 and PC2. Given that the response of conditional winter SAT quantiles to ENSO events is modeled in the quantile SAT functions as a weighted linear aggregate of its sensitivity to PC1 and PC2 indices, these effects by PC1 or PC2 indices on the conditional winter SAT probability distributions may get amplified or suppressed.

5.3.4 Change in Likelihood of Cold/Warm Winters due to ENSO Events

The modulating effect of ENSO events on the conditional wintertime SAT in North America can be assessed by estimating the change in risk of lower and upper quartile winter SAT for archetypical ENSO flavors. To that end, the representative amplitudes of archetypical ENSO patterns were derived by computing the centroid of PC1-PC2 index for the five selected EP, CP El Niño and La Niña events in previous section (see Figure 5.2c and Table D.1). These indices were then used to estimate conditional winter SAT distribution using a set of quantile functions for wintertime SATs at 30 equally spaced quantile values ($0.06 < \tau < 0.94$). The results are as follows:

CP El Niño

The spatial pattern of CP El Niño related changes in the likelihood of colder than normal ($\tau < 0.25$) winter SATs in North America has a broad northwest-southeast dipole pattern, where there is an increase in the relative likelihood of lower quantile winter SATs over much of Canada and north central and Pacific regions of US and vice versa for the mid-Atlantic and southern coastal plain regions (see Figure 5.4a). For instance, for much of

Alaska and northern part of Manitoba and Ontario, decreases in relative likelihood of colder than average SAT can exceed 80%, while the US Gulf states show an increase in exceedance probability of cold winters by at least 40%. On the other hand, the impact of CP El Niño on the relative likelihood of warmer than normal ($\tau > 0.75$) wintertime SATs is limited to the mid-Atlantic, southern coastal plain and the Pacific regions of North America (see Figure 5.4b). The western parts of Washington and Oregon, for example, show an increase in the relative risk of warm winters by nearly doubled, while there is a 40-60% decrease in the risk of warmer than average winters over the southeastern US.

EP El Niño

The modulating effect of EP El Niño on the exceedance probability of both lower and upper quartile wintertime SATs in North America can be characterized broadly as a north-south dipole pattern, where there is a substantial increase (decrease) in the exceedance probability of warmer (colder) than normal winters over much of Canada and northern US states and a modest increase in the relative probability of colder than normal winter SATs for Northern Mexico and Texas (see Figure 5.4c,d). In particular, southern provinces of Canada and northern tier US states show approximately 80% decrease in risk for cold wintertime SATs and doubling of risk for warm winters during EP El Niño winters.

La Niña

The effect of La Niña on the likelihood of lower quartile wintertime SATs in North America is concentrated along the Pacific and Atlantic regions of North America (see Figure 5.4e). During La Niña winters, there is largely a modest increase in the probability of colder than normal winters along the Pacific regions of US and Canada, while there is a substantially reduction in the likelihood of colder than normal winters over the eastern and southern US states and northern Mexico. On the other hand, the spatial pattern of La Niña related changes in the likelihood of upper quartile ($\tau > 0.75$) wintertime SATs in North America has a broad northwest-southeast dipole pattern, where there is a modest

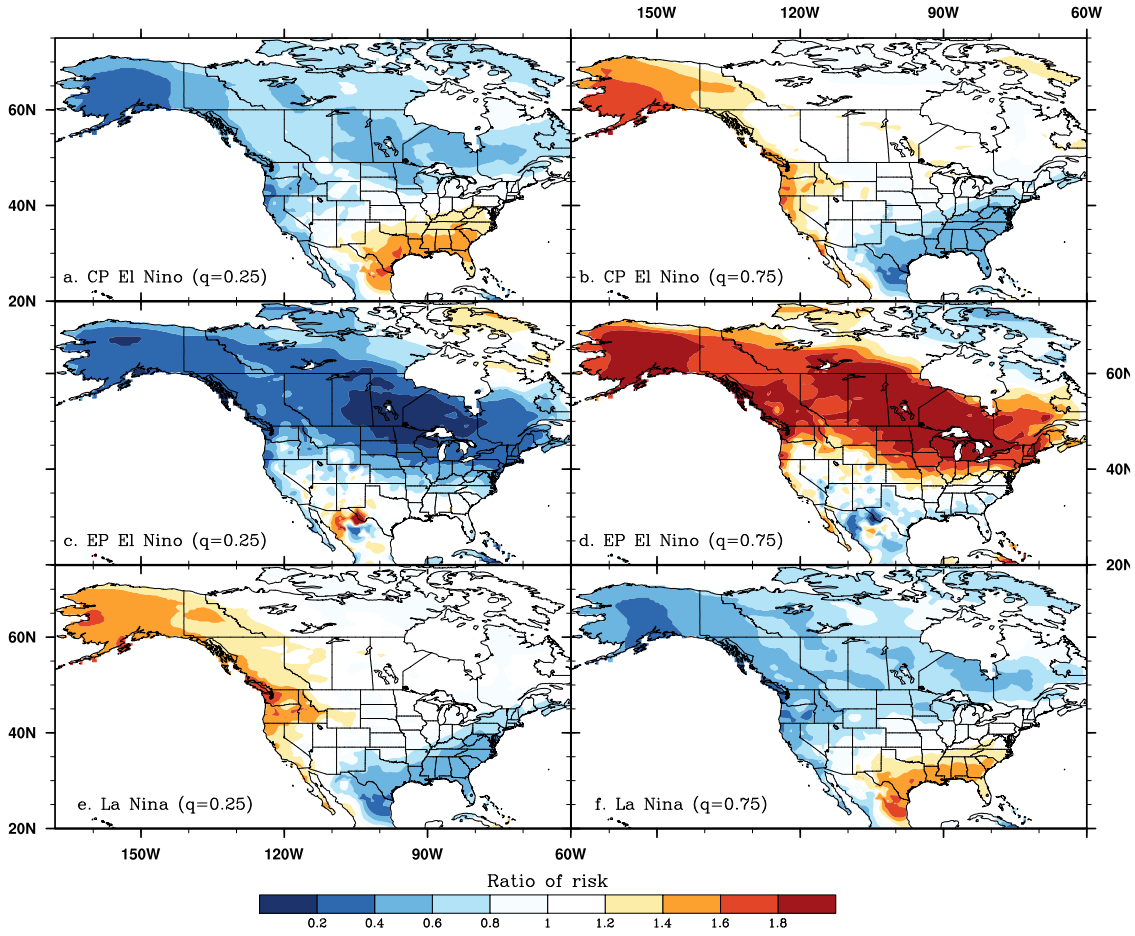

Figure 5.4. Relative exceedance probability of winters Relative exceedance probability of winters with **a**,**c** and **e** unusually cold ($\tau < 0.25$) and **b**,**d** and **f** warm ($\tau > 0.75$) temperatures during archetypical **a**,**b** CP El Niño, **c**,**d** EP El Niño and **e**,**f** La Niña event to that of the unconditional for the entire North American fields.

decrease in the relative likelihood of warm winter SATs over much of Canada and north central and Pacific regions of US and vice versa for the gulf coast of US (see Figure 5.4f). For instance, in Louisiana and southeastern Texas, the relative increase in risk of warm winters can exceed 40% during La Niña while western coast of US and Canadian regions show a reduction in risk of warm winters by at least 80%. A recurring theme in this study is to characterize the heterogeneous nature of winter SAT EPDF conditioned on ENSO events. As such, using results shown in figure 5.4a-f, the nature of the joint change in the conditional likelihood of upper and lower quartile winter SATs due to archetypical ENSO flavors is summarized using the vector plot shown in figure 5.5a-c. In these, the length and

angle of vectors denote the magnitude and direction of the joint change in the likelihood of upper and lower quartile winter SATs due to selected ENSO events. It should be noted that ENSO induced modulation of the upper and lower tails of the conditional winter SAT probability distribution is considered symmetric and uni-directional (as is in the traditional assumption) only when the vectors are at 135° and 315° angle. A summary of the results is given as follows:

Asymmetry in North American Winter SAT Response: CP El Niño

For most western North American regions, CP El Niño events typically reduce the likelihood of lower quartile winter SATs and also increase the likelihood of upper quartile winter SATs, such that related winters have warmer SATs (see Figure 5.5a). However the degree of decrease in the conditional likelihood of lower quartile winter SATs is higher than that of the increase in the occurrence probability of higher quartile winter SATs. In contrast, for regions in the eastern coast of the US, CP El Niñ events are associated with an increase in the occurrence probability of lower quartile winter SATs and a decrease in the likelihood of upper quartile winter SATs, such that these events are typically linked with colder winter SATs in the region. Furthermore in these regions, the magnitude of change in the conditional risk of the upper and lower quartile winter SATs CP El Niño events appears to be symmetric. CP El Niño events, on the other hand, are associated with a slight increase the likelihood of both upper and lower quartile winter SATs for western part of Nunavut province in Canada. Moreover, the amplitude of change in the conditional occurrence probability on both tails of the winter SAT distribution appears to be symmetric.

Asymmetry in North American Winter SAT Response: EP El Niño

For North American regions north of 40°N (except for Baffin Islands), the archetypical EP El Niño pattern is associated with a decrease in the occurrence probability lower quartile winter SATs and an increase in the likelihood of upper quartile winter SATs, such

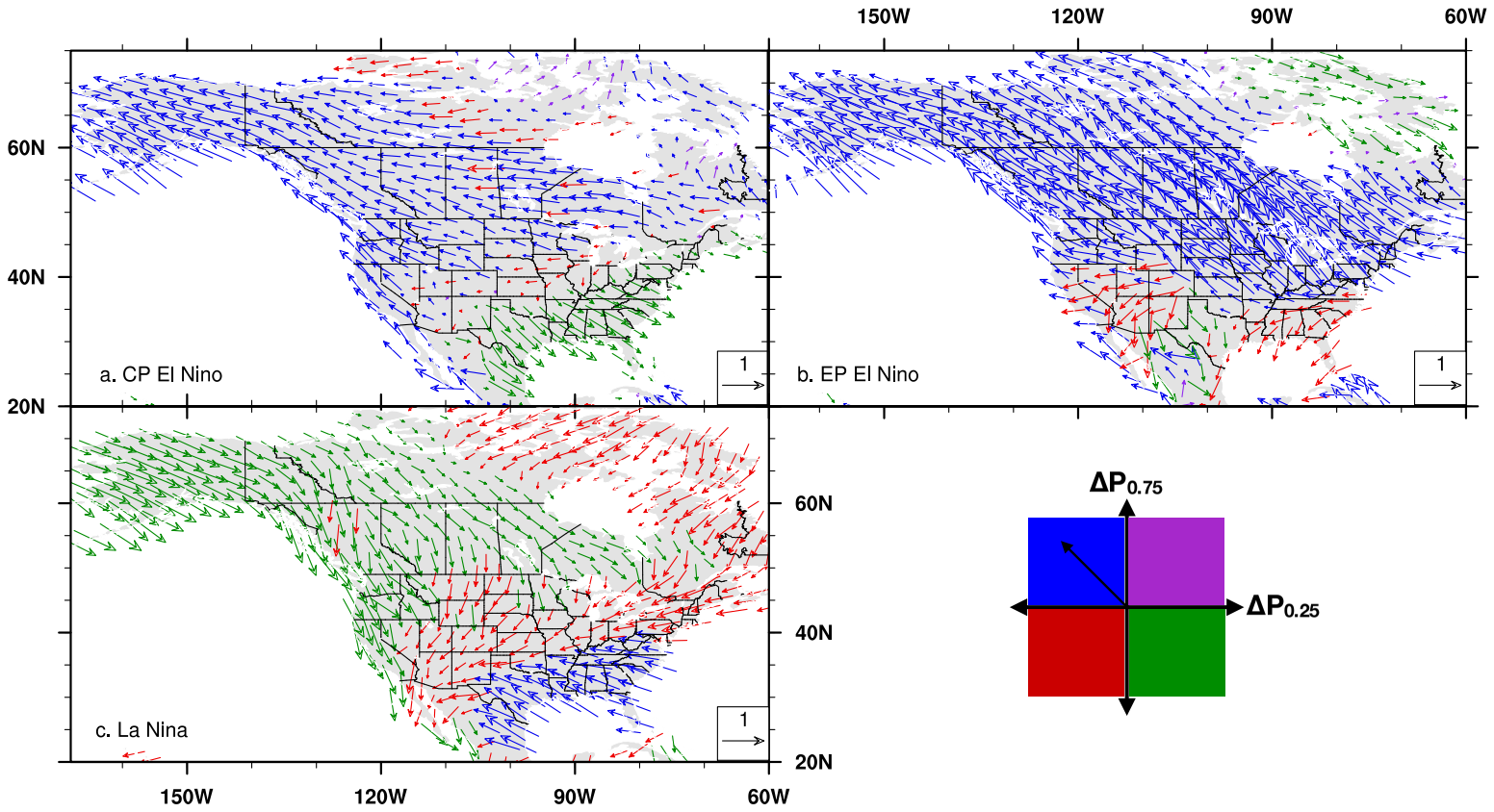

Figure 5.5. The joint change in the exceedance probability of upper and lower quartile winter SATs for North American regions conditioned on archetypical ENSO patterns The joint change in the exceedance probability of upper and lower quartile winter SATs for North American regions conditioned on archetypical ENSO patterns: **a** CP El Niño, **b** EP El Niño, and **c** La Niña. The *length of vector* represents the magnitude of change in risk of upper and lower quartile winter SATs, while the *direction of vector* denotes the relative increase/decrease in upper and lower quartile winter SATs conditioned on archetypical ENSO flavors.

that this pattern is associated with warmer winter SATs in the region (see Figure 5.5b). Moreover in these regions, the magnitude of change in the conditional risk of the upper and lower quartile winter SATs during typical EP El Niño appears to be symmetric. In contrast, EP El Niño events reduce the likelihood of both lower quartile and upper quartile winter SATs for southeastern and southwestern US states. However for most of these regions, the amplitude of change in the conditional risk of lower quartile winter SATs is higher than that of upper quartile winter SATs. For Texas and northern Mexico regions, EP El Niño events are related to an increase in the risk of lower quartile winter SATs and a decrease in the likelihood of upper quartile winter SATs such that they are associated with colder winter SATs in the region. However for this region, the degree of increase in the risk of upper quartile winter SATs is much higher than that of lower quartile winter SATs.

Asymmetry in North American Winter SAT Response: La Niña

For western North American regions north of 50°N, the typical La Niñ pattern is associated with a decrease in the conditional risk of upper quartile winter SAT and an increase in the conditional likelihood of lower quartile winter SATs such that it is related to colder winter SATs in the region (see Figure 5.5c). However for most of these regions (except for Alaska), the magnitude of decrease in the conditional occurrence probability of upper quartile winter SATs is much higher than the increase in the conditional risk of lower quartile winter SATs. In contrast, La Niña events are linked to a decrease in both the conditional risk of upper and lower quartile winter SATs for regions in northeastern Canada, northeastern and north-central US and Nunavut province. For northeastern and north-central US regions, the degree of change in the conditional likelihood of lower quartile winter SATs during these events is higher than that of upper quartile winter SATs. On the other hand, for southeastern and south central US regions, La Niña events reduce the conditional occurrence probability of lower quartile winter SATs and increase the conditional risk of upper quartile winter SATs such that they are related to warmer winter

SATs in the region. Moreover in these regions, the magnitude of increase in the conditional risk of upper quartile winter SATs during typical La Niña events is symmetric to that of the decrease in lower quartile winter SATs.

In summary, assessment of ENSO induced changes in the occurrence probability of warm and cold winter SAT anomalies over North America reveals three key features: asymmetry, multi-linearity and non-linearity. Typical CP El Niño (La Niña) pattern induce wintertime SAT anomalies in North America primarily by modulating the lower (upper) tail distributions, which indicates that the impact of ENSO across the two tails is asymmetric. Furthermore, the influence of archetypical CP and EP El Niño patterns in the TP on North American winter SATs varies both spatially and across the SAT variability range, which implies that ENSO flavors have differential teleconnection patterns (multi-linear). Again, North American winter SATs show differential sensitivity to the warm and cold phases of ENSO both spatially and across the entire SAT variability range, indicating of a non-linear response.

5.3.5 Case Study: Lake Superior Winter SATs

Analysis of composite patterns (Section 5.3.1) revealed that the unusually warm/cold winters at Lake Superior and Fort Nelson are strongly associated with diverse ENSO flavors (see Figure 5.1a-j). The efficacy of conditional quantile SAT functions, with the two ENSO indices as covariates, in explaining these linkages was examined by contrasting the conditional wintertime SAT distributions at Lake Superior and Fort Nelson for archetypical ENSO patterns. The conditional winter SAT distributions to typical ENSO flavors were generated using conditional quantile SAT functions at thirty evenly-spaced quantile points ($0.06 < \tau < 0.94$). While the following discussion describes the result of our analyses for Lake Superior (see Figure 5.6), the results for Fort Nelson are depicted in Figure D.3.

During EP El Niño pattern, there is a strong shift both in the location and tails (particularly in the lower tail) of the conditional SAT distribution for Lake Superior toward

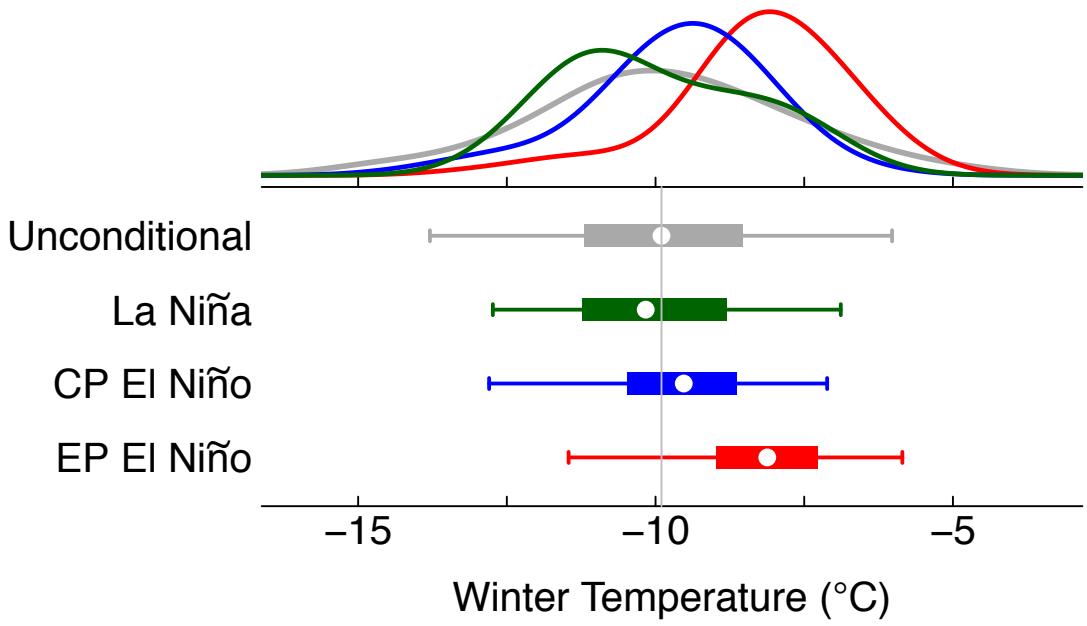

Figure 5.6. The empirical conditional winter air temperature distribution for Lake Superior during archetypical CP El Niño (blue), EP El Niño (red), and La Niña (green) events. The empirical conditional winter air temperature distribution for Lake Superior during archetypical CP El Niño (blue), EP El Niño (red), and La Niña (green) events. The grey boxplot/curve represents the climatological empirical winter air temperature distribution.

relatively warmer winter SATs (see Figure 5.6). Consequently, there is a high likelihood of unusually warm winters and a low likelihood of unusually cold winters at Lake Superior during EP El Niño winters. This is consistent with the findings of the composite analysis (see Figure 5.1e), where the warmest 10% winters at Lake Superior are observed to be strongly associated with warmer than normal wintertime SSTs particularly in the eastern TP. It should be noted that the spread in the conditional SAT distribution associated with EP El Niño at Lake Superior is relatively smaller than that of the climatology (unconditional), confirming that the change in the likelihood of extremely warm/cold winters due to EP El Niño is not only due to the change in the location but also the scale and other moments of the conditional SAT distribution. In contrast, during typical CP El Niño, there is a slight shift in the location of the conditional SAT distribution for Lake Superior toward warmer winter SATs (see Figure 5.6), however, both the warm and cold tails of the conditional SAT distribution are relatively thinner and the spread in the

conditional distribution smaller as compared with the unconditional distribution. Thus, warming of the central tropical Pacific SSTs mainly suppresses the occurrence of unusually warm/cold wintertime SATs at Lake Superior. Results from the composite analysis (see Figure 5.1a-e) indirectly support this conclusion in that the unusually warm ($\tau > 0.75$) or cold ($\tau < 0.25$) winters for Lake Superior do not show a strong association with a concurrent SST warming in the central TP. Furthermore, the suppressing influence of CP El Niño pattern on the occurrence of unusually warm or cold winter SAT conditions at Lake Superior mainly resides in its effect on the spread rather than the location of the conditional wintertime SAT distribution. Similarly during typical La Niña, there is a shift in the location and right tail of the conditional winter SAT distribution towards colder than normal winter temperatures (see Figure 5.6). This result suggests that La Niña events raise (reduce) the relative likelihood of unusually cold (warm) wintertime SATs at Lake Superior. Such inference is consistent with the findings of the composite analysis (see Figure 1b), where colder than normal ($\tau < 0.25$) winters at Lake Superior are ob-served to have a strong association with the cooling of SSTs in the central TP. The above analyses suggest that the sensitivity of winter SATs at Lake Superior to ENSO extends beyond that associated with the typical TP SST distribution.

5.4 Discussion and Summary

Observational studies of ENSO teleconnections show significant nonlinearities, phase-related asymmetry, and diverse responses to location-specific warm anomalies (e.g., CP and EP patterns). To date, ENSO-related changes in the EPDFs of SAT and precipitation have been analyzed mostly from the standpoint of shifts in the mean, and in rare instances, variance. Examined in that manner, the symmetric shifts in the location and shape of probability distributions often render inaccurate probability and risk estimates. This concern is rooted in the heterogeneous nature of the ENSO-related modulation of the scale and higher moments of the conditional distributions. A conditional

quantile function estimation approach presented here affords both quantile-specific conditional regression estimates, as well conditional EPDF that are not restricted by the limited flexibility afforded by parametric distributions (such as, Normal, Log-normal etc.). With appropriately chosen set of ENSO covariates, this study presented results at local-to-regional scales for North American wintertime SATs, wherein risk estimates were readily quantified for diverse tropical Pacific SST conditions. In what follows, we summarize the key findings from this study:

1. The sensitivity of North American winter SATs to the two leading empirical patterns of tropical Pacific SST anomaly patterns (PC1 & PC2) varies both spatially and across different quantiles (see Figure 5.3). Spatially, the modulating effect of PC1 patterns on North American wintertime SATs across key quantiles ($\tau = 0.25, 0.5, 0.75$) can be broadly characterized as a north-south dipole pattern, while PC2 pattern has a weak east-west dipole pattern, one dominantly concentrated in the eastern half of the United States. However, the response of the conditional SAT distribution across these quantiles have unequal amplitude (magnitude and direction) for most North American locations, with lower tails showing larger shifts as compared to the upper tails (as illustrated in Figure 5.3).

2. The observed heterogeneity of the sensitivity of North American winter SAT to particular tropical Pacific SST anomaly (represented as a point within the PC1-PC2 space; Figure 5.2) can be related to differential shifts throughout the SAT EPDF. In conventional terms, this would translate into changes in the central tendency, as well as higher moments. The resulting conditional EPDFs reflect contributions from PC1 and PC2 patterns amplitudes, which in turn may cause amplified or muted shifts for a particular SAT quantile.

3. The conditional quantile approach allows for a detailed assessment of the changes in the upper and lower tail SAT probabilities, which in general terms, represents the

likelihood of unusually mild and cold winters respectively. Examined as a ratio of conditional to unconditional probabilities (Figure 5.4), the contrasting spatial patterns and amplitudes of change in risk for lower and up-per quartile wintertime SATs related to archetypical CP and EP El Niño event are noteworthy, as are the La Niña patterns when contrasted the EP and CP events. Conditional quantiles for selected PC1-PC2 amplitudes capture the complexity linked to spatial patterns and amplitudes of tropical SST anomalies (Figure 5.2). As such, diversity in ENSO conditions and their respective teleconnections patterns can be mapped, as well as translated into risk estimates. We also note that SAT anomaly composites (for instance, based on select set of historical events) offer rough estimates of the conditional mean. However, our results clarify that modulation of tail probabilities integrates effects stemming from conditional mean, as well as higher moments that shape the conditional EPDF. In this respect, the example case for Lake Superior underscores the detailed nature of shifts in EPDF linked to diverse ENSO conditions (Figure 5.6).

4. Conditional quantile approach presented here affords conditional risk estimates derived from a limited length observational record, with ENSO conditions (represented with two leading principal components) as the covariates. Atmospheric circulation variability intrinsic to the extra-tropics exerts significant influence on the observed wintertime weather and climate over North America), as do long-term trends [e.g., 19, 44, 46]. These aspects of extra-tropical weather and climate variability are sampled in the observational records, albeit in a limited manner, and their expression within the EPDFs resides in the non-ENSO components of the variance. In other words, there are regions within North America, where ENSO PC1-PC2 related changes in risk are relatively modest, which indicates: (a) ongoing research examining other climatic phenomenon can offer critical new insights, and (b)

improved characterization of stochastic weather noise, and the extent to which that may overwhelm otherwise modest tropical SST influences.

5. The conditional quantile approach broadens climate diagnostic studies by not only assessing the changes in mean and variances, but also the entire distribution by characterization of heterogeneities across quantiles. Such improved diagnosis of sensitivity to wintertime North American SAT anomalies affords important insights regarding anticipated SAT anomalies during particular EP and CP El Niño, and La Niña years, which is of import to numerous human-environmental systems. A telling example is the sensitive linkages between ENSO and lake ice, wherein wintertime SAT-related thresholds, when exceeded, have the potential to significantly impact ecosystem health, as well as water quality [e.g., 22]. In closing, we note that continued improvements in the understanding of ENSO teleconnections and linked inter-annual climatic anomalies, when commingled with warming trends have the potential for large near-term impacts, a topic of high salience both for ENSO predictability and attribution studies. Our empirical approach complements recent studies that assess ENSO teleconnections in coupled climate model-based simulation with an eye on event diversity [84].

CHAPTER 6
FREEZING DEGREE-DAY THRESHOLDS AND LAKE ICE PHENOLOGY: UNDERSTANDING THE ROLE OF EL NIÑO CONDITIONS

6.1 Introduction

In temperate and polar regions of North America, where lakes freeze during winter, wintertime accumulated freezing degree-day (AFDD)- calculated as the sum of mean daily temperature departures below the freezing point (0°C or 32°F)- is an important cold season weather-climate variable. AFDD determines the amount of freezing energy available in the air to grow surfical ice on lakes, and consequently analytical studies often estimate the thickness of lake ice cover to be roughly proportional to the square root of the winter AFDD [109]. However, the impacts of wintertime AFDD variations on lakes may not be limited to the cold season. For example, springtime ice-out dates for Maine (USA) lakes are linked to wintertime AFDD thresholds [22]. The prevailing winter climate, including the AFDD patterns over North America, has been shown to be sensitive to phases of El Niño-Southern Oscillation (ENSO), a coupled oceanic-atmospheric phenomenon in the tropical Pacific that affects weather and climate worldwide [e.g., 12, 15, 32]. For instance, during the 1997/98 El Niño event (warm phase of ENSO), northern US and southern Canada recorded one of their lowest winter AFDDs such that it resulted in the least extensive ice-cover in the Great Lakes over the past century. However, the severity and spatial extent of the North American weather and climate anomaly patterns associated with El Niño events is neither alike nor is it linearly opposite to that of La Niña (cold phase of ENSO) events [e.g., 78, 79, 180]. Studies have shown that such discrepancies may arise from differences in the location and amplitude of their signature SST anomalies in the tropical Pacific as variations in the location of the warmest waters (SST > 27.5°C) in the tropical Pacific generate differential atmospheric wave trains responsible for climate

variability worldwide [e.g., 18, 78]. Furthermore, Beyene and Jain [23] showed that the sensitivity of North American winter temperatures to diverse ENSO flavors is not uniform, both regionally and across different parts of the empirical probability density function (EPDF). In the present context, a salient question is: to what extent do distinct El Niño flavors affect North American lake ice-out dates through their differential effect on the (EPDF of) winter AFDD? Two aspects of current and future ENSO variability further motivate the above noted line of inquiry: (a) five-fold increase in the frequency of a new variant of ENSO is being projected under anthropogenic climate change [e.g., 39, 182], (b) ENSO-based climate forecasts on seasonal and longer lead-times have proven to be reliable [81]. To this end, this study aims to develop location specific risk functions for North American winter AFDD, that incorporate as covariates ENSO indices that capture the location and amplitude of tropical Pacific SST anomalies, in order to estimate ENSO-related changes in the relative occurrence probability of early/late lake ice out events in North America. In this study, the term occurrence probability is used interchangeably with risk and likelihood. Past lake ice studies often assessed ENSO-induced changes in lake ice season by characterizing the response of local meteorological variables (relevant to lake ice evolution) to large-scale climate patterns using traditional statistical methods such as linear regression and averaging of sub-samples. However, analyses employing these methods offer limited insight, as they primarily measure the shift in the conditional mean and not the conditional tails of the distribution, where climate-related thresholds in lakes usually reside. This study thus employs quantile functions, first proposed by Koenker and Bassett Jr [100], to investigate the response of North American winter AFDD, across its variability range, to the amplitude and location of tropical Pacific SST warming/cooling, linked to ENSO events. This approach provides a functional framework to estimate the winter AFDD conditioned on ENSO indices with three important features: (a) no distributional assumption, (b) quantification of differential sensitivity across quantiles, and (c) resistance to outlier effects. Beyene and Jain [23] have

shown that the change in the conditional risk of North American winter temperatures due to ENSO flavors varies both regionally and across different temperature quantiles. This study extends their work and aims to quantify ENSO related changes in North American lake ice out dates by characterizing its effect on winter AFDD variability. Two key tasks in this regard are as follows:

1. Quantify the nature of relationships between lake ice and winter AFDD variability, based on observational records for a select group of lakes across North America.

2. Estimate ENSO-related changes in the relative likelihood of early/late lake ice out events for eight North American lakes- location-specific risk functions for North American winter AFDD that incorporate ENSO indices as covariates are developed.

6.2 Data and Methods

Lake Ice-out (off) Dates: Lake ice-out date refers to the date when winter ice completely disappears from the lake surface. In this study, eight North American lakes (see Figure 6.1 for lake locations) that freeze during the winter were selected and their historical lake ice-out dates from 1950-2010 were downloaded from the following electronic databases: Global Lake and River Ice Phenology Database (at National Snow and Ice Data Center) and Lake Ice Clearance and Formation dataset (at Niwot Ridge Long Term Ecological Research Center). In Table 6.1, geomorphological data and site of observation for ice out dates is provided for the eight selected lakes.

North American Winter AFDD: Time series of gridded, daily mean temperature data for North America from 1951-2010 were derived from HadGHCND dataset [38], which provides station-based, daily observations of average temperature data on a 2.5°x3.75° grid resolution. The year-to-year winter AFDD for North American fields were then calculated as the daily degrees below freezing (0°C) summed over the total number of days (n) from December to February that the daily average temperature was below freezing:

Lake	Latitude (°N)	Longitude (°E)	Surface Elevation (m)	Surface area ($10^6 m^2$)	Mean Depth (m)	Site of ice-out observation
Damariscotta	44.19	−69.48	15	17.5	9.0	Northern End
Superior	47.70	−87.5	183	82.1	147	Bayfield
Winnipeg	52.12	−97.25	217	24.5	12	South Beach
Deadman's Pond	48.95	−54.57	NA	NA	NA	NA
Dease	58.42	−131	803	NA	NA	NA
Lesser Slave	55.30	−114.78	578	1168	11.4	NA
Long	62.47	−114.45	303	0.27	5.0	Yellowknife
Albion	40.05	−105.60	3345	NA	NA	NA

Table 6.1. Geomorphic data for selected Maine lakes.

$$AFDD = \sum_{i=1}^{i=n} (T_o - T_i), T_i < T_o \tag{6.1}$$

Where T_i is the daily average air temperature (°C) and T_o is the freezing point of water which is often taken as 0°C. Lake ice occurs predominantly in regions with regular occurrence of sub-freezing temperatures and wintertime AFDD. Climatological winter AFDD patterns over North America (Figure 6.1a, b) indicate that regions with pole ward of 35°N show appreciable below-freezing temperatures; this region will be the focus of investigation in the remainder of this study.

Relationship between AFDD and lake ice thickness: Lake ice formation and growth results from the dynamical heat balance at lake surface [109]. Given that the surface air temperature strongly relates to major energy fluxes from lake to atmosphere, analytical studies often use the degree-day method- first derived by Stefan (1891)- to approximate the thickness of winter ice formed on lake surface. In general, in a degree-day model, ice growth (h) in inches, is modeled as a function of the square root of the accumulated freezing degree-days (AFDD)

$$h = C\sqrt[2]{AFDD} \tag{6.2}$$

where C is a coefficient that accounts for local snow and atmospheric conditions and AFDD is in Degree-Day Celsius (DDC) [13]. In Appendix D2, we provide a detailed exposition of this physical basis of the relationship noted above.

ENSO Indices: The emergence, type and strength of El Niño /La Niña events are often based on areal averaged SST indices for four regions in the tropical Pacific: Niño 1+2, Niño 3, Niño 3.4 and Niño 4 (see Figure E.1). In this study, time series of monthly, spatially averaged SSTs for the four Niño regions from 1951-2010 were collected from a dataset prepared by NOAA Climate Prediction Center, based on extended, reconstructed sea surface temperature (ERSST) V4 dataset. Time series of winter Niño SST indices from 1951-2010 were then computed by averaging the December to February SST index for each Niño region (see Supplementary Figure E.1b). Geographical distributions of ENSO-related tropical Pacific SST anomalies (warming or cooling relative to long-term averages) have been identified as important contributors to the spatial patterns and severity of climatic impacts in remote regions. Thus, it is critical to identify a small set of ENSO indices that best represent the detailed pattern of SST warming or cooling in the tropical Pacific. In this study, Principal Component Analysis was performed on the time series of mean winter SST indices of the four Niño regions from 1951-2010 (see Appendix E.1). The resulting pair of indices (Principal Component 1 and 2, hereafter referred as PC1 and PC2) account for 99.8% of the total variance in the ENSO historical record (PC1 = 89% and PC2 =10.8%). While PC1 and PC2 time series comprehensively characterize the temporal variations in ENSO over the past six decades, the spatial loadings linked to these PCs offer helpful interpretation of the tropical Pacific warming and cooling patterns associated with ENSO events (see Figure E.2). PC1 loadings across the four Niño regions are of the same sign suggesting synchronous wintertime SST variation across all Niño regions (see Table E.1 and Figure E.2b). PC2 loadings are characterized by an east-west dipole pattern with the wintertime SSTs in Niño-1+2 (eastern Pacific) region varying out of phase with that of Niño-3.4 and Niño-4 (Central Pacific) regions (Figure E.2c). Beyene and Jain [23] and

others have showed that the joint indices of PC1 and PC2 allow characterization of the amplitude and location of maximum TP SST anomalies associated with diverse El Niño/La Niña events (see Appendix E.1). Therefore, PC1 and PC2 indices are used as covariates/predictors in the quantile regression pursued in this study. Finally, as noted in the previous section, recent improvements in the understanding on ENSO flavors imply distinct patterns of climatic impacts across North America, and projected trends for the 21^{st} century reveal dramatic shifts in ENSO frequency- the associated risk to environmental variables such as lake ice remains unclear. Quantile Regression: Historical winter AFDD variability at a particular location can be summarized based on a frequency distribution or probability density function (PDF). Characteristic AFDD values that correspond to specific quantiles (representing non-exceedance probability) can be obtained from the PDF. For instance, the AFDD value for the 0.25^{th} quantile is exceeded 75% of the time. An extension of this approach allows modelling of quantiles based on covariates or predictors (for example, ENSO conditions) that modulate the conditional quantile functions for the target variable (in our case, AFDD). In its general form, quantile regression [101] affords conditional quantile estimates for each quantile, and as such, conditional PDF. These estimates are superior to ones from linear regression, wherein covariate effects are restricted to affect on the mean of the target variables. Example applications of quantile regression in lake studies include [26, 59, 181]. In this study, the quantile regression approach is used to model and predict the linear response of North American winter AFDDs, across all or selected quantiles, to ENSO indices (X_i). Mathematically, this can be expressed as

$$AFDD(\tau) = \beta_0^{(\tau)} + \beta_1^{(\tau)} PC1 + \beta_2^{(\tau)} PC2 \tag{6.3}$$

where $\beta_0^{(\tau)}$ is the intercept, and $\beta_1^{(\tau)}$ and $\beta_2^{(\tau)}$ are the slope coefficients for PC1 and PC2 patterns at τ^{th} quantile. The regression parameters $\beta^{(\tau)}$ are obtained by solving for minimization of the sum of weighted absolute residuals. The quantile regression implementation in the R computing environment [99] is employed to provide the optimizing algorithm to estimate $\beta^{(\tau)}$ using linear programming techniques. Estimation of conditional

winter AFDD quantiles requires fitting of curves across each quantile independently and as such generating multiple conditional winter AFDD quantile functions may yield quantile curves that cross or overlap, creating an invalid distribution. To alleviate the crossing problem in quantile regression, a procedure introduced by Bondell et al. [31], which imposes a non-crossing constraint, is applied. The statistical significance for parameter estimates, $\beta^{(\tau)}$ in the conditional winter AFDD functions were assessed by constructing the confidence interval using the wild bootstrap method, an approach that is almost unaffected by residual heterogeneity [58].

6.3 Results

6.3.1 Winter AFDD and North American Spring Lake Ice-out Dates

Empirical and theoretical rationales are needed to establish the import of seasonal winter (December-February) AFDD on North American lake ice season. To this end, Appendix E.2 presents a synopsis of the theoretical-physical basis underlying AFDD-lake ice linkages. This section on the other hand, offers empirical findings by analyzing the observed response of spring lake ice-out dates to their antecedent winter AFDDs for eight North American lakes (see Figure 6.1c-j). Here, the efficacy of winter AFDD in conditioning the spring lake ice out dates was examined using non-parametric kernel regression approach, as the functional relationship between winter AFDD and spring ice-out dates is unknown and may vary across lakes. Kernel regression method [33] is based on a smoothing approach that is locally adaptive, thus allowing for the estimation of linear and nonlinear relationship from data. The degree of smoothing depends on the bandwidth, which is selected based on a minimization of integrated error. In the context of ice-out and winter AFDD relationship, of particular interest is the diagnosis of nonlinearity and potential break points in the relationship (akin to thresholds). Results of this analysis show that for all selected lakes, there is a positive (direct) relationship between winter AFDD and spring ice-out dates, which implies that winters with relatively low (high) winter

AFDDs are generally related to earlier (later) than normal lake ice-out dates the following spring (see 6.1c-j). However the degree of sensitivity of spring ice-out dates to winter AFDDs in these lakes varies both spatially and across different winter AFDD quantiles. For instance, contrasting the overall slope of the winter AFDD regression line across the eight lakes indicate that the response of spring ice-out dates to the antecedent winter AFDD variability is relatively stronger at Lake Superior (USA) and Damariscotta Lake (USA) as compared to those at Lake Albion (USA) and Long Lake (Canada). This implies that the strength of association between spring ice-out dates and the antecedent winter AFDDs for North American lakes shows geographical variation and locally, is also likely to be modulated by other factors such as morphometry, elevation, and continentality. On the other hand, examining the response of spring ice-out dates of the eight lakes across different winter AFDD quantities reveals that unusually low /high winter AFDDs are strongly related to early/late spring ice-out dates. For instance, for Damariscotta Lake, 5 of the 6 winters with AFDD less than 200 Degree Day Celsius (DDC) ($tau < 0.30^{th}$) are associated with ice-out dates earlier than April 3^{rd} (see figure 6.1H). Similarly for Lesser Slave Lake (Canada), 5 of the 6 winters with AFDD less than 2270 DDC ($\tau < 0.28^{th}$) are linked to ice out dates that occurred prior to May 15^{th} (see figure 6.1D).

These findings on the presence of winter AFDD quantities that correspond to early/late spring ice-out dates for North American lakes is consistent with the findings reported in [22]. This implies that the efficacy of ENSO events in modulating the variability of ice-out dates in lakes depends on their effect on the occurrence of winter AFDDs associated with ice-out dates. Thus, characterization of ENSO-related change in risk of early/late ice dates requires an understanding of the relationship between different El Niño (or La Niña) events and winter AFDD at specific quantiles, as well across the entire winter AFDD distribution. It should be noted that for studied lakes, the degree of coherence between winter AFDD and spring ice-out dates can generally be assumed to be independent of spring temperature

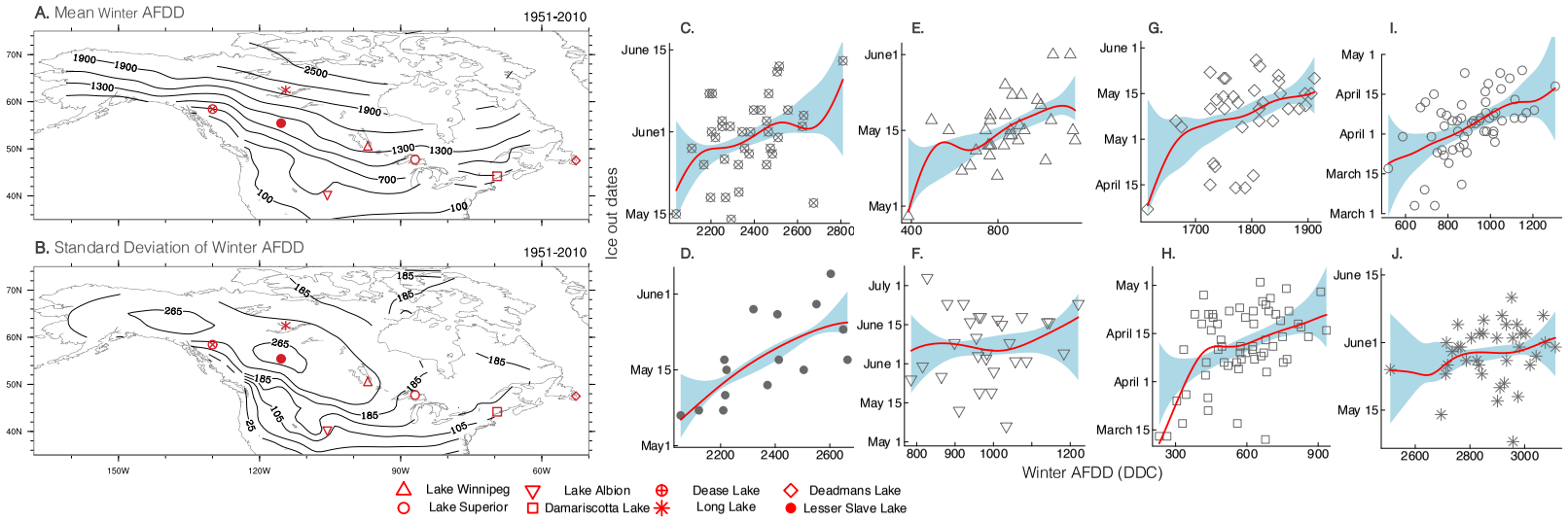

Figure 6.1. Climatology of winter accumulated freezing degree days (AFDD) over North America Climatology of winter accumulated freezing degree days (AFDD) over North America and its relationship with lake ice out dates.

conditions, as there is no significant ($p < 0.1$) correlation between winter and spring AFDD for almost all North American regions (see Figure E.4).

6.3.2 ENSO Diversity and North American Winter AFDD Variability

Differences in the location of peak ENSO-related Sea Surface Temperature (SST) warming/cooling in the Tropical Pacific (TP) contribute to the observed variability in ENSO-related climate patterns in North America [79]. To illustrate this difference in the context of North American winter AFDD, five years were selected where by majority agreement of different ENSO identification methods (EP/CP method, Niño3/4 method, EMI method and regression-EOF method) have been determined as Central Pacific (CP) El Niñoo (1969, 1988, 1995, 2003, 2005, 2010), Eastern Pacific (EP) El Niño (1973, 1983, 1987, 1998, 2007) and La Niña events (1956, 1971,1974, 1976, 1989) (see Table E.2). It should be noted that our use of EP and CP El Niño terminology in this study serves only to contrast the site of peak SST warming in TP between the two El Niño patterns, and is by no means implying that these patterns are distinct modes of El Niño. The composite TP winter SST anomaly (departure from the long-term average) pattern for the five CP El Niño events selected features peak SST warming confined in the central TP regions (Niño3.4 and Niño4 regions) flanked by cooler than normal SSTs on both sides of the equatorial Pacific (see Figure 6.2a bottom). While there is some inter-event differences, the pattern of North American winter AFDD variability pattern corresponding to CP El Niño events can broadly be characterized as southeast-northwest dipole pattern, where there is relatively strong increase in the seasonal winter AFDD (colder temperatures) over the Midwest and northeast US regions and decrease in winter AFDD (warmer temperatures) over western US and Canadian regions and northern edges of Canada (see Figure 6.2a top). In contrast, the location of maximum SST warming in the TP during EP El Niño winters is concentrated in eastern TP extending from the western coast of South America to the regions east of the dateline (Niño1+2 & Niño3 regions) (see Figure 6.2b). Moreover, these

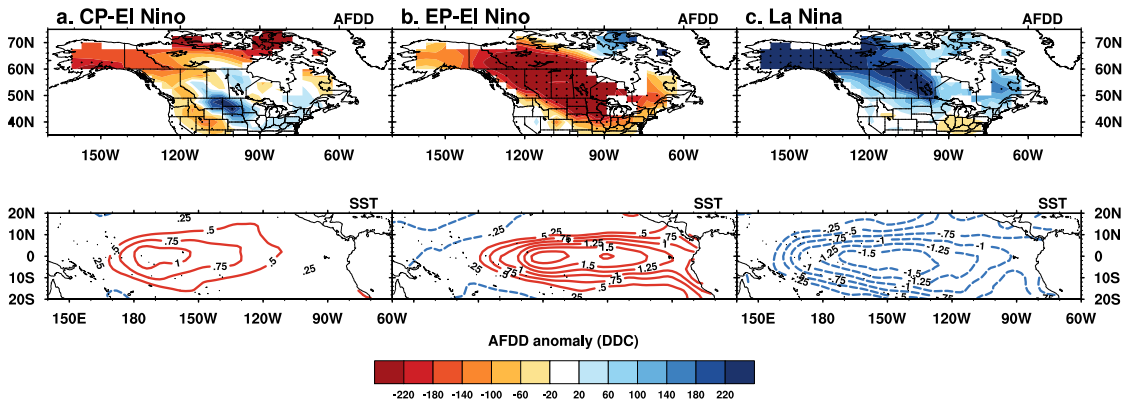

Figure 6.2. Composite maps of tropical Pacific winter SST warming/cooling and associated North American winter AFDD anomalies Composite maps of tropical Pacific winter SST warming/cooling and associated North American winter AFDD anomalies for select five (a) CP El Niño, (b) EP El Niño, and (c) La Niña events.

events are associated with a significant decrease of winter AFDD over much of North America (except for the Pacific US regions and Baffin Island). These results illustrate that the location of maximum SST warming in the tropical Pacific has important implication on the impact of individual El Niño events on the winter AFDD over US and Canada. On the other hand, the composite TP winter SST anomaly pattern for the five La Niña events exhibits peak SST cooling over central-eastern equatorial Pacific (Niño3 and Niño4 regions). Moreover, the North American winter AFDD anomaly patterns related to these events generally features a northwest-southeast dipole pattern with a relatively strong increase in winter AFDD over western Canada and Alaska and decrease in winter AFDD over the Southeast US states. These results reveal the effect of La Niño]a events on the winter AFDD of various North American regions is not a mirror opposite to that of El Niño events. They also establish the significance of tropical Pacific in producing non-linearity in the response of North American winter AFDD to opposite phases of ENSO.

In summary, the above findings show that the ENSO-winter AFDD relationship for North America varies with the location of peak ENSO-related SST warming and/or cooling in the TP. In other words, the efficacy of El Niño (or La Niña) events in modulating the conditional winter AFDD distribution for North American regions shown spatial variation.

Consequently, in the face of EP or CP El Niño/La Niña episodes, the likelihood associated with various AFDD magnitudes, including the ones that correspond to early/late spring ice-out dates in North American lakes, is marked by differential sensitivities. Quantile regression framework offers conditional risk estimates of AFDD at a location as well as regional scale.

6.3.3 ENSO Patterns and Lake Ice Season Risk Assessments

It was noted in earlier sections that there are winter AFDD quantities that correspond to early/late spring ice-out dates for North American lakes. The efficacy of quantile functions in generating AFDD quantiles conditioned on ENSO indices can thus offer usable risk estimates for unusually early/late ice-out events in these lakes. For instance, figure 6.3a shows that for Lake Superior, winters with AFDDs less than 820 Degree-day Celsius (DDC) ($\tau < 0.31^{th}$) are strongly associated with spring lake ice-out dates prior to March 30^th, and according to the climatology, the occurrence probability of such mild winters is 0.30. Please note that the method used here for determining the winter AFDD threshold is highly subjective and as such serves only for illustrative purposes only. To estimate the change in the conditional risk of early lake ice-out dates at Lake Superior due to ENSO patterns, a set of quantile functions for winter AFDD (that incorporate ENSO indices as covariates) were fitted at $\tau = 0.01$ intervals over the quantile range ($0.01 < \tau < 0.99$) and these function were used to compute winter AFDDs at the respective quantiles for sample combination of PC1-PC2 indices. Figure 6.3b shows the resulting conditional winter AFDD distribution as well as conditional risk of winter AFDDs less than 820 DDC for archetypical ENSO flavors (derived as centroids of PC1-PC2 index for the five selected EP, CP El Niño and La Niña events mentioned in the first result section). From these, it can be observed that during archetypical EP El Niño events, the likelihood of mild winters that engender early ice-out dates at Lake Superior increases by 2.16 times relative to that of the climatology (probability = 0.31). During typical CP El Niño pattern however, there is no

significant change in the occurrence probability of early ice out dates at Lake Superior relative to that of the climatology. Contrary to the traditional assumption, this result highlights that the effect of different El Niño flavors on North American lake ice-out dates are not alike. Figure 6.3c extend the results in figure 6.3b to depict the change in risk (relative to that of the climatology) of early ice-out dates for sample combinations of PC1 and PC2 indices. Broadly speaking, the conditional risk of early ice-out dates at Lake Superior increases from region of negative PC1 and positive PC2 to a region of positive PC1 and negative PC2. This means that strong EP El Niño patterns (PC1 $>$ 2 & PC2 $<$ 0) are related to an increase the relative likelihood of early ice-out dates at Lake Superior by 1.2 - 2.5 times that of the climatology, while strong CP El Niño events (PC1 $>$ 1 & PC2 $>$ 0) correspond to a rise in the relative risk of early ice out dates by 0.9-2.4 times. On the other hand, La Niña events (PC1 $<$ -1.5 & PC2 $<$ 0) reduce the relative occurrence probability of mild winters by 0.6-1.

Diversity in the influence of different ENSO patterns on North American lake ice-out dates can be illustrated by contrasting the change in the likelihood of mild winters that produce early ice-out dates, due to the three archetypical ENSO patterns, for the eight North American lakes. Results reveal that the effect of ENSO pattern on the timing of North American spring lake ice-out dates varies both spatially and for different ENSO events (see Figure 6.4). For seven of the eight lakes, the archetypical EP El Niño pattern increases the likelihood of mild winters that correspond to early ice-out dates, by 1.5-2.8 times to that of the climatology, while for Deadman Pond the occurrence probability of such winters decreases by 0.63 times relative to the climatology. In contrast, at Damariscotta Lake and Deadman Pond, typical CP El Niño pattern decreases the likelihood of mild winters that are associated with early ice out dates, by 0.4-0.8 times to that of the climatology, while for the other six lakes it has modest or no effect on the risk of such winters. On the other hand, for Lake Albion (Deadman Pond), archetypical La Niña pattern reduces (increases) the occurrence probability of mild winters by 0.46 (1.2)

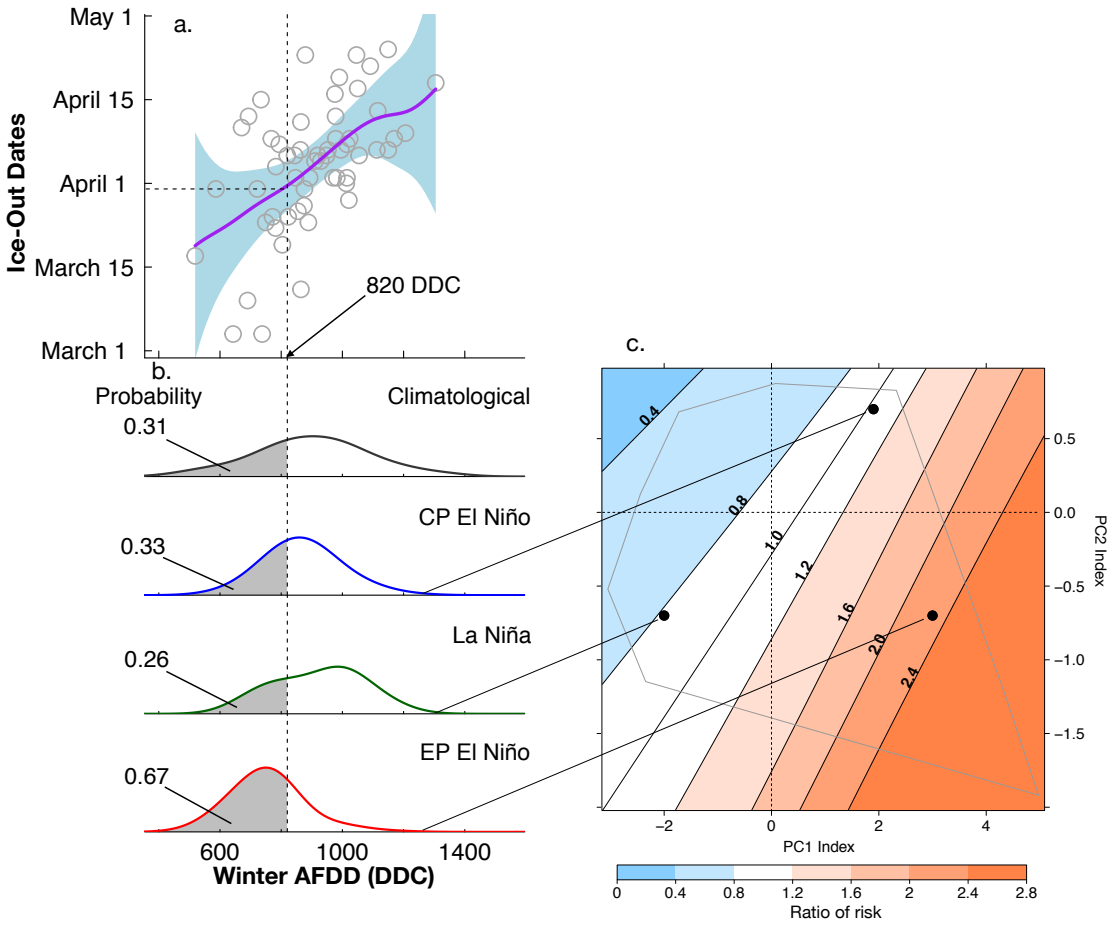

Figure 6.3. Risk estimates for winter AFDD quantiles, corresponding to spring ice-out dates, earlier than April 1 at Lake Superior, conditioned on different ENSO patterns.

times to that of the climatology, while for the other six lakes, it is associated with modest or no changes in risk of early ice out dates. These results taken together show that for North American lakes, (a) the effect of EP El Niño on the timing of ice-out dates is quite distinct to that of CP El Niño from local-to-regional scale, (b) El Niño related changes in the timing of spring ice-out dates is not a linear opposite to that of La Niña events. As discussed in earlier sections, these effects stem from the asymmetry in the regional AFDD patterns associated with El Niño/La Niña flavors and distinctness of AFDD thresholds for ice-out dates among local lakes. Figure D.6-D.10 depicts the wintertime AFDD quantities that correspond to early ice out date in lakes and the results of the conditional risk analysis for sample combinations of PC1 and PC2 for the seven other lakes.

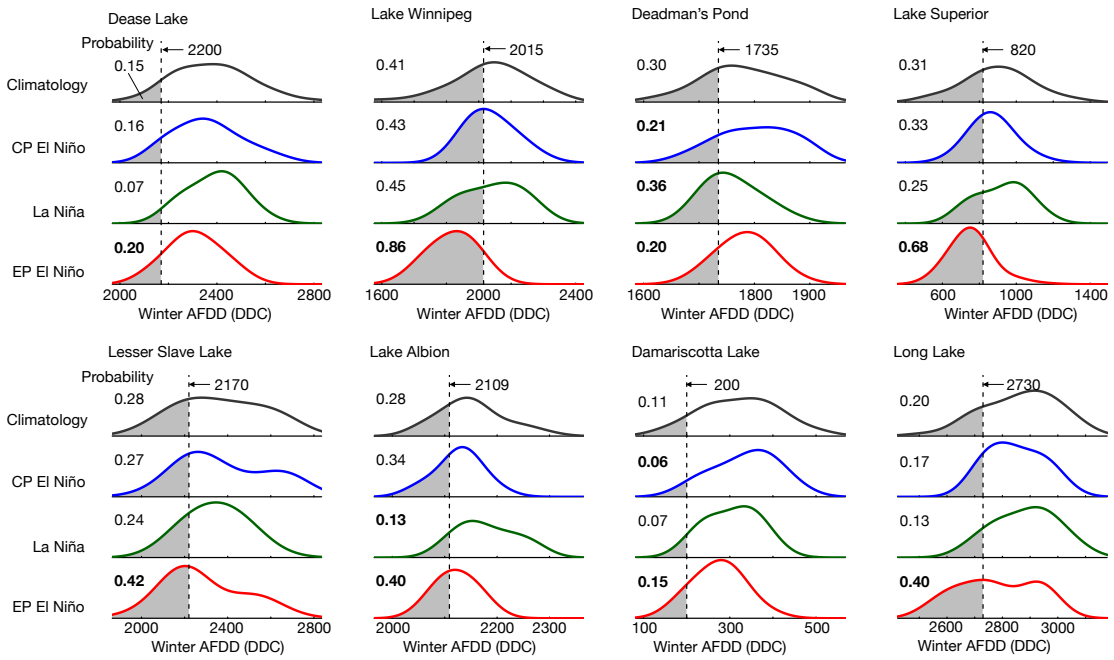

Figure 6.4. Risk estimates for winter AFDD quantities (corresponding to early lake ice out dates for selected North American lakes) conditioned on three archetypical ENSO flavors.

6.4 Discussion and Summary

ENSO-related warming/cooling in the tropical Pacific sea surface temperatures cause systematic shifts in the North American wintertime Accumulated Freezing Degree-days (AFDD) patterns. Winter AFDD governs the thermal flux between lake and atmosphere to grow lake ice, and early/late spring ice-out dates have been sensitively linked to seasonal winter AFDD thresholds. Consequently, changes in the magnitude and frequency ENSO has the potential to cause shifts and transitions in the ice regime of North American lakes. Our analysis of the response of spring ice-out dates to winter AFDD for select North American lakes reveals two important features. One is that for North American lakes, the relationship between winter AFDD and spring lake ice-out dates can be characterized from quasi-linear to highly non-linear. Second, in a number of these relationships, there are AFDDs (thresholds) that are strongly associated with specific ice out dates. Thus, the conditional quantile regression approach developed in this study allows a detailed characterization of quantile-specific ENSO-AFDD that can be readily used to estimate risk

functions for AFDD and lake ice out conditioned on ENSO. Results for seven out of the eight North American lakes show that typical Eastern Pacific (EP) El Niño pattern is associated with an increase in the risk of low winter AFDDs (that produce early ice-out dates in these lakes) by 1.5-2.8 times to that of the climatology, while the typical Central Pacific (CP) El Niño pattern corresponds to a decrease or no significant change in the likelihood of early ice-out dates in these lakes. On the other hand, for Deadman Pond (Lake Albion) the archetypical La Niña pattern induces an increase (decrease) the occurrence probability of early ice out dates by 1.2 (0.46) times relative to that of the climatology. To summarize: (a) the effect of CP and EP El Niño on the timing of spring ice-out dates of North American lakes is distinct from local-to-regional scale, (b) for North American lakes, the change in the timing of spring ice-out dates due to El Niño and La Niña patterns is not linearly opposite. In conclusion, we offer the following observations and discuss emerging research directions:

1. The results from this study and others [e.g., 15, 32] demonstrate that ENSO patterns greatly influence the local-to-regional patterns of lake ice-out dates for North America. Detection and evolution of ENSO events in the tropical Pacific is a well understood subject and as such, magnitudes of ENSO events are estimable up to 9 months in advance [e.g., 81, 137]. These imply that the ENSO-related conditional risk functions developed here pave the way for use of seasonal and longer-lead ENSO forecasts that can be profitably used to anticipate shifts in lake ice out dates.

2. The quantile regression risk framework advanced in this study, while specific to lake ice out, is applicable to other lake variables to assess climate-related risk and vulnerability. While a linear approach was taken here, nonlinear and non-parametric approach can be used to model complex relationships (for example, ones involving lake chemistry).

3. Changing weather/climate patterns reflect trends and inter-annual variability (for example, due to ENSO). Resulting seasonal temperatures can disrupt the lake phenology and linked processes, species dynamics and succession, and nutrient loading and mixing characteristics. For instance, for temperate and arctic North American lakes, winter climate variability has directly or indirectly been shown to affect ice cover phenology and extent [e.g., 15, 22], , water temperatures [e.g., 14], onset of stratification [e.g., 179], seasonal plankton composition, abundance and succession [e.g., 67, 70], fish population [56] and seasonal geo-chemical dynamics [e.g., 90, 132]. In a changing climate, successful conservation and restoration of lake ecosystems can benefit from climate-based risk framework presented here, thus affording pinpointed estimates of trends and transitions in lake variables. Finally, improved understanding and prediction of lake and river ice conditions has important environmental and socio-economic (e.g. recreational, hydro-power generation, cultural, commercial) implications, a point underscored in recent studies [e.g., 52, 135].

CHAPTER 7
SUMMARY AND FUTURE WORKS

This research was inspired by (a) the import of winter ice and related ecology on lake structure and function of northern Temperate and Arctic regions, (b) uncertainty over the efficacy of winter weather-climate conditions on winter lake ice cover duration, and (c) the advantage of incorporating winter weather-climate information for season-ahead or longer risk assessments of lake transitions at local and regional scale. This dissertation has focused broadly on two key aspects of the role of winter weather-climate variability on spring lake ice-out dates and related lake-watershed processes:

1. Assessing and quantifying the import of local-to-regional winter weather-climate patterns on lake ice cover duration

2. Evaluating the sensitivity of inter-linked ecological and social systems within lake watershed to shifts in winter ice cover duration.

All studies in this dissertation were based on long-term (1951-2010) records of observed ice-out dates for various Maine lakes and high-quality daily and monthly climate data. Most analyses were done using diagnostic statistical methods that employ fewer assumptions, preserve the inherent nature of data and are more descriptive. The main findings from this research can be divided into three categories: (a) those with applicability to regional climate studies, (b) those with applicability to climate and lake ice relationship researches, and (c) those with applicability to climate based risk assessments for lake transition studies.

7.1 Winter Weather-Climate Conditions and Local-to-Regional Lake Ice Cover Duration Relationship Studies

Ice-cover duration in North American regions shows significant dependency on the antecedent seasonal winter degree-days. However this dependency varies both at local and regional scale. Spatially, the seasonal winter degree-days has increased influence on the timing of spring ice-out dates for lakes at lower latitude, lower elevation and near the coast as compared with those at higher elevation, higher latitude and away from coast. For instance, results from Chapter 2 show that the inclusion of winter degree days in ice-out date models conditioned on a suite of predictor climate variables provides higher explanatory capacity for lakes in coastal and southern interior Maine regions as compared with those in northern interior regions. This is because in higher latitude/altitude and continental regions, late fall and/or early spring seasons provide some of the freezing energy to form and grow ice cover on lakes, and this reduces the efficacy of daily winter temperatures in modulating the ice cover season through their control over the lake ice cover growth. On the other hand, the variability of spring ice-out dates in large, deep lakes show higher response to the seasonal winter degree-days as compared with shallow and small lakes in the same region. For instance, results from Chapter 2 show that despite being in the same climate region, the spring ice-out dates at Lake Moosehead- the largest and deepest lake in Maine- shows relatively higher sensitivity to winter degree-days as compared with that of Lake Sebec.

For northern Temperate and Arctic regions, the relationship between seasonal winter degree-days and ice cover duration is often non-linear. In particular, the spring ice out dates of lakes shows higher sensitivity to lower AFDD and higher AMDD, as compared with higher AFDDs and lower AMDDs. This is mainly because of the temperature-ice thickness relationship, which in turn causes the observed non-linear relationship between spring ice out dates and antecedent winter degree-days. For instance results in chapter 3 show that for Lake Damariscotta, over 80% of the earliest 15 spring ice-out dates had

winters (January-February) with accumulated freezing degree days (AFDD) less than 310 degree day centigrade, while less than 7% of the latest 15 ice out dates occurred during these winters. On the other hand, over 75% of the latest 15 spring ice-out dates at Lake Damariscotta occurred during winters with AFDD greater than 370 DDC, while none of the 15 earliest spring ice-out dates occurred during such winters.

Inter-annual winter climate variability has as much influence as trends in modulating the statistics of early/late ice out dates of northern Temperate and Arctic lakes. For instance, results in Chapter 3 revealed that the pattern of Tropical/Northern Hemisphere (TNH)- a large-scale winter climate variability pattern that operates at inter-annual scale- is a primary climate determinant influencing the frequency of the earliest 10 ice-out dates from 1950-2010 for Maine lakes.

TNH and to a lesser extent the North Atlantic Oscillation (NAO) pattern were identified as the most relevant large-scale winter teleconnection patterns, operating at inter-annual time scale, that determine the statistics of lake ice-out dates in Maine. The efficacy of TNH and NAO patterns in engendering shifts in the lake ice season in Maine through its effect on the seasonal winter degree-days depends on (i) the sensitivity of spring ice-out dates of lakes to the antecedent winter degree-days (ii) the modulating influence of the two patterns on the winter degree-day statistics particularly the winter degree-day thresholds. Consequently, the effect of TNH and NAO patterns on the spring ice-out date of Maine lakes varies both spatially and locally. Results in Chapter 3 show that the pronounced negative phase of TNH ($TNH < -0.47$) pattern was found to increase the likelihood of early spring ice-out dates for studied Maine lakes, although this influence decreases for small, shallow lakes in interior regions. On the other hand, the efficacy of pronounced positive NAO ($NAO > 0.2$) patterns in increasing the risk of early ice-out dates in Maine lakes is limited to coastal lakes. Given that the occurrence of negative TNH phases is highly correlated to the state of the tropical Pacific SSTs, the efficacy of El Niño-Southern Oscillation pattern (ENSO) in modulating the local-to-regional patterns of

ice-out dates in North America through its effect on the winter AFDD statistics was also assessed. Results in Chapter 4 show that the response of North American winter AFDD to the location and amplitude of ENSO-induced tropical Pacific SST patterns differs both spatially and across different quantiles. For Maine lakes, the archetypical Eastern Pacific (EP) El Niño pattern was associated with an increase in the conditional risk of winter AFDD thresholds that engender early ice out dates by 60-80%, while the Central Pacific (CP) El Niño pattern was associated with a decrease in the conditional risk by 20-40%.

7.2 Climate based Risk Assessments for Shifts and Transition in Lake Ecosystem

The tentative conceptual SES framework for ice out dates in Chapter 5 reveals that shifts in ice cover duration potentially can produce perturbations that span across multiple lake watershed domains and seasons. Furthermore, it shows that effect of early ice-out dates on social and ecological domains within lake watershed system (may) stem from different pathways and feedbacks between different sub-systems. For instance, the warming influence of shorter ice cover duration on summer lake surface water temperature may arise from the commingled effect of one or more of this ice induced changes on lake system: increased absorption of solar radiation, increased surface phyto-plankton biomass and decline in lake water volume.

The presence of antecedent winter degree-day thresholds that engender shorter ice cover duration in lakes indicates that there (may be) are winter thresholds that cause regime shifts in vulnerable lake ecosystem through their effect on lake ice duration. For instance, for Lake Auburn, it was found that winters with AFDD less than 750 DDF are associated with early spring ice-out dates. Furthermore, depending on the degree to which regional-to-global winter climate patterns influence the statistics of these lake winter thresholds, information on these patterns allows local-to-regional assessments of risk of changes in lake characteristics and stability from seasonal or multi-decadal time scale.

The efficacy of winter ice and related ecology in modulating the lake structure and functions in northern cold regions can be enhanced/moderated by the commingling effect of other stressors in the lake-watershed. For instance, heavy spring rainfall events increase the availability of nutrients and suspended matters across the lake water column. With the effect of early ice-out dates in increasing the level of radiation reaching lake surface, lengthening the growing season for heterotrophic algae, heavy spring precipitation events add to the potency of early ice-out date impacts on lake water temperatures, lake water quality and quantity and eco-system health and services.

7.3 Regional Climate Studies

TNH and to a lesser extent NAO are identified as the most relevant large-scale winter teleconnection patterns, operating in inter-annual time scale, that influence the statistics of seasonal winter degree-days (AFDD and AMDD) in Maine (see Chapter 3). TNH is strongly associated with the winter AFDD, while NAO is related to the winter AMDD. The modulating effect of TNH and NAO patterns on the winter degree statistics in Maine varies both spatially and across different indices. Regionally the strength of influence of TNH increases towards interior regions while it is vice versa for NAO. Also the modulating effect of TNH (NAO) on winter temperatures is higher in its negative (positive) phase than in its positive (negative) phase.

The sensitivity of North American winter AFDDs to different ENSO flavors varies both spatially and across different quantiles. For instance, for most North American regions, the upper quantile Winter AFDDs have higher response to ENSO indices than those in the lower quantiles (see Chapter 4). Also the leading pattern of tropical Pacific winter SST variability (akin Eastern Pacific El Niño) has an inverse relationship with the winter AFDD for most Canadian and northern tier US States, while the second leading pattern (akin Central Pacific El Niño) has northwest-southeast dipole patterns.

The observed heterogeneity of the sensitivity of North American winter AFDD to particular tropical Pacific SST anomaly (represented as a point within the PC1-PC2 space) can be related to differential shifts throughout the SAT EPDF. In conventional terms, this would translate into changes in the central tendency, as well as higher moments. The resulting conditional EPDFs reflect contributions from PC1 and PC2 patterns amplitudes, which in turn may cause amplified or muted shifts for a particular winter AFDD quantile.

The conditional quantile approach broadens the climate diagnostic approaches to not only assess the changes in mean and variances, but also the entire distribution by characterization of heterogeneities across quantiles. Such improved diagnosis of sensitivity to wintertime North American winter AFDD affords important insights regarding anticipated winter AFDD anomalies during particular EP, CP El Niño, and La Niña years, which is of import to numerous human-environmental systems.

7.4 Future Studies

Studies have shown that the circular regression approach is the most appropriate for modeling circular data such as ice out dates. As such in this study, the efficacy of winter degree-days and other seasonal variables in modulating the timing of spring ice out dates was examined by developing circular regression model for ice out dates conditioned on an array of winter and spring climate variables. However, future works on this topic is still needed including determining the role of other climatic/non-climatic variables on the inter-annual lake ice-out date variability, the use of different link functions in circular ice-out date models and performance of non-parametric circular regression approach for modeling ice-out dates.

The empirical study of the response of spring lake ice out dates in Maine lakes has revealed that there are winter degree-day thresholds that produce early/late spring ice out dates. To assess the uncertainty in these results, future model based diagnostic studies

where ice-out dates are simulated for several prescribed winter degree-days using physical lake models are needed.

The delineated SES framework for ice out dates developed in this study offers an insight into the import of lake ice on the workings of lake watershed systems in northern Temperate and Arctic regions. However it is by no means comprehensive as there is scarcity of published research works in the topic of winter limnology. To this end, model based SES studies may be needed in mapping sensitivity of lake watershed processes to shorter ice cover durations, the inter-linkages between systems and in describing the uncertainty.

REFERENCES

[1] W. P. Adams. Diversity of lake cover and its implications. *Musk-Ox Journal*, 18: 86–98, 1976.

[2] Rita Adrian, Norbert Walz, Thomas Hintze, Sigrid Hoeg, and Renate Rusche. Effects of ice duration on plankton succession during spring in a shallow polymictic lake. *Freshwater Biology*, 41(3):621–634, 1999.

[3] Rita Adrian, Susann Wilhelm, and Dieter Gerten. Life-history traits of lake plankton species may govern their phenological response to climate warming. *Global Change Biology*, 12(4):652–661, 2006.

[4] C. Agostinelli and U. Lund. *R package Circular: Circular Statistics (version 0.4-7)*. CA: Department of Environmental Sciences, Informatics and Statistics, Ca' Foscari University, Venice, Italy. UL: Department of Statistics, California Polytechnic State University, San Luis Obispo, California, USA, 2013. URL `https://r-forge.r-project.org/projects/circular/`.

[5] Wendy L Anderson, Dale M Robertson, and John J Magnuson. Evidence of recent warming and el niño-related variations in ice breakup of wisconsin lakes. *Limnology and Oceanography*, 41(5):815–821, 1996.

[6] Lauri Arvola, Glen George, David M Livingstone, Marko Järvinen, Thorsten Blenckner, Martin T Dokulil, Eleanor Jennings, Caitriona Nic Aonghusa, Peeter Nõges, Tiina Nõges, et al. The impact of the changing climate on the thermal characteristics of lakes. In *The Impact of Climate Change on European Lakes*, pages 85–101. Springer, 2009.

[7] Karumuri Ashok, Swadhin K Behera, Suryachandra A Rao, Hengyi Weng, and Toshio Yamagata. El niño modoki and its possible teleconnection. *Journal of Geophysical Research: Oceans*, 112(C11), 2007.

[8] G. D. Ashton, editor. *River and Lake Ice Engineering*. Water Resources Publications, 1986.

[9] George D Ashton. Freshwater ice growth, motion, and decay. *Dynamics of Snow and Ice Masses*, pages 261–304, 1980.

[10] George D Ashton. Thin ice growth. *Water Resources Research*, 25(3):564–566, 1989.

[11] George D Ashton. River and lake ice thickening, thinning, and snow ice formation. *Cold Regions Science and Technology*, 68(1):3–19, 2011.

[12] Raymond Assel, Sheldon Drobot, and Thomas E Croley. Improving 30-day great lakes ice cover outlooks. *Journal of Hydrometeorology*, 5(4):713–717, 2004.

[13] Andrew Assur. *Airfields on floating ice sheets: for routine and emergency operations*. na, 1956.

[14] Jay A Austin and Steven M Colman. Lake superior summer water temperatures are increasing more rapidly than regional air temperatures: A positive ice-albedo feedback. *Geophysical Research Letters*, 34(6), 2007.

[15] Xuezhi Bai, Jia Wang, Cynthia Sellinger, Anne Clites, and Raymond Assel. Interannual variability of great lakes ice cover and its relationship to nao and enso. *Journal of Geophysical Research: Oceans*, 117(C3), 2012.

[16] Anthony G Barnston and Robert E Livezey. Classification, seasonality and persistence of low-frequency atmospheric circulation patterns. *Monthly weather review*, 115(6):1083–1126, 1987.

[17] Anthony G Barnston, Robert E Livezey, and Michael S Halpert. Modulation of southern oscillation-northern hemisphere mid-winter climate relationships by the qbo. *Journal of Climate*, 4(2):203–217, 1991.

[18] Joseph J Barsugli and Prashant D Sardeshmukh. Global atmospheric sensitivity to tropical sst anomalies throughout the indo-pacific basin. *Journal of Climate*, 15(23): 3427–3442, 2002.

[19] Soumik Basu, Xiangdong Zhang, Igor Polyakov, and Uma S Bhatt. North american winter-spring storms: Modeling investigation on tropical pacific sea surface temperature impacts. *Geophysical Research Letters*, 40(19):5228–5233, 2013.

[20] Barbara J Benson, John J Magnuson, Olaf P Jensen, Virginia M Card, Glenn Hodgkins, Johanna Korhonen, David M Livingstone, Kenton M Stewart, Gesa A Weyhenmeyer, and Nick G Granin. Extreme events, trends, and variability in northern hemisphere lake-ice phenology (1855–2005). *Climatic Change*, 112(2): 299–323, 2012.

[21] Stefan Bertilsson, Amy Burgin, Cayelan C Carey, Samuel B Fey, Hans-Peter Grossart, Lorena M Grubisic, Ian D Jones, Georgiy Kirillin, Jay T Lennon, Ashley Shade, et al. The under-ice microbiome of seasonally frozen lakes. *Limnology and Oceanography*, 58(6):1998–2012, 2013.

[22] Mussie T. Beyene and Shaleen Jain. Wintertime weather-climate variability and its links to early spring ice-out in Maine lakes. *Limnology and Oceanography*, 60(6): 1890–1905, 2015.

[23] Mussie T. Beyene and Shaleen Jain. North American wintertime temperature anomalies: The role of El Niño diversity and differential teleconnections. *Climate Dynamics*, pages 1–13, 2017.

[24] Mussie T. Beyene and Shaleen Jain. Freezing degree-day thresholds and lake ice-out dates: Understanding the role of El Niño conditions. *International Journal of Climatology*, 38(11):4335–4344, 2018.

[25] Mussie T. Beyene, Shaleen Jain, and Ramesh C. Gupta. Linear-circular statistical modeling of lake ice-out dates. *Water Resources Research*, 54(10):7841–7858, 2018.

[26] Jan E Bissinger, David JS Montagnes, Jonathan harples, and David Atkinson. Predicting marine phytoplankton maximum growth rates from temperature: Improving on the eppley curve using quantile regression. *Limnology and Oceanography*, 53(2):487–493, 2008.

[27] Kätlin Blank, Juta Haberman, Marina Haldna, and Reet Laugaste. Effect of winter conditions on spring nutrient concentrations and plankton in a large shallow lake peipsi (estonia/russia). *Aquatic Ecology*, 43(3):745–753, 2009.

[28] Thorsten Blenckner, Rita Adrian, David M Livingstone, Eleanor Jennings, Gesa A Weyhenmeyer, D Glen George, Thomas Jankowski, Marko Järvinen, Caitriona Nic Aonghusa, Tiina Nõges, et al. Large-scale climatic signatures in lakes across europe: A meta-analysis. *Global Change Biology*, 13(7):1314–1326, 2007.

[29] Benjamin D Block, Blaize A Denfeld, Jason D Stockwell, Giovanna Flaim, Hans-Peter F Grossart, Lesley B Knoll, Dominique B Maier, Rebecca L North, Milla Rautio, James A Rusak, et al. The unique methodological challenges of winter limnology. *Limnology and Oceanography: Methods*, 17(1):42–57, 2019.

[30] Kelsey A Boeff, Kristin E Strock, and Jasmine E Saros. Evaluating planktonic diatom response to climate change across three lakes with differing morphometry. *Journal of Paleolimnology*, 56(1):33–47, 2016.

[31] Howard D Bondell, Brian J Reich, and Huixia Wang. Noncrossing quantile regression curve estimation. *Biometrika*, 97(4):825–838, 2010.

[32] Barrie R Bonsal, Terry D Prowse, Claude R Duguay, and Martin P Lacroix. Impacts of large-scale teleconnections on freshwater-ice break/freeze-up dates over canada. *Journal of Hydrology*, 330(1):340–353, 2006.

[33] Adrian W Bowman and Adelchi Azzalini. *Applied smoothing techniques for data analysis: the kernel approach with S-Plus illustrations*, volume 18. OUP Oxford, 1997.

[34] James A Bradbury, Barry D Keim, and Cameron P Wake. Us east coast trough indices at 500 hpa and new england winter climate variability. *Journal of Climate*, 15 (23):3509–3517, 2002.

[35] Laura C Brown and Claude R Duguay. The response and role of ice cover in lake-climate interactions. *Progress in Physical Geography*, 34(5):671–704, 2010.

[36] Adam W Burnett, Matthew E Kirby, Henry T Mullins, and William P Patterson. Increasing great lake–effect snowfall during the twentieth century: A regional response to global warming? *Journal of Climate*, 16(21):3535–3542, 2003.

[37] Jonathan B Butcher, Daniel Nover, Thomas E Johnson, and Christopher M Clark. Sensitivity of lake thermal and mixing dynamics to climate change. *Climatic Change*, 129(1-2):295–305, 2015.

[38] John Caesar, Lisa Alexander, and Russell Vose. Large-scale changes in observed daily maximum and minimum temperatures: Creation and analysis of a new gridded data set. *Journal of Geophysical Research: Atmospheres*, 111(D5), 2006.

[39] Wenju Cai, Simon Borlace, Matthieu Lengaigne, Peter Van Rensch, Mat Collins, Gabriel Vecchi, Axel Timmermann, Agus Santoso, Michael J McPhaden, Lixin Wu, et al. Increasing frequency of extreme el niño events due to greenhouse warming. *Nature Climate Change*, 4(2):111, 2014.

[40] Wenju Cai, Agus Santoso, Guojian Wang, Sang-Wook Yeh, Soon-Il An, Kim M Cobb, Mat Collins, Eric Guilyardi, Fei-Fei Jin, Jong-Seong Kug, et al. Enso and greenhouse warming. *Nature Climate Change*, 5(9):849, 2015.

[41] Antonietta Capotondi, Andrew T Wittenberg, Matthew Newman, Emanuele Di Lorenzo, Jin-Yi Yu, Pascale Braconnot, Julia Cole, Boris Dewitte, Benjamin Giese, Eric Guilyardi, et al. Understanding enso diversity. *Bulletin of the American Meteorological Society*, 96(6):921–938, 2015.

[42] Stephen R Carpenter, Eric G Booth, and Christopher J Kucharik. Extreme precipitation and phosphorus loads from two agricultural watersheds. *Limnology and Oceanography*, 63(3):1221–1233, 2018.

[43] Thomas N Chase, Roger A Pielke, and Roni Avissar. Teleconnections in the earth system. *Encyclopedia of Hydrological Sciences*, 2007.

[44] Wilbur Y Chen and Huug M van den Dool. Asymmetric impact of tropical sst anomalies on atmospheric internal variability over the north pacific. *Journal of the Atmospheric Sciences*, 54(6):725–740, 1997.

[45] Judah Cohen and Justin Jones. A new index for more accurate winter predictions. *Geophysical Research Letters*, 38(21), 2011.

[46] Judah Cohen, James A Screen, Jason C Furtado, Mathew Barlow, David Whittleston, Dim Coumou, Jennifer Francis, Klaus Dethloff, Dara Entekhabi, James Overland, et al. Recent arctic amplification and extreme mid-latitude weather. *Nature Geoscience*, 7(9):627, 2014.

[47] Jason M Cordeira and Neil F Laird. The influence of ice cover on two lake-effect snow events over lake erie. *Monthly Weather Review*, 136(7):2747–2763, 2008.

[48] Clara Deser. On the teleconnectivity of the "arctic oscillation". *Geophysical Research Letters*, 27(6):779–782, 2000.

[49] Clara Deser, Michael A Alexander, Shang-Ping Xie, and Adam S Phillips. Sea surface temperature variability: Patterns and mechanisms. *Annual Review of Marine Science*, 2:115–143, 2010.

[50] Sushil S Dixit, John P Smol, Donald F Charles, Robert M Hughes, Steven G Paulsen, and Gary B Collins. Assessing water quality changes in the lakes of the northeastern united states using sediment diatoms. *Canadian Journal of Fisheries and Aquatic Sciences*, 56(1):131–152, 1999.

[51] Claude R Duguay, Terry D Prowse, Barrie R Bonsal, Ross D Brown, Martin P Lacroix, and Patrick Ménard. Recent trends in canadian lake ice cover. *Hydrological Processes: An International Journal*, 20(4):781–801, 2006.

[52] D Durnford, V Fortin, GC Smith, B Archambault, D Deacu, F Dupont, S Dyck, Y Martinez, E Klyszejko, M MacKay, et al. Toward an operational water cycle prediction system for the great lakes and st. lawrence river. *Bulletin of the American Meteorological Society*, 99(3):521–546, 2018.

[53] Bradley Efron. *The jackknife, the bootstrap, and other resampling plans*, volume 38. Siam, 1982.

[54] Yun Fan and Huug Van den Dool. A global monthly land surface air temperature analysis for 1948–present. *Journal of Geophysical Research: Atmospheres*, 113(D1), 2008.

[55] Xing Fang and Heinz G Stefan. Simulations of climate effects on water temperature, dissolved oxygen, and ice and snow covers in lakes of the contiguous us under past and future climate scenarios. *Limnology and Oceanography*, 54(6(2)):2359–2370, 2009.

[56] Troy M Farmer, Elizabeth A Marschall, Konrad Dabrowski, and Stuart A Ludsin. Short winters threaten temperate fish populations. *Nature Communications*, 6:7724, 2015.

[57] B. D. Fekedulegn, J. J. Colbert, R. R. Hicks, and M. Schuckers. Coping with multicollinearity: An example on application of principal components regression in dendroecology. Technical report, Department of Agriculture, Forest Service, Northeastern Research Station: Newton Square, PA, USA, 2002.

[58] Xingdong Feng, Xuming He, and Jianhua Hu. Wild bootstrap for quantile regression. *Biometrika*, 98(4):995–999, 2011.

[59] Samuel R Fielding. Emiliania huxleyi specific growth rate dependence on temperature. *Limnology and Oceanography*, 58(2):663–666, 2013.

[60] N. I. Fisher. *Statistical analysis of circular data*. Statistical analysis of circular data, 1992.

[61] N. I. Fisher and A. J. Lee. Regression models for an angular response. *Biometrics*, 48 (3):665–677, 1992.

[62] Glen George. The impact of climate change on european lakes. In *The Impact of Climate Change on European Lakes*, pages 1–13. Springer, 2010.

[63] Dieter Gerten and Rita Adrian. Climate-driven changes in spring plankton dynamics and the sensitivity of shallow polymictic lakes to the north atlantic oscillation. *Limnology and Oceanography*, 45(5):1058–1066, 2000.

[64] Dieter Gerten and Rita Adrian. Differences in the persistency of the north atlantic oscillation signal among lakes. *Limnology and Oceanography*, 46(2):448–455, 2001.

[65] Dieter Gerten and Rita Adrian. Effects of climate warming, north atlantic oscillation, and el niño-southern oscillation on thermal conditions and plankton dynamics in northern hemispheric lakes. *The Scientific World Journal*, 2:586–606, 2002.

[66] Reza Namdar Ghanbari and Hector R Bravo. Coherence between atmospheric teleconnections, great lakes water levels, and regional climate. *Advances in water resources*, 31(10):1284–1298, 2008.

[67] Charles R Goldman, Alan Jassby, and Thomas Powell. Interannual fluctuations in primary production: meteorological forcing at two subalpine lakes. *Limnology and Oceanography*, 34(2):310–323, 1989.

[68] Mikael Gyllström, L-A Hansson, Erik Jeppesen, F García Criado, Elisabeth Gross, Kenneth Irvine, Timo Kairesalo, Ryszard Kornijów, Maria Rosa Miracle, Mirva Nykänen, et al. The role of climate in shaping zooplankton communities of shallow lakes. *Limnology and Oceanography*, 50(6):2008–2021, 2005.

[69] Stephanie E Hampton, Marianne V Moore, Tedy Ozersky, Emily H Stanley, Christopher M Polashenski, and Aaron WE Galloway. Heating up a cold subject: prospects for under-ice plankton research in lakes. *Journal of Plankton Research*, 37 (2):277–284, 2015.

[70] Stephanie E Hampton, Aaron WE Galloway, Stephen M Powers, Ted Ozersky, Kara H Woo, Ryan D Batt, Stephanie G Labou, Catherine M O'Reilly, Sapna Sharma, Noah R Lottig, et al. Ecology under lake ice. *Ecology Letters*, 20(1):98–111, 2017.

[71] Dörthe Handorf, Ralf Jaiser, Klaus Dethloff, Annette Rinke, and Judah Cohen. Impacts of arctic sea ice and continental snow cover changes on atmospheric winter teleconnections. *Geophysical Research Letters*, 42(7):2367–2377, 2015.

[72] Suzanne Hartley and Michael J Keables. Synoptic associations of winter climate and snowfall variability in new england, usa, 1950–1992. *International Journal of Climatology: A Journal of the Royal Meteorological Society*, 18(3):281–298, 1998.

[73] Xuming He and Li-Xing Zhu. A lack-of-fit test for quantile regression. *Journal of the American Statistical Association*, 98(464):1013–1022, 2003.

[74] A Louise Heathwaite, Penny J Johnes, and Norman E Peters. Trends in nutrients. *Hydrological Processes*, 10(2):263–293, 1996.

[75] Ingeborg P Helland, Anders G Finstad, Torbjørn Forseth, Trygve Hesthagen, and Ola Ugedal. Ice-cover effects on competitive interactions between two fish species. *Journal of Animal Ecology*, 80(3):539–547, 2011.

[76] G. Hodgkins. Historical ice out dates for 29 lakes in New England, 1807-2008. Open-File Report 2010-1214, U. S. Geological Survey, 2010.

[77] Glenn A Hodgkins, Ivan C James, and Thomas G Huntington. Historical changes in lake ice-out dates as indicators of climate change in New England, 1850–2000. *International Journal of Climatology*, 22(15):1819–1827, 2002.

[78] Martin P Hoerling and Arun Kumar. Why do north american climate anomalies differ from one el niño event to another? *Geophysical Research Letters*, 24(9): 1059–1062, 1997.

[79] Martin P Hoerling, Arun Kumar, and Min Zhong. El niño, la niña, and the nonlinearity of their teleconnections. *Journal of Climate*, 10(8):1769–1786, 1997.

[80] Martin P Hoerling, James W Hurrell, and Taiyi Xu. Tropical origins for recent north atlantic climate change. *Science*, 292(5514):90–92, 2001.

[81] Brian Hoskins. The potential for skill across the range of the seamless weather-climate prediction problem: a stimulus for our science. *Quarterly Journal of the Royal Meteorological Society*, 139(672):573–584, 2013.

[82] Veronika Huber, Rita Adrian, and Dieter Gerten. Phytoplankton response to climate warming modified by trophic state. *Limnology and Oceanography*, 53(1):1–13, 2008.

[83] James W Hurrell. Influence of variations in extratropical wintertime teleconnections on northern hemisphere temperature. *Geophysical Research Letters*, 23(6):665–668, 1996.

[84] Johnna M Infanti and Ben P Kirtman. North american rainfall and temperature prediction response to the diversity of enso. *Climate Dynamics*, 46(9-10):3007–3023, 2016.

[85] George L Jacobson, Ivan J Fernandez, Paul Andrew Mayewski, and Catherine V Schmitt. Maine's climate future: an initial assessment. 2009.

[86] S. R. Jammalamadaka and A. Sengupta. *Topics in Circular Statistics*. World Scientific, 2001.

[87] M Järvinen, M Rask, J Ruuhijärvi, and L Arvola. Temporal coherence in water temperature and chemistry under the ice of boreal lakes (finland). *Water Research*, 36(16):3949–3956, 2002.

[88] Alan D Jassby, Thomas M Powell, and Charles R Goldman. Interannual fluctuations in primary production: Direct physical effects and the trophic cascade at Castle Lake, California. *Limnology and Oceanography*, 35(5):1021–1038, 1990.

[89] Ian Jolliffe. Principal component analysis. In *International Encyclopedia of Statistical Science*, pages 1094–1096. Springer, 2011.

[90] DongJoo Joung, Meagan Leduc, Benjamin Ramcharitar, Yaoyang Xu, Peter DF Isles, Jason D Stockwell, Gregory K Druschel, Tom Manley, and Andrew W Schroth. Winter weather and lake-watershed physical configuration drive phosphorus, iron, and manganese dynamics in water and sediment of ice-covered lakes. *Limnology and Oceanography*, 62(4):1620–1635, 2017.

[91] Eugenia Kalnay, Masao Kanamitsu, Robert Kistler, William Collins, Dennis Deaven, Lev Gandin, Mark Iredell, Suranjana Saha, Glenn White, John Woollen, et al. The ncep/ncar 40-year reanalysis project. *Bulletin of the American meteorological Society*, 77(3):437–472, 1996.

[92] Hsun-Ying Kao and Jin-Yi Yu. Contrasting eastern-pacific and central-pacific types of enso. *Journal of Climate*, 22(3):615–632, 2009.

[93] Thomas R Karl and Claude N Williams Jr. An approach to adjusting climatological time series for discontinuous inhomogeneities. *Journal of Climate and Applied Meteorology*, 26(12):1744–1763, 1987.

[94] Sujay S Kaushal, Paul M Mayer, Philippe G Vidon, Rose M Smith, Michael J Pennino, Tamara A Newcomer, Shuiwang Duan, Claire Welty, and Kenneth T Belt. Land use and climate variability amplify carbon, nutrient, and contaminant pulses: a review with management implications. *JAWRA Journal of the American Water Resources Association*, 50(3):585–614, 2014.

[95] Georgiy Kirillin, Matti Leppäranta, Arkady Terzhevik, Nikolai Granin, Juliane Bernhardt, Christof Engelhardt, and Tatyana Efremova. Physics of seasonally ice-covered lakes: A review. *Aquatic Sciences*, 74(4):659–682, 2012.

[96] Andreas Kleeberg. Phosphorus sedimentation in seasonal anoxic lake scharmützel, ne germany. *Hydrobiologia*, 472(1-3):53–65, 2002.

[97] George W Kling, Katharine Hayhoe, Lucinda B Johnson, Donald J Magnuson, Stephen Polasky, Scott K Robinson, Brian J Shuter, Michelle M Wander, Donald J Wuebbles, and Donald R Zak. Confronting climate change in the great lakes region: impacts on our communities and ecosystems. 2003.

[98] Lesley B Knoll, Sapna Sharma, Blaize A Denfeld, Giovanna Flaim, Yukari Hori, John J Magnuson, Dietmar Straile, and Gesa A Weyhenmeyer. Consequences of lake and river ice loss on cultural ecosystem services. *Limnology and Oceanography Letters*, 2019.

[99] R Koenker. Quantreg: Quantile regression (r package version 5.29)[computer software], 2016.

[100] Roger Koenker and Gilbert Bassett Jr. Regression quantiles. *Econometrica: journal of the Econometric Society*, pages 33–50, 1978.

[101] Roger Koenker and Kevin Hallock. Quantile regression: An introduction. *Journal of Economic Perspectives*, 15(4):43–56, 2001.

[102] T. K. Kratz, B. P. Hayden, B. J. Benson, and W. Y. B. Chang. Patterns in the interannual variability of lake freeze and thaw dates. *Internationale Vereinigung fur Theoretische und Angewandte Limnologie Verhandlungen*, 27(5):2796–2799, 2001.

[103] Jong-Seong Kug, Fei-Fei Jin, and Soon-Il An. Two types of el niño events: cold tongue el niño and warm pool el niño. *Journal of Climate*, 22(6):1499–1515, 2009.

[104] Yochanan Kushnir, Walter A Robinson, Ping Chang, and Andrew W Robertson. The physical basis for predicting atlantic sector seasonal-to-interannual climate variability. *Journal of Climate*, 19(23):5949–5970, 2006.

[105] Narasimhan K Larkin and DE Harrison. On the definition of el niño and associated seasonal average us weather anomalies. *Geophysical Research Letters*, 32(13), 2005.

[106] RE Lautzenheiser. The climate of maine. us department of commerce, national oceanic and atmospheric administration. *Environmental Data Service, Silver Springs, Maryland*, 1972.

[107] A. Lee. Circular data. *Wiley Interdisciplinary Reviews: Computational Statistics*, 2 (4):477–486, 2010.

[108] Matti Leppäranta. Modelling the formation and decay of lake ice. In *The Impact of Climate Change on European Lakes*, pages 63–83. Springer, 2010.

[109] Matti Leppäranta. *Freezing of lakes and the evolution of their ice cover*. Springer Science & Business Media, 2014.

[110] Robert E Livezey and WY Chen. Statistical field significance and its determination by monte carlo techniques. *Monthly Weather Review*, 111(1):46–59, 1983.

[111] David M. Livingstone. Break-up dates of alpine lakes as proxy data for local and regional mean surface air temperatures. *Climatic Change*, 37(2):407–439, 1997.

[112] David M Livingstone. A change of climate provokes a change of paradigm: taking leave of two tacit assumptions about physical lake forcing. *International Review of Hydrobiology*, 93(4-5):404–414, 2008.

[113] R. A. Lockhart and M. A. Stephens. Tests of fit for the von mises distribution. *Biometrika*, 72(3):647–652, 1985.

[114] Ulric Lund. Least circular distance regression for directional data. *Journal of Applied Statistics*, 26(6):723–733, 1992.

[115] John J Magnuson, Dale M Robertson, Barbara J Benson, Randolph H Wynne, David M Livingstone, Tadashi Arai, Raymond A Assel, Roger G Barry, Virginia Card, Esko Kuusisto, et al. Historical trends in lake and river ice cover in the northern hemisphere. *Science*, 289(5485):1743–1746, 2000.

[116] Heera I Malik, Kate A Warner, and Jasmine E Saros. Comparison of seasonal distribution patterns of discostella stelligera and lindavia bodanica in a boreal lake during two years with differing ice-off timing. *Diatom Research*, 33(1):1–11, 2018.

[117] C. Mallows. The zeroth problem. *The American Statistician*, 52(1):1–9, 1998.

[118] K. V. Mardia. Linear-circular correlation coefficients and rhythmometry. *Biometrika*, 63(2):403–405, 1976.

[119] Kanti V. Mardia and Peter E. Jupp. *Directional Statistics*, volume 494. John Wiley & Sons, 2009.

[120] John Marshall, Yochanan Kushnir, David Battisti, Ping Chang, Arnaud Czaja, Robert Dickson, James Hurrell, MICHAEL McCARTNEY, R Saravanan, and Martin Visbeck. North atlantic climate variability: phenomena, impacts and mechanisms. *International Journal of Climatology*, 21(15):1863–1898, 2001.

[121] Ian M McCullough, Cynthia S Loftin, and Steven A Sader. Combining lake and watershed characteristics with landsat tm data for remote estimation of regional lake clarity. *Remote Sensing of Environment*, 123:109–115, 2012.

[122] Dmitrii V Mironov. *Parameterization of lakes in numerical weather prediction: Description of a lake model*. DWD, 2008.

[123] Omid Mohseni, Heinz G. Stefan, and Troy R. Erickson. A nonlinear regression model for weekly stream temperatures. *Water Resources Research*, 34(10):2685–2692, 1998.

[124] S Nigam. Teleconnections. *Encyclopedia of Atmospheric Sciences, Six-Volume Set*, pages 2243–2269, 2003.

[125] Peeter Nõges, Rita Adrian, Orlane Anneville, Lauri Arvola, Thorsten Blenckner, Glen George, Thomas Jankowski, Marko Järvinen, Stephen Maberly, Judit Padisák, et al. The impact of variations in the climate on seasonal dynamics of phytoplankton. In *The Impact of Climate Change on European Lakes*, pages 253–274. Springer, 2010.

[126] Tiina Noges, Lea Tuvikene, and Peeter Noges. Contemporary trends of temperature, nutrient loading, and water quality in large Lakes Peipsi and Vortsjärv, Estonia. *Aquatic Ecosystem Health & Management*, 13(2):143–153, 2010.

[127] Catherine M O'Reilly, Sapna Sharma, Derek K Gray, Stephanie E Hampton, Jordan S Read, Rex J Rowley, Philipp Schneider, John D Lenters, Peter B McIntyre, Benjamin M Kraemer, et al. Rapid and highly variable warming of lake surface waters around the globe. *Geophysical Research Letters*, 42(24):10–773, 2015.

[128] Hans W Paerl and Jef Huisman. Blooms like it hot. *Science*, 320(5872):57–58, 2008.

[129] MA Palecki and RG Barry. Freeze-up and break-up of lakes as an index of temperature changes during the transition seasons: a case study for finland. *Journal of Climate and Applied Meteorology*, 25(7):893–902, 1986.

[130] Sangkyu Park, Michael T Brett, Anke Müller-Solger, and Charles R Goldman. Climatic forcing and primary productivity in a subalpine lake: Interannual variability as a natural experiment. *Limnology and Oceanography*, 49(2):614–619, 2004.

[131] Michael R Penn, Martin T Auer, Susan M Doerr, Charles T Driscoll, Carol M Brooks, and Steven W Effler. Seasonality in phosphorus release rates from the sediments of a hypereutrophic lake under a matrix of ph and redox conditions. *Canadian Journal of Fisheries and Aquatic Sciences*, 57(5):1033–1041, 2000.

[132] Stephen M Powers and Stephanie E Hampton. Winter limnology as a new frontier. *Limnology and Oceanography Bulletin*, 25(4):103–108, 2016.

[133] D. L. Preston, N. Caine, D. M. McKnight, M. W. Williams, K. Hell, M. P. Miller, S. J. Hart, and P. T. J. Johnson. Climate regulates alpine lake ice cover phenology and aquatic ecosystem structure. *Geophysical Research Letters*, 43:5353–536, 2016.

[134] Terry Prowse, Knut Alfredsen, Spyros Beltaos, Barrie Bonsal, Claude Duguay, Atte Korhola, James McNamara, Warwick F Vincent, Valery Vuglinsky, and Gesa Weyhenmeyer. Changing lake and river ice regimes: Trends, effects and implications. 2011.

[135] Terry Prowse, Knut Alfredsen, Spyros Beltaos, Barrie R Bonsal, William B Bowden, Claude R Duguay, Atte Korhola, Jim McNamara, Warwick F Vincent, Valery Vuglinsky, et al. Effects of changes in arctic lake and river ice. *AMBIO: A Journal of the Human Environment*, (40):63–74, 2011.

[136] Robert G Quayle, David R Easterline, Thomas R Karl, and Pamela Y Hughes. Effects of recent thermometer changes in the cooperative station network. *Bulletin of the American Meteorological Society*, 72(11):1718–1724, 1991.

[137] Nandini Ramesh and Raghu Murtugudde. All flavours of el niño have similar early subsurface origins. *Nature Climate Change*, 3(1):42, 2013.

[138] Sergei Rodionov and Raymond Assel. Atmospheric teleconnection patterns and severity of winters in the laurentian great lakes basin. *Atmosphere-Ocean*, 38(4): 601–635, 2000.

[139] Wayne R Rouse, Claire M Oswald, Jacqueline Binyamin, Peter D Blanken, William M Schertzer, and Christopher Spence. Interannual and seasonal variability of the surface energy balance and temperature of central great slave lake. *Journal of Hydrometeorology*, 4(4):720–730, 2003.

[140] Kathleen Rühland, Andrew M Paterson, and John P Smol. Hemispheric-scale patterns of climate-related shifts in planktonic diatoms from north american and european lakes. *Global Change Biology*, 14(11):2740–2754, 2008.

[141] K Salonen, M Leppäranta, M Viljanen, and RD Gulati. Perspectives in winter limnology: closing the annual cycle of freezing lakes. *Aquatic Ecology*, 43(3):609–616, 2009.

[142] G Sánchez-López, A Hernández, S Pla-Rabes, M Toro, I Granados, J Sigró, RM Trigo, MJ Rubio-Inglés, L Camarero, B Valero-Garcés, et al. The effects of the nao on the ice phenology of spanish alpine lakes. *Climatic Change*, 130(2):101–113, 2015.

[143] Daniel E Schindler, Donald E Rogers, Mark D Scheuerell, and Caryn A Abrey. Effects of changing climate on zooplankton and juvenile sockeye salmon growth in southwestern alaska. *Ecology*, 86(1):198–209, 2005.

[144] David W Scott. *Multivariate density estimation: theory, practice, and visualization*. John Wiley & Sons, 1992.

[145] Sapna Sharma and John J Magnuson. Oscillatory dynamics do not mask linear trends in the timing of ice breakup for northern hemisphere lakes from 1855 to 2004. *Climatic Change*, 124(4):835–847, 2014.

[146] Sapna Sharma, John J Magnuson, Ryan D Batt, Luke A Winslow, Johanna Korhonen, and Yasuyuki Aono. Direct observations of ice seasonality reveal changes in climate over the past 320–570 years. *Scientific Reports*, 6:25061, 2016.

[147] Sapna Sharma, Kevin Blagrave, John J Magnuson, Catherine M O'Reilly, Samantha Oliver, Ryan D Batt, Madeline R Magee, Dietmar Straile, Gesa A Weyhenmeyer, Luke Winslow, et al. Widespread loss of lake ice around the northern hemisphere in a warming world. *Nature Climate Change*, 9(3):227, 2019.

[148] Simon J Sheather. Density estimation. *Statistical Science*, pages 588–597, 2004.

[149] Bernard W Silverman. *Density estimation for statistics and data analysis*. Routledge, 1986.

[150] Bernard W Silverman. *Density estimation for statistics and data analysis*. Routledge, 2004.

[151] E Sinha, AM Michalak, and V Balaji. Eutrophication will increase during the 21st century as a result of precipitation changes. *Science*, 357(6349):405–408, 2017.

[152] Doug M Smith, Adam A Scaife, and Ben P Kirtman. What is the current state of scientific knowledge with regard to seasonal and decadal forecasting? *Environmental Research Letters*, 7(1):015602, 2012.

[153] Thomas M Smith, Richard W Reynolds, Thomas C Peterson, and Jay Lawrimore. Improvements to noaa's historical merged land–ocean surface temperature analysis (1880–2006). *Journal of Climate*, 21(10):2283–2296, 2008.

[154] Martin Søndergaard, Jens Peder Jensen, and Erik Jeppesen. Role of sediment and internal loading of phosphorus in shallow lakes. *Hydrobiologia*, 506(1-3):135–145, 2003.

[155] MJ Stankiewicz. Breakup can be foretold. *Pulp Pap. Mag. Can*, 48:118–120, 1947.

[156] Thomas Stocker. *Climate change 2013: the physical science basis: Working Group I contribution to the Fifth assessment report of the Intergovernmental Panel on Climate Change*. Cambridge University Press, 2014.

[157] John L Stoddard, John Van Sickle, Alan T Herlihy, Janice Brahney, Steven Paulsen, David V Peck, Richard Mitchell, and Amina I Pollard. Continental-scale increase in lake and stream phosphorus: Are oligotrophic systems disappearing in the united states? *Environmental Science & Technology*, 50(7):3409–3415, 2016.

[158] Dietmar Straile, David M Livingstone, Gesa A Weyhenmeyer, and D Glen George. The response of freshwater ecosystems to climate variability associated with the north atlantic oscillation, 2003.

[159] K Takahashi, A Montecinos, K Goubanova, and Boris Dewitte. Enso regimes: Reinterpreting the canonical and modoki el niño. *Geophysical Research Letters*, 38 (10), 2011.

[160] David WJ Thompson and John M Wallace. The arctic oscillation signature in the wintertime geopotential height and temperature fields. *Geophysical Research Letters*, 25(9):1297–1300, 1998.

[161] Axel Timmermann, Josef Oberhuber, Andreas Bacher, Monika Esch, Mojib Latif, and Erich Roeckner. Increased el niño frequency in a climate model forced by future greenhouse warming. *Nature*, 398(6729):694, 1999.

[162] Kevin E Trenberth and David P Stepaniak. Indices of el niño evolution. *Journal of Climate*, 14(8):1697–1701, 2001.

[163] Kevin E Trenberth, Grant W Branstator, David Karoly, Arun Kumar, Ngar-Cheung Lau, and Chester Ropelewski. Progress during toga in understanding and modeling global teleconnections associated with tropical sea surface temperatures. *Journal of Geophysical Research: Oceans*, 103(C7):14291–14324, 1998.

[164] Stephen J. Vavrus, Randolph H. Wynne, and Jonathan A. Foley. Measuring the sensitivity of southern wisconsin lake ice to climate variations and lake depth using a numerical model. *Limnology and Oceanography*, 41(5):822–831, 1996.

[165] Charles Verpoorter, Tiit Kutser, David A Seekell, and Lars J Tranvik. A global inventory of lakes based on high-resolution satellite imagery. *Geophysical Research Letters*, 41(18):6396–6402, 2014.

[166] John M Wallace. North atlantic oscillatiodannular mode: two paradigms—one phenomenon. *Quarterly Journal of the Royal Meteorological Society*, 126(564): 791–805, 2000.

[167] Kate Warner, Rachel Fowler, Robert Northington, Heera Malik, Joan McCue, and Jasmine Saros. How does changing ice-out affect arctic versus boreal lakes? a comparison using two years with ice-out that differed by more than three weeks. *Water*, 10(1):78, 2018.

[168] Gesa A Weyhenmeyer. Do warmer winters change variability patterns of physical and chemical lake conditions in sweden? *Aquatic Ecology*, 43(3):653–659, 2009.

[169] Gesa A Weyhenmeyer, Thorsten Blenckner, and Kurt Pettersson. Changes of the plankton spring outburst related to the north atlantic oscillation. *Limnology and Oceanography*, 44(7):1788–1792, 1999.

[170] Gesa A Weyhenmeyer, Anna-Karin Westöö, and Eva Willén. Increasingly ice-free winters and their effects on water quality in sweden's largest lakes. In *European Large Lakes Ecosystem Changes and Their Ecological and Socioeconomic Impacts*, pages 111–118. Springer, 2007.

[171] Gesa A. Weyhenmeyer, David M. Livingstone, Markus Meili, Olaf Jensen, Barbara Benson, and John J. Magnuson. Large geographical differences in the sensitivity of ice-covered lakes and rivers in the northern hemisphere to temperature changes. *Global Change Biology*, 17(1):822–831, 2011.

[172] Daniel S Wilks. *Statistical Methods in the Atmospheric Sciences (International Geophysics Series; V. 91)*. Academic Press, 2006.

[173] C. N. Williams, M. J. Menne, R. S. Vose, and D. R. Easterling. United states historical climatology network monthly temperature and precipitation data. Technical Report ORNL, CDIAC-187, NDP-019, Carbon Dioxide Information Analysis Center, Oak Ridge National Laboratory, Oak Ridge, Tennessee, USA, 2007.

[174] Gaynor P Williams. Correlating freeze-up and break-up with weather conditions. *Canadian Geotechnical Journal*, 2(4):313–326, 1965.

[175] Gaynor P Williams. Predicting the date of lake ice breakup. *Water Resources Research*, 7(2):323–333, 1971.

[176] Greg Williams, Kari L Layman, and Heinz G Stefan. Dependence of lake ice covers on climatic, geographic and bathymetric variables. *Cold Regions Science and Technology*, 40(3):145–164, 2004.

[177] S. Williams. Maine lakes report. Technical report, Maine Volunteer Lake Program, http://www.mainevlmp.org/wp-content/uploads/2013/07/2012-VLMP-Annual-Report-Color.pdf, 2012.

[178] Sterling Greg Williams and Heinz G Stefan. Modeling of lake ice characteristics in north america using climate, geography, and lake bathymetry. *Journal of Cold Regions Engineering*, 20(4):140–167, 2006.

[179] Monika Winder and Daniel E Schindler. Climate change uncouples trophic interactions in an aquatic ecosystem. *Ecology*, 85(8):2100–2106, 2004.

[180] Klaus Wyrtki. El niño—the dynamic response of the equatorial pacific oceanto atmospheric forcing. *Journal of Physical Oceanography*, 5(4):572–584, 1975.

[181] Yaoyang Xu, Andrew W Schroth, and Donna M Rizzo. Developing a 21st century framework for lake-specific eutrophication assessment using quantile regression. *Limnology and Oceanography: Methods*, 13(5):237–249, 2015.

[182] Sang-Wook Yeh, Jong-Seong Kug, Boris Dewitte, Min-Ho Kwon, Ben P. Kirtman, and Fei-Fei Jin. El niño in a changing climate. *Nature*, 461(7263):511–514, 2009.

[183] Jin-Yi Yu, Yuhao Zou, Seon Tae Kim, and Tong Lee. The changing impact of el niño on us winter temperatures. *Geophysical Research Letters*, 39(15), 2012.

[184] Tao Zhang, Judith Perlwitz, and Martin P Hoerling. What is responsible for the strong observed asymmetry in teleconnections between el niño and la niña? *Geophysical Research Letters*, 41(3):1019–1025, 2014.

[185] Yunlin Zhang, Erik Jeppesen, Xiaohan Liu, Boqiang Qin, Kun Shi, Yongqiang Zhou, Sidinei Magela Thomaz, and Jianmin Deng. Global loss of aquatic vegetation in lakes. *Earth-Science Reviews*, 173:259–265, 2017.

[186] Yafang Zhong, Michael Notaro, Stephen J Vavrus, and Michael J Foster. Recent accelerated warming of the laurentian great lakes: Physical drivers. *Limnology and Oceanography*, 61(5):1762–1786, 2016.

APPENDIX A

This appendix provides additional supporting tables and figures for Chapter 2.

Citation	System & Region	Lake Parameter
Adrian et al. [2]	Lake Müggelsee, Germany	Physical, Biological
Adrian et al. [3]	Lake Müggelsee, Germany	Biological
Arvola et al. [6]	Multiple lakes, Europe	Biological
Austin and Colman [14]	Lake Superior, USA/Canada	Physical
Boeff et al. [30]	Multiple lakes, USA	Biological
Blank et al. [27]	Lake Peipsi, Estonia/Russia	Physical, Chemical, Biological
Blenckner et al. [28]	Multiple lakes, Europe	Physical, Biological
Burnett et al. [36]	Laurentian Great Lakes, USA	Climate
Butcher et al. [37]	Multiple lakes, USA	Biological
Cordeira and Laird [47]	Lake Eerie, USA	Climate
Fang and Stefan [55]	Multiple lakes, USA	Physical, Chemical
Farmer et al. [56]	Lake Eerie, USA	Biological
Gerten and Adrian [63]	Lake Müggelsee, Germany	Physical, Biological
Gerten and Adrian [64]	Multiple lakes, Germany	Physical
Gyllström et al. [68]	Multiple lakes, Europe	Biological
Hampton et al. [69]	-	Biological
Hampton et al. [70]	Multiple lakes, Europe/USA/Canada	Chemical, Biological
Helland et al. [75]	Multiple lakes, Norway	Biological
Jassby et al. [88]	Castle lake, USA	Biological
Joung et al. [90]	Multiple lakes, USA	Physical, Chemical
Kleeberg [96]	Lake Scharmützel, Germany	Physical, Chemical
Kling et al. [97]	Great Lakes, USA/Canada	Social
Leppäranta [108]	Multiple lakes, Europe	Social
Malik et al. [116]	Jordan Pond, USA	Physical, Biological
Nõges et al. [125]	Multiple lakes, Europe	Biological
O'Reilly et al. [127]	Multiple lakes, Global	Physical
Paerl and Huisman [128]	-	Biological
Park et al. [130]	Castle Lake, USA	Physical, Biological
Penn et al. [131]	Onondaga Lake, USA	Physical, Chemical
Preston et al. [133]	Multiple lakes, USA	Physical, Chemical, Biological
Prowse et al. [134]	Multiple lakes, USA	Physical, Chemical, Biological, Social
Rouse et al. [139]	Central Great Slave Lake, Canada	Physical
Rühland et al. [140]	Multiple lakes, USA/Canada/Europe	Biological
Schindler et al. [143]	Lake Aleknagik, USA	Physical
Straile et al. [158]	Multiple lakes, Europe	Physical, Biological
Warner et al. [167]	Multiple lakes, USA	Physical, Biological
Weyhenmeyer et al. [169]	Lake Erken, Sweden	Physical, Biological
Weyhenmeyer et al. [170]	Multiple lakes, Sweden	Physical, Chemical
Weyhenmeyer [168]	Multiple lakes, Sweden	Physical, Chemical, Biological
Zhong et al. [186]	Laurentian Great Lakes, USA/Canada	Physical

Table A.1. Reviewed articles on the impact of shorter ice cover period on lake social and ecological systems.

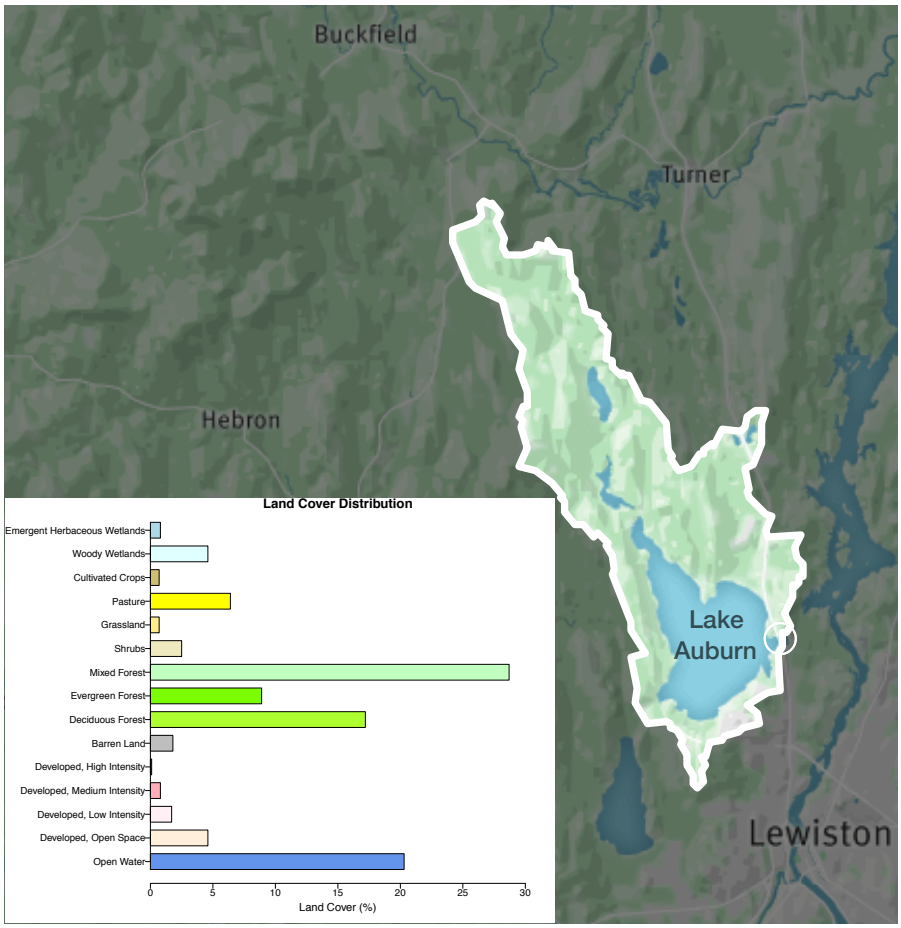

Figure A.1. Land cover distribution for Lake Auburn Watershed.

APPENDIX B

This appendix provides additional supporting tables and figures for Chapter 3.

Lake	Latitude (°N)	Longitude (°)	Surface area ($10^6 m^2$)	Mean Depth (m)	Elevation (m)	$\frac{\text{Surface area}}{\text{Mean depth}}$
Damariscotta	44.14	−69.49	18.96	9.14	17	2.07
China	44.43	−69.55	15.94	8.53	60	1.87
Maranacook	44.34	−69.95	7.46	9.14	64	0.82
Auburn	44.15	−70.25	9.15	10.97	90	0.83
West Grand	45.24	−67.84	58.54	11.28	91	5.19
Norway	44.23	−70.58	3.73	5.48	128	0.68
Sebec	4.26	−69.23	25.74	12.80	98	2.01
Mooselucmeguntic	44.91	−70.89	66.2	18.28	447	3.62
Rangeley	44.95	−70.70	25.5	18.29	463	1.39
Moosehead	45.66	−69.69	305.42	16.76	313	18.22
Squapan	46.57	−68.32	20.72	6.40	183	3.24
Portage	46.78	−68.50	8.54	3.05	220	2.80

Table B.1. Morphometric data for studied Maine lakes.

	Seasonal Winter AFDD	Seasonal Winter AMDD	Seasonal Spring AMDD	Seasonal Spring AFDD	Accumulated Winter Snowfall	Accumulated Spring Snowfall	Lake Maranacook	Lake China	Lake Damariscotta
Seasonal Winter AFDD	**1**								
Seasonal Winter AMDD	**-0.48**	**1**							
Seasonal Spring AMDD	**-0.26**	**0.33**	**1**						
Seasonal Spring AFDD	0.19	-0.13	**-0.60**	**1**					
Accumulated Winter Snowfall	-0.05	**-0.26**	**-0.27**	0.10	**1**				
Accumulated Spring Snowfall	0.13	-0.06	**-0.38**	**0.38**	0.05	**1**			
Lake Maranacook	**0.36**	**-0.53**	**-0.77**	**0.45**	**0.36**	**0.42**	**1**		
Lake China	**0.34**	**-0.53**	**-0.79**	**0.47**	**0.39**	**0.48**	**0.95**	**1**	
Lake Damariscotta	**0.36**	**-0.51**	**-0.72**	**0.50**	**0.42**	**0.43**	**0.89**	**0.92**	**1**

Table B.2. Pearson correlation between lake ice-out dates and winter and spring degree-days and snowfall at Gardiner Station. Correlation coefficients in bold are significant at $p < 0.05$.

	Seasonal Winter AFDD	Seasonal Winter AMDD	Seasonal Spring AMDD	Seasonal Spring AFDD	Accumulated Winter Snowfall	Accumulated Spring Snowfall	Lake Auburn	Lake Norway
Seasonal Winter AFDD	**1**							
Seasonal Winter AMDD	**0.44**	**1**						
Seasonal Spring AMDD	0.12	**0.32**	**1**					
Seasonal Spring AFDD	0.08	-0.09	**-0.56**	**1**				
Accumulated Winter Snowfall	-0.11	**-0.36**	-0.24	0.02	**1**			
Accumulated Spring Snowfall	**-0.27**	**-0.31**	**-0.36**	**0.39**	0.02	**1**		
Lake Auburn	**-0.31**	**-0.44**	**-0.78**	**0.47**	**0.37**	**0.40**	**1**	
Lake Norway	**-0.28**	**-0.44**	**-0.76**	**0.45**	0.25	**0.43**	**0.88**	**1**

Table B.3. Correlation between lake ice-out dates and winter and spring degree-days and snowfall at Lewiston Station. Correlation between lake ice-out dates and winter and spring degree-days and snowfall at Lewiston Station. Correlation coefficients in bold are significant at $p < 0.05$.

	Seasonal Winter AFDD	Seasonal Winter AMDD	Seasonal Spring AMDD	Seasonal Spring AFDD	Accumulated Winter Snowfall	Accumulated Spring Snowfall	Lake Sebec
Seasonal Winter AFDD	**1**						
Seasonal Winter AMDD	**-0.47**	**1**					
Seasonal Spring AMDD	**-0.27**	**0.34**	**1**				
Seasonal Spring AFDD	**0.26**	-0.18	**-0.54**	**1**			
Accumulated Winter Snowfall	0.12	-0.22	**-0.30**	0.14	**1**		
Accumulated Spring Snowfall	0.20	-0.18	**-0.32**	**0.35**	0.21	1	
Lake Sebec	**0.37**	**-0.40**	**-0.77**	**0.55**	**0.35**	**0.45**	**1**

Table B.4. Correlation between lake ice-out dates and winter and spring degree-days and snowfall at Corinna Station. Correlation between lake ice-out dates and winter and spring degree-days and snowfall at Corinna Station. Correlation coefficients in bold are significant at $p < 0.05$.

	Seasonal Winter AFDD	Seasonal Winter AMDD	Seasonal Spring AMDD	Seasonal Spring AFDD	Accumulated Winter Snowfall	Accumulated Spring Snowfall	Lake Mooselucmeguntic	Lake Rangeley
Seasonal Winter AFDD	**1**							
Seasonal Winter AMDD	**-0.50**	**1**						
Seasonal Spring AMDD	**-0.39**	**0.26**	**1**					
Seasonal Spring AFDD	**0.37**	-0.23	**-0.65**	**1**				
Accumulated Winter Snowfall	0.06	-0.23	-0.18	0.09	**1**			
Accumulated Spring Snowfall	0.21	-0.10	**-0.35**	**0.33**	0.17	**1**		
Lake Mooselucmeguntic	**0.39**	-0.28	**-0.85**	**0.45**	0.20	**0.35**	**1**	
Lake Rangeley	**0.38**	**-0.31**	**-0.83**	**0.42**	0.20	**0.39**	**0.98**	**1**

Table B.5. Correlation between lake ice-out dates and winter and spring degree-days and snowfall at Farmington Station. Correlation between lake ice-out dates and winter and spring degree-days and snowfall at Farmington Station. Correlation coefficients in bold are significant at $p < 0.05$.

	Seasonal Winter AFDD	Seasonal Winter AMDD	Seasonal Spring AMDD	Seasonal Spring AFDD	Accumulated Winter Snowfall	Accumulated Spring Snowfall	Lake Moosehead
Seasonal Winter AFDD	**1**						
Seasonal Winter AMDD	**-0.34**	**1**					
Seasonal Spring AMDD	-0.24	0.22	**1**				
Seasonal Spring AFDD	0.22	-0.20	**-0.60**	**1**			
Accumulated Winter Snowfall	0.08	-0.06	-0.27	0.17	1		
Accumulated Spring Snowfall	0.17	0.02	**-0.38**	**0.50**	0.28	1	
Lake Moosehead	**0.46**	-0.25	**-0.74**	**0.64**	0.26	**0.56**	**1**

Table B.6. Correlation between lake ice-out dates and winter and spring degree-days and snowfall at Brassua Station. Correlation between lake ice-out dates and winter and spring degree-days and snowfall at Brassua Station. Correlation coefficients in bold are significant at $p < 0.05$.

	Seasonal Winter AFDD	Seasonal Winter AMDD	Seasonal Spring AMDD	Seasonal Spring AFDD	Accumulated Winter Snowfall	Accumulated Spring Snowfall	Lake Portage	Lake Squapan
Seasonal Winter AFDD	**1**							
Seasonal Winter AMDD	-0.21	**1**						
Seasonal Spring AMDD	-0.11	0.19	**1**					
Seasonal Spring AFDD	0.16	-0.21	**-0.56**	**1**				
Accumulated Winter Snowfall	-0.15	0.13	-0.01	-0.01	**1**			
Accumulated Spring Snowfall	0.25	0.09	-0.15	0.26	0.03	**1**		
Lake Portage	0.25	-0.09	**-0.74**	**0.39**	-0.05	**0.40**	**1**	
Lake Squapan	**0.34**	0.20	**0.50**	**0.81**	0.28	**0.50**	**0.90**	**1**

Table B.7. Correlation between lake ice-out dates and winter and spring degree-days and snowfall at Presque Isle Station. Correlation between lake ice-out dates and winter and spring degree-days and snowfall at Presque Isle Station. Correlation coefficients in bold are significant at $p < 0.05$.

Station	PC1	PC2
Gardiner	0.98	0.02
Lewiston	0.97	0.03
Eastport	0.97	0.03
Corinna	0.99	0.01
Farmington	0.99	0.01
Brassua Dam	0.99	0.01
Presque Isle	0.99	0.01

Station	PC1		PC2	
	AFDD	AMDD	AFDD	AMDD
Gardiner	0.997	-0.079	-0.079	-0.997
Lewiston	0.996	-0.090	-0.090	-0.996
Eastport	0.994	-0.110	-0.110	-0.994
Corinna	0.999	-0.047	-0.047	-0.999
Farmington	0.999	-0.044	-0.044	-0.999
Brassua Dam	0.999	-0.025	-0.025	-0.999
Presque Isle	0.999	-0.013	-0.013	-0.999

Table B.8. Results of Principal Component Analysis (PCA) on the 1950-2010 winter AFDD and AMDD time series in each of the six USHCN stations in Maine.

Station	PC1	PC2
Gardiner	0.83	0.17
Lewiston	0.87	0.13
Eastport	0.86	0.14
Corinna	0.78	0.22
Farmington	0.83	0.17
Brassua Dam	0.87	0.13
Presque Isle	0.77	0.23

Station	PC1		PC2	
	AFDD	AMDD	AFDD	AMDD
Gardiner	-0.51	0.86	0.86	0.51
Lewiston	-0.32	0.95	0.95	0.32
Eastport	-0.40	0.92	0.92	0.40
Corinna	-0.61	0.79	0.79	0.61
Farmington	-0.67	0.74	0.74	0.67
Brassua Dam	-0.93	0.37	0.37	0.93
Presque Isle	-0.73	0.68	0.68	0.73

Table B.9. Results of Principal Component Analysis (PCA) on the 1950-2010 spring AFDD and AMDD time series in each of the six USHCN stations in Maine.

Lake	Weather-Station	Regression Coefficients		Model Fitness		
		Spring		$\ell\ell$	R^2	AICc
		PC1 (10^{-4})	PC2 (10^{-4})			
Maranacook	Gardiner	−6.0 ***	3.9 ***	134.1	0.60	−261.6
Damariscotta	Gardiner	−6.9 ***	2.2	120.9	0.53	−235.50
China	Gardiner	−6.6 ***	3.9 ***	132.5	0.63	−258.5
Auburn	Lewiston	−5.6 ***	1.4	129.7	0.63	−252.7
Norway	Lewiston	−4.7 ***	0.9	133.6	0.59	−260.6
West Grand	Eastport	−6.6 ***	4.0 **	147.0	0.61	−287.5
Sebec	Corinna	−4.6 ***	1.7 **	147.0	0.61	−287.5
Mooselucmeguntic	Farmington	−3.9 ***	5.3 ***	188.7	0.74	−370.9
Rangeley	Farmington	−3.7 ***	5.3 ***	184.7	0.71	−362.9
Moosehead	Brassua Dam	−4.0 ***	4.9 ***	135.1	0.62	−263.6
Squapan	Presque Isle	−3.7 ***	3.4 ***	150.7	0.65	−294.7
Portage	Presque Isle	−3.2 ***	3.7 ***	148.3	0.58	−289.9

$\ell\ell$- log-likelihood

Table B.10. Key statistics for circular regression model M_0 across selected lakes. Key statistics for circular regression model M_0 across selected lakes. Circular regression parameters with *, **, and *** are significant at 0.1, 0.05 and 0.01 significance level respectively.

Lake	Weather Station	Regression Coefficients				Model Fitness		
		Spring				$\ell\ell$	R^2	AICc
		PC1 (10^{-4})	PC2 (10^{-4})	Snowfall (10^{-3})				
Maranacook	Gardiner	−5.4 ***	4.1 ***	1.1 ***	135.5	0.62	−263.2	
Damariscotta	Gardiner	−6.2 ***	2.5	1.5 ***	122.3	0.55	−236.9	
China	Gardiner	−5.8 ***	4.3 ***	1.6 ***	135.3	0.67	−262.8	
Auburn	Lewiston	−5.2 ***	1.9	6.8 ***	130.5	0.64	−253.0	
Norway	Lewiston	−4.3 ***	1.5	0.8 ***	134.9	0.62	−261.8	
West Grand	Eastport	−6.1 ***	4.2 ***	1.0 ***	148.1	0.62	−288.4	
Sebec	Corinna	−4.2 ***	1.8 **	1.2 ***	172.3	0.65	−336.9	
Mooselucmeguntic	Farmington	−3.7 ***	5.3 ***	3.5 **	188.7	0.74	−370.9	
Rangeley	Farmington	−3.4 ***	5.3 ***	0.6 ***	186.4	0.73	−365.0	
Moosehead	Brassua Dam	−3.2 ***	4.9 ***	1.3 ***	139.5	0.69	−271.0	
Squapan	Presque Isle	−3.3 ***	3.9 ***	1.5 ***	156.2	0.73	−304.5	
Portage	Presque Isle	−2.8 ***	4.1 ***	1.4 ***	153.7	0.67	−299.4	

$\ell\ell$- log-likelihood

Table B.11. Key statistics for circular regression model M_1 across selected lakes. Key statistics for circular regression model M_1 across selected lakes. Circular regression parameters with *, **, and *** are significant at 0.1, 0.05 and 0.01 significance level respectively

Lake	Weather Station	Regression Coefficients					Model Fitness		
		Winter		Spring			$\ell\ell$	R^2	AICc
		PC1 (10^{-4})	PC2 (10^{-4})	PC1 (10^{-4})	PC2 (10^{-4})	Snowfall (10^{-3})			
Maranacook	Gardiner	0.8 **	−8.1 ***	−4.6 ***	3.2 ***	1.3 ***	143.6	0.72	−276.6
Damariscotta	Gardiner	1.0 **	−9.7 ***	−5.1 ***	1.4	1.6 **	128.1	0.64	−245.6
China	Gardiner	0.8 **	−9.0 ***	−4.9 ***	3.3 ***	1.8 ***	143.8	0.76	−277.0
Auburn	Lewiston	1.2 ***	−2.8	−5.1 ***	6.5	2.2	135.1	0.71	−259.3
Norway	Lewiston	0.8 **	−3.4 *	−4.1 ***	0.6	0.5 **	138.2	0.67	−265.5
West Grand	Eastport	1.2 ***	−4.6 **	−5.1 ***	3.6 **	1.0 ***	153.1	0.68	−295.7
Sebec	Corinna	0.4 **	−3.2	−3.8 ***	1.7 **	1.1 **	174.2	0.68	−338.1
Mooselucmeguntic	Farmington	0.3 *	−1.6	−3.5 ***	5.2 ***	3.3 **	190.4	0.76	−370.4
Rangeley	Farmington	0.3 *	−3.4 *	−3.2 ***	5.3 ***	0.6 ***	188.0	0.74	−365.6
Moosehead	Brassua Dam	0.9 ***	−1.5 *	−2.8 ***	4.4 ***	1.2 ***	143.6	0.74	−276.3
Squapan	Presque Isle	0.5 **	−0.1	−3.2 ***	3.9 ***	1.3 ***	158.4	0.74	−306
Portage	Presque Isle	0.2	−1.6	−2.8 ***	4.1 ***	1.3 ***	154.1	0.67	−297.4

$\ell\ell$- log-likelihood

Table B.12. Key statistics for circular regression model M_2 across selected lakes. Key statistics for circular regression model M_2 across selected lakes. Circular regression parameters with *, **, and *** are significant at 0.1, 0.05 and 0.01 significance level respectively

Lake	Weather Station	Regression Coefficients						Model Fitness		
		Winter			Spring			$\ell\ell$	R^2	AICc
		PC1 (10^{-4})	PC2 (10^{-4})	Snowfall (10^{-4})	PC1 (10^{-4})	PC2 (10^{-4})	Snowfall (10^{-3})			
Maranacook	Gardiner	0.9 ***	−7.1 ***	7.0 ***	−4.3 ***	3.0 **	1.3 ***	145.0	0.74	−277.8
Damariscotta	Gardiner	1.1 ***	−7.5 ***	1.5 ***	−4.6 ***	7.9	1.7 ***	131.9	0.7	−251.8
China	Gardiner	0.8 ***	−7.6 ***	9.5 ***	−4.6 ***	3.0 **	1.8 ***	146.6	0.79	−281.1
Auburn	Lewiston	1.1 ***	−1.1	8.1 ***	−4.9 ***	0.3	0.3	137.6	0.74	−262.8
Norway	Lewiston	0.7 **	−3.1 *	1.3	−4.1 ***	4.9	4.8 *	138.4	0.67	−264.4
West Grand	Eastport	1.3 ***	−3.9 *	7.7 **	−4.9 ***	3.3 **	1.1 ***	154.8	0.70	−297.8
Sebec	Corinna	0.4 **	−2.8	3.8 **	−3.7 ***	1.5 **	1.0 ***	174.9	0.68	−338.1
Mooselucmeguntic	Farmington	0.3 *	−1.3	1.2	−3.5 ***	5.2 ***	3.1	190.5	0.76	−369.2
Rangeley	Farmington	0.3 *	−3.3	5.5	−3.2 ***	5.3 ***	5.9 **	188	0.74	−364.3
Moosehead	Brassua Dam	0.9 ***	−1.5	5.9	−2.8 ***	4.4 ***	1.2 ***	143.6	0.74	−274.8
Squapan	Presque Isle	0.4 **	1.0	−2.5	3.2 ***	−4.0 ***	1.3 ***	158.8	0.75	−305.2
Portage	Presque Isle	0.2	−1.6	3.2 *	−2.8 ***	4.2 ***	1.3 ***	154.3	0.68	−296.3

$\ell\ell$- log-likelihood

Table B.13. Key statistics for circular regression model M_3 across selected lakes. Key statistics for circular regression model M_3 across selected lakes. Circular regression parameters with *, **, and *** are significant at 0.1, 0.05 and 0.01 significance level respectively.

Lake	Weather-Station	Regression Coefficients		Model Fitness		
		Spring		$\ell\ell$	R^2	AICc
		PC1 (10^{-4})	PC2 (10^{-4})			
Maranacook	Gardiner	−11.9 ***	7.8 **	41.92	0.59	−75.58
Damariscotta	Gardiner	−13.3 ***	4.2	30.25	0.60	−49.57
China	Gardiner	−13.1 ***	7.8 **	40.50	0.62	−72.74
Auburn	Lewiston	−11.2 ***	2.9	44.52	0.63	−80.76
Norway	Lewiston	−9.5 ***	1.8	48.20	0.57	−88.11
West Grand	Eastport	−13.1 ***	7.9 **	47.65	0.60	−87.07
Sebec	Corinna	−9.1 ***	3.3 *	47.65	0.62	−87.07
Mooselucmeguntic	Farmington	−7.7 ***	10.5 ***	80.20	0.75	−152.18
Rangeley	Farmington	−7.4 ***	10.6 ***	76.23	0.71	−144.26
Moosehead	Brassua Dam	−7.9 ***	9.8 ***	50.07	0.61	−91.87
Portage	Presque Isle	−6.4 ***	7.4 ***	61.9	0.58	−115.53
Squapan	Presque Isle	−6.4 ***	7.4 ***	63.72	0.58	−119.17

Table B.14. Key statistics for standard linear model M_0 across selected lakes. Key statistics for standard linear model M_0 across selected lakes. Linear regression parameters with *, **, and *** are significant at 0.1, 0.05 and 0.01 significance level respectively.

Lake	Weather Station	Regression Coefficients			Model Fitness		
		Spring			$\ell\ell$	R^2	AICc
		PC1 (10^{-4})	PC2 (10^{-4})	Snowfall (10^{-3})			
Maranacook	Gardiner	−10.8 ***	8.2 **	2.3	41.92	0.62	−75.78
Damariscotta	Gardiner	−12.3 ***	4.9	2.9	0.54		
China	Gardiner	−11.5 ***	8.5 **	3.3 **	43.24	0.66	−75.96
Auburn	Lewiston	−10.4 ***	3.9	1.4	45.5	0.63	−80.72
Norway	Lewiston	−8.6 ***	2.9	1.6 *	49.8	0.60	−89.32
West Grand	Eastport	−12.1 ***	8.4 **	2.0	48.77	0.62	−87.31
Sebec	Corinna	−8.3 ***	3.6 **	2.5 **	67.47	0.66	−124.72
Mooselucmeguntic	Farmington	−7.4 ***	10.5 ***	0.7	80.82	0.75	−151.42
Rangeley	Farmington	−6.8 ***	10.6 ***	1.23*	77.91	0.72	−145.6
Moosehead	Brassua Dam	−6.4 ***	9.7 ***	2.6 **	53.5	0.67	−96.72
Portage	Presque Isle	−5.6 ***	8.2 ***	2.7 ***	66.64	0.66	−122.72
Squapan	Presque Isle	−6.5 ***	7.7 ***	3.0 ***	69.88	0.73	−129.49

Table B.15. Key statistics for standard linear model M_1 across selected lakes. Key statistics for standard linear model M_1 across selected lakes. Linear regression parameters with *, **, and *** are significant at 0.1, 0.05 and 0.01 significance level respectively.

Lake	Weather Station	Regression Coefficients					Model Fitness		
		Winter		Spring			$\ell\ell$	R^2	AICc
		PC1 (10^{-4})	PC2 (10^{-4})	PC1 (10^{-4})	PC2 (10^{-4})	Snowfall (10^{-3})			
Maranacook	Gardiner	1.6 **	−16.2 ***	−9.1 ***	6.5 **	2.5 *	49.97	0.71	−84.57
Damariscotta	Gardiner	2.1 **	−19.3 ***	−10.2 ***	2.8	3.3 *	36.1	0.64	−56.83
China	Gardiner	1.5 **	−17.8 ***	−9.7 ***	6.6 **	3.6 ***	50.7	0.75	−86.04
Auburn	Lewiston	2.3 **	−5.5	−10.2 ***	1.3	0.5	49.43	0.69	−84.59
Norway	Lewiston	1.5 *	−6.7	−8.2 ***	1.1	0.9	52.39	0.68	−90.49
West Grand	Eastport	2.5 ***	−9.3 *	−10.2 ***	7.2 *	2.0	53.8	0.68	−93.36
Sebec	Corinna	0.8	−6.3	−7.6 ***	3.3 *	2.2 **	69.43	0.68	−124.75
Mooselucmeguntic	Farmington	0.5	−3.2	−7.0 ***	10.4 ***	0.7	0.76		
Rangeley	Farmington	0.5	−6.8	−6.4 ***	10.5 ***	1.2 *	79.56	0.74	−144.9
Moosehead	Brassua Dam	1.7 ***	−3.1	−5.7 ***	8.8 ***	2.5 **	58.5	0.73	−102.73
Portage	Presque Isle	0.4 *	−3.3	−5.6 ***	8.2 ***	2.5 **	67.2	0.67	−117.63
Squapan	Presque Isle	0.9 *	−1.8	−6.3 ***	7.8 ***	2.5 ***	72	0.75	−129.7

Table B.16. Key statistics for standard linear model M_2 across selected lakes. Key statistics for standard linear model M_2 across selected lakes. Linear regression parameters with *, **, and *** are significant at 0.1, 0.05 and 0.01 significance level respectively.

Lake	Weather Station	Regression Coefficients						Model Fitness		
		Winter			Spring			$\ell\ell$	R^2	AICc
		PC1 (10^{-4})	PC2 (10^{-4})	Snowfall (10^{-4})	PC1 (10^{-4})	PC2 (10^{-4})	Snowfall (10^{-3})			
Maranacook	Gardiner	1.7 **	−14.2 **	1.4	−8.6 ***	6.0 **	2.6 **	51.17	0.72	−84.38
Damariscotta	Gardiner	2.3 **	−14.8 **	3.0 **	−9.2 ***	1.7	3.3 **	0.69		
China	Gardiner	1.7 **	−15.1 ***	1.9 **	−9.1 ***	6.0 **	3.6 ***	52.98	0.77	−88.01
Auburn	Lewiston	2.1 **	−2.2	1.6 *	−9.7 ***	0.6	0.7	51.72	0.72	−87.17
Norway	Lewiston	1.5 *	−6.2	0.3	−8.1 ***	1.0	1.0	52.46	0.65	−88.63
West Grand	Eastport	2.6 ***	−7.8	1.5 *	−9.7 ***	6.5 *	2.2 *	55.6	0.70	−94.95
Sebec	Corinna	0.8 **	−5.6	0.8 *	−7.4 ***	3.1	2.1	70.2	0.69	−124.18
Mooselucmeguntic	Corinna	0.5	−2.6	0.2	−7.0 ***	10.4 ***	0.6	81.91	0.76	−147.61
Rangeley	Corinna	0.5	−6.5	0.1	−6.4 ***	10.5 ***	1.2 *	79.58	0.74	−142.94
Moosehead	Brassua Dam	1.7 ***	−3.0	0.1	−5.7 ***	8.8 ***	2.4 **	58.51	0.73	−100.75
Portage	Presque Isle	0.4	−3.3	0.6	−5.6 ***	8.3 ***	2.6 ***	67.54	0.67	−116.99
Squapan	Presque Isle	0.9 *	−1.8	0.5	−6.3 ***	8.0 ***	2.6 ***	72.27	0.75	−128.26

Table B.17. Key statistics for standard linear model M_3 across selected lakes. Key statistics for standard linear model M_3 across selected lakes. Linear regression parameters with *, **, and *** are significant at 0.1, 0.05 and 0.01 significance level respectively.

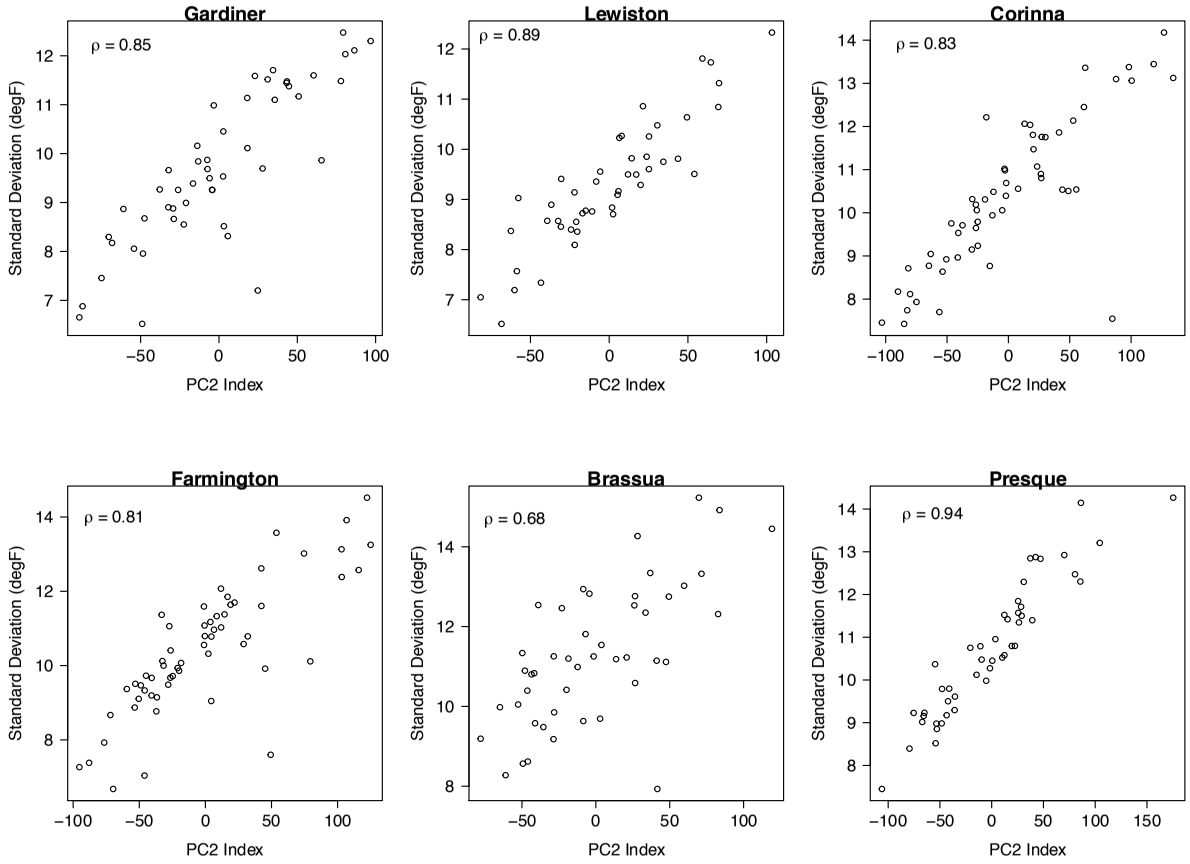

Figure B.1. Scatter plot of intra-seasonal standard deviation of spring temperatures as a function of the indices of second principal component (PC2) of spring degree-days across the six stations.

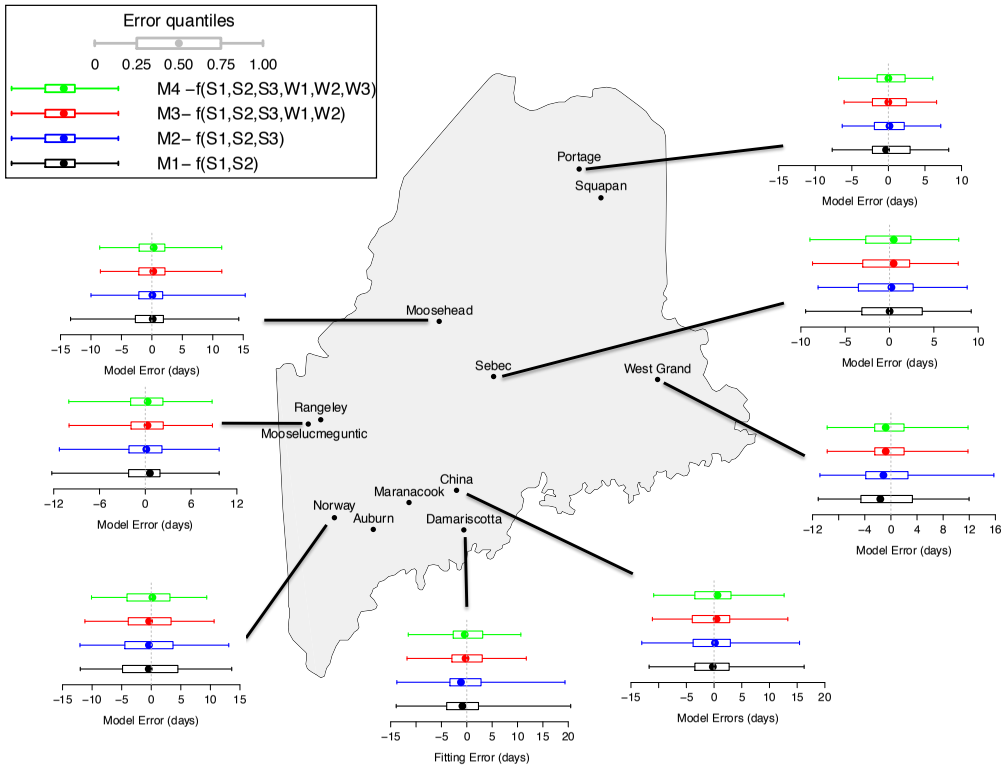

Figure B.2. Model bias and uncertainty across studied lakes.

APPENDIX C

This appendix provides supplementary tables and figures for Chapter 4.

C.1 Spatial and temporal patterns of ice break up dates in Maine lakes

To assess whether the PC1 for the ice-out date of eight Maine lakes used in this study is a good representation of the dominant temporal pattern of ice out date in Maine lakes, we performed Principal component analysis (PCA) on the ice-out date of sixteen Maine lakes for the period between 1950-2010 with some years missing. The leading principal component (PC1) retains 79% of the total variance in ice out date of the sixteen lakes and therefore may be considered as the leading pattern of ice-out date variability (see Table C.1). Figure C.1a shows the strong similarity between the time series of the PC1 of the two sets of lakes and the correlation is 0.98 ($p < 0.05$). Furthermore the homogeneity of signs in the sixteen lakes indicates that there is coherence between these lakes in their pattern of ice out dates, which was also observed in the PC1 of the eight lakes (see Figure C.1b).

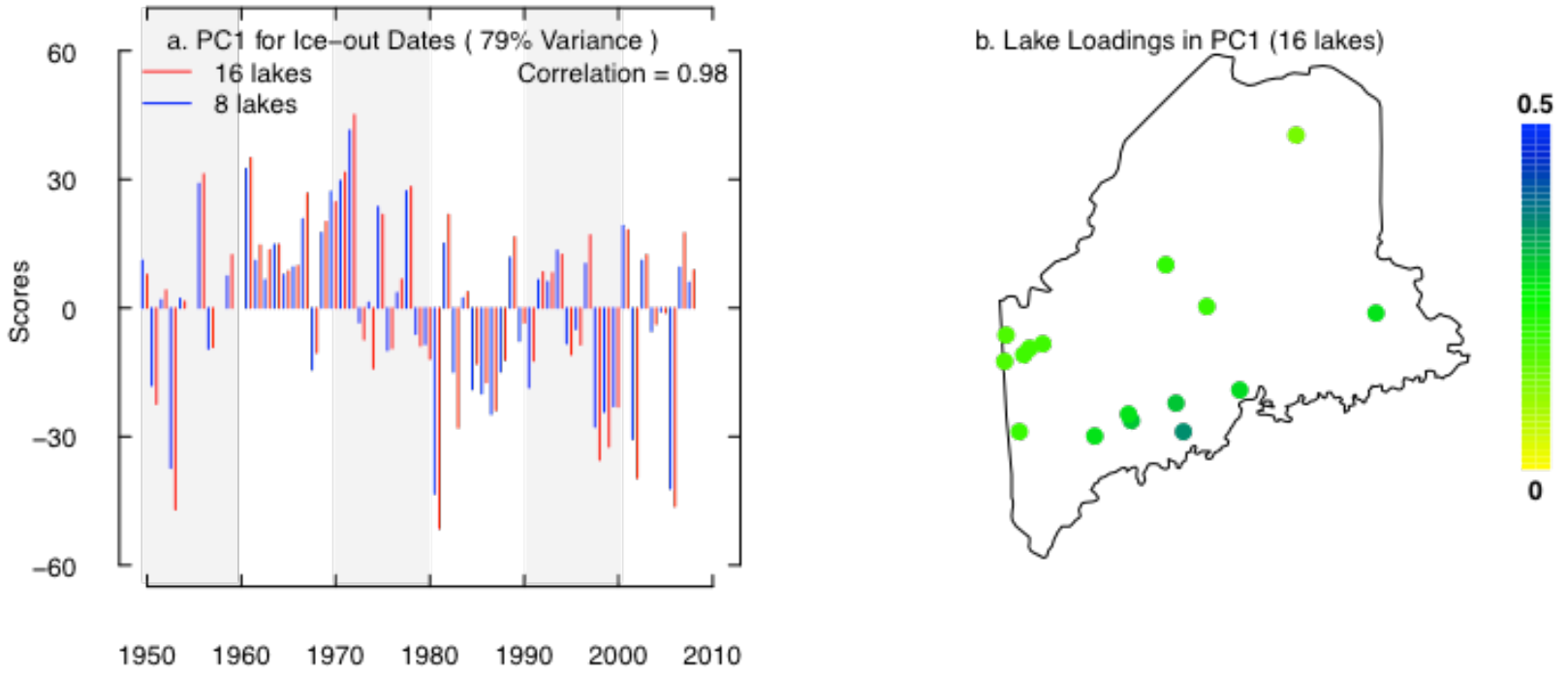

Figure C.1. The time series and loadings for the first principal component (PC1) of lake ice 27 out dates in Maine for the period 1950-2010.

	PC1	PC2	PC3
Standard Deviation	29.09	11.05	4.95
Proportion of Variance	0.79	0.11	0.02
Cumulative Proportion	0.79	0.91	0.93

Lake	PC1 Loading	PC2 Loading
Mooselucmeguntic	0.20	-0.35
Richardson	0.20	-0.34
Rangeley	0.20	-0.33
Aziscohos	0.18	-0.33
Umbagog	0.18	-0.30
Moosehead	0.22	-0.27
Portage	0.15	-0.25
Sebec	0.21	-0.10
Kezar	0.21	-0.05
West Grand	0.28	0.07
Auburn	0.29	0.17
Swan	0.29	0.18
Maranacook	0.29	0.21
China	0.31	0.22
Cobbosseecontee	0.23	-0.20
Damariscotta	0.33	0.73

Table C.1. Results of Principal Component Analysis (PCA) performed on the ice out date of eight lakes with serially complete data for the period 1950-2010.

C.2 Influence of Northern Hemisphere Sea Surface Temperatures on Maine Winter Temperature

For the sake of comprehensiveness, the PC1 time series of winter AFDD and AMDD in Maine were correlated with sea surface temperatures to determine other oceanic-atmospheric circulation patterns that influence winter temperature variability and in turn spring ice out date in Maine. The PC1 of winter AFDD and AMDD showed a significant correlation largely with sea surface temperature anomalies along North Atlantic and Pacific and Tropical Atlantic (see Figure C.2). This result indicates that teleconnection patterns such as Atlantic tripole (ATI), Atlantic multidecadal oscillation (AMO) and Pacific decadal oscillation (PDO) with sensitivity to sea surface anomalies in this region may shape inter-annual variability of winter degree-days and spring ice off dates in Maine (see Table C.2). However the mechanisms that underlie the mode of these sea surface temperature anomalies (and their teleconnections), their persistence and seasonality are less understood. Thus, we limit our focus to the understanding the season-ahead causal relationships between select teleconnection patterns, suitable degree-day indices in the context of lake ice out.

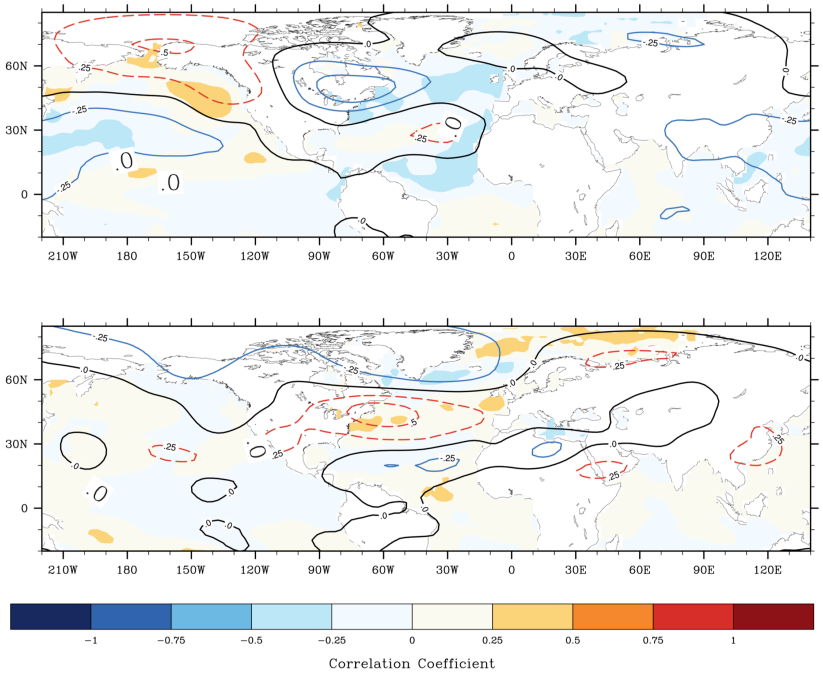

Figure C.2. The 1950-2010 composite winter sea surface temperature and 500mb geo- potential height anomaly maps correlated against the time series of PC1 for winter AFDD (top) and PC1 for winter AMDD in Maine (bottom).

	Year	PC1 of Winter AFDD	PC1 of Winter AMDD	PC1 of Spring AFDD	PC1 of Spring AMDD	Winter TNH Index	Winter NAO Index	Winter PNA Index	Winter PDO Index	Winter AMO Index	Winter AO Index	Winter SAI Index	PC1 of Lake Ice-dates
Year	**1**												
PC1 of Winter AFDD	-0.15	**1**											
PC1 of Winter AMDD	-0.09	**-0.50**	**1**										
PC1 of Spring AFDD	-0.07	0.20	-0.14	**1**									
PC1 of Spring AMDD	0.24	0.26	-0.26	**0.61**	**1**								
Winter TNH Index	0.14	**0.38**	-0.24	-0.17	-0.07	**1**							
Winter NAO Index	**0.44**	0.06	**0.44**	-0.02	0.19	0.12	**1**						
Winter PNA Index	**0.35**	0.10	-0.07	0.19	**0.29**	-0.11	-0.05	**1**					
Winter PDO Index	**0.40**	0.16	-0.06	-0.03	0.26	-0.09	-0.09	**0.74**	**1**				
Winter AMO Index	-0.16	**-0.50**	0.11	0.08	-0.05	-0.15	-0.14	0.05	0.01	**1**			
Winter AO Index	**0.30**	0.01	**-0.31**	-0.20	0.06	0.26	**0.82**	-0.21	-0.24	-0.11	**1**		
Winter SAI Index	0.16	**-0.52**	**0.56**	**-0.38**	**-0.47**	**-0.56**	**-0.79**	**0.72**	**0.50**	-0.07	**0.80**	**1**	
PC1 of Lake ice dates	-0.26	**0.38**	**-0.51**	0.13	**-0.85**	**-0.27**	0.21	**0.29**	0.24	0.08	-0.10	**-0.43**	**1**

Table C.2. Correlation between the first principal component (PC1) of lake ice out dates, winter and spring degree-days and winter teleconnection patterns.

C.3 Analyzing the effect of changing the teleconnection thresholds on the results of this study

In this paper, analyses and observations on the influence of "strong" or "extreme" teleconnection patterns on lake ice out dates/winter degree-days in Maine is based on the threshold of the selected teleconnection patterns being in the upper and lower quartiles of the historical indices. The selection of this threshold was made based on the limited sample size ($n = 61$) and higher thresholds would limit the number of subsamples that can be re-sampled. In our case, we have a sample size of 15, wherein mean, median, and box-plot statistics can be meaningfully computed and compared.

However, to explore if alterations in this threshold would result in a whole sale change in our observations and conclusions about the efficacy of TNH and NAO phases in engendering early spring ice breakup dates in Maine lakes, the significance of the shift in the median ice out date of select eight lakes during different lower/upper percentiles (0.1, 0.15, 0.2, 0.25, 0.3) of TNH/NAO phases were compared with the unconditional median ice out dates for randomly chosen subsamples years in the study period (see Figure C.3). It should be noted that the size of the random sub-samples depends on the percentile chosen. For instance, for the upper/lower terciles of TNH/NAO patterns, the subsample size for the random sub-sample is six ($61 \times 6 \approx 6$). It can be observed in Figure C.3 that indeed strongly negative TNH phases during winter induces a shift towards earlier dates in the spring ice out date of lakes for all regions of Maine although the shift in the median ice out dates for one or two lakes is not highly significant ($p < 0.05$) during the different percentiles. It can also be noted that the influence of strongly positive NAO phases during winter in engendering earlier spring lake ice out dates is limited to the coastal regions since in most cases the shift in the median ice out date of northern or southern interior lakes is not significant ($p < 0.1$). The basis for such observations is that the strength of positive NAO phases in producing warmer winter degree-days is weak in the interior regions as observed in the figure C.5.

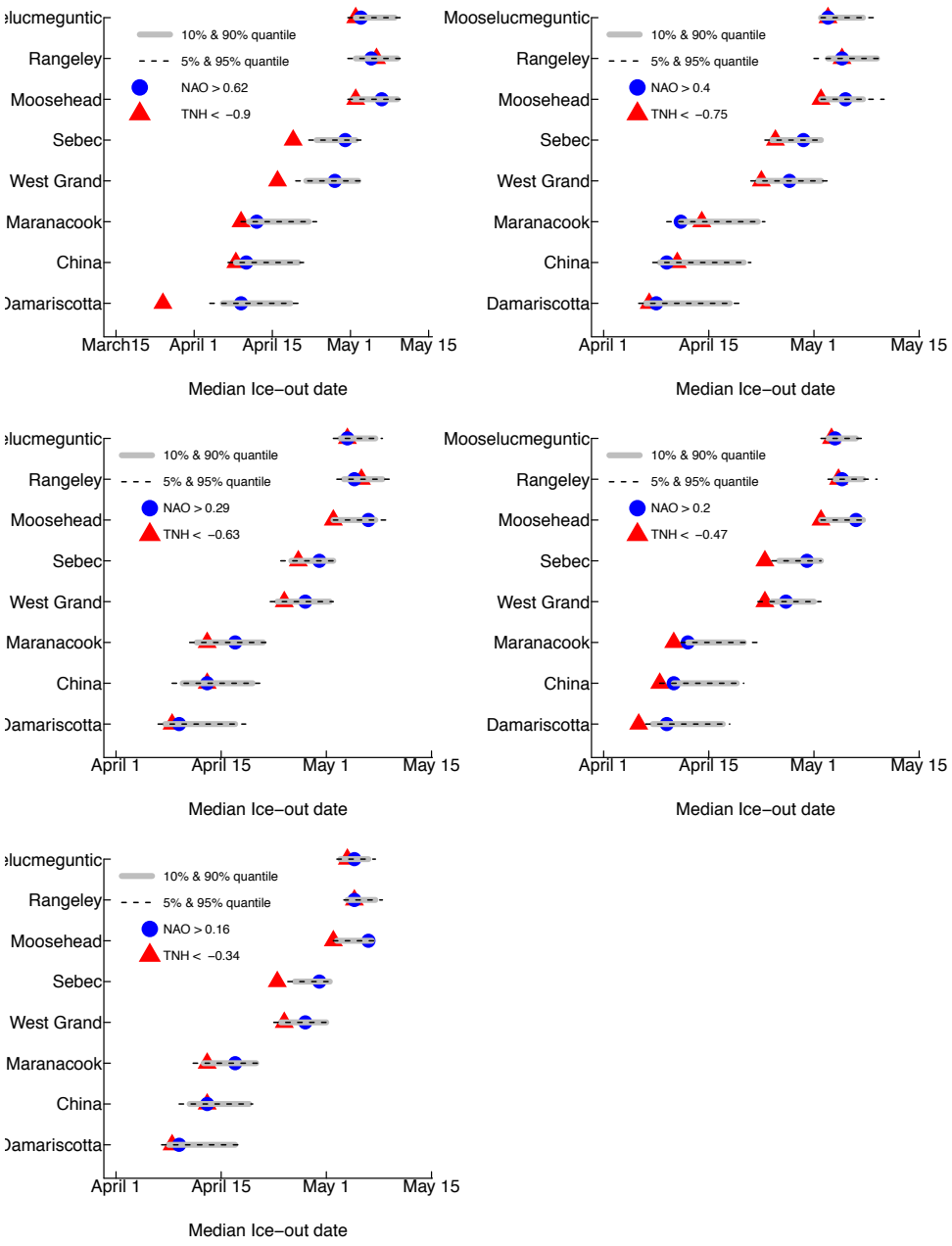

Figure C.3. Shifts in median ice out dates and its significance for eight selected lakes from 1950-2010 Shifts in median ice out dates and its significance for eight selected lakes from 1950-2010 during (a) lower tercile TNH pattern (TNH $<$ -0.9) and upper tercile of NAO (NAO $>$ 0.62) phases (b) lower 15^{th} percentile TNH pattern (TNH $<$ -0.75) and upper 15^{th} percentile NAO (NAO $>$ 0.4) phases (c) lower 20^{th} percentile TNH phases (TNH $<$ -0.63) and upper 20^{th} percentile NAO (NAO $>$ 0.29) phases (d) lower quartile TNH indices (TNH $<$ -0.47) and upper quartile NAO phases (NAO $>$ 0.2) (e) lower 30^{th} percentile TNH indices (TNH $<$ -0.34) and upper quartile NAO phases (NAO $>$ 0.16). The variability band for the median ice out date of each lake was constructed using the bootstrap method.

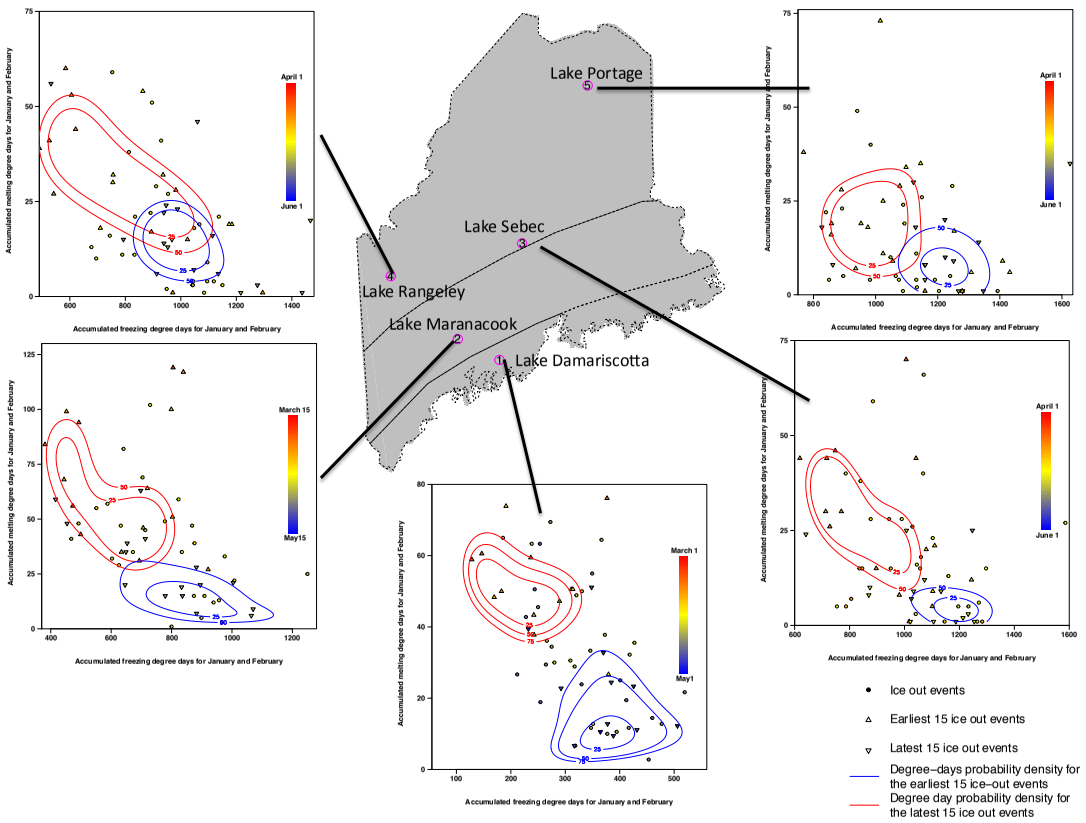

Figure C.4. The joint probability density of winter AFDD and AMDD for the earliest and latest fifteen (upper and lower quartiles) ice breakup dates in five Maine lakes The joint probability density of winter AFDD and AMDD for the earliest and latest fifteen (upper and lower quartiles) ice breakup dates in five Maine lakes (Lake Portage, Lake Maranacook, Lake Damariscotta, Lake Rangeley, and Lake Sebec).

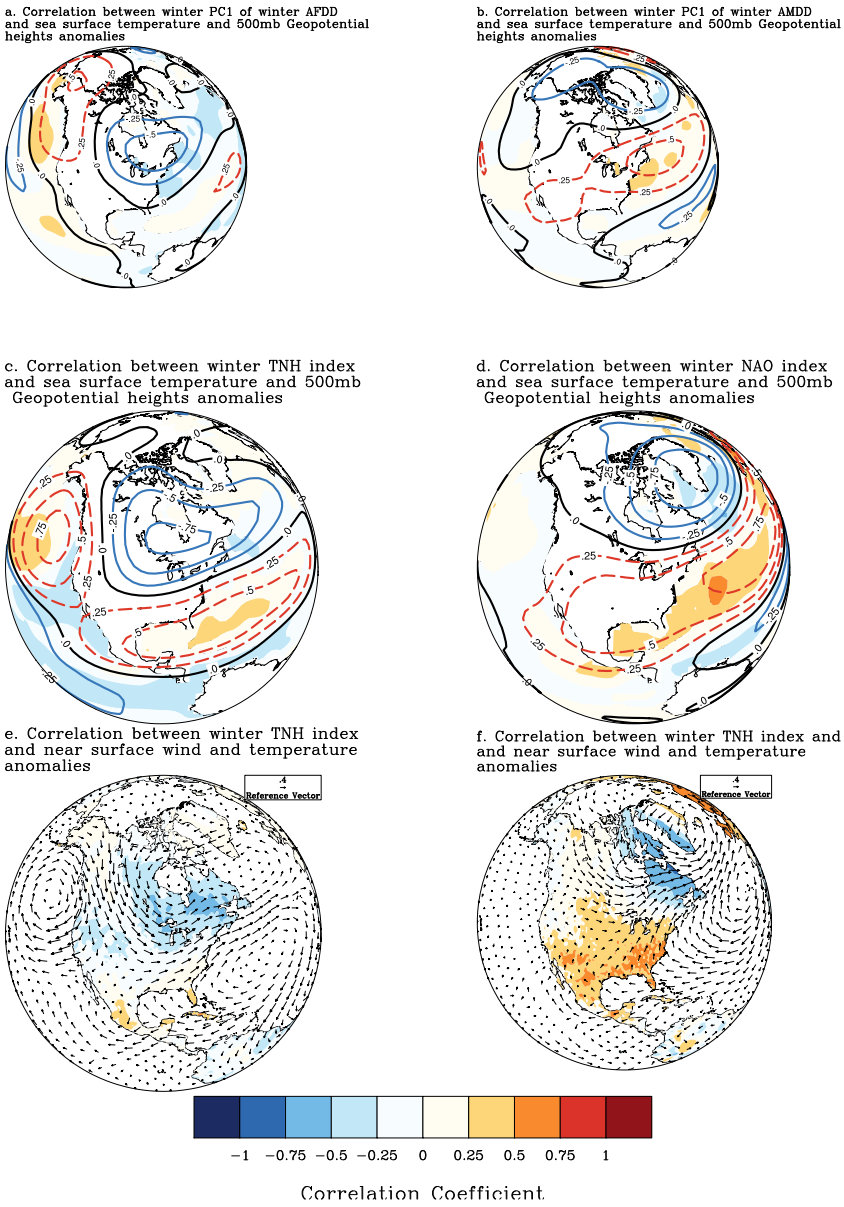

Figure C.5. The 1950-2010 composite winter 500mb geo-potential heights and sea surface anomaly maps The 1950-2010 composite winter 500mb geo-potential heights and sea surface anomaly maps correlated against the time series of (a) PC1 for winter AFDD (b) PC1 for winter AMDD in Maine (c) average winter TNH indices (d) average winter NAO indices. Correlation coefficients above 0.25 (colored areas) are significant at 95% confidence level. (e) and (f) show the anomalous near surface (850mb) wind and temperature anomaly maps regressed against the time series of average winter TNH and NAO indices respectively. The unit of anomalous winds at 850mb is in 7m/sec as shown in the vector at the top.

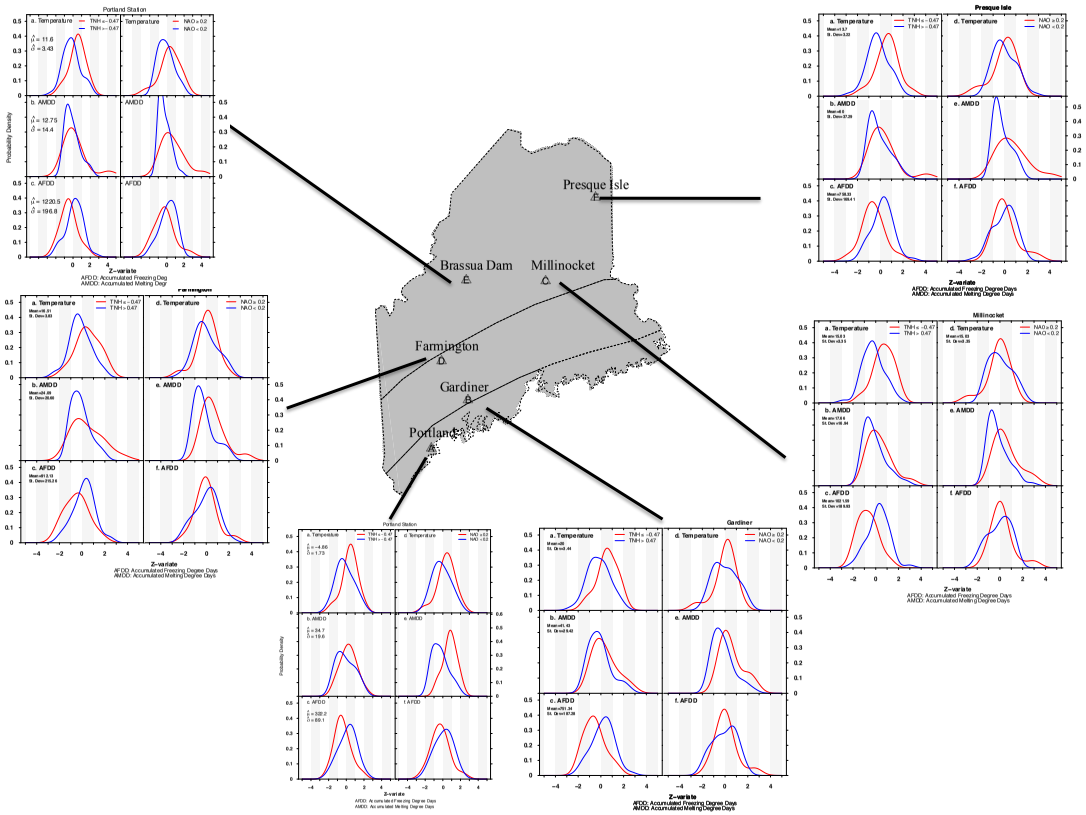

Figure C.6. The Conditional probability density curves for winter temperature (and derived variables) The Conditional probability density curves for winter temperature (and derived variables during (a-c) lower quartile TNH phases (d-f) upper quartile NAO phases in six USHCN stations (Portland, Farmington, Presque Isle, Brassua Dam, Gardiner and Millinocket).

APPENDIX D

This supplementary document contains additional analyses and figures that support the results and/or assumptions for Chapter 5. For instance, D.1 details the identification of ENSO events based on a comprehensive survey of existing approach in published literature. On the other hand, Section D.1 performs lack of fit test to check the adequacy of linear quantile regression in characterizing the link between tropical Pacific SST patterns and surface temperature anomalies, across different quantiles, for North American temperature fields. Discussion on the methods and procedures for Section D.1 to Section D.3 are given in those sections.

Year	Classification Method					
	EMI	Nino3/4	EP/CP	NCP/NWP	Network Method	Consensus
1955/56	La Niña	La Niña	La Niña	La Niña	La Niña	La Niña
1968/69	CP El Niño	CP El Niño	CP El Niño	CP El Niño	CP El Niño	CP El Niño
1972/73	EP El Niño	EP El Niño	EP El Niño	EP El Niño	EP El Niño	EP El Niño
1973/74	La Niña	La Niña	La Niña	La Niña	La Niña	La Niña
1975/76	La Niña	La Niña	La Niña	La Niña	La Niña	La Niña
1982/83	EP El Niño	EP El Niño	EP El Niño	EP El Niño	EP El Niño	EP El Niño
1988/89	La Niña	La Niña	La Niña	La Niña	La Niña	La Niña
1994/95	CP El Niño	CP El Niño	CP El Niño	CP El Niño	CP El Niño	CP El Niño
1997/98	EP El Niño	EP El Niño	EP El Niño	EP El Niño	EP El Niño	EP El Niño
2004/05	CP El Niño	CP El Niño	CP El Niño	CP El Niño	CP El Niño	CP El Niño
2006/07	EP El Niño	EP El Niño	EP El Niño	EP El Niño	EP El Niño	CP El Niño
2007/08	La Niña	La Niña	La Niña	La Niña	La Niña	La Niña
2009/10	CP El Niño	CP El Niño	CP El Niño	CP El Niño	CP El Niño	CP El Niño
2014/15	CP El Niño	CP El Niño	CP El Niño	CP El Niño	-	CP El Niño
2015/16	EP El Niño	EP El Niño	EP El Niño	EP El Niño	EP El Niño	EP El Niño

Table D.1. Classification of major ENSO events based on different identification methods Classification of major ENSO events based on different identification methods: EMI (Ashok et al. 2007), Niño 3/4 (Yeh et al. 2009), EP/CP (Kao and Yu 2009), NCT/NWP (Ren and Jin 2011) and climate network based (Wiedermann et al. 2016) index. A hyphen indicates that there has been no classification made for that event.

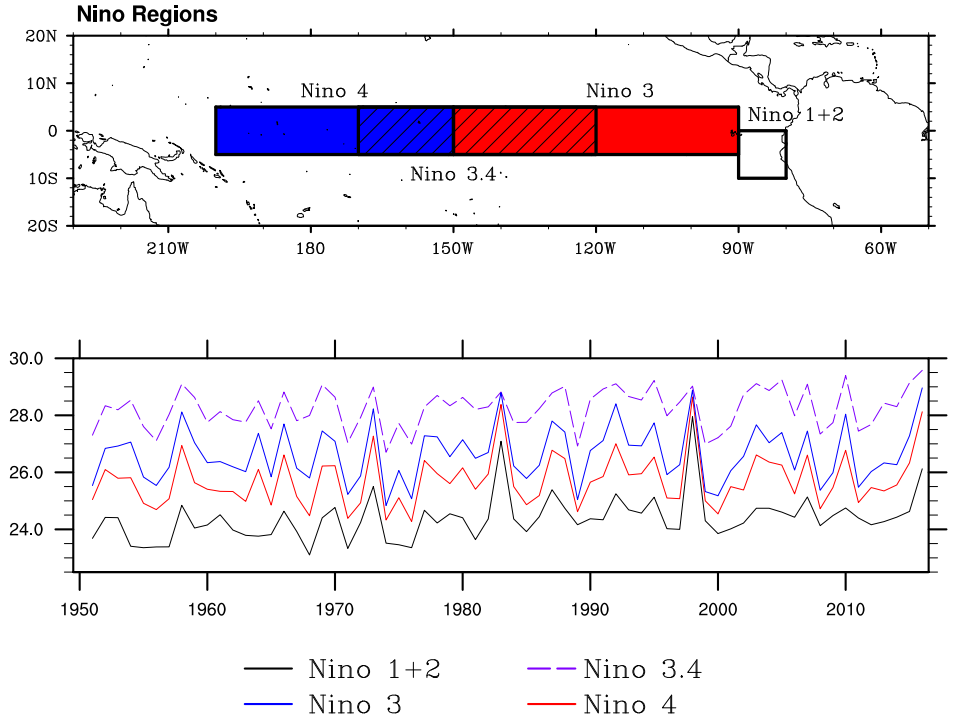

Figure D.1. Time series of the winter sea surface temperature (SST) index for the four Niño regions in the Tropical Pacific from 1951-2016 Time series of the winter sea surface temperature (SST) index for the four Niño regions in the Tropical Pacific from 1951-2016: Niño1+2 (black line), Niño 3 (red line), Niño 3.4 (blue line) and Niño 4 (purple dashed line). These SST indices represent the spatially averaged sea surface temperatures for different Tropical Pacific region: Niño 1 (white), Niño 3 (red), Niño 4 (blue) and Niño 3.4 (black hatches).

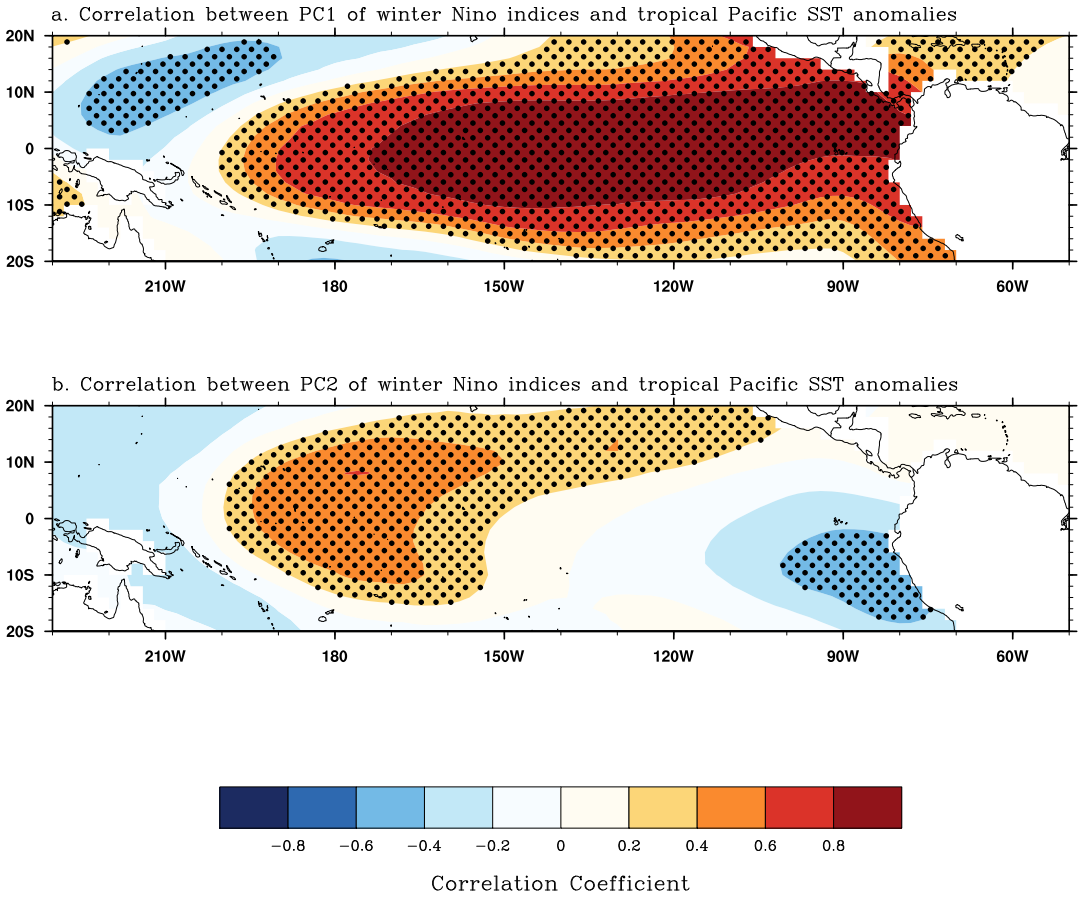

Figure D.2. Correlation maps of tropical Pacific winter SST anomaly fields against (a) PC1 and (b) PC2 patterns. Correlation maps of tropical Pacific winter SST anomaly fields against (a) PC1 and (b) PC2 patterns. Contour interval for the correlation coefficient is set at 0.2. Stipples represent correlation coefficients that are significant at $p < 0.1$ based on two-tailed student t-test.

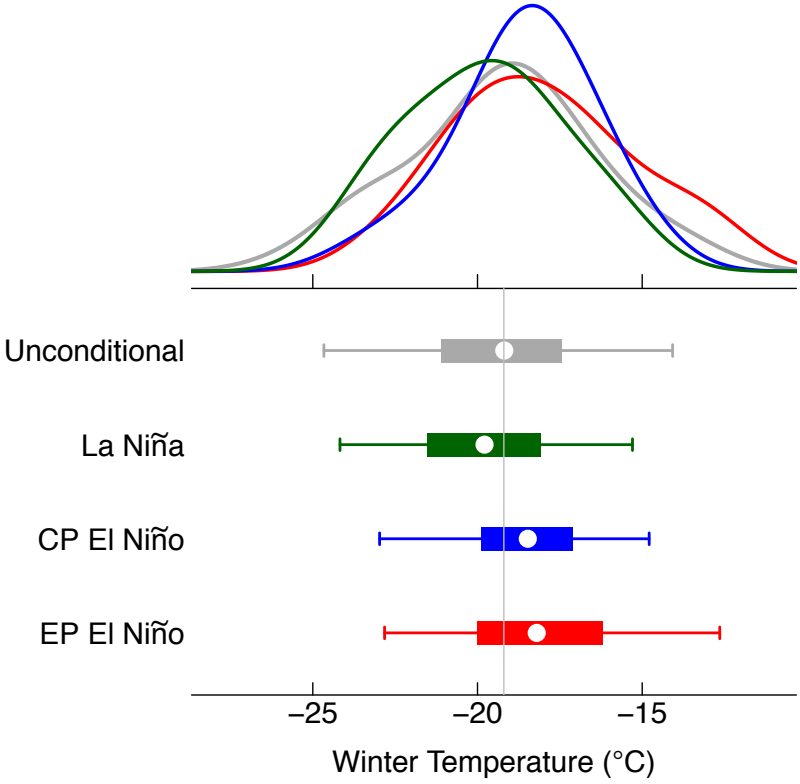

Figure D.3. The empirical conditional winter air temperature distribution for Fort Nelson during archetypical EP Niño (red), CP El Niño (blue) and La Niña (green) events. The empirical conditional winter air temperature distribution for Fort Nelson during archetypical EP Niño (red), CP El Niño (blue) and La Niña (green) events. The grey boxplot/curve represents the climatological empirical winter air temperature distribution. The probability density curves were constructed using non-parametric kernel density estimators. The boxplot shows the 0.05th (left end), 0.25th (left end of box), 0.5th (centroid of white circle inside box), 0.75th (right end of the box) and 0.95th (right end) quantile of the winter temperature range.

D.1 Adequacy of Linearity

To check adequacy of the linearity specification within quantile regression of winter temperatures over North America, this study implemented a lack of fit test following the procedure by He and Zhu [73]. This approach is based on the cumulative sum (cusum) process of model residuals, which also utilizes a resampling method for obtaining the p-value in the test statistics. All p-values less than 0.10 suggest that the response of winter temperatures to ENSO patterns at specified quantile is not linear. The p-value of the test for the conditional winter temperature quantile functions of North American regions at quantile levels $\tau = 0.25^{th}$, 0.50^{th}, and 0.75^{th} is depicted in Figure D.4a-c. Results indicate that the linearity assumption for the conditional quantiles is reasonable for most North American regions (except for northwestern territories and Nunavut).

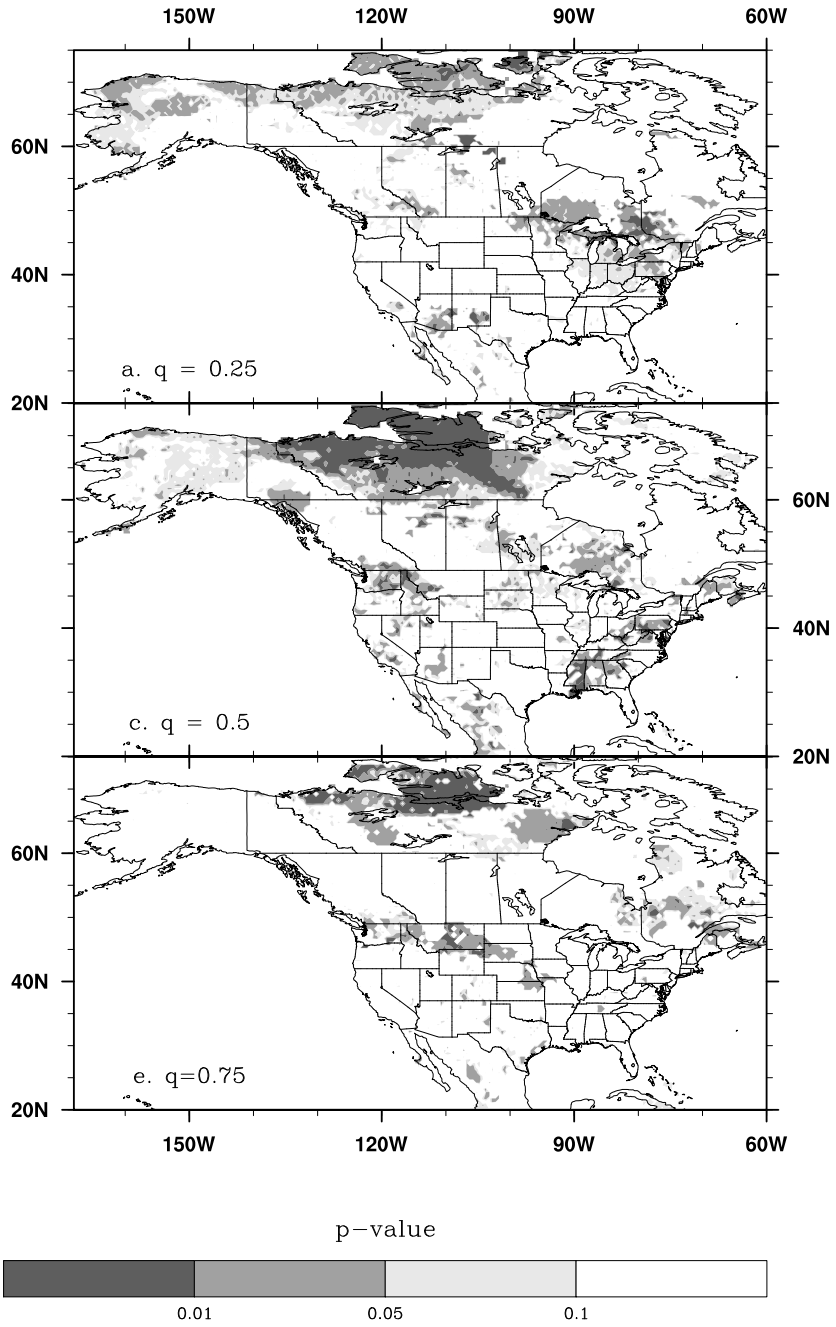

Figure D.4. Appropriateness of linear quantile functions for examining the relationship between ENSO indices and North American winter temperatures across different quantiles. Appropriateness of linear quantile functions for examining the relationship between ENSO indices and North American winter temperatures across different quantiles. The Lack of fit test was performed across (a) 0.25^{th}, (b) 0.50^{th} and (c) 0.75^{th} quantile winter temperatures and gray dots represent North American temperature fields where the p-value for lack of fit is significant at 90% confidence level.

D.2 Atmospheric Teleconnection Patterns associated with ENSO Flavors

The mid-tropospheric circulation is a key driver of the regional pattern of climate anomalies at surface. As such, contrasting the winter 500mb height anomalies among diverse ENSO flavors can offer a physical basis to explain how diversity in tropical Pacific SST anomaly patterns engenders asymmetries in ENSO-related winter climate anomalies over North America. To this end, three sets of five years were selected where by majority agreement of different identification methods have been identified as CP El Niño, EP El Niño and La Niña (see Table D.1). While there is year-to-year variation within each set of ENSO flavors, differences in the upper air height anomaly patterns over North America are prominent across the three ENSO flavors. The 500mb height anomaly patterns associated with CP El Niño winters have strong resemblance to the positive phase of Pacific North America (PNA) pattern, where there is below normal pressure centers over the gulf of Alaska and eastern coast of US and above normal height center over Pacific-North American regions (see Figure D.5a-e). As such, CP El Niño winters over North America typically correspond to positive temperature anomaly over much of Canada and north western US and a negative temperature anomaly over much of the eastern coast of US. In contrast, the upper air height anomaly patterns corresponding to EP El Niño winters have strong similarities with the negative phase of Tropical/Northern Hemisphere (TNH) pattern, where there are negative height anomaly centers over the Aleutians and northern Mexico and above normal pressure center over eastern Canada (see Figure D.5f-j). Consequently, EP El Niño winters over North America typically relate to warmer than normal winter temperatures over much of the eastern North America and cooler than average winter temperatures over southwestern US and northern Mexico. On the other hand, typical La Niña winters feature above normal pressure center over Aleutians and a negative height anomaly center over much of the Canadian regions, which correspond to below normal winter temperatures over much of Canada and north-western part of US and above normal winter temperatures over the southeastern part of the US (see Figure D.5k-o).

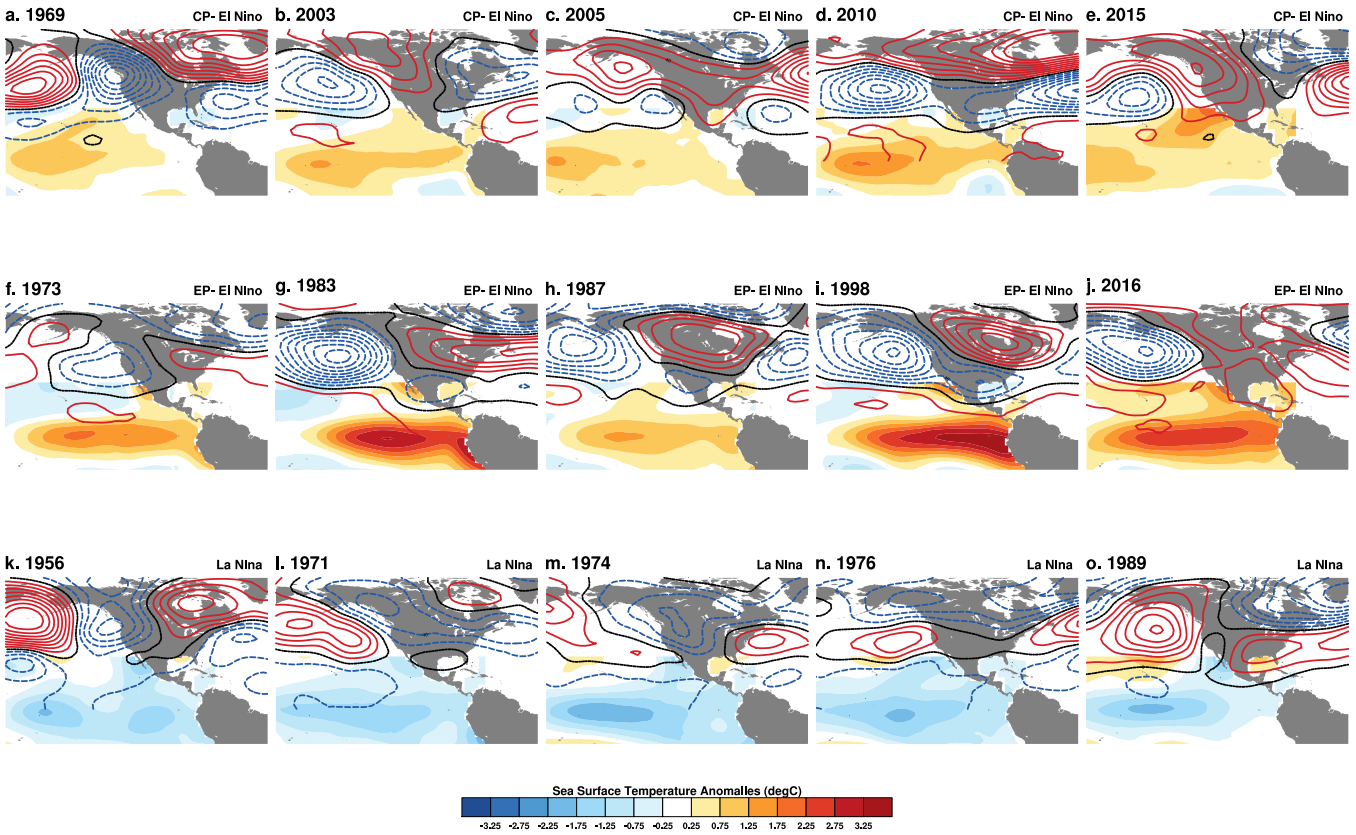

Figure D.5. Map of contemporaneous North American winter 500mb geo-potential height and tropical Pacific SST anomalies Map of contemporaneous North American winter 500mb geo-potential height and tropical Pacific SST anomalies, for five (a-e) CP El Niño (f-j) EP El Niño (k-o) La Niña years. These years were determined by majority consensus of different "ENSO identification" methods. Red contours indicate positive anomaly while blue contours represent negative anomalies. The contours for the 500mb geo-potential height and SST anomalies are set at 20m and $0.5°C$.

D.3 De-trending North American Surface Air Temperatures

D.3.1 Method

To determine if any, the effect of trends and low frequency variability on the results of our analysis, the linear winter trend was removed from the time series of winter Niño SST indices and North American winter SATs from 1951 to 2016. Using this data, all the analyses performed in the main article were repeated.

D.3.2 Results

D.3.2.1 ENSO Indices

The leading two empirical pattern of variability for the detrended wintertime SSTs in Niño regions was determined by performing Principal Component Analysis (PCA) on the time series of de-trended winter SST indices in the four Niño regions. Similar to the result for the un-detrended SSTs, the first two principal components (PCs) explain over 97% of the total Niño winter SST variability with PC1 representing just over 87% of the total variability (see Supplementary Table D.2). Moreover the loadings from the four Niño regions in the PC1 and PC2 of the detrended SST data are the same as that for the un-detrended data. Consequently, the correlation between the new PC1 and PC2 time series to that of the old (un-detrended) is 0.97 and 0.98 respectively (see Figure D.6).

	PC1	PC2	PC3	PC4
Standard Deviation	1.87	0.67	0.24	0.09
Proportion of Variance	0.87	0.11	0.01	0.002
Cumulative Proportion	0.87	0.98	0.99	1.00

PC	Niño1.2	Niño3	Niño3.4	Niño4
PC1	0.47	0.52	0.53	0.48
PC2	-0.72	-0.15	0.19	0.65
PC3	0.51	-0.58	-0.35	0.53
PC4	-0.09	0.60	-0.75	0.26

Table D.2. Empirical orthogonal modes of wintertime sea surface temperature variability in Niño regions Empirical orthogonal modes of wintertime sea surface temperature variability in Niño regions: (a) proportion of variance explained (b) loadings of Niño regions

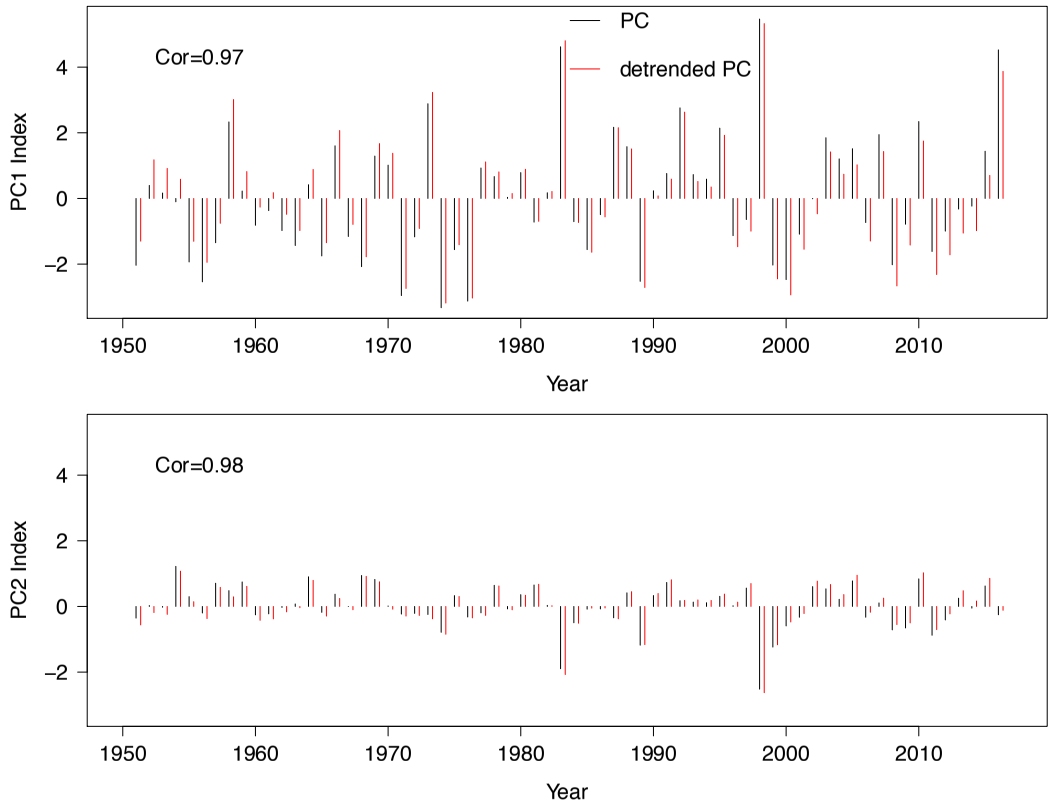

Figure D.6. Time series of the leading two empirical patterns (PC1 and PC2) for the detrended winter sea surface temperature variability in Nino regions of the tropical Pacific from 1951-2016. Time series of the leading two empirical patterns (PC1 and PC2) for the detrended winter sea surface temperature variability in Nino regions of the tropical Pacific from 1951-2016. The first principal component represents 87% of the total winter sea surface temperature (SST) variability in Niño regions while the second principal component explains 11%. The red histograms represent time series of PC1 and PC2 indices for the detrended winter SST variability in Niño regions while the black histogram is for the un-detrended one. The correlations results show the coherence between the new (detrended) PC1 and PC2 patterns to that of the old (un-detrended).

D.3.2.2 Response of De-trended North American Wintertime SAT Distribution to Leading EOFs of SST variability in Niño regions

Similar to the analysis in section 3.3 of the main paper, quantile functions for detrended winter SATs that employ the joint PC1-PC2 indices as covariates were generated at three quantile thresholds ($\tau = 0.25, 0.50$, and 0.75). The field significance of parameter estimates for PC1 and PC2 were computed using the wild bootstrap procedure. For North American regions, the parameter estimates for PC1 and PC2 patterns across the three quantiles are depicted in D.7.

Comparison of supplementary figure D.7 and figure 3 (in the main paper) show that for North America, the detrending process results in modest alteration in the parameter estimates (and their significance) for PC1 and PC2 patterns particularly for North American regions north of $60°N$ and at $\tau = 0.75$ (see Supplementary figure D.7). For instance after detrending the winter SATs, the parameter estimate for PC2 at 0.75^{th} quantile changes not only their magnitudes but also sign for some locations in Alaska. However, this can be explained as follows: the strongest trends in winter SATs are observed in northern most North American regions (see supplementary figure D.8) and removing this trends results in changes not only in the location of the winter SAT distribution but also the scale and other higher moments. Given these alterations in the characteristics (e.g. mean, spread, etc) of winter SAT distribution, it is not surprising that changes in the response of winter SATs to PC1 and PC2 patterns at specific quantiles are observed in North American regions with strong trends in their winter SATs.

Despite this, the main findings and conclusions from our previous analyses in section 3.3 remain valid. Both results show that there is asymmetry both spatially and across different quantiles in the response of North American winter SATs to the leading patterns of winter SST variability in the tropical Pacific. As such, the two leading patterns of winter SST anomaly in the tropical Pacific modulate not only the conditional mean but also the scale and higher moments (e.g., kurtosis, skewness) of the conditional winter SAT

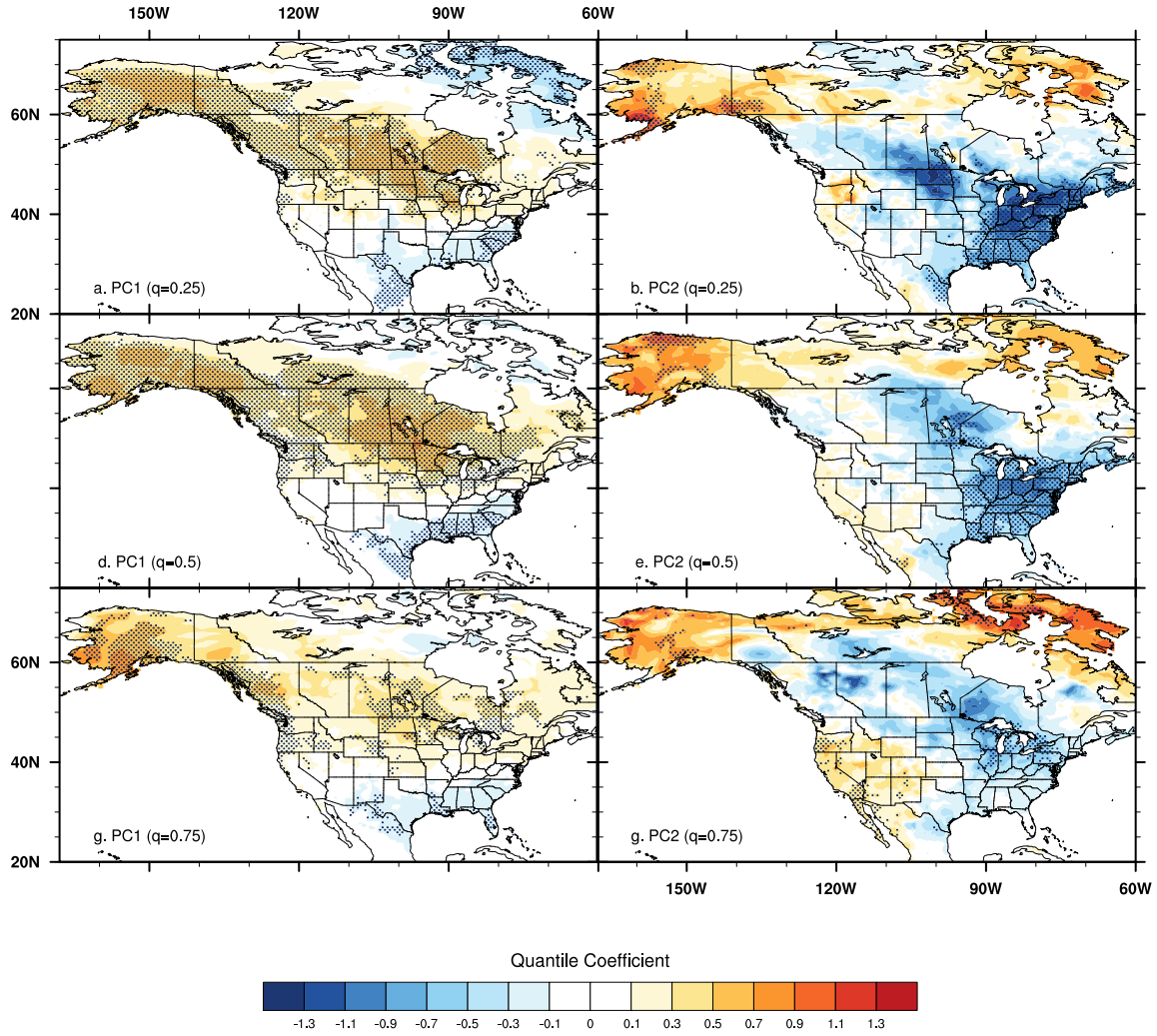

Figure D.7. Regression analysis results for (de-trended) North American winter temperature at various quantiles Regression analysis results for (de-trended) North American winter temperature at various quantiles: (a,b) $\tau = 0.25^{th}$, (b,d) $\tau = 0.50^{th}$, and (c,e) $\tau = 0.75^{th}$ quantiles against PC1 and PC2 patterns. The quantile slope coefficient for (a, c, and e) PC1 and (b, d, and f) PC2 patterns, across key quantile thresholds, were generated using quantile functions that employ both PC1 and PC2 patterns as covariates, for the entire North American temperature fields. Contour interval for quantile coefficients is 0.20. Confidence interval for estimated quantile coefficients were constructed using wild bootstrap method and stippled region signifies regression quantile coefficients at 95% confidence level.

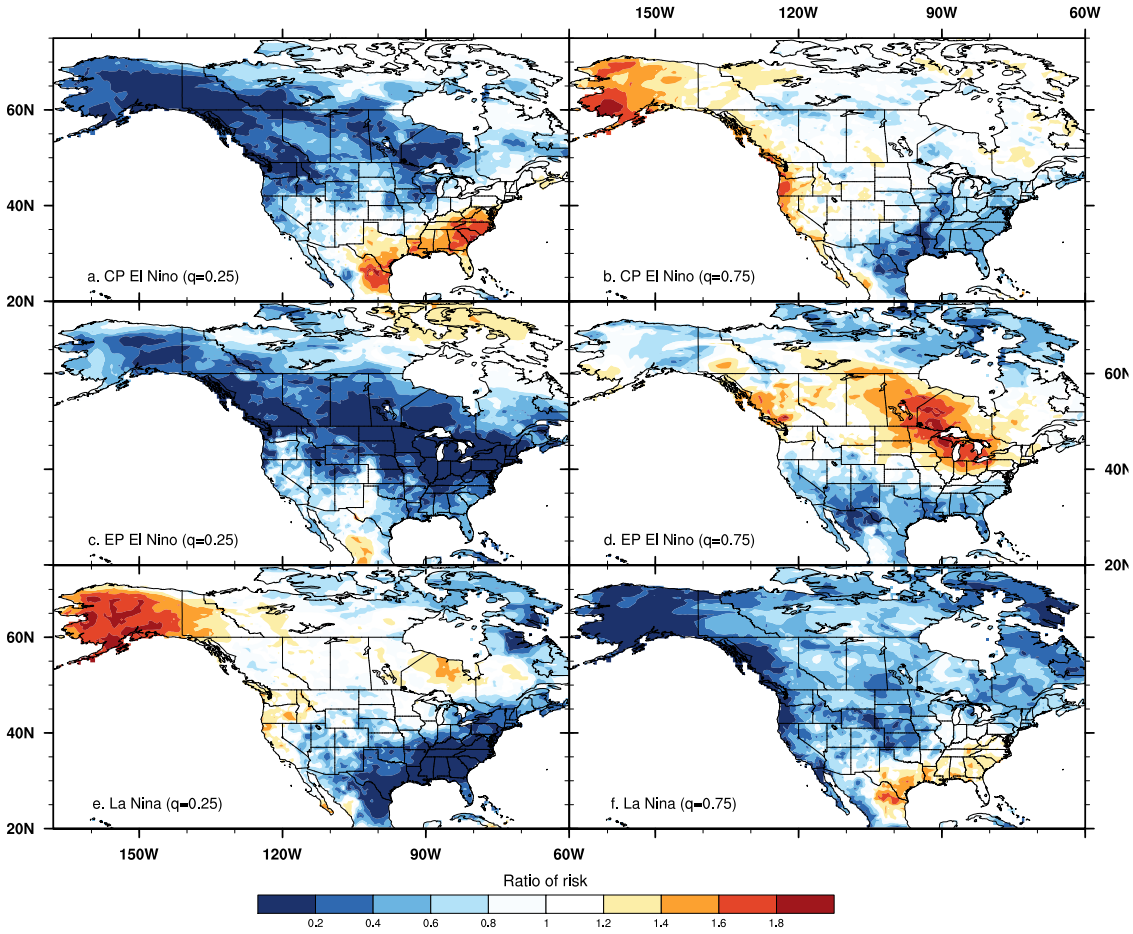

Figure D.8. Trends in North American winter SATs Trends in North American winter SATs. The red colors indicate positive (warming) trend, while the blue colors represent negative (cooling) trends. The black dots denote trends which are significant at $p < 0.10$ significance level based on Student's t-test.

variability range. Furthermore, given that the response of conditional winter SAT quantiles to ENSO events is modeled in the quantile SAT functions as a weighted linear aggregate of its sensitivity to PC1 and PC2 indices, these effects by PC1 or PC2 indices on the conditional winter SAT distributions may get amplified or suppressed.

D.3.2.3 Change in Likelihood of Cold/Warm Winters due to ENSO events

For all North American SAT fields, the change in the conditional risk of upper and lower quartile winter SATs (de-trended) due to archetypical ENSO flavors was assessed

using the same procedures described in section 3.4 of the main paper and supplementary figure 9 depicts the resulting estimates. Comparison of figure 4 and supplementary figure D.9 shows that for most North American regions, the detrending process (a) increases the conditional risk estimates for upper and lower quartile winter SATs associated with typical CP El Niño and La Niña pattern, (b) decreases the conditional risk estimates for upper quartile winter SATs related to EP El Niño. Again, it should be noted that removing the linear trend from the winter SAT time series alters the distributional characteristics of winter SATs, which in turn results in the observed difference in the computed conditional risk estimates associated with the different ENSO flavors.

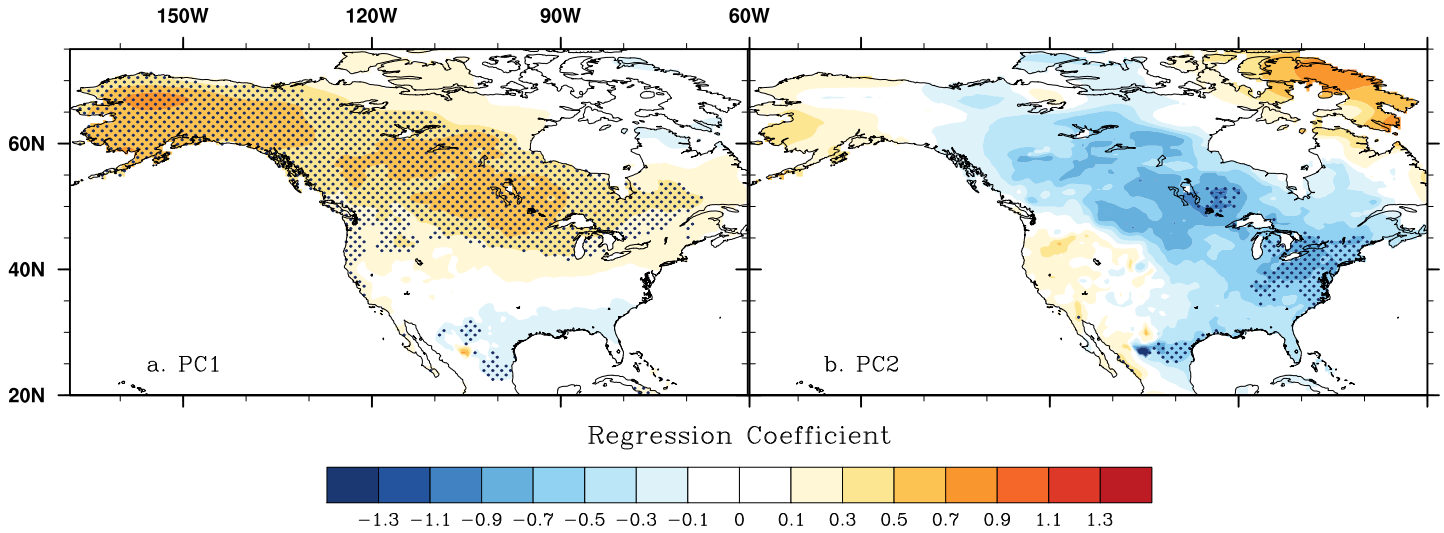

Figure D.9. Relative exceedance probability of winters with (a, c, and e) unusually cold ($\tau < 0.25^{th}$) and (b, d and f) warm ($\tau > 0.75^{th}$) temperatures Relative exceedance probability of winters with (a, c, and e) unusually cold ($\tau < 0.25^{th}$) and (b, d and f) warm ($\tau > 0.75^{th}$) temperatures during archetypical (a, b) CP El Niño, (c, d) EP El Niño, and (e, f) La Niña event to that of the unconditional for the entire North American fields. Conditional distribution for the detrended winter temperatures during ENSO events was estimated based on thirty conditional quantile functions for $0.06 < \tau < 0.94$, at equal intervals; winter temperatures at equal intervals and estimating the conditional winter temperature quantiles for centroid PC1 and PC2 indices for the five selected samples of ENSO flavors. Contour interval for the ratio is set at 0.20. A value of 1 indicates that there is no change in the relative likelihood of unusually cold/warm winters due to ENSO events.

APPENDIX E

This supplementary document contains analyses and figures that elaborate the results and/or assumptions for Chapter 6.

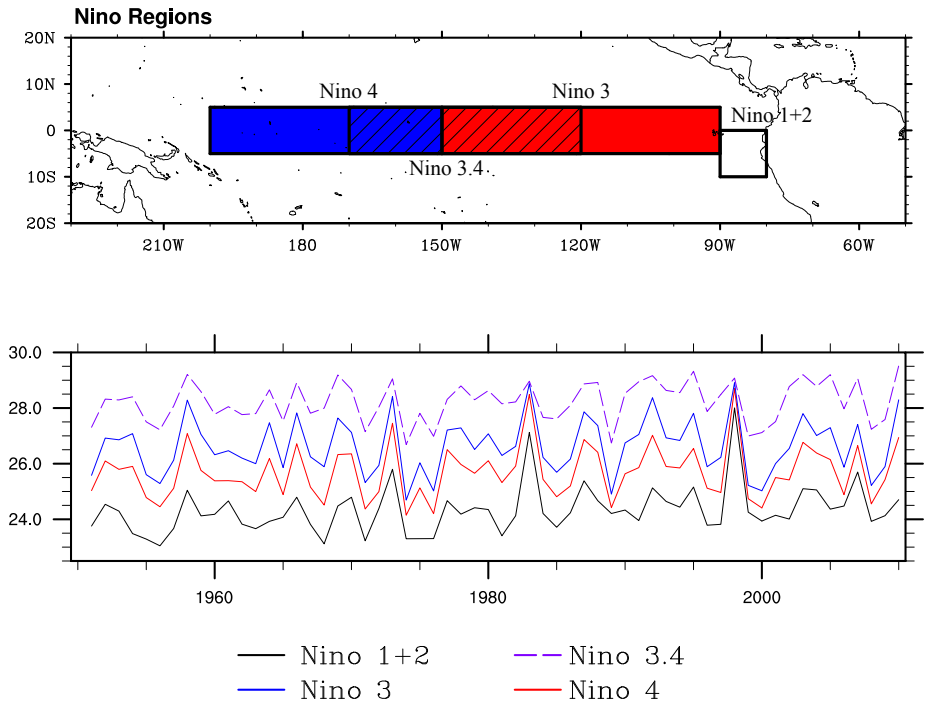

Figure E.1. Time series of wintertime sea surface temperatures (SST) for Niño regions from 1951-2010. Time series of wintertime sea surface temperatures (SST) for Niño regions from 1951-2010. (a) Delineation of the four Niño regions in the tropical Pacific: Niño 1+2 (white), Niño 3 (red), Niño 3.4 (hatched), Niño 4 (blue). (b) Time series of winter SST indices in Niño regions from 1951-2010: Niño1+2 (black), Niño 4 (red), Niño 3 (blue) and Niño 3.4 (violet). These SST indices represent the spatially averaged SST for different TP region.

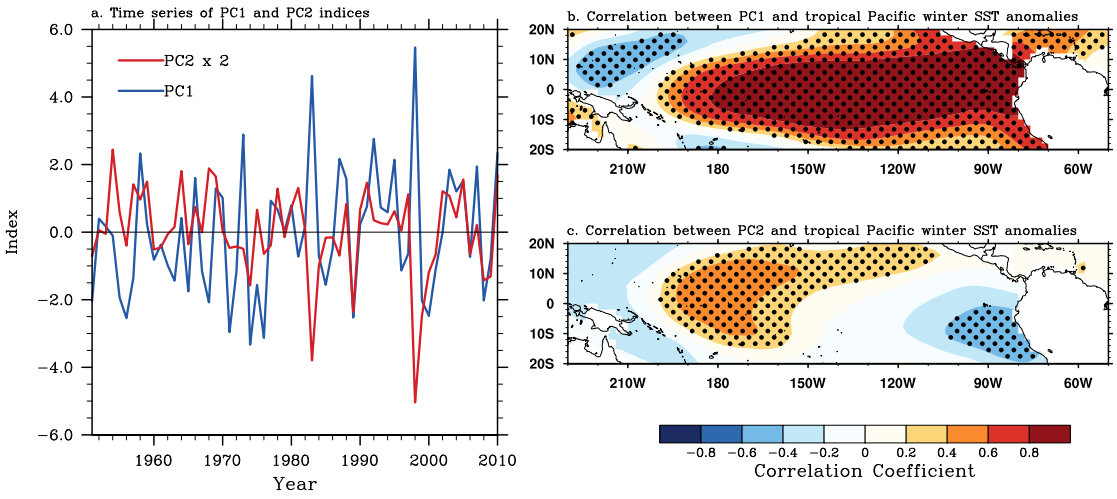

Figure E.2. The two leading empirical patterns (PC1 & PC2) of winter SST warming/cooling in Niño regions from 1951-2010. The two leading empirical patterns (PC1 & PC2) of winter SST warming/cooling in Niño regions from 1951-2010. PC1 pattern represents 89% of the total variability while PC2 pattern reproduces 9.8%. (a) Time series of PC1 (blue) and PC2 (red) scores from 1951-2010. (b) Correlation map of PC1 pattern and tropical Pacific winter SST fields. (c) Correlation map of PC2 pattern and tropical Pacific winter SST fields. Stippled areas denote regions where the correlation coefficient is significant at 90% confidence level based student t-test.

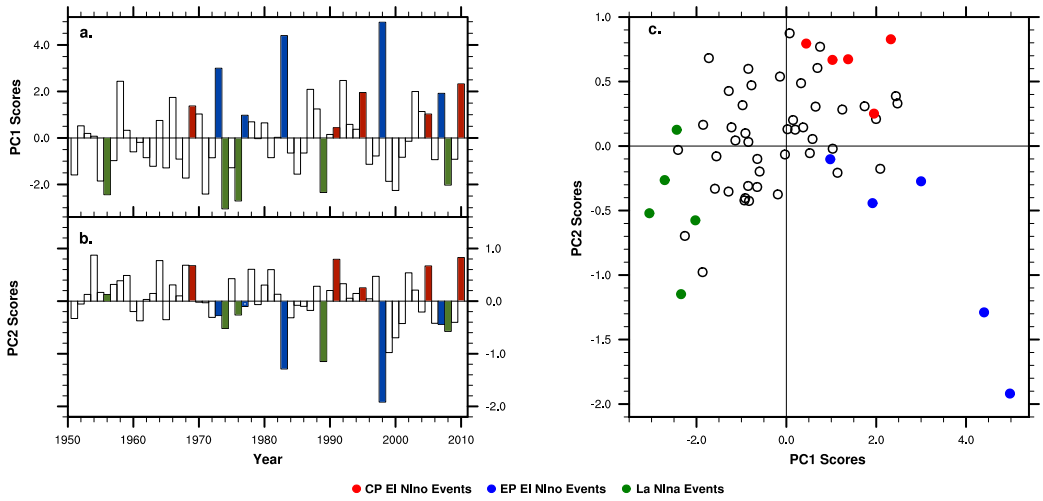

Figure E.3. Location of select five eastern Pacific El Niño (1973, 1977, 1983, 1998, and 2016), central Pacific El Niño (1969, 1991, 1995, 2005, and 2010) and La Niña (1956, 1974, 1976, 1989, and 2008) years, Location of select five eastern Pacific El Niño (1973, 1977, 1983, 1998, and 2016), central Pacific El Niño (1969, 1991, 1995, 2005, and 2010) and La Niña (1956, 1974, 1976, 1989, and 2008) years, identified from majority consensus of different identification methods (see Supplementary Table 1), within PC1-PC2 phase space. Red, blue and green bars/dots signify select CP El Niño, EP El Niño and La Niña events respectively.

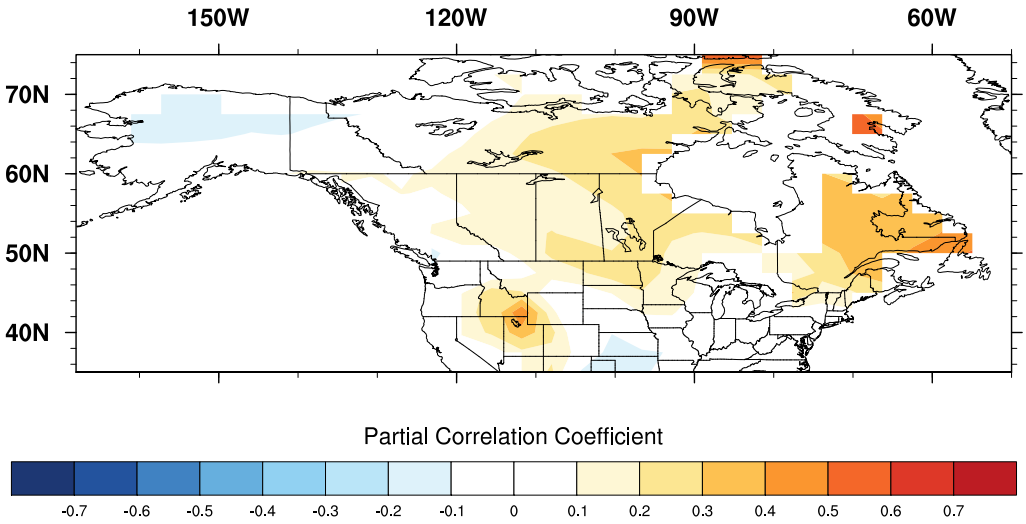

Figure E.4. The association between winter and spring AFDD for North American regions. The association between winter and spring AFDD for North American regions. Contour interval for the partial correlation coefficients is set at 0.10. It should be noted that only the partial correlation coefficients that are greater than 0.22 are statistically significant at level of 0.10 ($p < 0.10$).

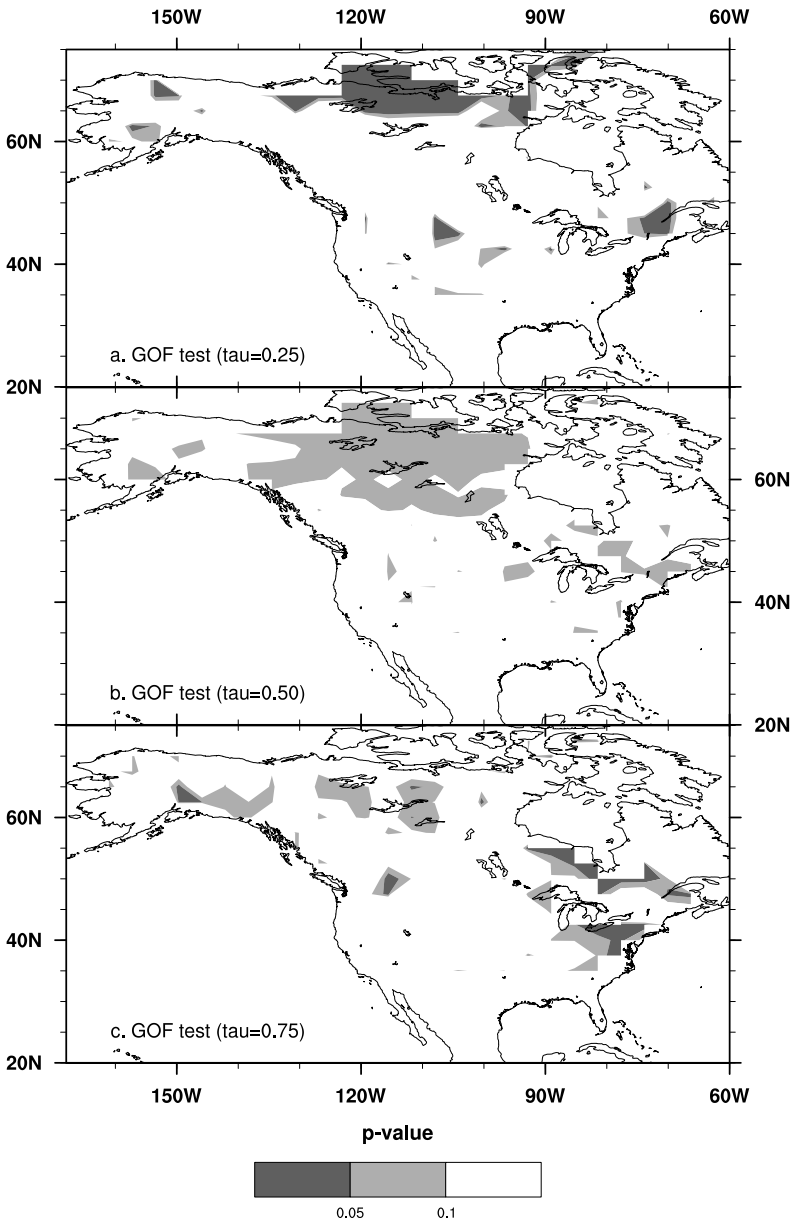

Figure E.5. Appropriateness of linear quantile functions for examining the relationship between ENSO indices and North American winter Accumulated Freezing Degree Days (AFDD) across three key quantiles. Appropriateness of linear quantile functions for examining the relationship between ENSO indices and North American winter Accumulated Freezing Degree Days (AFDD) across three key quantiles. Gray dots represent North American AFDD fields where the p-value for lack of fit is significant at 90% confidence level.

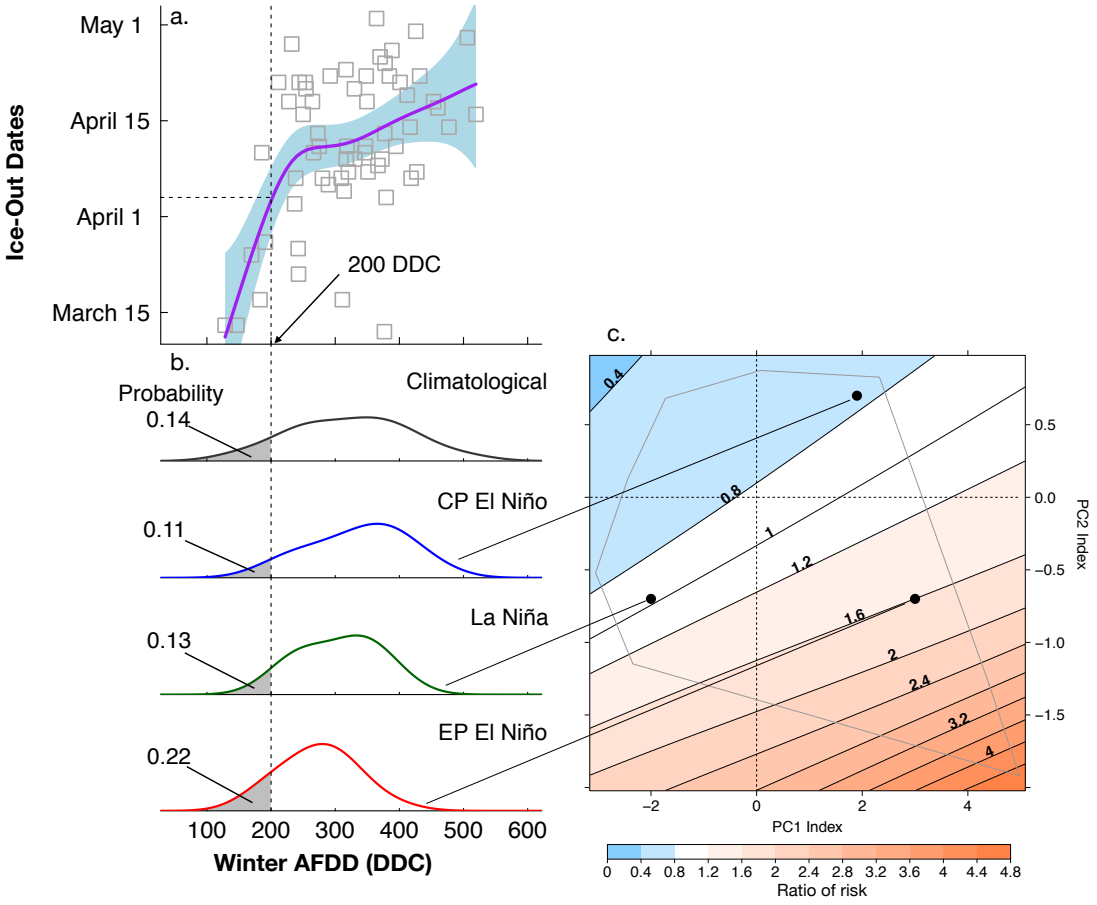

Figure E.6. Risk estimates for winter AFDD quantities, corresponding to spring ice out dates earlier than April 3^{rd} at Lake Damariscotta, conditioned on three El Niño/Southern Oscillation patterns Risk estimates for winter AFDD quantities, corresponding to spring ice out dates earlier than April 3^{rd} at Lake Damariscotta, conditioned on three El Niño/Southern Oscillation patterns (CP El Niño, La Niña, and EP El Niño). (a) Scatter plot for spring ice-out dates at Lake Damariscotta as a function of the antecedent winter AFDD. The blue shadings denote the 90% confidence interval for computed regression line. (b) Conditional winter AFDD distribution at Lake Damariscotta associated with archetypical ENSO patterns: CP El Niño (blue), La Niña (green) and EP El Niño (red). The gray area represents part of the conditional distribution less or equal to 200 DDC. (c) Contour surface plot of estimated conditional risk for winter AFDD at Lake Damariscotta to be less or equal to 200 DDC, relative to the unconditional (climatology).

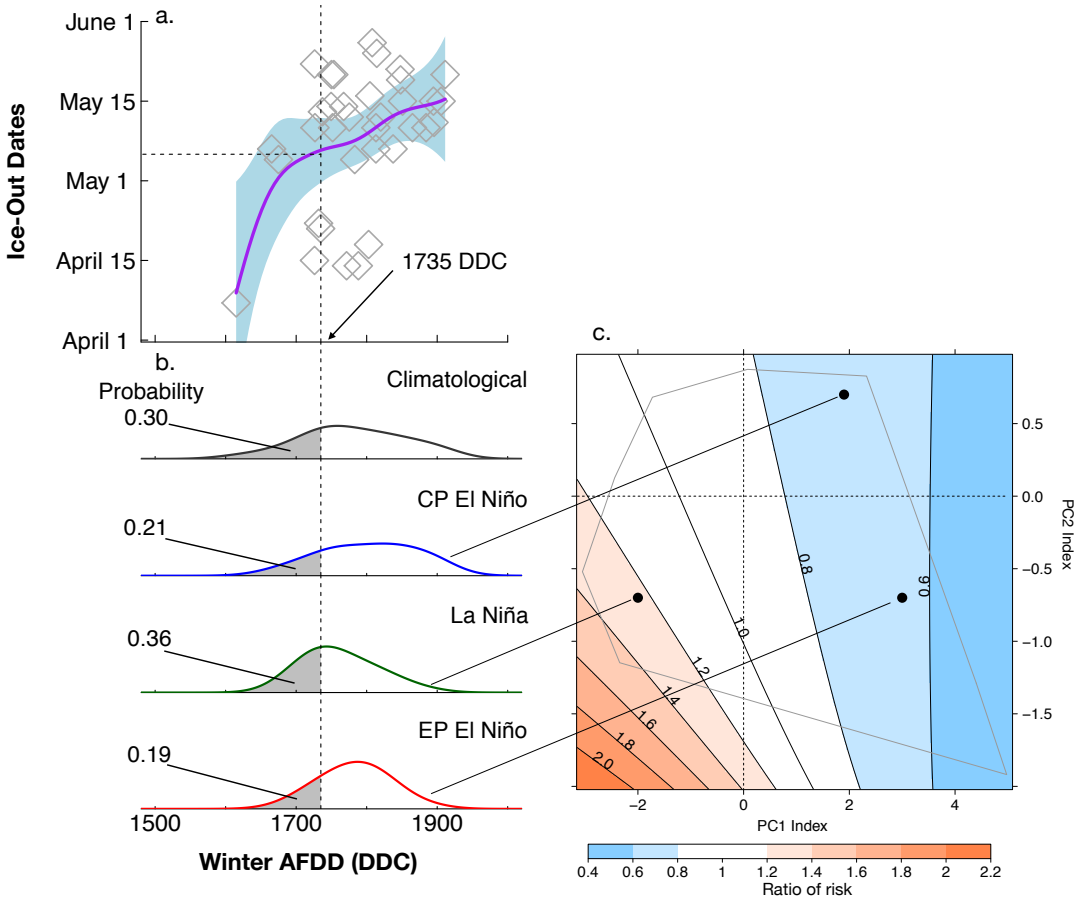

Figure E.7. Risk estimates for winter AFDD quantities, corresponding to spring ice out dates earlier than May 3^{rd} at Deadman Lake, conditioned on three El Niño/Southern Oscillation patterns Risk estimates for winter AFDD quantities, corresponding to spring ice out dates earlier than May 3^{rd} at Deadman Lake, conditioned on three El Niño/Southern Oscillation patterns (CP El Niño, La Niña, and EP El Niño). Results are computed using similar techniques as in supplementary figure S6.

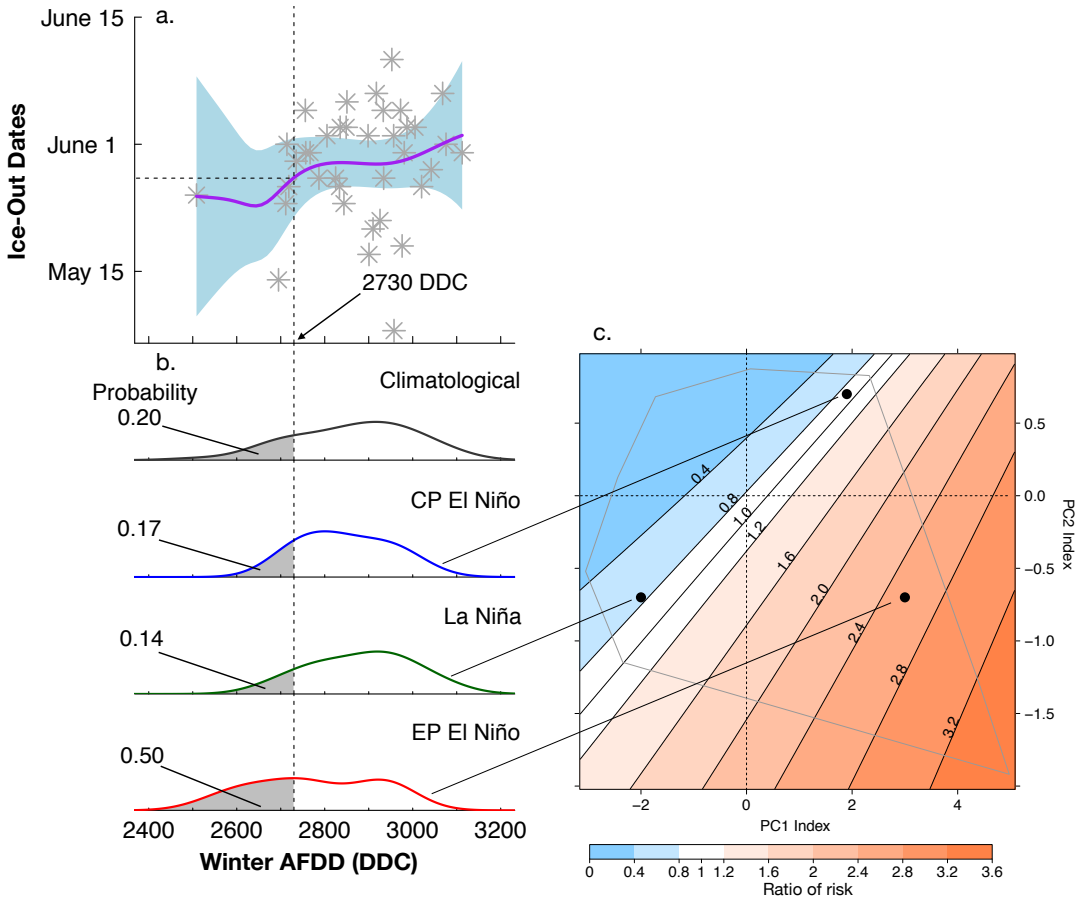

Figure E.8. Risk estimates for winter AFDD quantities, corresponding to spring ice out dates earlier than May 26^{th} at Long Lake, conditioned on three El Niño/Southern Oscillation patterns Risk estimates for winter AFDD quantities, corresponding to spring ice out dates earlier than May 26^{th} at Long Lake, conditioned on three El Niño/Southern Oscillation patterns (CP El Niño, La Niña, and EP El Niño). Results are computed using similar techniques as in supplementary figure S6.

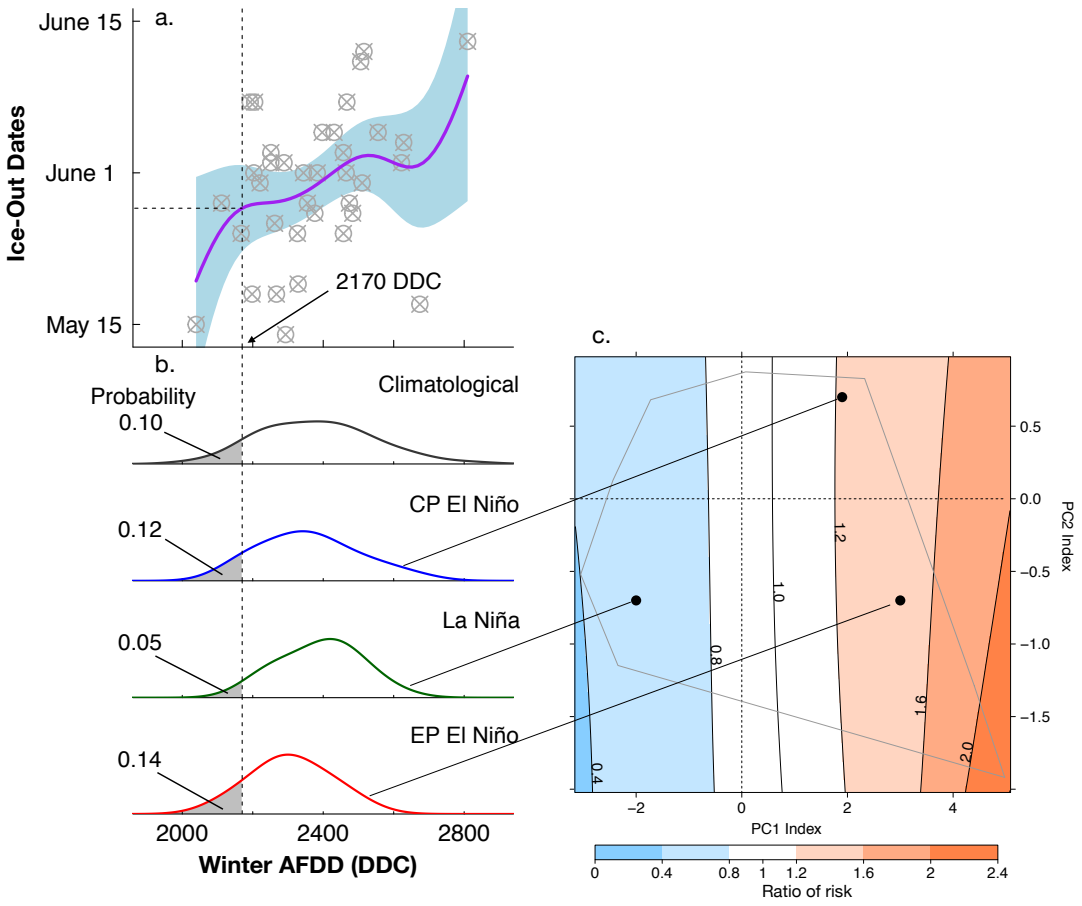

Figure E.9. Risk estimates for winter AFDD quantities, corresponding to spring ice out dates earlier than May 28^{th} at Dease Lake, conditioned on three El Niño/Southern Oscillation patterns Risk estimates for winter AFDD quantities, corresponding to spring ice out dates earlier than May 28^{th} at Dease Lake, conditioned on three El Niño/Southern Oscillation patterns (CP El Niño, La Niña, and EP El Niño). Results are computed using similar techniques as in supplementary figure S6.

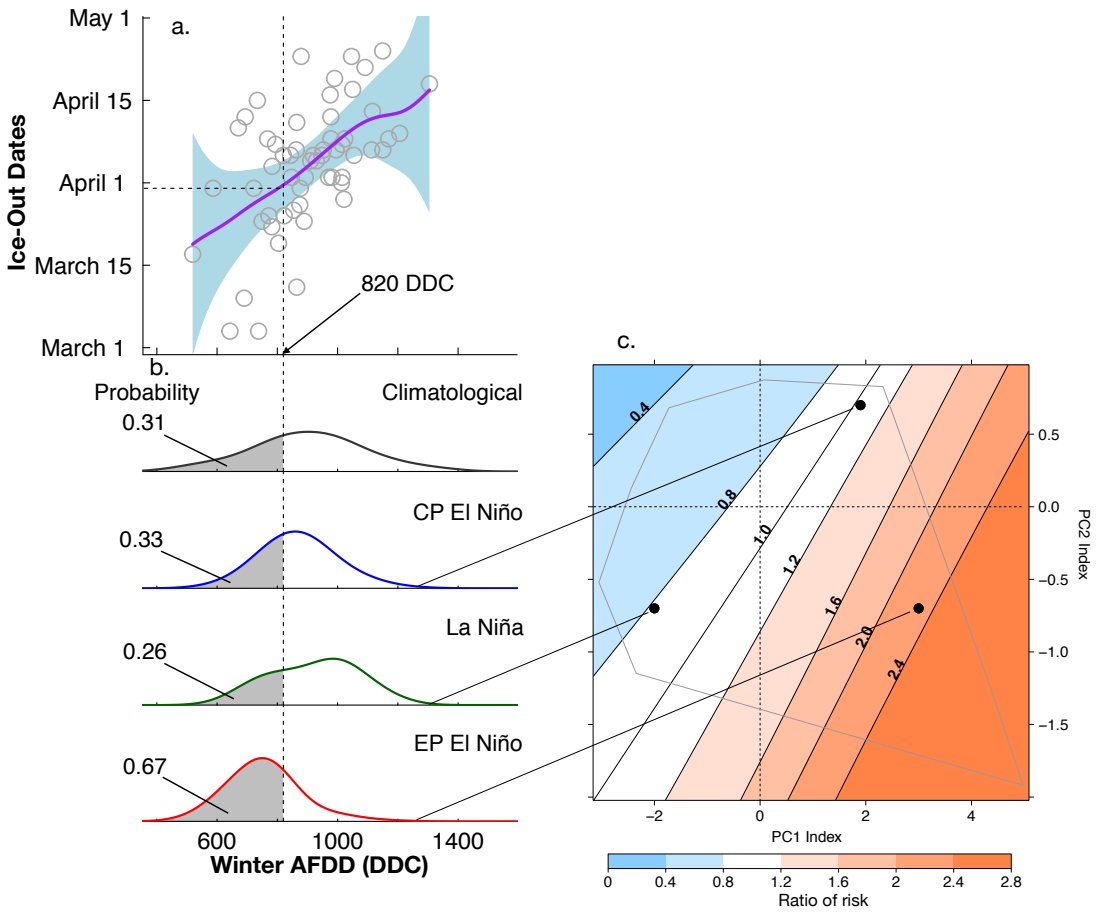

Figure E.10. Risk estimates for winter AFDD quantities, corresponding to spring ice out dates earlier than May 13^{th} at Lesser Slave Lake, conditioned on three El Niño/Southern Oscillation patterns Risk estimates for winter AFDD quantities, corresponding to spring ice out dates earlier than May 13^{th} at Lesser Slave Lake, conditioned on three El Niño/Southern Oscillation patterns (CP El Niño, La Niña, and EP El Niño). Results are computed using similar techniques as in supplementary figure S6.

	PC1	PC2	PC3	PC4
Standard Deviation	1.87	0.67	0.24	0.09
Proportion of Variance	0.87	0.11	0.01	0.002
Cumulative Proportion	0.87	0.98	0.99	1.00

PC	Niño1.2	Niño3	Niño3.4	Niño4
PC1	0.47	0.52	0.53	0.48
PC2	-0.72	-0.15	0.19	0.65
PC3	0.51	-0.58	-0.35	0.53
PC4	-0.09	0.60	-0.75	0.26

Table E.1. Empirical orthogonal modes of wintertime SST variability in Niño regions Empirical orthogonal modes of wintertime SST variability in Niño regions: (a) proportion of variance explained (b) loadings of Niño regions

Year	Classification Method					
	EMI	Nino3/4	EP/CP	NCP/NWP	Network Method	Consensus
1955/56	La Niña	La Niña	La Niña	La Niña	La Niña	La Niña
1968/69	CP El Niño	CP El Niño	CP El Niño	CP El Niño	CP El Niño	CP El Niño
1972/73	EP El Niño	EP El Niño	EP El Niño	EP El Niño	EP El Niño	EP El Niño
1973/74	La Niña	La Niña	La Niña	La Niña	La Niña	La Niña
1975/76	La Niña	La Niña	La Niña	La Niña	La Niña	La Niña
1982/83	EP El Niño	EP El Niño	EP El Niño	EP El Niño	EP El Niño	EP El Niño
1988/89	La Niña	La Niña	La Niña	La Niña	La Niña	La Niña
1994/95	CP El Niño	CP El Niño	CP El Niño	CP El Niño	CP El Niño	CP El Niño
1997/98	EP El Niño	EP El Niño	EP El Niño	EP El Niño	EP El Niño	EP El Niño
2004/05	CP El Niño	CP El Niño	CP El Niño	CP El Niño	CP El Niño	CP El Niño
2006/07	EP El Niño	EP El Niño	EP El Niño	EP El Niño	EP El Niño	CP El Niño
2007/08	La Niña	La Niña	La Niña	La Niña	La Niña	La Niña
2009/10	CP El Niño	CP El Niño	CP El Niño	CP El Niño	CP El Niño	CP El Niño

Table E.2. Classification of major ENSO events based on different identification methods Classification of major ENSO events based on different identification methods: EMI (Ashok et al., 2007), Niño 3/4 (Yeh et al., 2009), EP/CP (Kao and Yu, 2009), NCT/NWP (Ren and Jin, 2011) and climate network based (Wiedermann et al., 2016) index. A hyphen indicates that there has been no classification made for that event.

E.1 ENSO Indices for Diverse Flavors

Using the quantile regression approach, a robust characterization of ENSO-related AFDD risk for North America requires the inclusion of ENSO indices that well represent the strength and location of abnormal SST warming/cooling in the TP. Trenberth and Stepaniak [162] suggested the use of at least two TP SST indices to approximate the amplitude and spatial patterns associated with warm and cold ENSO SST anomalies, as the SST index in one region of the TP cannot effectively describe diverse ENSO flavors. To this end, principal component analysis was performed on the time series of mean winter SST indices of the four Niño regions from 1951-2010. The first principal component (PC1) reproduces 89% of the total winter SST variability across the four Niño regions and thus may be considered as the leading pattern of winter SST variability across eastern and central TP (see Table E.1a). In PC1, the loadings across the four Niño regions are of the same sign suggesting synchronous wintertime SST variation across all Niño regions (see Table E.1b). In fact, correlation between PC1 pattern and SST fields in the TP reveals that positive PC1 patterns have a spatial pattern resembling mature phase of El Niño: peak SST warming concentrated in eastern TP bounded by a horse-shoe shaped cold SST anomalies in western TP (see Figure E.2b). On the other hand, the second principal component (PC2), which is orthogonal (uncorrelated) to PC1, represents 9.8% of the total SST variability across all Niño regions (eastern and central TP). The loadings in PC2 are characterized by an east-west dipole pattern with the wintertime SSTs in Niño-1+2 (eastern Pacific) region varying out of phase with that of Niño-3.4 and Niño-4 (Central Pacific) regions. Correlation between PC2 patterns and SST fields in the TP reveal that positive PC2 phases have a SST structure that is akin to El Niño Modoki [7]: warmer than normal SSTs in the central TP extending eastwards in both hemisphere, flanked by cooler than normal temperatures on both sides of the equatorial TP (see Figure E.2c). While PC1 and PC2 patterns are uncorrelated (orthogonal) by design, extreme PC2 patterns have substantial projections within PC1. This means that PC2 patterns are primarily

indicators of the east-west asymmetry in the warming/cooling of wintertime SSTs in the TP during different El Niño/La Niña events. Figure E.3 shows the location of different ENSO events, shown in Figure E.2, within the PC1-PC2 subspace. For instance, the five EP- El Niño events selected are found in the fourth quadrant where the PC1 and PC2 indices are positive and negative respectively. This indicates that the maximum SST warming during these events is localized in the eastern equatorial Pacific and the south American coast (Niño 1+2 and Niño 3), as some of the warming in central equatorial Pacific (Niño 3.4 & Niño 4) SSTs due to positive PC1 mode is attenuated by the cooling effect in the region due to negative PC2 phases. On the other hand, the five CP-El Niño events are situated in the first quadrant where PC1 and PC2 indices are both positive. This in turn implies that the peak anomalous SST warming in the Tropical Pacific during this phenomenon is confined in central equatorial Pacific region because some of the anomalous SST warming in Niño 1+2 and Niño 3 due to positive PC1 phase is offsetted by the cooling effect in the region due to positive PC2 mode. All of the La Niña episodes are found in the third quadrant where PC1 and PC2 modes are both negative which suggests that peak SST cooling in the Niño regions is concentrated along the central equatorial Pacific. These results taken together show that the joint indices of the two leading patterns of wintertime tropical Pacific SST variability can describe the detailed nature of the amplitude and location of the tropical Pacific SST anomalies for diverse ENSO events.

E.2 Theory on the Relationship between Winter AFDD and Lake Ice Thickness

Analytical studies often estimate the wintertime lake ice growth as a function of the square root of the accumulated freezing degree days: sum of mean daily temperature departures below the freezing point (0°C or 32°F) [109]. Stefan (1891) derived the first ice growth model that employs AFDD as a covariate and today several versions of this model exist due to its simplicity and performance. The purpose of this section is to offer a limited exposition of the physical basis causal links between wintertime AFDD and lake ice phenomena. Congelation (black) ice forms when water freezes at the bottom of an ice cover [109]. This process requires the conduction of latent heat of freezing, released during the freezing of water at the water-ice interface, through the ice to the atmosphere [108]. Therefore, the rate of ice thickening commensurate to the rate of heat flux transferred from the bottom of the ice cover to the atmosphere. The growth of ice is predominantly a vertical process and as such the conduction of heat through ice can simply be expressed as a one-dimensional thermodynamic process [95]:

$$\frac{\partial \rho_i c_i T_i}{\partial t} = \frac{\partial}{\partial z}\left(\kappa \frac{\partial T_i}{\partial z} - Q_{sw}\right), T_i \leq T_f \tag{E.1}$$

where ρ_i is the density of ice, c_i is the specific heat of fusion for ice, T_i is the temperature of ice, T_f is the freezing temperature of water, κ is the thermal conductivity of ice, z is the vertical coordinate (positive downwards and zero at surface) and Q_{sw} is the solar radiation absorbed. During boreal winter, the incoming solar radiation reaching the mid-latitudes is relatively very weak as compared with other seasons and the albedo and light attenuation coefficient of ice surface is much higher than that of water. In addition, the specific heat capacity of ice is much smaller than its latent heat of fusion [9]. Thus the above equation can be reduced by (a) neglecting Q_{sw}, (b) assuming quasi-steady conditions ($\frac{\partial T_i}{\partial t} = 0$), and (c) the thickness is not large, to a steady state heat conduction equation:

$$\phi_i = \frac{\kappa_i dT_i}{dz} \tag{E.2}$$

where ϕ_i is the heat flux through the ice and κ_i is the thermal conductivity of ice. Equation E.2 states that the temperature profile within ice is linear. The boundary conditions may be determined by accounting for the heat fluxes into the system: Top of the ice cover ($z = 0$)

$$\kappa \frac{\partial T_i}{\partial z} = Q_0 - m(T_i \rho L \frac{dh}{dt}) \tag{E.3}$$

Bottom of the ice cover ($z = h$)

$$\kappa \frac{\partial T_i}{\partial z} = Q_w - \rho L \frac{dh}{dt} \tag{E.4}$$

where Q_w is the heat flux from he water to the bottom of the ice cover, L is the heat of fusion, $m(T_i) = 1$ for $T_i = 0°C$ and 0 otherwise and Q_0 is the net heat flux at the top surface of the ice cover. Equation E.3 and equation E.4 explain that the heat flux through ice cover equals the heat flux due to phase change plus external heat sources [108].

The temperature at the bottom of ice cover is zero while the temperature of lake water beneath the ice cover is greater than zero. The difference in temperature means that there is transfer of heat from the underlying water body to the bottom of the ice cover. However, this heat flux is small during winter as the turbulence under ice is either very weak or absent [95]. Furthermore at the top of the ice cover, the short wave radiation absorbed is small and the temperature is less than zero if no phase change is assumed. Therefore, the transfer of heat at the top and bottom surface of the ice cover can be approximated as: Top of the ice cover ($z = 0$)

$$\phi_i = H_{sa}(T_s - T_a), \tag{E.5}$$

Bottom of the ice cover ($z = h$)

$$\phi_i = \rho L \frac{dh}{dt}, \tag{E.6}$$

where T_s and T_a is the temperature at the top ice cover and the overlying air respectively, and H_{sa} is the bulk heat transfer coefficient between air and top ice cover surface. Equation E.5 and E.6 state that the rate of ice production is balanced by the rate of heat transfer from the top ice cover surface to the overlying air [11]. It has been pointed out that equation E.5 only takes into account the heat flux due convection and net long wave radiation [174]. Assuming homogenous ice cover, equation E.2, equation E.5, and equation E.6 can be combined to approximate the rate of ice production as

$$\rho L \frac{dh}{dt} = \frac{T_m - T_a}{\left(\frac{h_i}{\kappa_i} + \frac{1}{H_{sa}}\right)} \tag{E.7}$$

where T_m is the temperature at the bottom of the ice cover, which is equal to the freezing point of water ($T_m = 0$). These may be integrated with the boundary condition that $h = 0$ when $t = 0$ resulting in

$$h = \left[\left(\frac{\kappa}{H_{sa}}\right)^2 + \int_{t=0}^{t} \frac{2\kappa}{\rho L}(T_m - T_a)dt\right] - \frac{\kappa}{H_{sa}} \tag{E.8}$$

the effect of the term $\frac{H}{sa}$ has appreciable effect when the ice is thin [10]. On the other hand for large values of $\int(T_m - T_a)dt$, equation (E.8) converges to

$$h = \left(\frac{2\kappa}{\rho L}\right)^{1/2} \left(\int_{t=0}^{t} (T_m - T_a)dt\right)^{1/2}, T_a < T_m \tag{E.9}$$

If the time interval Δt is in days, equation E.9 produces a well-known approach for estimating the bulk ice thickness referred to as Stefan's equation. Furthermore, the second bracketed term in this equation represents the sum of the freezing degree-days and thus lake ice thickness is approximated as a function of the square root of the accumulated freezing degree days. Given the myriad of assumptions and approximations employed in deriving this equation, empirical data reveals that an additional correcting factor often in the range 0.5-0.8 must be applied to the right hand side of equation E.9, so that its estimates are close to actual ice thickness measurements [10].

BIOGRAPHY OF THE AUTHOR

Mussie Tekie Beyene was born in Addis Ababa, Ethiopia. For his B.Sc., he studied Civil and Environmental Engineering from University of Asmara, Eritrea. For the next few years, Mussie worked as a water/waste water design engineer at Asmara Water Supply and Sewerage Department. He was admitted to the PhD program in Civil and Environmental Engineering at the University of Maine in 2011. During his graduate studies at the University of Maine, Mussie was awarded Michael J. Eckardt's Dissertation Fellowship and Summer Dissertation Writing Fellowship. His research interest lies in winter limnology, hydro-climatology and environmental risk assessment. Mussie is currently an ORISE Post-doctoral Fellow at the Western Ecological Division (of the US Environmental Protection Agency) in Corvallis, Oregon.

Mussie Tekie Beyene is a candidate for the Doctor of Philosophy degree in Civil and Environmental Engineering from the University of Maine in December 2019.